Vol. 178 No. 2, December 15, 1985
Completing Vol. 178

ISSN 0003-2670

ANALYTICA CHIMICA ACTA

International journal devoted to all branches of analytical chemistry

ELSEVIER

ANALYTICA CHIMICA ACTA

International journal devoted to all branches of analytical chemistry
Revue internationale consacrée à tous les domaines de la chimie analytique
Internationale Zeitschrift für alle Gebiete der analytischen Chemie

PUBLICATION SCHEDULE FOR 1986

	J	F	M	A	M	J	J	A	S	O	N	D
Analytica Chimica Acta	179	180	181	182 183/1	183/2 184	185	186	187	188	189	190	191

Scope. *Analytica Chimica Acta* publishes original papers, short communications, and reviews dealing with ever aspect of modern chemical analysis both fundamental and applied.

Submission of Papers. Manuscripts (three copies) should be submitted as designated below for rapid and efficier handling:

Papers from the Americas to: Professor Harry L. Pardue, Department of Chemistry, Purdue University, West Lafayett IN 47907, U.S.A.

Papers from all other countries to: Dr. A. M. G. Macdonald, Department of Chemistry, The University, P.O. Box 36 Birmingham B15 2TT, England. Papers dealing particularly with computer techniques to: Professor J. T. Cler Universität Bern, Pharmazeutisches Institut, Baltzerstrasse 5, CH-3012 Bern, Switzerland.

Submission of an article is understood to imply that the article is original and unpublished and is not being considere for publication elsewhere. Upon acceptance of an article by the journal, authors will be asked to transfer the copyrigl of the article to the publisher. This transfer will ensure the widest possible dissemination of information.

Information for Authors. Papers in English, French and German are published. There are no page charge Manuscripts should conform in layout and style to the papers published in this Volume. Authors should consu Vol. 170 for detailed information. Reprints of this information are available from the Editors or from: Elsevier Editori Services Ltd., Mayfield House, 256 Banbury Road, Oxford OX2 7DH (Great Britain).

Reprints. Fifty reprints will be supplied free of charge. Additional reprints (minimum 100) can be ordered. An ord form containing price quotations will be sent to the authors together with the proofs of their article.

Advertisements. Advertisement rates are available from the publisher.

Subscriptions. Subscriptions should be sent to: Elsevier Science Publishers B.V., Journals Department, P.O. Bc 211, 1000 AE Amsterdam, The Netherlands. Tel: 5803 911, Telex: 18582.

Publication. *Analytica Chimica Acta* appears in 13 volumes in 1986. The subscription for 1986 (Vols. 179–191) Dfl. 2730.00 plus Dfl. 312.00 (p.p.h.) (total approx. US $1049.00). All earlier volumes (Vols. 1–178) except Vols. 2 and 28 are available at Dfl. 231.00 (US $85.56), plus Dfl. 15.00 (US $5.56) p.p.h., per volume.

Our p.p.h. (postage, packing and handling) charge includes surface delivery of all issues, except to subscribers in th U.S.A., Canada, Japan, Australia, New Zealand, P.R. China, India, Israel, South Africa, Malaysia, Thailand, Singapor South Korea, Taiwan, Pakistan, Hong Kong, Brazil, Argentina and Mexico who receive all issues by air delivery (S.A.L — Surface Air Lifted) at no extra cost. For the rest of the world, airmail and S.A.L. charges are available upon reques Claims for issues not received should be made within three months of publication of the issues. If not they cannot b honoured free of charge.

For further information, or a free sample copy of this or any other Elsevier Science Publishers journal, readers in th U.S.A. and Canada can contact the following address: Elsevier Science Publishing Co. Inc., Journal Informatio Center, 52 Vanderbilt Avenue, New York, NY 10017, U.S.A., Tel: (212) 916-1250.

0003-2670/85/$03.

Printed in The Netherlands

Analytica Chimica Acta, 178 (1985) 159—167
Elsevier Science Publishers B.V., Amsterdam — Printed in The Netherlands

A NEW SAMPLING TECHNIQUE FOR REVERSED-PHASE LIQUID CHROMATOGRAPHY/FOURIER-TRANSFORM INFRARED SPECTROMETRY

C. FUJIMOTO, T. OOSUKA and K. JINNO*
School of Materials Science, Toyohashi University of Technology, Toyohashi 440 (Japan)
(Received 12th April 1985)

SUMMARY

A systematic study of the utility of stainless-steel wire nets (SSWN) as a substrate for infrared sampling is described. The nets can be used with polar solvents including water, as well as non-polar solvents, without harming the surface. The use of the SSWN simplifies interfacing between a reversed-phase liquid chromatograph (l.c.) and a Fourier-transform infrared spectrometer. It is used as a l.c. detector cell by collecting the effluent from l.c. on the cell itself. The technique is tested extensively with carbaryl as sample and is applied successfully to the detection of a pharmaceutical mixture (phenacetin, caffeine and aspirin) separated by reversed-phase l.c. with a (3:2, v/v) methanol/water mobile phase.

In recent years, several laboratories have worked on the development of modern liquid chromatography/Fourier-transform infrared spectrometry (l.c./F.t.i.r.). Much of this work has focused on dealing with the fact that most l.c. mobile phases absorb strongly in the mid-infrared region, which makes the measurement of the spectrum of the solute by a flow-cell technique nearly impossible. The subject has been reviewed by Vidrine [1].

Some procedures have been described to eliminate the mobile phase prior to the measurement of infrared spectrum. In the buffer-memory technique [2—4], the effluent from a micro l.c. column was deposited onto a moving KBr plate where the mobile phase was evaporated and the solutes were condensed on the plate. After the chromatogram was complete, the plate was simply transferred to the infrared spectrometer and transmittance spectra were measured across the region of the plate where the solutes had been deposited. In another procedure, developed for conventional (4.6 mm i.d.) l.c. columns, Kuehl and Griffiths [5, 6] used diffuse-reflectance F.t.i.r.; the effluent was concentrated by differential evaporation and the solutes were deposited on powdered KCl which was held in small sample cups on a carousel. A drop monitor and controlling electronics moved the carousel after each drop has been deposited. The diffuse-reflectance spectra of the solutes were then measured. Conroy et al. [7] have recently reported the use of micro columns for l.c./F.t.i.r. with diffuse reflectance.

However, neither technique is readily applicable to reversed-phase l.c./F.t.i.r. because of the presence of water in most reversed-phase solvent

0003-2670/85/$03.30

systems, in spite of their success in size-exclusion and normal-phase chromatography. The prime problem with reversed-phase l.c. is that because of the high latent heat of evaporation, it is difficult to remove the final traces of water from the substrate before the F.t.i.r. spectra are measured, leading to large spectroscopic interferences.

More recently, some modifications of the above-mentioned l.c./F.t.i.r. with diffuse reflectance have been studied to solve the water elimination problem. Conroy et al. [8] have developed a new solvent elimination interface which includes extraction of solutes into dichloromethane; subsequently, the interface is operated in a manner similar to that described above. Kalasinsky and co-workers [9—11] have utilized a post-column dehydrating agent (an acetal) which reacts with water in the effluent to form volatile products before being deposited on a moving sample "train" which contains a KCl substrate. The spectra of the solutes were measured by diffuse-reflectance F.t.i.r.

In the work reported here, stainless-steel wire net (SSWN) was evaluated for use as a cell in the buffer-memory technique. One of the major reasons to switch over to this SSWN is its insolubility in water.

EXPERIMENTAL

Equipment

An F.t.i.r. spectrometer (model JIR-40X, JEOL, Tokyo) equipped with a triglycine sulfate detector, the standard KBr/Ge beam splitter, and water-cooled Globar source was used to obtain all of the spectral results. The infrared spectra were measured with the aid of a 3× beam condenser (model BC-1, JASCO, Tokyo) situated in the front channel of the spectrometer. The SSWN disk (see below), after sample deposition, was secured onto the standard sample holder supplied with the beam condenser. At the sampling site the beam image was reduced to such an appropriate area as to fill the whole sample-deposited area. After both the sample and blank spectra had been scanned 200 times in the double-beam mode, infrared subtraction was used to remove the background interference from the sample. The blank spectrum was obtained from the SSWN disk before the solution was deposited. Spectra were all obtained at a resolution of 4.0 cm^{-1}.

Separations were obtained on Develosil ODS-3 packings in a fused-silica capillary (0.5 mm i.d. × 50 mm) or on Develosil ODS-10 packings in a larger fused-silica capillary (0.5 mm i.d. × 240 mm), with aqueous mobile phases at 4 $\mu l\ min^{-1}$. An ultraviolet detector (Uvidec 100-II, JASCO) equipped with a micro flow-cell (0.2-μl volume) was used as an auxiliary detector. The samples were injected into the columns by the "microfeeder" sampling technique; the necessary details are available elsewhere [12, 13].

The stainless-steel wire net and interface

Commercially available SSWNs were formed into round disks (7 mm) or strips (10 mm × 50 mm) and, prior to use, were cleaned by rinsing in various

solvents, e.g., methanol and carbon tetrachloride, and air-drying. The SSWN was obtained from Iuchi-Seieido (Osaka, Japan).

A microfeeder pump (model MF-2, Azumadenki Kogyo, Tokyo) equipped with an air-tight microsyringe (250- or 500-μl volume) was used to feed solutions of sample and solvent to the SSWN disks. The pump was also used to feed mobile phases into reversed-phase columns. For preliminary studies, the needle of the microsyringe was connected to a piece of stainless-steel capillary (0.31 mm o.d., 0.13 mm i.d.) via a polytetrafluoroethylene tubing so that the solutions were concentrated into an appropriate small area on the surface of the SSWN disks. After the solutions had been deposited, the disks were thoroughly dried with a hot air stream to eliminate residual solvent and leave a spot of the sample. The spot diameter varied from 0.4 to 1 mm depending on the solvent type and flow rate used. The exact length of this evaporation period appeared to have no significant influence on the band intensity of the resulting spectrum, provided that the sample-deposited disks were not subjected to the stream for an extended period of time. The evaporation period was usually 3—5 min.

The interface for the buffer-memory technique has been described elsewhere [2]. Only minor modification of the interface was required for use in this study. The present version of the depositor consisted of a few centimeter of a stainless-steel capillary (0.13 mm i.d., 0.31 mm o.d.) which was bent to keep it in contact with the surface of the SSWN (Fig. 1). A strip of SSWN was mounted on a newly constructed sample holder which was attached to the interface. All infrared spectra were obtained by measuring the single-beam spectra of the solutes and ratioing this against the single-beam spectrum of the blank (no-sample retained area). Each stored spectrum (representing a 0.8-μl elution volume or 0.38 mm on the SSWN surface along the direction of the movement) was the result of averaging 100 individual spectra obtained at a resolution of 8 cm^{-1}. Other details of the construction and operation of the interface are similar to those outlined earlier [2].

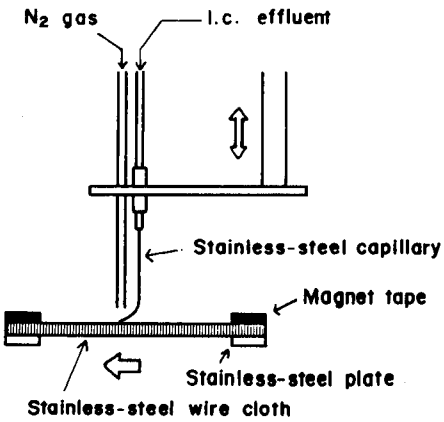

Fig. 1. Sampling arrangement for l.c./F.t.i.r. based on the buffer-memory technique.

RESULTS AND DISCUSSION

The SSWNs have many of the properties required of a substrate for infrared sampling, in that they are completely insoluble in all solvents including water, not very fragile, conveniently handled, and easily regenerated. In addition, they possess enough open area to transmit the incident radiation to the detector, allowing the transmittance spectrum of a sample on them to be measured. Therefore, if KBr plates, which have been used previously in the buffer-memory technique, are replaced by SSWNs, the water problem will be circumvented.

Initially, several SSWNs having different screen-size openings (see Table 1) were tested. At first sight, none of these SSWNs looks to be tight enough to trap the sample. However, all the sample seems to be retained on the surface because no breakthrough of solution was ever observed. The spectra obtained by depositing 2 μg of carbaryl in (1:1, v/v) methanol/water onto each SSWN surface are shown in Fig. 2. It can be seen that the intensities of the absorption bands increase substantially as the opening is reduced, and the 846-mesh SSWN gives the most intense spectrum. Only a slight increase in background noise level was observed on the spectrum from the 846-mesh net. It is interesting to note that the band intensity is independent of the energy impinging on the detector. The percentage of open area (listed in Table 1) reflects the efficiency of incident radiation transmitted through the net without a beam condenser. Based on these results, the 846-mesh SSWN was chosen for all further studies.

For comparative purposes, the carbaryl solutions were deposited onto a SSWN disk and a KBr plate under the same conditions. The spectra were scanned 10 000 times; the results are shown in Fig. 3. There are differences in the bandwidths and relative band intensities; the former is noticeable for the C=O band at 1712 cm^{-1} while the latter is noticeable for the N—H band at

TABLE 1

The SSWNs tested

Screen-size opening (μm)	Taylor equivalent designation (mesh)	Nominal wire diam. (mm)	Open area[b] (%)
15	846	0.012	30.9
20	635	0.015	32.7
37[a]	400	0.026	34.5
46	300	0.035	32.3
53[a]	270	0.038	33.9
74[a]	200	0.053	34.0
105[a]	145	0.070	36.0

[a]These screens correspond to those proposed as a Japanese Industrial Standard (JIS). [b]Percentage of open area (P) was calculated from $P = [(O^2/(O + D)^2] \times 100$, where O is the size of the opening (column 1) and D is the diameter of wire (column 3).

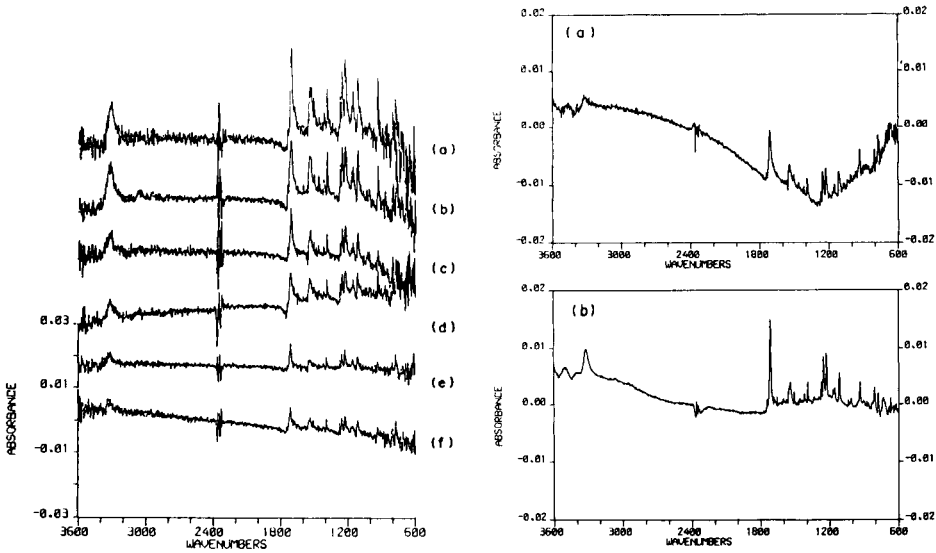

Fig. 2. F.t.i.r. spectra of carbaryl deposited on SSWN with different screen-size opening (μm): (a) 15, (b) 20, (c) 37, (d) 53, (e) 74, (f) 105 μm. Conditions: carbaryl solution, 10 mg ml^{-1}; flow rate, 1 μl min^{-1}; collection time, 12 s.

Fig. 3. F.t.i.r. spectra of carbaryl (0.5 μg) deposited on (a) 846 mesh SSWN and (b) KBr plate.

3320 cm^{-1}. These differences can be attributed to the contribution of diffusely reflected components of the infrared beam to the spectrum in Fig. 3(a). If it is assumed that the surface of the 846-mesh SSWN is uniformly covered with the sample molecules, the intensities (in absorbance) should be about 70% of those obtained from KBr plates, as the percentage open area is about 30.9% (Table 1). The loss in intensity with the SSWN is <30%, which suggests that much of the sample is retained in the open portions of the net, rather than on the wires; this was confirmed by microphotography.

To explore the likelihood that the spectral intensity varies with the solvent type used, some experiments were conducted with methanol, (1:1) methanol/water, and n-hexane as the sample carrier. Samples of constant concentration in each carrier were deposited for different times. With methanol as carrier, samples of different concentration were also deposited for the same period of time. The plots of the absorbance of the C=O stretching band (1712 cm^{-1}) against the quantity of sample deposited with (1:1) methanol/water and pure methanol are shown in Fig. 4a and 4b, respectively. For a given collection time, absorbances are higher with the aqueous solution. It was observed that when methanol was used as the carrier, the wetted area spread further than with the aqueous carrier, so that the sample spot was larger after solvent evaporation. Thus, the results seem to be explained by the different surface tensions of the solvents (22.55 and 35.31 dyne cm^{-1} for methanol and (1:1)

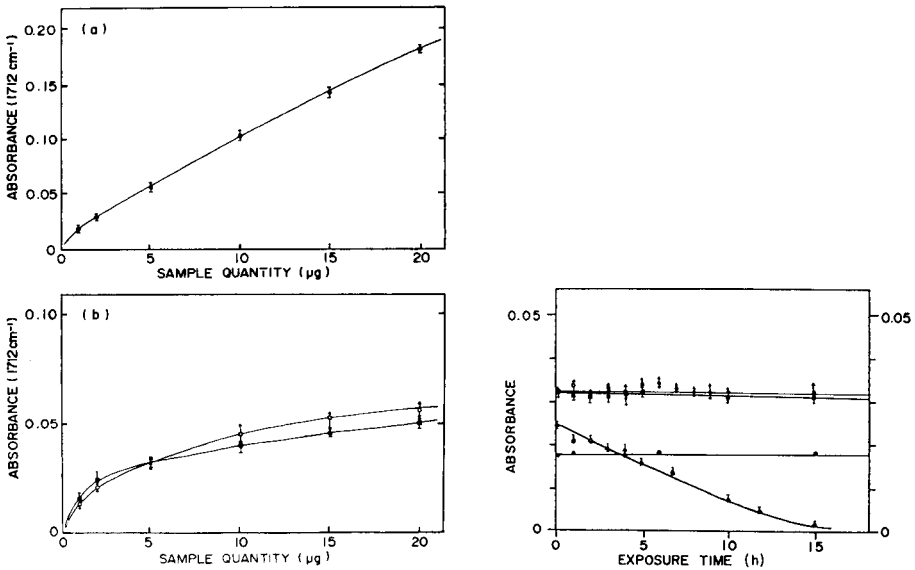

Fig. 4. Band intensity vs. sample quantity. (a) Samples (1% w/v) dissolved in (1:1) methanol/water with a collection time of 6—120 s. (b) Samples dissolved in pure methanol: (○) sample concentration of 0.2—4% with 30-s collection time; (■) sample concentration of 1% with a collection time of 6—120 s. In all cases, flow rate was 1 μl min^{-1}. Bars show the spread of 3—6 experiments.

Fig. 5. Variation of band intensity of sample with exposure time. Each sample (5 μg) was deposited on 846-mesh SSWN. (●) *p,p'*-DDT (1100 cm^{-1}); (○) n-butyl stearate (2920 cm^{-1}); (■) carbaryl (1712 cm^{-1}); (△) n-octadecane (2930 cm^{-1}). Conditions: 5 μg of sample in methanol or carbon tetrachloride was deposited; temperature ca. 27° C, relative humidity 40%.

methanol/water at 20° C, respectively). The larger the spot, the more sample will adhere to the wires as the solvent evaporates; an increasing fraction of the sample will then not be "seen" by the beam. It is clear, however, that the SSWN substrate is useful for reversed-phase l.c. for which water/methanol is a common mobile phase. Nevertheless, these results indicate a problem; as the intensity is solvent-dependent, quantitation will be more difficult when gradient elution chromatography is used.

Close inspection of the data in Fig. 4(b) shows that the absorbance is sensitive to the volume of the solution deposited; for a given sample size, higher absorbances are obtained from smaller volumes of solution. Analogously, lengthened collection times produce enlarged sample areas, lowering the apparent absorbance.

It can also be seen that all the plots in Fig. 4 display downward curvature; the absorbance may be suppressed by the increase in the deposited area accompanying the increase in the collection volume. In contrast, excellent linearity was obtained when n-octadecane dissolved in n-hexane was deposited.

In this case, the carrier evaporated immediately, leaving a small sample spot. It could be concluded that if the heat of vaporization of the sample carrier is sufficiently small, then there will be no decrease in absorbance caused by spreading of the deposited area.

Another point to be considered is the possible loss of sample deposited on exposure to the atmosphere, as well as losses during the solvent evaporation. It should be realized that in all the l.c./F.t.i.r. techniques involving solvent elimination, nonvolatility of the sample is a prerequisite to their success; this is not a serious limitation because volatile samples are usually separated by gas chromatography.

It has been noted previously that sample loss can occur during sample preparation for infrared spectrometry. Griffiths and Block [14] tested methylphosphonate monoesters having a vapor pressure of about 10^{-4} torr at 20°C; a large fraction of the sample evaporated during transfer of KBr powders and sample to the microdie and over 90% of the sample disappeared in a few minutes after it had been pressed into a microdisk. King [15] studied the loss of 2,6-dimethoxyphenol, which has an even lower vapor pressure than the esters. When carbon disulfide was used as the sample carrier, and evaporated on the KBr powder, sample loss was observed during the deposition, but not subsequently. In order to establish the suitability of the buffer-memory technique with the SSWN for different samples, some compounds of relatively low volatility were tested. One advantage of the buffer-memory technique over other solvent-elimination techniques is that the solutes are retained on a single substrate as a permanent record of the chromatogram so that the solutes can be characterized by other analytical techniques if required [4].

The selected compounds were n-octadecane, carbaryl, n-butyl stearate, and *p,p'*-DDT, of which vapor pressures at 20°C are of the order of 10^{-4}, 10^{-5}, 10^{-6}, and 10^{-7} torr, respectively. Variations of absorbance of each compound with exposure time are shown in Fig. 5. Obviously, the relative evaporation rate of the sample decreases with decreasing vapor pressure. The evaporation loss is very rapid with n-octadecane, which is liquid at room temperature. In these measurements, the SSWN disks with sample deposited were placed at a small focus between the source and beam splitter in the JIR-40X and absorbances were obtained from 200 co-added, 4-cm^{-1} resolution spectra (requiring ca. 13 min). Therefore, the heating effect of the source radiation on the sample also creates sample losses. In fact, at higher data collection rates (e.g., ca. 7 min for 200 scans at 8-cm^{-1} resolution), the absorbances decreased much more slowly. Such losses can be greatly reduced by placing the SSWN disks just in front of the detector. Compounds having a vapor pressure of not more than 10^{-5} torr or so could be handled by the buffer-memory technique.

The present work was directed primarily toward reversed-phase chromatography with aqueous mobile phases. An F.t.i.r. chromatogram obtained by injecting 2 μg of carbaryl is shown in Fig. 6; the lower trace indicates the

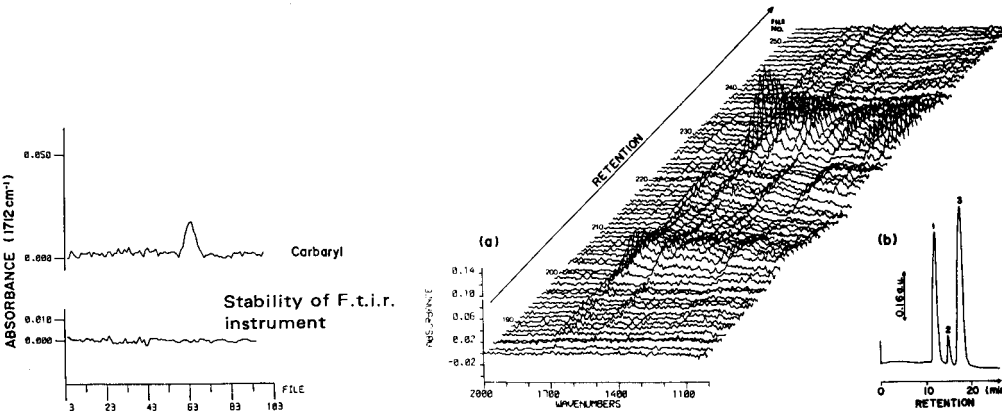

Fig. 6. F.t.i.r. chromatogram of carbaryl (2 μg). Conditions: 3-μm ODS column, (4:1) methanol/water eluent at 4 μl min^{-1}; effluent collected on SSWN strip drawn across deposition point at 1.88 mm min^{-1}; N_2 stream at 50° C. The lower trace is the response without the strip in the i.r. beam.

Fig. 7. F.t.i.r. (a) and u.v. (b) chromatograms. Peaks: (1) caffeine; (2) aspirin; (3) phenacetin.

response of the spectrometer without the strip in the beam, i.e., the stability of the F.t.i.r. instrument itself. Clearly, there is no base-line drift or excessive noise caused by the movement of the strip across the beam. A plot of the relative area of the chromatographic peak against the quantity of carbaryl injected was linear (correlation coefficient 0.998) over the 1–20 μg range; the linear range may actually be wider. These results are inconsistent with the trends of band intensity against sample quantity shown in Fig. 4, possibly because the surface of the SSWN strip was specially prepared for the effluent.

In further tests, a mixture of phenacetin, caffeine, and aspirin (8.4 μg of each) was separated on a 10-μm ODS column with methanol/water (3:2) at 4 μl min^{-1}; a u.v. detector was placed before the deposition point. In this case, efficient evaporation required heating of the nitrogen stream to roughly 80° C. The u.v. and F.t.i.r. chromatograms are shown in Fig. 7. As can be seen, even with the high water content of the mobile phase, the F.t.i.r. chromatogram maintains the peak shape and resolution. The response obviously depends on the properties of the sample molecules, e.g., the sensitivity for phenacetin is about seven times higher than that for aspirin. An i.r. spectrum of phenacetin taken from a file used in Fig. 7 was compared with a spectrum obtained by depositing a phenacetin solution onto a KBr crystal directly without the column. There were some differences in the intensities of certain bands but the changes of bandwidths were less marked than those noted in Fig. 3.

Conclusion

The incompatibility between reversed-phase l.c. and F.t.i.r. seems to be largely overcome by the buffer-memory procedure with a SSWN substrate. Even with the substrate, the concept of the buffer-memory technique remains the same; continuous infrared chromatograms can be measured without interference from the mobile phase. The substrate serves as a sample collector, concentrator, infrared cell, and storage device. A major limitation on the technique is, at present, the rather severe dependence of the spectral intensities on the mobile-phase composition and difficulties with sensitivities. Work is in progress on these problems.

REFERENCES

1 D. W. Vidrine, in J. R. Ferraro and L. T. Basile (Eds.), Fourier Transform Infrared Spectroscopy, Vol. 2, Academic Press, New York, 1979, p. 129.
2 K. Jinno, C. Fujimoto and Y. Hirata, Appl. Spectrosc., 36 (1982) 67.
3 K. Jinno, C. Fujimoto and D. Ishii, J. Chromatogr., 239 (1982) 625.
4 C. Fujimoto, K. Jinno and Y. Hirata, J. Chromatogr., 258 (1983) 81.
5 D. Kuehl and P. R. Griffiths, J. Chromatogr. Sci., 17 (1979) 471.
6 D. T. Kuehl and P. R. Griffiths, Anal. Chem., 52 (1980) 1394.
7 C. M. Conroy, P. R. Griffiths and K. Jinno, Anal. Chem., 57 (1985) 822.
8 C. M. Conroy, P. R. Griffiths, P. J. Duff and L. V. Azarraga, Anal. Chem., 56 (1984) 2636.
9 K. S. Kalasinsky, J. T. McDonald, Jr. and V. F. Kalasinsky, in J. Christenson (Ed.), FT-IR Spectral Lines, Vol. 5, Nicolet Instrument Corp., Madison, WI, 1983, p. 14 (No. 1).
10 K. S. Kalasinsky, J. T. McDonald and V. F. Kalasinsky, paper presented at the Pittsburgh Conference on Analytical Chemistry and Applied Spectroscopy, Atlantic City, NJ, March, 1983, No. 357.
11 K. S. Kalasinsky, J. A. Smooter Smith and V. F. Kalasinsky, paper presented at the Pittsburgh Conference on Analytical Chemistry and Applied Spectroscopy, New Orleans, LA, February, 1985, No. 636.
12 T. Tsuda, K. Hibi, T. Nakanishi, T. Takeuchi and D. Ishii, J. Chromatogr., 158 (1978) 227.
13 Y. Hirata and M. Novotny, J. Chromatogr., 186 (1980) 521.
14 P. R. Griffiths and F. Block, Appl. Spectrosc., 27 (1973) 431.
15 S. S. T. King, J. Agric. Food Chem., 21 (1973) 526.

Analytica Chimica Acta, 178 (1985) 169—177
Elsevier Science Publishers B.V., Amsterdam — Printed in The Netherlands

HIGH-PERFORMANCE LIQUID CHROMATOGRAPHIC DETERMINATION OF NICKEL, COPPER AND ZINC AS THEIR TETRAPHENYLPORPHINE CHELATES

KOICHI SAITOH and NOBUO SUZUKI*

Department of Chemistry, Faculty of Science, Tohoku University, Sendai, Miyagi 980 (Japan)

(Received 21st June 1985)

SUMMARY

Nickel(II), copper(II) and zinc(II) ions are extracted from an aqueous solution into carbon tetrachloride as their diethyldithiocarbamate (DDC) chelates. The extract, after removal of the solvent, is treated with *meso*-tetraphenylporphine (TPP) in benzyl alcohol at 140° C for 60 min. Quantitative conversion of the DDC chelate to the TPP chelate is obtained over the range 0.25—4.5 μg of each metal by use of 3 μmol of TPP. The reaction mixture is analysed by reversed-phase high-performance liquid chromatography with spectrophotometric detection at 412 nm. Simultaneous determination of Cu and Zn in NBS bovine liver is possible by this procedure.

Porphyrins and their metal chelates generally have intense absorption bands in the visible region. The band at about 400 nm, which is called the Soret band, shows the most intense absorption; molar absorptivities of the order of 10^5 are often recorded. The Soret band is regarded as the band of choice for spectrophotometric determination of these compounds. If a porphyrin reacts easily with a metal ion, and quantitative formation of the metal porphyrin chelate occurs, the porphyrin must be useful as a sensitive spectrophotometric reagent for the metal. In most studies on the spectrophotometric determination of metals as their porphyrin chelates, the reagents used have been water-soluble porphyrins, such as *meso*-tetraphenylporphinetrisulfonic acid [1], *meso*-tetrakis(4-N-methylpyridyl)porphine [2], *meso*-tetrakis-(4-carboxyphenyl)porphine [3], *meso*-tetrakis(4-N-trimethylaminophenyl)-porphine [4] and *meso*-tetrakis(5-sulfothienyl)porphine [5].

There are two problems in utilizing a porphyrin for the spectrophotometric determination of metals; (1) the formation of the metal chelates is often not easily achieved; (2) the Soret bands of many of the metal chelates overlap so closely that simultaneous determination of different metals is rarely effective. At most two metals have so far been determined together by use of a water-soluble porphyrin as the spectrophotometric reagent, and this technique has only been applied practically for simple samples such as river water or tap water [1—5]. If the metal chelates formed could be separated sufficiently, the latter problem would be solved.

0003-2670/85/$03.30

Many porphyrins are available and are used in various fields of chemistry such as coordination chemistry and petroleum chemistry, but almost all these porphyrins are lipophilic and insoluble in water. If these porphyrins could be actively used for analytical purposes, more interesting applications including multi-element determinations would become available. It has already been reported that several metal chelates of lipophilic porphyrins can be separated by reversed-phase high-performance liquid chromatography (h.p.l.c.) [6, 7] and high-performance thin-layer chromatography [8—10]. If an easy means of forming the porphyrin chelates were available for some metals, any new procedure for determination of the metals must still couple the metal chelate formation with h.p.l.c. separation to be useful in practice.

In this paper, *meso*-tetraphenylporphine (TPP) is chosen; TPP is the most popular porphyrin applied so far and can easily be synthesized with high yield. Procedures are described for the quantitative formation of the TPP chelates of Ni(II), Cu(II) and Zn(II) and for the determination of these metals in an aqueous solution by means of h.p.l.c. The TPP reagent is quite insoluble in water but is slightly soluble in various organic solvents. This means that the metal/TPP chelate formation is simpler in an organic solution rather than in aqueous media. Chelation in an organic solution is achieved by using diethyldithiocarbamate (DDC) chelates as the metal carriers.

EXPERIMENTAL

Reagents

The TPP reagent was prepared by the method of Adler et al. [11], followed by purification as described by Barnett et al. [12]. Sodium diethyldithiocarbamate (NaDDC) was of analytical-reagent grade (Wako Pure Chemicals). Stock solutions of Ni(II), Cu(II) and Zn(II) (1000 mg l^{-1}) were prepared by dissolving the corresponding metals (purity $\geqslant$99.99%) in diluted nitric acid. The TPP chelates of Ni(II), Cu(II) and Zn(II) (hereafter NiTPP, CuTPP, and ZnTPP, respectively) were prepared by reaction of the corresponding chloride with TPP in refluxing *N,N*-dimethylformamide [13], followed by purification on an alumina column. The metal DDC chelates tested were prepared by extraction from aqueous solutions containing the metal ions into carbon tetrachloride with NaDDC as the extractant. Double-distilled water was used throughout. All other reagents and solvents were of analytical-reagent grade.

Chromatography

The h.p.l.c. system used consisted of a Hitachi Model 655-15 liquid chromatographic pump, a Rheodyne 7125 sample injection valve with a 5-μl sample loop, a home-made variable-wavelength u.v.-visible detector with an 8-μl flow cell, and a Shimadzu CR-1A data processor. The column used was a 4.0 mm $\times$ 25 cm LiChrosorb RP-18 (7 μm) pre-packed column (Merck).

The mobile phase used was a mixture of acetone and acetonitrile at a volume ratio of 40:60. The flow rate was 1.3 ml min^{-1}. The detection

wavelength and the spectral bandpass of the detector were set at 412 nm and 2 nm, respectively.

Typical procedure

Step 1: Extraction of metal DDC chelates. In a 50-ml shaking tube, take about 10 ml of sample solution containing a total of $\gtrsim 50$ μg of nickel, copper and zinc ions. Add 5 ml of 20% (w/v) ammonium citrate solution, 2 drops of 0.1% cresol red in ethanol, and aqueous ammonia (1 + 1) until the solution changes to red (pH 8.8—9.1). Dilute the solution to 20 ml with water, and finally add 1 ml of aqueous 1% (w/v) NaDDC solution. Shake the resulting solution with 10 ml of carbon tetrachloride for 10 min at 350 strokes/min. After centrifugation at 2000 rpm for 5 min, wash the organic phase with 100 ml of water in a 200-ml separatory funnel. Remove the organic phase as the final extract to be used.

Step 2: Conversion to TPP chelates. Transfer a 1-ml aliquot (or more if necessary) of the above extract, i.e., the carbon tetrachloride solution containing the metal/DDC chelate(s), to a 10-ml volumetric flask. Put the flask in a hole in a heating duralumin block regulated at 140°C (reaction temperature), and evaporate the solvent with the aid of a nitrogen stream. Add 1 ml of benzyl alcohol and 1 ml of 2×10^{-3} mol l^{-1} TPP in benzene. Keep the flask at the reaction temperature for 10 min (preliminary heating). After the addition of a further 2 ml of benzyl alcohol to the flask, maintain the contents at the same temperature for 60 min (main heating time).

Step 3: H.p.l.c. After cooling the contents of the flask to room temperature, dilute the solution to 10 ml by addition of benzene. Submit the solution to h.p.l.c. (sample injection, 5 μl). Measure the heights or areas of the chromatographic peaks corresponding to the metal/TPP chelates. Calculate the concentration of the metal ion in the original sample solution by comparing the peak height (or area) of the chelate derived from the sample with that derived by the same procedure from a standard of known metal concentration.

Procedure for conversion studies

An aqueous solution of the metal was prepared at a concentration of 10 mg l^{-1}, just prior to the following procedures, by dilution of the 1000-mg l^{-1} stock solution of the metal. A carbon tetrachloride solution of a metal/DDC chelate at a known concentration was prepared by transferring the desired quantity of the 10 mg l^{-1} solution of the metal ion to be tested to the shaking tube, and extracting the metal into 10 ml of carbon tetrachloride as outlined above (step 1) except for the use of water instead of the ammonium citrate solution and also the omission of the washing of extract with water. The required volume of the carbon tetrachloride extract was transferred to a 10-ml volumetric flask and the conversion was examined at various heating temperatures for different times of the main heating. After the general treatment for making up the reaction mixture, h.p.l.c. was applied as outlined above. The percentage conversion was calculated by comparing the peak

height (or area) obtained for the metal/TPP chelate with that obtained by dissolving a known amount of the pure metal/TPP chelate in benzene and chromatographing directly.

RESULTS AND DISCUSSION

The scheme for the determination of metals has two essential points: quantitative derivation of the metal/TPP chelates at the microgram level, and separation and measurement of the metal chelates within a short time. Reversed-phase h.p.l.c. is known to be a promising technique for the separation of several metal/TPP chelates [6]. Accordingly, the most urgent need was to establish a suitable procedure for the preparation of these chelates. Several methods are available for the preparation of metal porphyrin chelates [14]. These are useful on a preparative scale rather than an analytical scale. A large excess of metal carrier (e.g., chloride [13]) is normally used for the reaction with a porphyrin. The quantitative nature of the reaction has been little studied.

The TPP reagent is quite insoluble in water but slightly soluble in various organic solvents (e.g., about 3×10^{-3} mol l^{-1} and about 4×10^{-4} mol l^{-1} in benzene and benzyl alcohol, respectively). Accordingly, reaction of a metal ion with TPP is more viable in an organic solution rather than in an aqueous solution, but the metal ions in the aqueous sample solution must first be transferred to an organic phase. This can be done by use of a DDC extraction prior to the conversion reaction to the TPP chelates for nickel, copper and zinc ions. The organic phase is carbon tetrachloride in the first step and benzyl alcohol in the second step.

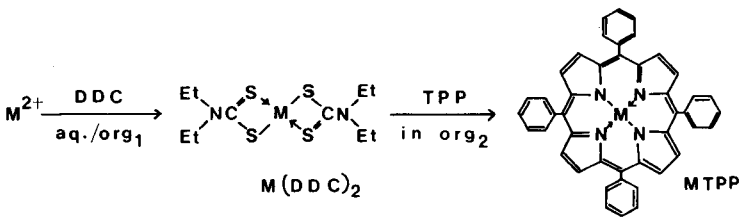

Extraction

For the extraction of the metal ions NaDDC was chosen as the chelating reagent primarily because it is a popular reagent for the liquid-liquid extraction of metals and because many metal/DDC chelates can be extracted into a non-polar solvent such as carbon tetrachloride without auxiliary reagents. Further, a large amount of useful extraction data is available for choosing appropriate conditions for the extraction [15—17].

Initially, the extractions were examined without either the addition of ammonium citrate to the aqueous phase or washing of the organic phase after separation from the aqueous phase. Nickel, copper and zinc were

quantitatively extracted as their DDC chelates from the aqueous phase at pH 8.8—9.1 into carbon tetrachloride. However, when the DDC extraction was applied to a sample solution containing quite large amounts of iron(III) and manganese(II), the extracted Fe and Mn chelates interfered with the quantitative conversion of the DDC chelates of Ni, Cu and Zn DDC to the TPP chelates. The addition of ammonium citrate to the aqueous phase [15, 16] effectively masked Fe(III) and Mn(II) in the extraction; the percentage extraction was lowered to less than 5% for Fe(III) and to about 60% for Mn(II). The percentage extraction for manganese was lowered to about 5% after subsequent back-washing of the carbon tetrachloride phase with 10-times its volume of water.

Conversion studies

The feasibility of the DDC-to-TPP chelate conversion method was surveyed for various metal ions including Mn(II), Fe(III), Co(II), Ni(II), Cu(II), Zn(II), Pd(II), Cd(II), Hg(II), Pb(II) and Bi(III). It was found that the TPP chelates of Ni(II), Cu(II) and Zn(II) could be derived from the respective DDC chelates and then measured by h.p.l.c. The h.p.l.c. peaks observed were assigned unambiguously to these TPP chelates, by recording the spectra of the column effluent with a rapid-scanning u.v.-visible absorption detector [18] as well as by comparing their retention times with those of the corresponding pure metal/TPP chelates. The h.p.l.c. peaks of the TPP chelates were not observed, within a 60-min run, for metal ions other than Ni, Cu and Zn, even when the DDC-to-TPP chelate conversions were attempted for those metal ions under vigorous conditions, e.g., at 160°C for 90 min. The conversion studies described below relate to Ni, Cu and Zn only.

The extent of the conversion depended on the reaction temperature and on the reaction time (the main heating period). When the reaction time was fixed at 60 min, the percentage conversion for Ni(II), Cu(II) and Zn(II) (2 μg of each) varied with the reaction temperature as shown in Fig. 1. When the reaction temperature was fixed at 120 or 140°C, the percentage conversion changed with the reaction time, as shown in Fig. 2. It is clear from these figures that quantitative formation of NiTPP is less easily attained than those of CuTPP and ZnTPP. The reaction at 140°C for 60 min is recommended for simultaneous conversion of the three metals.

The reproducibility of the conversion was examined for the treatment of a 1-ml aliquot of the carbon tetrachloride solution containing 2 μg of the metal as its DDC chelate. The results for the Ni(II), Cu(II) and Zn(II) systems are summarized in Table 1. The linearity of the conversion was examined for the Ni(II), Cu(II) and Zn(II) systems, and was found to be satisfactory in the range from 0.25 μg to at least 4.5 μg of each metal treated.

The feasibility of simultaneous conversion for Ni(II), Cu(II) and Zn(II) was examined as follows. A mixture of the DDC chelates of Ni(II), Cu(II) and Zn(II) in a mole ratio of 1.00:1.13:1.00 was treated by the conversion procedure under typical conditions (reaction at 140°C for 60 min), except

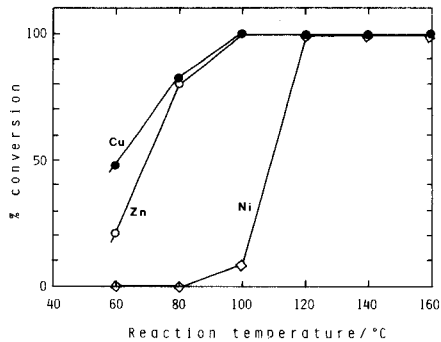

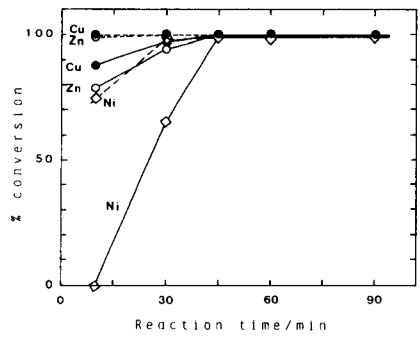

Fig. 1. Percentage conversion vs. reaction temperature plots: (◇) Ni(II); (•) Cu(II); (○) Zn(II). Amount of metal, 2 μg for each; reaction time, 60 min.

Fig. 2. Percentage conversion vs. reaction time plots for Ni(II), Cu(II) and Zn(II) at two reaction temperatures: (——) 120°C; (———) 140°C. Metal: (•) Cu; (○) Zn; (◇) Ni. Amount of metal, 2 μg in each case.

TABLE 1

Reproducibility of the DDC-to-TPP chelate conversion[a]

Run	Conversion (%)		
	Ni	Cu	Zn
1	98	100	101
2	100	98	98
3	100	104	98
4	93	102	99
Mean	97.8	101.0	99.0
RSD (%)[b]	3.4	2.6	1.4

[a]The metal (2 μg) as its DDC chelate was allowed to react with TPP at 140°C for 60 min.
[b]Relative standard deviation.

that the amount of TPP used was 1.2 μmol for convenience (the quantity of TPP used in the recommended procedure in the experimental section was 3 μmol). The reaction mixture was subjected to h.p.l.c. to determine the quantities of unreacted TPP and the metal/TPP chelates produced. The percentage reaction of TPP was calculated from the equation

$$\text{Reaction (\%)} = 100 \times (Q^0_{TPP} - Q_{TPP})/Q^0_{TPP}$$

where Q^0_{TPP} and Q_{TPP} are the total quantity (in mol) of TPP and the quantity (in mol) of unreacted TPP, respectively. The percentage reaction of TPP varied with the mole ratio of the total quantity of metals (Q^0_M) to Q^0_{TPP}, as shown in Fig. 3. When the Q^0_M/Q^0_{TPP} mole ratio was smaller than about 0.7, the percentage reaction of TPP increased proportionally to the amount of the metals to be reacted. The percentage conversion for each metal is also plotted against the Q^0_M/Q^0_{TPP} ratio in Fig. 3. A significant decrease in the per-

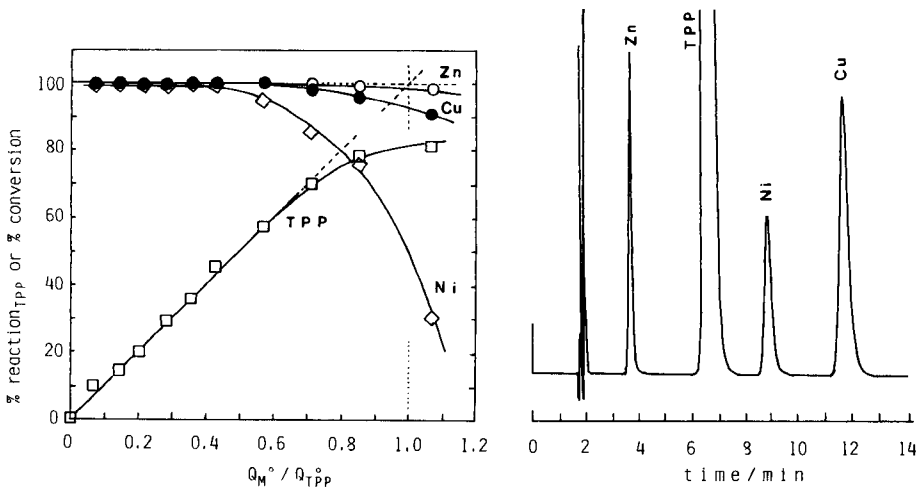

Fig. 3. Percentage reaction for TPP and percentage conversion for Ni, Cu and Zn plotted against the Q_M^0/Q_{TPP}^0 ratio in the simultaneous conversion system. Curves: (□) TPP; (●) Cu; (○) Zn; (◇) Ni. The Ni/Cu/Zn mole ratio was 1.00:1.13:1.00; Q_{TPP}^0 = 1.2 μmol; reaction at 140° C for 60 min.

Fig. 4. H.p.l.c. separation of Ni, Cu and Zn as their TPP chelates. The injected sample (4 μl) contained each metal at 0.2 μg ml^{-1}. Column, LiChrosorb RP-18 (7 μm), 250 mm × 4-mm i.d.; mobile phase, acetone/acetonitrile (40:60 v/v) at 1.3 ml min^{-1}; detection at 412 nm.

centage conversion is found for Ni(II) when the Q_M^0/Q_{TPP}^0 ratio is larger than about 0.5. This tendency is not observed for Zn(II), even when the Q_M^0/Q_{TPP}^0 ratio is about 1.0. According to the above results, the permissible upper limit of the Q_M^0/Q_{TPP}^0 ratio for the simultaneous conversion for Ni(II), Cu(II) and Zn(II) is about 0.5, if the quantities of these metals are almost the same.

Separation by h.p.l.c.

Figure 4 shows a chromatogram for the separation of TPP and its Ni(II), Cu(II) and Zn(II) chelates which were prepared from these metal ions in an aqueous solution. The metal ions (5 μg of each) were extracted as their DDC chelates from an aqueous solution into 10 ml of carbon tetrachloride, and then a 4-ml aliquot of the extract was used in the conversion procedure to form the TPP chelates. The TPP chelates were eluted in the following order of retention times: ZnTPP < TPP < NiTPP < CuTPP. The wavelengths of maximum absorption recorded for TPP, NiTPP, CuTPP and ZnTPP in the acetone/acetonitrile (40:60 v/v) used as the mobile phase were 415, 411, 412 and 421 nm, respectively. In consideration of the sharp chromatographic peak of ZnTPP compared to NiTPP and CuTPP, the detection wavelength was conveniently set at 412 nm. When the zinc content of a sample is considerably smaller than the nickel and copper contents, a rather longer wavelength is recommended.

TABLE 2

Determination of nickel, copper and zinc in NBS SRM 1577 bovine liver by h.p.l.c. after conversion to their TPP chelates

Sample taken (mg)	Metal content found ($\mu g\ g^{-1}$)		
	Ni	Cu	Zn
285	ND[a]	180	137
	ND	184	138
298	ND	193	137
	ND	186	138
296	ND	195	131
Mean	ND	188	136
NBS values	—	193 ± 10	130 ± 10
Literature [19]	0.4 ± 0.4	189 ± 21	132 ± 10

[a]Not detected on the chromatogram.

Application to NBS bovine liver

The NBS bovine liver standard (SRM 1577) was dried by lyophilization for 24 h in preference to heating. About 290 mg of the bovine liver sample was treated with nitric acid for 22 h on a hot plate at 120° C. The resulting solution was evaporated to dryness and then taken into solution with 25 ml of 0.1 mol l^{-1} hydrochloric acid. A 10-ml aliquot of this solution was used for the extraction procedure with DDC, followed by the conversion to the TPP chelate and h.p.l.c. as outlined in the experimental section; a 1-ml aliquot of the carbon tetrachloride extract was used in the conversion step. To prepare a calibration curve, aqueous solutions with known metal contents were taken through the entire procedure.

The results are shown in Table 2. The nickel content of the bovine liver sample could not be determined but the copper and zinc contents obtained were in fair agreement with the NBS and literature [19] values.

Conclusion

The new h.p.l.c. method for the determination of Ni, Cu and Zn is based on the use of TPP as the chelating reagent. The TPP chelates of these metals are sufficiently stable for h.p.l.c. separation and are sensitively detected at about 412 nm. The extraction step with DDC not only facilitates the metal/TPP chelate formation but also pre-separates the metals of interest from a complicated actual sample.

Financial support by the Ministry of Education, Science and Culture (Grant-in-Aid for Scientific Research 58 470 027) is gratefully acknowledged.

REFERENCES

1 J. Itoh, T. Yotsuyanagi and K. Aomura, Anal. Chim. Acta, 74 (1975) 53.
2 H. Ishii and H. Koh, Bunseki Kagaku, 28 (1979) 474.
3 H. Ishii and H. Koh, Talanta, 24 (1977) 317.
4 T. Makino and J. Itoh, Clin. Chim. Acta, 111 (1981) 1.
5 S. Igarashi, T. Saeki and T. Yotsuyanagi, Bunseki Kagaku, 32 (1983) 39.
6 K. Saitoh, M. Kobayashi and N. Suzuki, J. Chromatogr., 243 (1982) 291.
7 M. Kobayashi, K. Saitoh and N. Suzuki, Chromatographia, 20 (1985) 72.
8 K. Saitoh, M. Kobayashi and N. Suzuki, Anal. Chem., 53 (1981) 2309.
9 M. Kobayashi, K. Saitoh and N. Suzuki, Chromatographia, 18 (1984) 441; 20 (1985) 49.
10 S. Miyake, K. Saitoh and N. Suzuki, Chromatographia, 20 (1985) 417.
11 A. D. Adler, F. R. Longo, J. D. Finavilli, J. Goldmacher, J. Assour and L. Korsakiff, J. Org. Chem., 32 (1967) 476.
12 G. H. Barnett, M. F. Hudson and K. M. Smith, J. Chem. Soc., Perkin Trans. I: (1975) 1401.
13 A. D. Adler, F. R. Longo, F. Kampas and J. Kim, J. Inorg. Nucl. Chem., 32 (1970) 2443.
14 J. W. Buchler, in D. Dolphin (Ed.), The Porphyrins, Vol. 10, Academic Press, New York, 1978, Chap. 10.
15 H. Bode, Fresenius' Z. Anal. Chem., 143 (1954) 182.
16 J. Stary and K. Kratzer, Anal. Chim. Acta, 40 (1968) 93.
17 N. Suzuki, K. Saitoh and H. Watarai, Bunseki Kagaku, 33 (1984) T52.
18 K. Saitoh and N. Suzuki, Anal. Chem., 51 (1979) 1683.
19 E. S. Gladney, Anal. Chim. Acta, 118 (1980) 385.

Analytica Chimica Acta, 178 (1985) 179—188
Elsevier Science Publishers B.V., Amsterdam — Printed in The Netherlands

CHARACTERIZATION OF MICELLAR MOBILE PHASES FOR REVERSED-PHASE CHROMATOGRAPHY

JOHN S. LANDY[a] and JOHN G. DORSEY*
Department of Chemistry, University of Florida, Gainesville, FL 32611 (U.S.A.)
(Received 6th June 1985)

SUMMARY

Cationic, anionic, and nonionic surfactants are characterized for their usefulness as micellar mobile phases in reversed-phase chromatography. Conditions found previously to provide optimum chromatographic efficiency for sodium dodecyl sulfate also provide high efficiency for the cationic and nonionic surfactants studied. The use of 3% n-propanol in the micellar mobile phase and column temperatures of 40°C appear to offer a broadly applicable solution to the low efficiency previously reported for micellar mobile phases. A chromatographic method for the determination of critical micelle concentrations is reported; it compares favorably with literature methods. Micellar mobile phases are shown to mimic ion-pairing mobile phases, allowing the separation of neutral solutes as well as solutes charged oppositely to the surfactant and offer a more rugged method of analysis than hydro-organic ion-pairing methods.

The micellization of surfactant solutions has been heavily studied for many years [1]. However, only recently have many analytical chemists become aware of the effect micellar solutions can have on the determination of many solutes [2]. Since the first report by Armstrong and Henry [3], interest in micellar mobile phases for reversed-phase liquid chromatography has grown rapidly, and unusual advantages are now moving these systems from laboratory curiosity to practical utility.

From the first report, the advantages of enhanced selectivity, low cost and low toxicity have been promulgated. Indeed, enhanced selectivity can come both from the actual separation [4, 5], and also from unusual detection schemes. Micellar mobile phases have been shown to increase fluorescent quantum efficiencies, thereby lowering limits of detection, and also to allow room-temperature, liquid-phase phosphorescence [6, 7].

More compelling arguments for the use of these mobile phases have been made recently. Arunyanart and Cline Love [8] have developed equations relating capacity factor to micellar mobile phase concentration which allow calculation of the equilibrium constant for the solute between the bulk aqueous phase and micellar aggregate. More importantly, if the equilibrium

[a]Present address: Revlon Health Care Group, 1 Scarsdale Road, Tuckahoe, NY 10707, U.S.A.

0003-2670/85/$03.30

constant is available from independent methods, the equations can accurately predict the chromatographic capacity factor at zero or greater micelle concentration in the mobile phase. This means that for the first time spectroscopic measurements can accurately predict chromatographic retention, a goal not yet realized for hydro-organic mobile phases.

A dramatic chromatographic advantage of these mobile phase systems has also been shown for gradient elution techniques [9, 10]. An unusual property of micellar solutions is that there is always an approximately constant amount of free surfactant present in solution, and any change in total surfactant concentration serves only to change the concentration of micelles. This means that a micelle concentration gradient can be run without altering the composition of the stationary phase, so no column re-equilibration is necessary before the next injection. This property of micellar solutions is also a major factor in improving the compatibility of electrochemical detection with gradient elution techniques [10, 11].

Micellar mobile phases are also finding use for fundamental study of both micelles themselves, and also for micelle/solute interactions [12, 13]. Thus, micellar chromatography is an exceedingly information-rich technique which can be exploited for both fundamental and analytical purposes.

Along with the fundamental chromatographic advantages, these mobile phases are proving to be useful for a wide range of important sample types. Any compound which will partition to a micellar aggregate is capable of being eluted from a chromatographic column with these mobile phases. Virtually all organic compounds are then amenable to this technique, and the chromatographic advantages previously discussed become available. Furthermore, Mullins and Kirkbright [14] have demonstrated the determination of inorganic anions on a C_{18} column, thus providing a rational alternative to ion chromatography. Kirkman et al. [15] have shown the usefulness of micellar mobile phases for the separation of metallo-organic compounds, including the capability of separating both neutral and charged complexes in the same chromatogram.

One of the early problems with micellar mobile phases was rather poor chromatographic efficiency. This inefficiency was shown to be caused by slow mass transfer which comes principally from poor wetting of the stationary phase by a purely aqueous micellar mobile phase [16]. The addition of 3% n-propanol to the mobile phase and column temperatures of 40°C improve mass transfer to the point that plate heights are similar to those found with hydro-organic mobile phases [16].

This work extends the efficiency optimization scheme to both cationic and nonionic surfactants, classes of compounds heretofore not investigated. A chromatographic method for determination of critical micelle concentration (c.m.c.) values is presented; results for all three surfactants compare favorably to literature values. Also, selectivity differences for selected solutes are noted among the three surfactants investigated.

EXPERIMENTAL

An Altex (Berkeley, CA) Model 322 gradient liquid chromatograph incorporating two Model 100A pumps, a model 210 sample injection valve with a 5-μl loop, and a model 153 detector (254 nm) with an 8-μl flow cell was used. The columns used were Altex Ultrasphere ODS (4.6 × 250 and 4.6 × 150 mm) and were water jacketed and thermostated at 40°C with a Techne (Princeton, NJ) TE-7 circulator. A thermostated silica pre-column was used before the injector to saturate the mobile phase with silicates and to equilibrate the mobile phase thermally before it reached the analytical column. To avoid such problems as precipitation, incomplete removal of adsorbed surfactant from the stationary phase and possible mixed retention mechanisms, a separate column was dedicated for each different surfactant mobile phase.

Acetophenone, nitrobenzene (Fisher Scientific), phenol, benzene, anilinium chloride, sodium benzoate, and toluene (Mallinckrodt) were reagent grade and were dissolved in chromatographic-grade methanol (Fisher Scientific). n-Propanol was reagent grade (Fisher Scientific). Surfactants used were sodium dodecyl sulfate (SDS) (puriss. grade), hexadecyltrimethylammonium bromide (CTAB) (purum grade) and Brij-35, polyoxyethylene lauryl ether (practical grade); all were from Fluka Chemical and were used as received. Deionized water was from a Barnstead Nanopure system (Boston, MA) and was further irradiated for 24 h by ultraviolet light in a Photronix Model 816 HPLC reservoir (Medway, MA). The appropriate weight of surfactant was dissolved in 97:3 water/propanol and the solution was filtered through a 0.45-μm Nylon-66 membrane filter (Rainin Instruments, Woburn, MA).

All capacity-factor and plate-count values are averages of at least duplicate determinations. Efficiency (number of theoretical plates, N) was evaluated by using an equation which corrects for the asymmetry of skewed peaks [17]:

$$N = 41.7\ (t_R/W_{0.1})^2/(B/A + 1.25) \quad (1)$$

where t_R is the retention time, $W_{0.1}$ is the peak width at 10% peak height, and B/A is the asymmetry ratio measured at 10% peak height. This equation was recently found to be the most accurate manual method of calculation of column efficiency [18].

The reduced plate height was calculated from $h = H/d_p$, where H is the plate height ($H = L/N$), L is the column length, and d_p is the particle diameter of the stationary phase.

RESULTS AND DISCUSSION

Efficiency

There has been some disagreement in published work about the efficiency achievable with micellar mobile phases, and about schemes to improve the

inherently low efficiency obtained. Dorsey et al. [16] were the first to address this problem, and showed through the use of Knox plots that the primary source of inefficiency in purely aqueous micellar mobile phases is slow mass transfer, arising from poor wetting of the hydrophobic stationary phase by a purely aqueous mobile phase. This can be overcome by the addition of 3% n-propanol to the mobile phase and using column temperatures of 40°C.

Yarmchuk et al. [19] reported a similar study and also suggested higher operating temperatures, but not organic modifiers, to improve slow mass transfer. The major difference in this work was that a C_1 (methyl) stationary phase was used, and the serious wetting problem found with C_8 and C_{18} stationary phases did not exist. They found that addition of small amounts of organic modifier would displace adsorbed surfactant and have a large effect on retention, while not improving efficiency significantly. They showed that poor efficiency can also arise from slow exit rates of solutes from the micellar aggregate, and with weakly polar stationary phases this is the dominant problem.

Kirkman et al. [15] attempted to improve efficiency by adding 5% methanol to an SDS micellar mobile phase; however, they did not report any improvements in efficiency. While this work was on a nitrile bonded phase, and methanol may have some effect for this weakly polar stationary phase, methanol is not effective for C_8 or C_{18} phases [16].

That the significant problem is wetting of the stationary phase has recently been confirmed by Foley and May [20]. In a study of optimization of pH for the separation of weak organic acids on hydrophobic stationary phases, they studied column efficiencies with purely aqueous (non-micellar) mobile phases and investigated adding small amounts of methanol, ethanol, n-propanol, and acetonitrile as a means of improving efficiency. They found that n-propanol was by far the most effective organic solvent, with 3—6% (v/v) improving chromatographic efficiencies by factors of 10—15, which approached the efficiencies obtained with traditional hydro-organic mobile phases. Furthermore, they observed only slight improvements with the other solvents. This is consistent with previous findings that methanol, ethanol and acetonitrile are ineffective at increasing the efficiency of micellar mobile phases [16]. Scott and Simpson [21] studied modification of C_{18} phases by organic modifiers and showed that over 90% of the surface is covered with the alcohol at a concentration of 3% (w/v) propanol, but there is only about 50% coverage with the same concentration of methanol. This coating of the hydrophobic surface (and solvation of the stationary phase chains) with a solvent of intermediate polarity then must serve as a phase transfer catalyst for the transfer of solutes from the mobile to stationary phase. While SDS and all surfactants will themselves adsorb on a hydrophobic stationary phase, thus technically "wetting" the phase, they do not solvate the stationary phase chains, and are then also ineffective at improving efficiency.

TABLE 1

Variation of efficiency and asymmetry with propanol concentration[a]

Propanol (%)	N m^{-1}	B/A	k'	Propanol (%)	N m^{-1}	B/A	k'
0	36 000	1.62	23.8	4	61 000	1.00	16.9
1	56 000	1.15	21.3	6	60 000	1.01	14.9
2	57 000	1.03	19.6	8	59 000	1.01	13.2
3	58 000	1.02	18.2	10	61 000	1.01	11.7

[a]250 × 4.6 mm Ultrasphere ODS, mobile phase 5 × 10^{-2} M SDS, 40°C, benzene solute.

Table 1 shows the plate count in plates per meter, asymmetry factor, and capacity factor for benzene in a mobile phase of 5 × 10^{-2} M SDS at 40°C as the n-propanol concentration is varied from 0 to 10%. Several factors are apparent. First, temperature alone is not sufficient to overcome the mass-transfer problem with very hydrophobic stationary phases. Secondly, there is no significant improvement in either efficiency or asymmetry above 2% propanol, and it is clear that the efficiency is not dependent on k', as has been incorrectly argued. For the propanol concentrations of 3—10% the average plate count is 59 800, with a standard deviation (s) of 1300, or 2.2%, which is within the precision limits of these manual plate count methods [17]. Finally, the small amounts of propanol needed do affect the capacity factor to a small extent, but are certainly not deleterious to overall retention.

Yarmchuk et al. [19] have shown that the exit rate of solutes from micelles becomes slower as the hydrophobicity of the solute increases. This means that for a wide range of solute polarities, the chromatographic efficiency would decrease with increasing hydrophobicity. It is likely, however, that the small amount of propanol necessary for wetting of the stationary phase also changes the micelle structure and thereby increases the exit rates of solutes, thus lessening this other source of slow mass transfer. This possibility is presently being investigated.

Table 2 shows the efficiency data in plates per meter for all three surfactants used throughout this study with the "SDS efficiency-optimized" conditions (3% n-propanol and 40°C). Data obtained without propanol

TABLE 2

Efficiency data vs. surfactant for "optimized" conditions[a]

Column	Propanol (%)	Surfactant	h	L (cm)	N m^{-1}	B/A
1	0	5 × 10^{-2} M SDS	5.5	25	36 000	1.62
1	3	5 × 10^{-2} M SDS	3.4	25	58 000	1.02
2	3	5 × 10^{-2} M Brij-35	4.1	15	48 000	1.03
3	3	5 × 10^{-2} M CTAB	4.1	15	49 000	1.04

[a]Altex Ultrasphere ODS, 40°C, benzene solute.

present are included to show the improvement in the reduced plate height with 3% n-propanol. Both the nonionic surfactant (Brij-35) and the cationic surfactant (CTAB) show low reduced plate heights, indicating good mass transfer, and showing that the efficiency optimization scheme [16] appears to be a broadly-based solution for micellar mobile phases of any surfactant. This means that the surfactant type can be varied to affect separational selectivity with no loss in column efficiency. To illustrate the efficiencies and separations possible with the optimized conditions, Fig. 1 shows separations of a five-component test mixture using the three different surfactants. Interestingly, the elution order of phenol and acetophenone reverses with a CTAB mobile phase, as compared to SDS and Brij-35. This is an example of the useful selectivity differences possible from changing surfactant type. Here the weakly acidic phenol (pK_a 9.9) is likely electrostatically attracted to the CTAB adsorbed on the stationary phase, thus increasing its retention. Selectivity differences from changing surfactant type have been addressed in detail by Yarmchuk et al. [4].

Determinations of c.m.c.

For any aqueous surfactant solution there is a relatively small range of concentration below which virtually all surfactant is present as monomers,

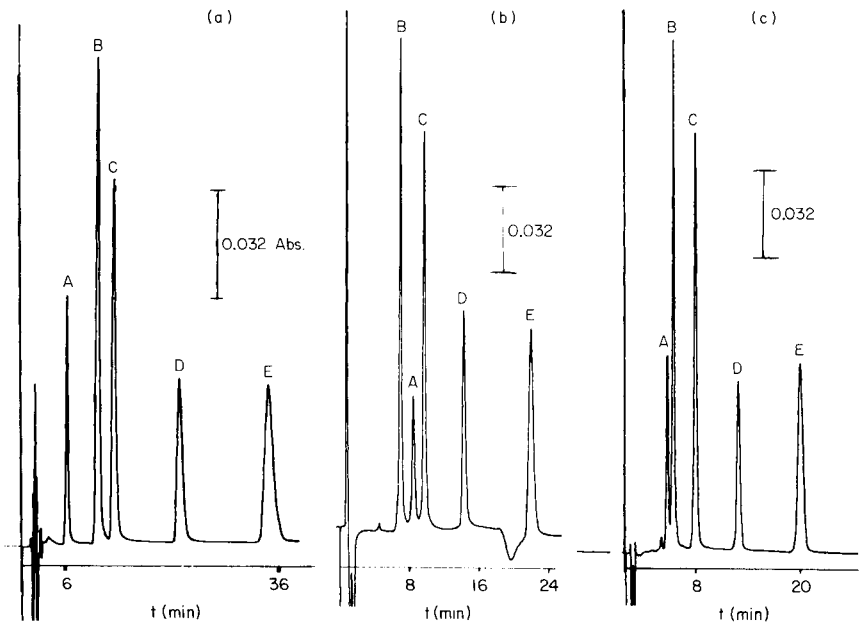

Fig. 1. Chromatograms of five-component test mixture. Conditions: Ultrasphere ODS (25 cm for SDS, 15 cm for CTAB and Brij-35), mobile phase 3:97 n-propanol/water with surfactant added, flow rate 1.5 ml min^{-1}. Surfactant added: (a) 0.1 M SDS; (b) 0.05 M CTAB; (c) 0.05 M Brij-35. Solutes: (A) phenol; (B) acetophenone; (C) nitrobenzene; (D) benzene; (E) toluene.

and above which virtually all additional surfactant is present in micellar form. This micellization phenomenon causes significant changes in bulk physical properties of the solution. The determination of the c.m.c. then involves the measurement of some property of the surfactant solution as a function of concentration, and the c.m.c. is taken as the point of intersection of the extrapolated segments of the measured property at concentrations both below and above the c.m.c. The c.m.c. value can also be determined chromatographically, using the capacity factor, k', of a neutral solute that associates strongly with the micelles as the measured property. Figure 2 shows plots of log k' vs. log surfactant concentration for the solutes phenol, acetophenone, nitrobenzene and benzene for the three surfactants used in this work, all under the efficiency-optimized conditions of 3:97 n-propanol/water. Figure 2(a) (SDS) also includes anilinium chloride (pK_b 9.4), and Fig. 2(b) (CTAB) includes sodium benzoate (pK_a 4.2). The dramatic change in retention as micellization occurs is quite obvious. Values of c.m.c. for all three surfactants were calculated from these plots (using nitrobenzene and benzene solutes) by extrapolation of the linear regression lines both below and above the apparent c.m.c. These results are presented in Table 3 and compared to literature values and in the case of SDS to a conductimetric value obtained in this laboratory [11]. The good agreement of the chromatographic and literature values for three different surfactants is evidence that it is truly solubilization of the solutes by the micelles, and not surface-tension effects, as suggested by others, that causes elution at high surfactant concentrations. The small differences that are observed are probably due to temperature differences and to the 3% propanol present in the chromatographic determinations. Both temperature and added solvents can affect the c.m.c., the aggregation number, and the actual structure of the micellar assembly. Furthermore, the necessity of having a solute residing in (or on) the micelle for the chromatographic determination will likely affect the c.m.c. value slightly. However, this offers the possibility of simultaneously studying the effects of various solutes on micellization because of the separation provided by the chromatographic column.

Selectivity

One of the major differences between hydro-organic and micellar mobile phases is in the selectivity of separation. The choice of surfactant gives added control of selectivity, primarily through electrostatic interactions, while the concentration controls the strength of the mobile phase. With electrostatic interactions playing a major role in the selectivity, it is important to specify the pH of the mobile phases. The measured pH of a 0.1 M SDS solution is 6.1 and that of 0.5 M CTAB is 4.2. These pH values can obviously be changed by the use of appropriate buffers, and this provides another means of controlling selectivity.

Changing the surfactant type from cationic, to anionic, to nonionic greatly affects the retention of ionizable and ionic compounds. Figure 2(a)

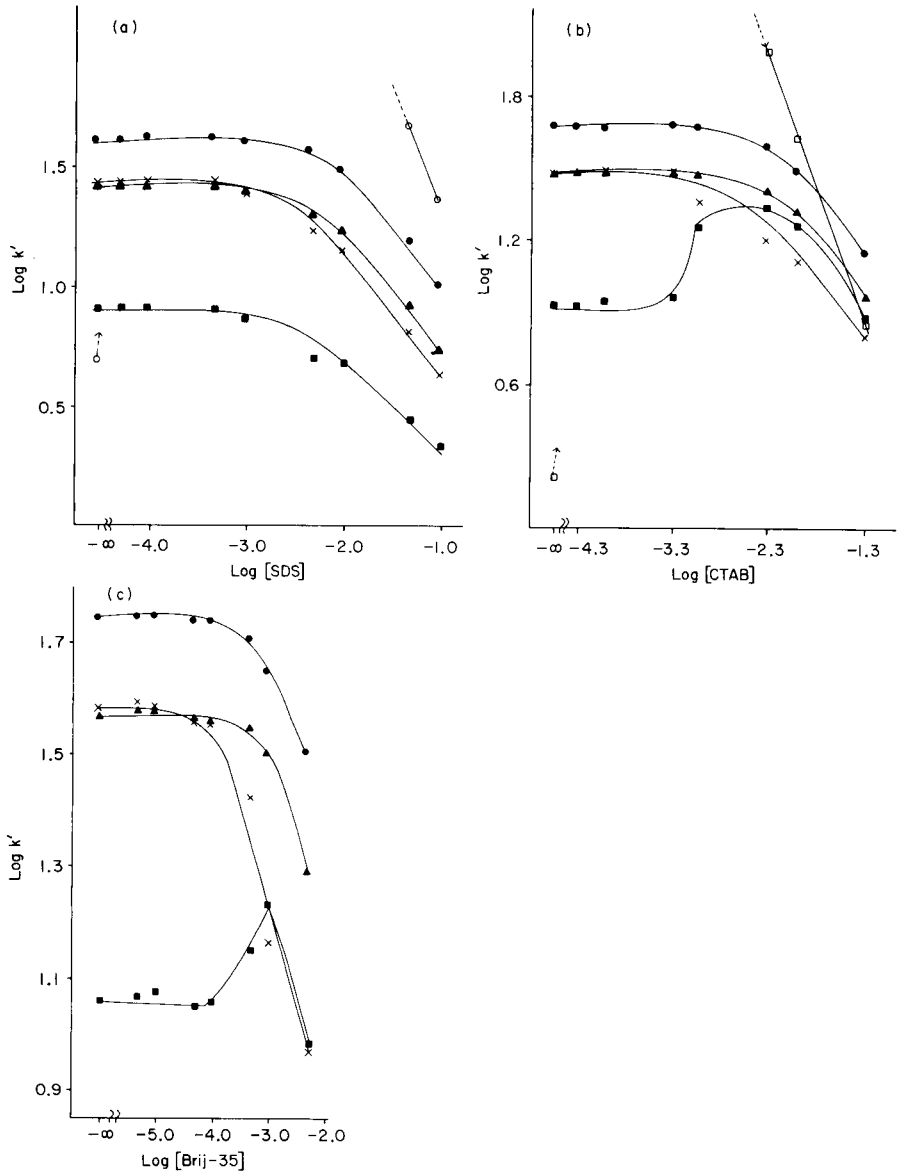

Fig. 2. Log k' vs. log [surfactant]. Surfactant: (a) SDS; (b) CTAB; (c) Brij-35. Solutes: (•) benzene; (▲) nitrobenzene; (×) acetophenone; (■) phenol; (○) anilinium chloride in (a) only; (□) sodium benzoate in (b) only. Conditions: Ultrasphere ODS columns, mobile phase and flow rate as in Fig. 1.

and (b) show the behavior of both neutral solutes and solutes oppositely charged to the surfactant. At zero surfactant concentration, the neutral solutes are strongly retained, as there is neither organic modifier nor micelles

TABLE 3

Critical micelle concentrations

Surfactant	C.m.c. (10^{-3} M)	
	Chromatographic method[a]	Literature
SDS	4.7	8.1 [2] 7.3[b] [11]
CTAB	3.6	1.3 [2]
Brij-35	0.34	0.1 [2]

[a]Average of nitrobenzene and benzene solutes, 40°C, 3:97 n-propanol/water. [b]30°C, 3:97 n-propanol/water.

present to cause their elution. However, there is little retention of the ionic compounds, as the charged site prevents their retention by the hydrophobic stationary phase. At surfactant concentrations below the c.m.c., retention of the neutral solutes is only slightly affected, but the solutes oppositely charged to the surfactant are totally retained, as they are electrostatically attracted to the adsorbed surfactant. The operative mechanism is similar to that of ion-pair chromatography, as common ion-pairing reagents are surfactants added to the mobile phase at concentrations below the c.m.c. Here there is some amount of adsorbed surfactant present on the stationary phase, and still there are neither micelles nor organic modifier in the mobile phase to cause elution. Above the c.m.c. all solutes show a decrease in retention, as now they can partition from the stationary phase to the micellar aggregates.

Micellar mobile phases composed of charged surfactants can therefore be used in the same manner as traditional ion-pairing mobile phases to provide the simultaneous separation of both neutral solutes and those charged oppositely to the surfactant. While this may seem to offer no advantage over ion-pairing with hydro-organic mobile phases, there is a dramatic difference. Hydro-organic ion-pairing chromatography is not a rugged method. That is, the concentration of surfactant present in solution is such that separations are performed on the steep slope of the adsorption isotherm of the surfactant on the stationary phase. This means that any change in temperature, ionic strength or surfactant concentration will change the amount of surfactant adsorbed, and thereby change the separation. This is the major factor causing poor reproducibility of ion-pairing separations. Furthermore, if a hydro-organic gradient is applied, not only must the column be re-equilibrated with the initial mobile phase composition, but the change in organic composition will have also changed the amount of surfactant present on the surface, and this must be re-equilibrated as well. In micellar mobile phases, however, there is no change in the amount of adsorbed surfactant at any concentration above the c.m.c. [10]. This then provides a much more rugged method which should offer greater long-term reproducibility. We are further investigating ion-pairing methods using micellar mobile phases.

Figure 2(b) and (c) also show anomalous retention behavior for phenol at surfactant concentrations just below the c.m.c. This is yet unexplained, but is likely due to increased retention from strongly polar interactions between the weakly acidic phenol and the surfactant as the stationary phase becomes more coated with adsorbed surfactant. Again there is a reversal of the elution order between phenol and acetophenone with the CTAB micellar mobile phase (Fig. 1b).

The authors gratefully acknowledge Nelson H. C. Cooke, Altex Scientific, for a gift of the Ultrasphere columns. J. G. D. acknowledges Eli Lilly and Company and the Alcoa Foundation for support of this work.

REFERENCES

1 C. Tanford, The Hydrophobic Effect: Formation of Micelles and Biological Membranes, Wiley-Interscience, New York, 2nd edn., 1980.
2 L. J. Cline Love, J. G. Habarta and J. G. Dorsey, Anal. Chem., 56 (1984) 1132A.
3 D. W. Armstrong and S. J. Henry, J. Liq. Chromatogr., 3 (1980) 657.
4 P. Yarmchuk, R. Weinberger, R. F. Hirsch and L. J. Cline Love, Anal. Chem., 54 (1982) 2233.
5 R. A. Barford and B. J. Sliwinski, Anal. Chem., 56 (1984) 1554.
6 D. W. Armstrong, W. L. Hinze, K. H. Bui and H. N. Singh, Anal. Lett., 14 (1981) 1659.
7 R. Weinberger, P. Yarmchuk and L. J. Cline Love, Anal. Chem., 54 (1982) 1552.
8 M. Arunyanart and L. J. Cline Love, Anal. Chem., 56 (1984) 1557.
9 J. S. Landy and J. G. Dorsey, J. Chromatogr. Sci., 22 (1984) 68.
10 J. G. Dorsey, M. G. Khaledi, J. S. Landy and J.-L. Lin, J. Chromatogr., 316 (1984) 183.
11 M. G. Khaledi and J. G. Dorsey, Anal. Chem., 57 (1985) 2190.
12 E. Pramauro, G. Saini and E. Pelizzetti, Anal. Chim. Acta, 166 (1984) 233.
13 E. Pelizzetti and E. Pramauro, J. Phys. Chem., 88 (1984) 990.
14 F. G. P. Mullins and G. F. Kirkbright, Analyst (London), 109 (1984) 1217.
15 C. M. Kirkman, C. Zu-Ben, P. C. Uden, W. J. Stratton and D. E. Henderson, J. Chromatogr., 317 (1984) 569.
16 J. G. Dorsey, M. T. DeEchegaray and J. S. Landy, Anal. Chem., 55 (1983) 924.
17 J. P. Foley and J. G. Dorsey, Anal. Chem., 55 (1983) 730.
18 B. A. Bidlingmeyer and F. V. Warren, Jr., Anal. Chem., 56 (1984) 1583A.
19 P. Yarmchuk, R. Weinberger, R. F. Hirsch and L. J. Cline Love, J. Chromatogr., 283 (1984) 47.
20 J. P. Foley and W. E. May, Pittsburgh Conference and Exposition, 1985, Abstract 1207.
21 R. P. W. Scott and C. F. Simpson, Faraday Symp. Chem. Soc., 15 (1980) 69.

Analytica Chimica Acta, 178 (1985) 189—195
Elsevier Science Publishers B.V., Amsterdam — Printed in The Netherlands

EXTRACTION OF ORGANIC ACIDS BY ION-PAIR FORMATION WITH TRI-n-OCTYLAMINE
Part 4. Influence of Organic Phase Composition

M. PUTTEMANS, L. DRYON and D. L. MASSART*

Farmaceutisch Instituut, Vrije Universiteit Brussel, Laarbeeklaan 103, B-1090 Brussels (Belgium)

(Received 4th July 1985)

SUMMARY

Synthetic food dyes are extracted by ion-pair formation with tri-n-octylamine. Mixed organic phases are used, consisting of mixtures of hexane with one of the following solvent modifiers: chloroform, dichloromethane, methyl isobutyl ketone, butyl acetate or pentanol. Logarithmic plots of the distribution ratio versus the volume fraction of the solvent modifier are linear for dichloromethane, chloroform and pentanol. The efficiency of the solvents is classified as follows: dichloromethane > pentanol > chloroform > methyl isobutyl ketone > butyl acetate > hexane. The addition of pentanol to chloroform provides nearly quantitative recovery for hydrophilic solutes.

The chromatographic or spectrophotometric determination of synthetic food dyes, after their extraction by ion-pair formation with tri-n-octylamine (TOA), has been described in several papers [1—3]. Factors affecting the recovery, such as the counter-ion concentration [4] and the pH and ionic strength of the aqueous phase [5] have been discussed. Another important parameter to be considered is the composition of the organic phase. In most cases, organic phases consisting of a single solvent are used for extraction, but mixed organic solvents can also be useful. One reason for the use of mixtures is the demand for an efficient extraction solvent which will form the upper phase, thus greatly facilitating sample manipulation in the extraction of complex samples (e.g., whole blood) [6, 7]. Mixed solvents have also been used for the ion-pair extraction of inorganic ions [8, 9] and hydrophilic organic compounds [10].

Solutes partition between immiscible phases because of competition between the solvating forces in the aqueous phase and the organic solvent. For non-ionic polar substances, the main interactions between solute and solvent are ion/dipole, dipole/dipole interactions and hydrogen bonding [10]. Based on Snyder's classification triangle [11], solvents are characterized as proton donors, proton acceptors or promoters of dipole/dipole interactions. Based on these interactions, the polarity index (or solvent strength) calculated [11] can be used in high-performance liquid chromatography to predict

0003-2670/85/$03.30

eluent compositions which will maintain the retention, but will result in different selectivities [12].

In previous papers in which ion-pair extractions with mixed organic phases were described, the efficient extraction obtained in ion-pair systems was ascribed to specific solvation effects. In the case of chloroform/cyclohexane mixtures, ion-pairs produced a great deal of ordering or structure formation in the organic phase [13]. For example, dextromethorphane/bromide ion-pairs were found to be associated with as many as five proton-donating solvent molecules [14]. Selective solvation of the ion-pairs was also observed with chloroform/carbon tetrachloride [15], dichloromethane/cyclohexane [16] and pentanol/chloroform mixtures [10]. These findings were based on the linear relation between the logarithms of the extraction constant and the molar concentration of the solvent modifier in the organic phase [10, 15, 16]. Similar experiments are conducted here with different solvents (i.e., chloroform dichloromethane, methyl isobutyl ketone, butyl acetate and pentanol) in mixtures with hexane, in order to establish which of them is the most powerful.

EXPERIMENTAL

Apparatus and reagents

The equipment included a Perkin-Elmer Lambda 3 u.v.-visible spectrophotometer, an Orion 601 Ionalyzer and a combined glass/calomel electrode.

Tri-n-octylamine, 4-hydroxybenzoic acid (99%) and 3,4-dihydroxybenzoic acid (97%) were obtained from Aldrich. Dyes were from the Dutch Colorants Industry (Amersfoort, The Netherlands). All other reagents and solvents used were of analytical grade (Merck). The composition of the buffer (pH 5.5, ionic strength 0.1) was 24.650 g of $NaH_2PO_4 \cdot H_2O$ and 1.260 g of $Na_2HPO_4 \cdot 2H_2O$ made up to 2 l with double-distilled water.

Extractions

Extractions were done in glass, screw-capped, centrifuge tubes, with equal volumes (10.0 ml) of aqueous and organic phase. The aqueous phase, consisting of a solution of the acid with given concentration in the phosphate buffer (pH 5.5) was shaken for 30 min with the organic phase. The tube was then centrifuged for 10 min at 2000 rpm. The concentration of the acid was determined in the aqueous phase by spectrophotometry. Each partition experiment was done in triplicate. The extraction efficiency is expressed as a percentage or as the distribution ratio, D = concentration of solute in the organic phase/concentration of solute in the aqueous phase.

RESULTS AND DISCUSSION

Three dyes (tartrazine, amaranth and patent blue) were extracted from a buffered aqueous solution with 5 mM TOA dissolved in a mixed organic

phase. The following solvents were mixed with hexane: chloroform, dichloromethane, methyl isobutyl ketone (MIBK), butyl acetate and pentanol. The hexane levels were 0, 20, 40, 60, 80 and 100%. The choice of these solvents was based on two criteria. First, TOA had to be soluble in the solvent modifier chosen. Solvents were then selected which represent, according to Snyder's classification, different characteristics and therefore interact by a different mechanism with the ion-pair. Dichloromethane promotes mainly dipole/dipole interactions, chloroform is a good proton donor, and pentanol is a strong proton acceptor; butyl acetate and MIBK appear at intermediate positions in this classification [11].

A relatively low TOA concentration (i.e., 5 mM) was chosen so that the effect of the organic solvent on the extraction efficiency would be more obvious. Indeed, at higher TOA concentrations (50 mM) significant extractions were obtained even with pure hexane. Blank extractions, without TOA, indicated no extraction by any of the solvents alone, except in the case of patent blue for which ca. 45% was extracted by pentanol. With a hexane/pentanol (80:20) mixture, however, the extraction of patent blue was negligible.

The results of these experiments, expressed as plots of the logarithm of the distribution ratio versus the volume fraction of the solvent modifier, are given in Fig. 1. As can be seen in Fig. 1(a) for tartrazine, 1(b) for amaranth and 1(c) for patent blue, the ion-pair extraction of these dyes with hexane alone is negligible. The addition of small amounts of dichloromethane or pentanol to the organic phase results in an immediate increase of the extraction yield for all three dyes. In the case of chloroform, amaranth and patent blue show an increased extraction yield starting with 20% chloroform; for tartrazine, 60% chloroform is needed to improve the extraction. For MIBK, this critical level is about 60% for patent blue and 80% for tartrazine and amaranth. Butyl acetate permits the extraction of amaranth starting from the 20% level; however, for tartrazine and patent blue, 100% of the ester is needed.

As can be seen in Table 1, ion-pair extraction of various food dyes is possible with the different solvents tested. The efficiency of these solvents can be classified in the following order: hexane < butyl acetate < MIBK < chloroform < dichloromethane. No systematic study of the efficiency of pentanol was undertaken because of the problems encountered in the spectrophotometric evaluation of the remaining dye concentrations in pentanol-saturated buffer solutions. Nevertheless, a few results, expressed as % extraction, were obtained for tartrazine (95.2 ± 0.2%), amaranth (100.0 ± 0.1%) and patent blue (97.1 ± 0.2%), which enable the extraction efficiency of pentanol to be classified as intermediate between chloroform and dichloromethane.

In Part 3 of this series [5], it was found that, although quantitative recovery was obtained in most ion-pair extractions with TOA in chloroform, the recovery was still insufficient for very hydrophilic substances. Effectively,

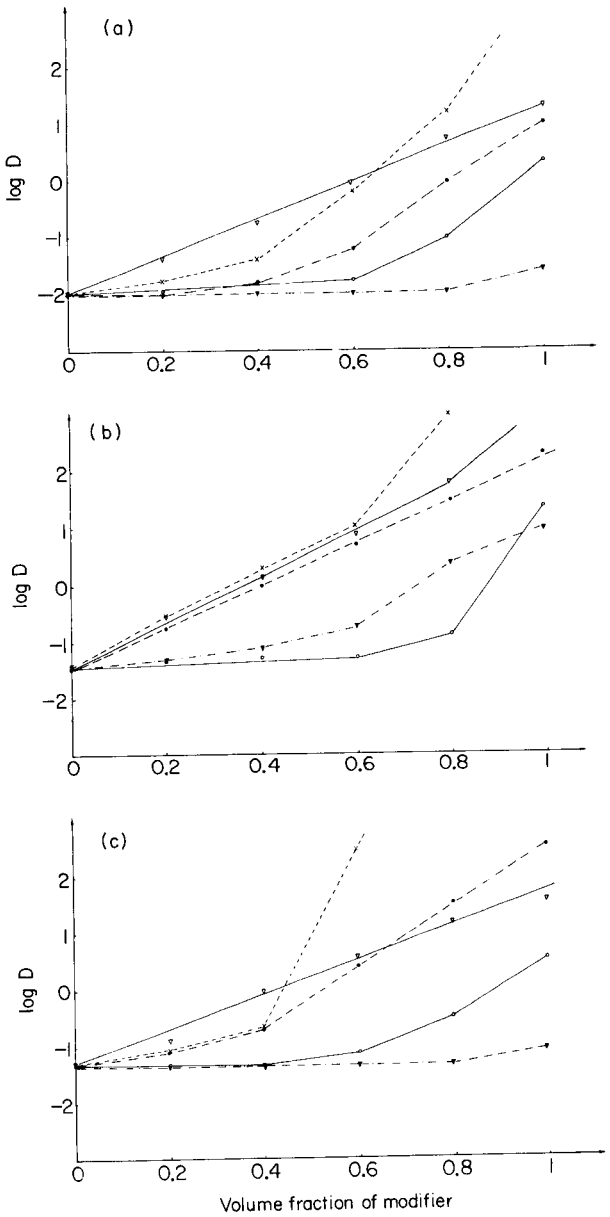

Fig. 1. Influence of the addition of a modifying solvent to hexane on the ion-pair extraction of synthetic dyes: (a) tartrazine; (b) amaranth; (c) patent blue. Modifier: (X) dichloromethane; (▽) pentanol; (•) chloroform; (○) methyl isobutyl ketone; (▼) butyl acetate.

TABLE 1

Percentage extraction of dyes with various solvents (dye concentration 5×10^{-5} M; counter-ion concentration 5×10^{-3} M)

Dye	CI No.	Extraction yield (%)[a]				
		CH_2Cl_2	$CHCl_3$	MIBK	Butyl acetate	Hexane
Tartrazine	19140	100.0 (0.1)	92.4 (0.9)	69.4 (0.1)	2.1 (0.1)	1.0 (0.1)
Quinoline yellow	47005	100.0 (0.1)	100.0 (0.1)	97.5 (0.1)	51.0 (0.1)	2.3 (0.3)
Sunset yellow	15985	100.0 (0.1)	100.0 (0.1)	98.0 (0.1)	92.3 (0.2)	54.3 (1.3)
Azorubine	14720	100.0 (0.2)	100.0 (0.2)	100.0 (0.1)	99.9 (0.1)	50.6 (0.3)
Amaranth	16185	100.0 (0.1)	99.9 (0.1)	95.6 (1.1)	91.4 (0.5)	3.3 (0.3)
New Coccine	16255	99.6 (0.1)	99.6 (0.1)	98.5 (0.1)	97.3 (0.1)	63.0 (1.0)
Erythrosine	45430	100.0 (0.1)	100.0 (0.1)	99.9 (0.2)	99.9 (0.1)	1.9 (0.1)
Patent blue	42051	100.0 (0.1)	99.7 (0.2)	78.2 (0.6)	6.9 (0.5)	2.0 (0.3)
Indigotin	73015	100.0 (0.1)	88.2 (0.2)	66.0 (0.1)	4.5 (0.2)	3.0 (0.4)
Brilliant green	44090	100.0 (0.1)	100.0 (0.1)	50.8 (0.1)	20.1 (0.1)	1.3 (0.2)
Brilliant black	28440	99.8 (0.2)	100.0 (0.2)	99.1 (0.2)	6.7 (0.1)	2.5 (0.1)

[a]Standard deviations (n = 3) are given in parentheses.

only ca. 50% of hydroxylated derivatives of *p*-hydroxybenzoic acid were extracted with 0.1 M TOA in chloroform In the past, several investigators have extracted hydrophilic compounds by adding small amounts of a lipophilic alcohol (e.g., pentanol) to the organic phase. In the present work, pentanol was added to chloroform in order to combine the solvating effects of both solvents. The increases in the extraction yield observed on the addition of increasing amounts of pentanol to chloroform are summarized in Table 2. The extraction by the solvent alone was negligible in each case.

The effect of the addition of pentanol to chloroform on the extraction constant and the composition of the extracted complex was tested for patent blue. Patent blue, at an initial concentration of 10^{-5} M, was extracted with TOA (0, 1, 5, 10, 25 and 50×10^{-5} M) in chloroform/pentanol mixtures

TABLE 2

Percentage extraction of hydroxylated derivatives of benzoic acid as a function of the pentanol concentration in chloroform (initial concentration 100 mg l^{-1}; TOA concentration 0.1 M)

Compound	Extraction (%) at different % pentanol added						
	0	2.5	5	7.5	10	15	20
4-Hydroxybenzoic acid	54.3	60.9	77.1	76.4	81.0	86.4	91.3
3,4-Dihydroxybenzoic acid	55.2	70.8	86.1	86.5	90.7	93.4	98.5

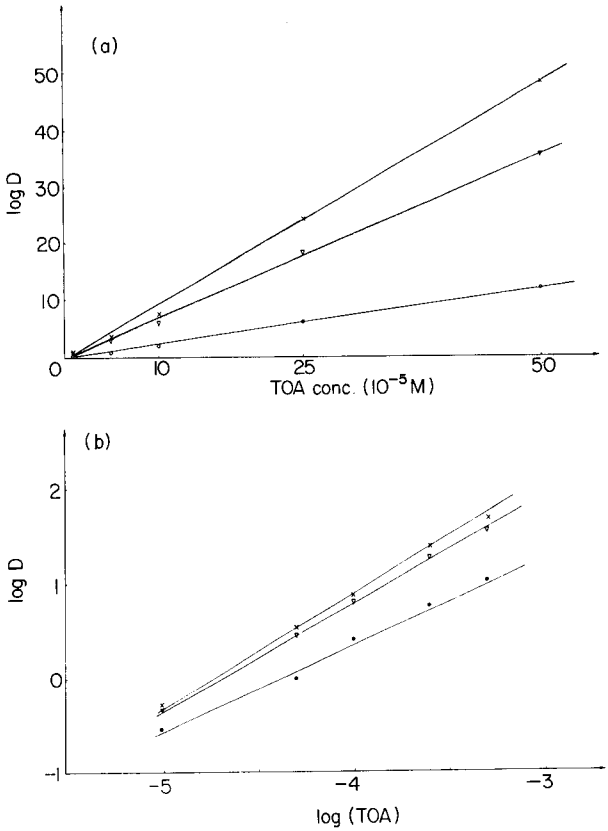

Fig. 2. Influence of the addition of pentanol to chloroform on the ion-pair extraction of patent blue. Pentanol added: (○) 0%; (▽) 10%; (×) 20%. (a) Plot of D vs. TOA concentration in the organic phase; (b) plot of log D vs. the logarithm of the TOA concentration in the organic phase.

(100:0; 90:10; 80:20). Figure 2(a) shows the graphs of the distribution ratio versus the counter-ion concentration. Logarithmic plots, obtained for the same values, are shown in Fig. 2(b). In each case, correlations were higher than 0.999. The slopes of the graphs in Fig. 2(a) yield the extraction constant [4, 5]. This constant, expressed as its logarithm, increases from 4.38 to 4.86 and 4.99, when the pentanol content is increased from 0 to 10 and 20%, respectively. The slope of the logarithmic plot (Fig. 2b), which is equal to the number of moles of amine for 1 mole of acid in the complex [4, 5], is not significantly increased by the addition of pentanol. This indicates that, in this case, the extraction is enhanced by better solvation of the ion-pair and not by the formation of a different amine/dye complex.

An important means of affecting the extraction yield in ion-pair extraction with TOA is the selection of the appropriate solvent. Although, in most cases, chloroform permits quantitative recovery, the efficiency can still be improved

through the use of dichloromethane or a chloroform/pentanol mixture as the extracting solvent.

The authors thank A. De Schrijver, K. Decq and M. De Vreese for technical assistance.

REFERENCES

1 M. Puttemans, L. Dryon and D. L. Massart, J. Assoc. Off. Anal. Chem., 65 (1982) 737.
2 M. Puttemans, L. Dryon and D. L. Massart, J. Assoc. Off. Anal. Chem., 66 (1983) 670.
3 M. Puttemans, L. Dryon and D. L. Massart, J. Assoc. Off. Anal. Chem., 66 (1983) 1039.
4 M. Puttemans, L. Dryon and D. L. Massart, Anal. Chim. Acta, 161 (1984) 221.
5 M. Puttemans, L. Dryon and D. L. Massart, Anal. Chim. Acta, 165 (1984) 245. (Part 3 of this series.)
6 M. Puttemans, M. Bogaert, G. Hoogewijs, L. Dryon, D. L. Massart and L. Vanhaelst, J. Liq. Chromatogr., 7 (1984) 2237.
7 G. Hoogewijs, Y. Michotte, J. Lambrecht and D. L. Massart, J. Chromatogr. Biomed. Appl., 226 (1981) 423.
8 K. O. Borg, Acta Pharm. Suecica, 6 (1969) 425.
9 B. A. Persson, Acta Pharm. Suecica, 7 (1970) 343.
10 R. Modin and S. Back, Acta Pharm. Suecica, 8 (1971) 585.
11 L. R. Snyder, J. Chromatogr. Sci., 16 (1978) 223.
12 M. De Smet, G. Hoogewijs, M. Puttemans and D. L. Massart, Anal. Chem., 56 (1984) 2662.
13 A. F. Michaelis and T. Higuchi, J. Pharm. Sci., 58 (1969) 201.
14 T. Higuchi, A. Michaelis and J. H. Rytting, Anal. Chem., 43 (1971) 287.
15 M. J. Harris, T. Higuchi and J. H. Rytting, J. Phys. Chem., 77 (1973) 2694.
16 T. D. Doyle and J. B. Proctor, J. Assoc. Off. Anal. Chem., 59 (1976) 1175.

Analytica Chimica Acta, 178 (1985) 197—208
Elsevier Science Publishers B.V., Amsterdam — Printed in The Netherlands

DETERMINATION OF ALUMINIUM, COPPER, IRON AND MANGANESE IN BIOLOGICAL AND OTHER SAMPLES AS 8-QUINOLINOL COMPLEXES BY HIGH-PERFORMANCE LIQUID CHROMATOGRAPHY WITH ELECTROCHEMICAL AND SPECTROPHOTOMETRIC DETECTION

A. M. BOND* and Y. NAGAOSA[a]

Division of Chemical and Physical Sciences, Deakin University, Waurn Ponds 3217, Victoria (Australia)

(Received 17th July 1985)

SUMMARY

A range of methods based on reverse-phase high-performance liquid chromatography is described for determining Al, Cu, Fe and Mn. The simplest method for determining Fe, Cu and Al involves direct formation and separation of the 8-quinolinol complexes on the column, with 1:1 acetonitrile/water containing 5×10^{-3} M 8-quinolinol, 0.4 M potassium nitrate and 0.02 M acetate buffer (pH 6.0) as the mobile phase, followed by electrochemical detection at −0.5 V vs. Ag/AgCl and/or spectrophotometric detection at 400 nm. Electrochemical detection enables < 2 ng Cu and < 1 ng Fe to be quantified for injection volumes of 20 μl. Spectrophotometric detection allows simultaneous determinations of Al, Cu and Fe with lower sensitivity. The method is applied to the determination of Cu, Fe and Al in bovine liver and oyster tissue. Down to 1 ng of manganese (in the 20 μl injected) can be determined in biological samples by liquid chromatography with a mobile phase containing 1 mM Tris buffer (pH 8.8) after injection of an externally prepared 8-quinolinol complex. Preconcentration on Sep-Pak cartridges after dichloromethane extraction is used for the determination of low concentrations of iron in water. A sensitive determination of aluminium based on detection at 254 nm is also reported.

Recently, considerable attention has been focused on the use of high-performance liquid chromatography (h.p.l.c.) for the separation and sensitive multi-element determination of metals as chelated complexes formed externally or directly on the chromatographic column [1—3]. In particular, the reverse-phase h.p.l.c. method seems to offer excellent potential for the routine determination of heavy metals owing to its simplicity of operation and general convenience [4—23]. The most extensively studied type of chelating agent in this branch of elemental analysis is probably dithiocarbamate [9, 11—14] although several papers have dealt with the h.p.l.c. of β-diketones [15, 16], nitrogen-oxygen-coordinated metal chelates [4, 5] and other metal complexes [1—3]. The study of the separation of 8-quinolinol metal chelates by reverse-phase h.p.l.c. was first reported by Berthod et al.

[a] On leave from Faculty of Engineering, Fukui University, Bunkyo, Fukui 910, Japan.

0003-2670/85/$03.30

[17], who used a 55:45 methanol/water mobile phase (at pH 8.5) and a Lichrosorb RP8 (5 μm) column for the separation of Cu(II), Co(II), Fe(III), Ni(II) and Hg(II). Both electrochemical and spectrophotometric detection methods were examined but no attempts were made to quantify the data by the examination of real samples. Other reports are also available [18—23]. For example, Lajunen et al. [22] reported the h.p.l.c. and thin-layer chromatography of Co(II), Cr(III) and V(V) complexes with 8-quinolinol, using a reverse-phase column and a 63:37 methanol/water eluent with a u.v. detector; Hoffmann and Schwedt [21] examined the determination of manganese in water and soils, using both pre-column and on-column derivatization for separation of the various metal complexes.

Various detection methods have been developed to quantify species in an eluate flowing from a separation column. In general, the u.v./visible spectrophotometric detector enables a wide range of components to be quantified with fairly good sensitivity, while the electrochemical (e.c.) detector can usually enhance the selectivity as well as sensitivity of the chromatographic determination. Atomic absorption spectrometry and inductively-coupled plasma techniques provide more selective but more expensive detectors than the spectrophotometric or electrochemical counterparts considered here. After liquid-liquid extraction, metal 8-quinolinol complexes, such as Cu(II), Fe(III), Mo(VI) and U(VI) [24—26], exhibit well-defined polarograms (reduction) in non-aqueous solvents. Thus, h.p.l.c./e.c. of 8-quinolinol complexes should provide simultaneous determinations of metals even though polarographic methods do not necessarily provide sufficient selectivity for multi-element determination of real samples. In the work described here, the determination of Cu(II), Fe(III) and Mn(III) was investigated by l.c./e.c.; the reduction current of the 8-quinolinol complexes was measured at a glassy carbon working electrode in a thin-layer electrochemical cell. The problems associated with oxygen, which have frequently been reported [9, 27] in electrochemical detection based on reduction processes, was overcome by removing oxygen from the solutions with argon. In addition to the e.c. detection mode, spectrophotometric detection was examined for the determination of the above three metal ions and Al(III).

A wide range of possible procedures was considered in this work. For example, photometric detection at 254 nm was examined for the highly sensitive determination of Al(III) after 'external' complex formation; the direct-injection method was applied to the determination of metals in biological and other samples; and preconcentration on a Sep-Pak silica cartridge (Waters Associates) after extraction was examined for the determination of low concentration of Fe(III) in reticulated water. Watanabe et al. [28] have demonstrated that trace elements can be concentrated by complexation with 8-quinolinol and adsorption on C_{18} bonded silica gel followed by inductively-coupled plasma or atomic absorption spectrometric determination. The method used in this work is similar in principle but is more

efficient. This and other studies are presented to emphasise the broad potential of methods for metal determinations based on the use of 8-quinolinol complexes and their chromatographic separation.

EXPERIMENTAL

Reagents, standard solutions and apparatus

Analytical-reagent-grade metal nitrates and sulphates were used to prepare metal standard solutions. Commercially available 8-quinolinol was recrystallized from methanol. The organic solvents were of h.p.l.c. grade (Waters Associates). Acetonitrile was mixed with the required volume of water (buffer), degassed with argon, and used as the mobile phase. Acetate/acetic acid buffers were prepared in the conventional manner.

For liquid chromatography, Waters Associates Model 6000A solvent delivery system was used with a Rheodyne 7126 sample injection loop (20 μl) and an Altex Ultrasphere ODS column (internal diameter 4.6 mm, length 25 cm). A new guard column (internal diameter 3.9 mm, length 1 cm), packed with C_{18} material (Waters Associates), was prepared once a week for use with the Altex analytical column. A Model LC4 amperometric controller and a Model TL5 thin-layer cell with glassy carbon working electrode, Ag/AgCl (3 M KCl) reference electrode and platinum auxiliary electrode (all from Bioanalytical Systems) was used for electrochemical detection. A Model 450 variable-wavelength u.v./visible detector (Waters Associates) was used for spectrophotometric detection. Recording of chromatograms and data treatment were made with a Model 730 data module (Waters Associates).

A Varian-Techtron Model AA6 atomic absorption spectrometer with nitrous oxide/acetylene flame was used as an alternative method to h.p.l.c. for the determination of aluminium.

Procedure for in situ methods of complex formation

The direct injection method utilizing in situ complex formation was as follows. Aqueous solutions of metal ions, adjusted to pH 2.0 ± 0.1 with dilute hydrochloric acid or sodium hydroxide, were degassed with argon for 3 min and injected into the chromatographic column. Elutions were made with a mixed 1:1 acetonitrile/water solvent containing 5×10^{-3} M 8-quinolinol, 0.4 M potassium nitrate and 0.02 M acetate buffer (pH 6.0). The detectors were set to potentials and wavelengths appropriate for the detection of the metal complexes. The column temperature was kept at (25 ± 1)°C. All solutions were degassed with argon during the runs. Other procedures are included under Results and Discussion.

RESULTS AND DISCUSSION

Chromatograms of metal/8-quinolinol complexes

Previous studies [9, 11] in these laboratories have shown that the μ-Bondapak C_{18} column (10 μm, Waters Associates) is a versatile separation

column for determining heavy metal ions as diethyldithiocarbamate complexes by reverse-phase h.p.l.c. with acetonitrile/water (70:30) as the mobile phase in the presence of potassium nitrate and the ligand. Complex formation occurs in situ with this method. Therefore, this column, and equivalent chromatographic conditions were used initially to investigate the h.p.l.c. behaviour of the copper(II) and iron(III) complexes with 8-quinolinol in the running solvent. Unfortunately, poor reproducibility was observed for copper determinations. Data indicated that there is strong interaction between the support material and the species and/or dissociation of complexes in the eluent with this experimental arrangement. Further, it was found that the iron(III) complex could not be recovered quantitatively with this column. The iron(III) complex is partially decomposed during elution at higher concentrations of acetonitrile relative to water and at lower concentrations of 8-quinolinol in the eluent.

The chromatographic behaviour for the two 8-quinolinol complexes was improved by using a separation column packed with supporting material of smaller diameter (Spherisorb ODS, 5 μm; Altex) and with 1:1 acetonitrile/water as the eluent. Figure 1A shows a typical chromatogram for the separation of the Cu(II), Al(III), Ga(III), In(III), Fe(III) and Mo(VI) complexes under the recommended condition with spectrophotometric detection. In this and other work, peaks were identified by demonstrating

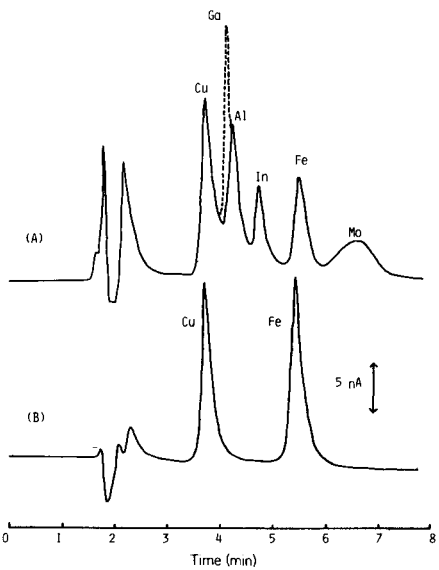

Fig. 1. Separation by h.p.l.c. of metal/8-quinolinol complexes on an Ultrasphere ODS column (Altex). Eluent: 1:1 acetonitrile/water (5×10^{-3} M 8-quinolinol, 0.4 M KNO_3, 0.02 M acetate buffer, pH 6.0). Sample: aqueous 1 mg l^{-1} solution directly injected on the column. Detection: (A) spectrophotometry at 400 nm; (B) d.c. amperometry at −0.05 V vs. Ag/AgCl (flow rate 2.0 ml min^{-1}; injection volume 20 μl).

that the height is proportional to the metal ion being considered via the use of spiked samples. It is clear that sharp and symmetric peaks were obtained with all elements except Mo(VI), provided that relatively high concentrations of 8-quinolinol were used in the eluent. The Mo(VI) complex showed a wide and asymmetric peak that is not suitable for its determination. The Ga(III) complex co-eluted with the Al(III) complex, and attempts to separate the two complexes failed under any experimental conditions investigated. It is interesting to note that the metal complexes examined are extracted into organic solvents from acidic solution below pH 3 [29]. Apparently the trivalent ions examined form very stable and hydrophobic complexes with 8-quinolinol under the conditions considered. In contrast, divalent metal ions, except copper(II), gave no chromatographic peak with 1:1 acetonitrile/water (pH 6.0) as the mobile phase. Berthod et al. [17] have reported that Co(II) and Ni(II) can be separated from Cu(II) and Fe(III) with a Lichrosorb RP8 column and 1:1 methanol/water containing 8-quinolinol at pH 8.5.

There was no retention of the Co(II) and Ni(II) complexes under the experimental conditions used here. Consequently, the present method offers a rather selective determination of a number of trivalent ions in addition to copper(II). As can be seen from Fig. 1B, electrochemical detection makes it possible to determine Cu(II) and Fe(III) selectively by measuring the electroactive species at −0.5 V vs. Ag/AgCl (3 M NaCl). Thus, the recommended direct sample-injection method is simple and complex formation is fast enough for automatic analysis and monitoring of samples, which is important when a number of samples must be examined in a short time.

Eluent composition and electrode potential

In establishing the optimum experimental conditions referred to above, the effects of some variables on the chromatographic behaviour of the Cu(II) and Fe(III) complexes were examined with the e.c. mode with a glassy carbon working electrode.

The content of acetonitrile in the eluent was varied from 70 to 40%. As can be seen from Table 1, the retention time of each chelate decreased with increasing acetonitrile content. Adequate separation of the two complexes was not achieved at acetonitrile contents more than 60%. At a content of 55%

TABLE 1

Effect of acetonitrile/water on retention time, t_R[a]

CH_3CN/H_2O	70:30	60:40	55:45	50:50	40:60
t_R (s)					
Cu	64	85	101	117	224
Fe	84	122	169	222	531

[a] Other experimental conditions as for Fig. 1.

acetonitrile, the two peaks were reasonably separated but not baseline-resolved. Well-resolved peaks suitable for the simultaneous determination of the two ions were obtained with 50% acetonitrile in the mobile phase. When 40% acetonitrile was used in the mobile phase, the peak heights were greatly decreased, despite good peak separation, and tailing took place during the elution. A longer retention time seems to cause the decomposition of complexes in the column. An acetonitrile content of 50% was the most suitable for both retention and separation.

The effect of the 8-quinolinol and potassium nitrate concentrations on peak height was also investigated in considerable detail. These reagents were necessary additions to the eluent in order that the complex formation of the chelates on the column was completed rapidly after sample injection and also so that decomposition was prevented during elution. In the absence of these reagents, the peak heights per unit concentration for Cu(II) and Fe(III) on the chromatogram were very small even if preformed complexes were injected onto the column. Data shown in Table 2 indicate that the peak heights become larger and that peak symmetry was improved at higher concentrations of the two reagents. In particular, the addition of potassium nitrate was found to be essential for fast and quantitative formation of the Fe(III) complex. High concentrations of 8-quinolinol in the eluent were unfavourable for determination of Cu(II). The optimum concentrations selected were, therefore, 5×10^{-3} M.

Another important factor affecting the chromatogram is the potential applied to the glassy carbon working electrode to detect the species in the eluate. The electrode potential was varied from −0.30 to −0.80 V vs. Ag/AgCl. Maximum peak heights for the Cu(II) and Fe(III) complexes were obtained at −0.50 V (Table 3). Away from this potential, the heights gradually decreased. An electrode potential of −0.5 V was therefore chosen for the remainder of this study.

TABLE 2

Effect of reagent concentrations on peak current with the glassy carbon working electrode held at −0.50 V vs. Ag/AgCl[a]

Reagent concentration (mM)		Peak current (nA)	
8-Quinolinol	KNO_3	Cu	Fe
2.0	200	34	29
2.0	300	35	31
5.0	40	28	18
5.0	100	34	25
5.0	200	35	32
5.0	400	35	37
5.0	500	36	38

[a]Metal concentration 2.0 mg l^{-1}; injection volume 20 μl; flow rate 2.0 ml min^{-1}; other conditions as for Fig. 1.

TABLE 3

Effect of electrode potential (E_{app} vs. Ag/AgCl) on peak current (i_p) with a glassy carbon working electrode[a]

E_{app}(V)	−0.30	−0.35	−0.40	−0.50	−0.60	−0.70	−0.80
i_p(nA)							
Cu	14	25	35	35	31	25	23
Fe	4	11	19	37	34	24	15

[a]Metal concentration 2.0 mg l^{-1} : injection volume 20 μl; eluent 5 × 10^{-3} M 8-quinolinol, 0.4 M KNO_3, 0.02 M acetate buffer, 1:1 acetonitrile/water; flow rate 2.0 ml min^{-1}.

Cyclic voltammetry for the Cu(II) and Fe(III) complexes in 1:1 acetonitrile/water containing 0.5 M tetrabutylammonium perchlorate was examined with a glassy carbon working electrode in a conventional electrochemical cell. When the metal concentration was 10^{-4} M and a scan rate of 100 mV s^{-1} was used, the reduction peak potentials were −0.50 V vs. Ag/AgCl for copper(II) and −0.45 V vs. Ag/AgCl for Fe(III), respectively. These potentials were almost coincident with the peak potentials of the corresponding differential-pulse voltammograms obtained with a modulation amplitude of −25 mV. Both processes appear to be reversible and correspond [24, 30, 31] to $Cu(Q)_2 + e^- \rightleftharpoons [Cu(Q)_2]^-$ and $Fe(Q)_3 + e^- \rightleftharpoons [Fe(Q_3)]^-$, respectively (Q = 8-quinolinol).

Calibration curves and detection limits

The calibration curves obtained for 20-μl injections were linear for 2.0—100 ng Cu(II) and for 1.0—100 ng Fe(III) when the peak heights were measured at −0.5 V vs. Ag/AgCl under the recommended conditions. When the spectrophotometric detector was used at 400 nm, detection limits were 10 ng for Cu(II), 5 ng for Al(III) and 5 ng for Fe(III), respectively. These detection limits correspond to a signal-to-noise (background) ratio of 3:1. It can be concluded from the zero intercept that either the three metal complexes undergo no substantial decomposition on the column during the elution or that any decomposition is constant. In both detection modes, the reagent blank was subtracted from the peak height observed. The relative standard deviations were 3.5% for Cu(II) and 2.7% for Fe(III), with ten replicate determinations of 20 ng for each metal ion and e.c. detection. The values were marginally lower for spectrophotometric detection under the same conditions.

ANALYTICAL APPLICATIONS

The above in situ method with direct calibration was applied to the determination of Cu, Fe and Al in biological and other samples. For the analysis of oyster tissue and bovine liver, 0.5 g of sample was weighed in

a 100-ml beaker and 20 ml of mixed acids (8 ml of concentrated nitric acid, 8 ml of concentrated sulphuric acid and 4 ml of 60% perchloric acid) was carefully added. The solution was heated gently until the contents became colourless, and then evaporated almost to dryness. After cooling, the solution was adjusted to pH 2.0 with 3 M sodium hydroxide and the total volume was made up to 10 or 100 ml with water, depending on the concentrations of the elements being determined. Drinking water (Deakin University), 200 ml, was filtered through a 0.45-μm membrane filter, and 6 M hydrochloric acid was added to the filtrate to adjust the pH to 2.0. A 20-μl portion of the sample solution was injected and the three metal ions were determined from the calibration curves previously obtained.

Table 4 summarizes the results obtained together with the certified values of Cu and Fe and the data obtained by the differential-pulse polarographic method in 0.2 M hydrochloric acid. It is clear that the Cu and Fe contents of oyster tissue and bovine liver as determined by the different methods are in satisfactory agreement with each other. Although the certified value for aluminium is not given, the Al content should be in the $\mu g\ g^{-1}$ to $mg\ g^{-1}$ range in such biological samples; the Al values are in excellent agreement with those obtained by atomic absorption spectrometry. Slightly variable results were obtained for copper in the drinking water; this may be due to different acidities of the sample solutions or to variable contact time with copper pipes. Acidification of all samples prior to direct injection is recommended for total copper determination. The iron and aluminium concentrations in the drinking water could not be detected as they were too low.

TABLE 4

Metal determinations in biological and water samples by the direct injection method

Sample	Metal	Concentration found ($mg\ kg^{-1}$)		Certified value
		Electrochemical	Ultraviolet	
Oyster tissue	Cu	60.5 ± 4.2[a]	65.2 ± 1.5[a]	63.0 ± 3.5
(NBS 1566)	Fe	203 ± 5[a]	200 ± 4[a]	195 ± 34
	Al	—[b]	366 ± 9[a]	(350 ± 10)[a,c]
Bovine liver	Cu	202 ± 4[a]	201 ± 4[a]	193 ± 10
(NBS 1577)	Fe	275 ± 6[a]	275 ± 4[a]	268 ± 8
	Al	—[b]	1.44 ± 0.10[a]	2[d]
Drinking water	Cu	0.468 ± 0.008[a]	0.480 ± 0.010[a]	0.520 ± 0.009[a,e]
	Fe	<0.05	<0.2	
	Al	—[b]	<0.2	

[a] Average of three determinations obtained via direct calibration. [b] Could not be determined by this method. [c] Determined by atomic absorption spectrometry in these laboratories. [d] Value provided by NBS for information only. [e] Determined by differential pulse polarography.

Determination of manganese based on 'external' complex formation

The elution behaviour of the 8-quinolinol complex with manganese(III) was investigated under a variety of experimental conditions. The direct-injection experiments showed that an acetate-buffered (pH 6.0) mobile phase was unfavourable because the Mn(III) complex was not formed in the column. An 'external' complex formation method was therefore applied: Mn(II) was added to an equal volume of a solution containing 1 mM tris-(hydroxymethyl)methylamine (Tris) buffer (pH 8.8), 5×10^{-3} M 8-quinolinol and 0.4 M KNO_3 in the presence of 50 mg of potassium periodate before sample injection. Figure 2 shows the elution curves for the Mn(III) complex, monitored by spectrophotometric (400 nm) and e.c. (−0.15 V) detection, respectively. The e.c. detection gave a better defined peak for the Mn(III) complex and very low noise on the baseline, compared with the spectrophotometric one. The calibration graph for Mn(III) was linear with a zero intercept over the concentration range 1—50 ng.

The manganese content of bovine liver was determined. A portion (20 ml) of the sample solution (0.5 g/100 ml), prepared as described previously, was transferred to a 100-ml beaker and the pH was adjusted to 10 with dilute sodium hydroxide. After addition of 50 mg of potassium periodate, the solution was shaken twice with 10 ml of dichloromethane containing 0.01 M 8-quinolinol. The dichloromethane extract was evaporated to dryness, and the residue was dissolved in 2.0 ml of methanol which was injected onto the column. Figure 2C shows the chromatogram obtained for this sample.

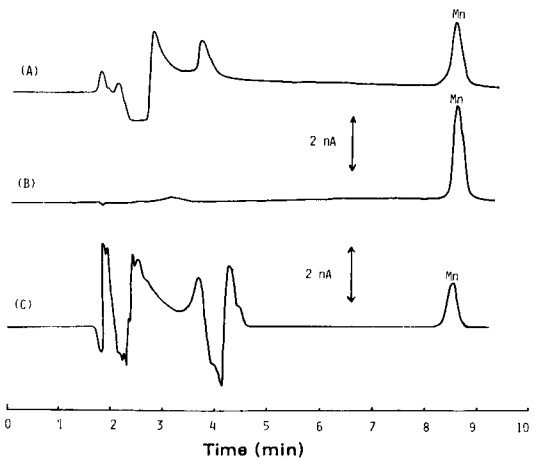

Fig. 2. Chromatograms of manganese obtained by 'external' complex formation with 1:1 acetonitrile/water (10^{-3} M Tris buffer, pH 8.8, containing 5×10^{-3} M 8-quinolinol and 0.4 M KNO_3) as eluent. (A) Spectrophotometry at 400 nm for 20 ng Mn; (B) d.c. amperometry at −0.15 V for 20 ng Mn; (C) d.c. amperometry at −0.15 V for a bovine liver sample (see text for detail). Conditions: Ultrasphere ODS column (Altex); flow rate 2.0 ml min^{-1}, injection volume 20 μl.

The result found was 10.2 ± 0.3 mg kg^{-1}, which is in good agreement with the certified value (10.3 ± 1.0 mg kg^{-1}). The dichloromethane extract was also directly injected onto the column, but the manganese peak was then very small and distorted; this is probably because the solvent forms an immiscible phase in the separation column.

Determination of iron with preconcentration on a Sep-Pak silica column

The concentration of iron in the drinking water was too low to be determined by the direct-injection method (Table 4). Therefore, preconcentration of the Fe(III) in the sample was examined with a Sep-Pak C_{18} column (Waters Associates); treatment was after the dichloromethane extraction and before the sample injection. First, an aqueous 0.5% 8-quinolinol solution (buffered to pH 4.0 with 1 M acetic acid/1 M sodium acetate) was purified by extracting it twice with dichloromethane (10 ml per 100 ml of the reagent solution). A portion (10 ml) of this purified solution was added to 100 ml of drinking water and left for 15 min for quantitative complex formation. After extraction with two 10-ml portions of dichloromethane, the separated extract was passed through a Sep-Pak C_{18} cartridge. It was ascertained that the column was capable of quantitatively retaining the species of interest. The dichloromethane absorbed onto the column was flushed out with air. The iron complex was then eluted with 2.5 ml of methanol. Examination of the recovered methanol solutions (2.0 ml) indicated that a 50-fold concentration factor was obtained with good reproducibility. A 20-μl portion of the solution was injected into a precolumn containing C_{18} supporting material (Waters) followed by separation with the Ultrasphere ODS column (Altex) as described under Experimental. Figure 3A shows the chromatogram obtained for the drinking water sample

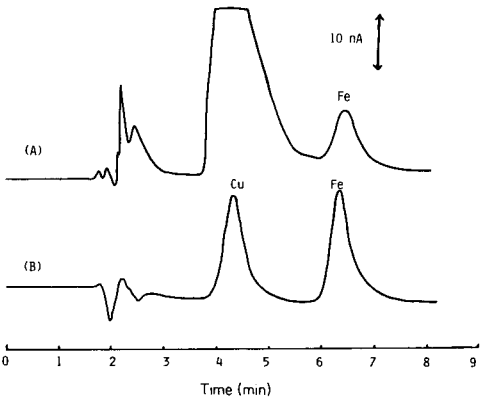

Fig. 3. Determination of iron in drinking water by dichloromethane extraction with 8-quinolinol, Sep-Pak preconcentration and elution with methanol. (A) Tap water concentrated 50-fold; (B) 20 μl of 1.0 mg l^{-1} Cu^{2+}/1.0 mg l^{-1} Fe^{3+} solution. For further details see text.

after this preconcentration method. By comparing with the chromatogram obtained for a standard solution of Fe(III) (Fig. 3B), the Fe(III) concentration of the sample solution was found to be 0.013 ± 0.001 mg l^{-1}; this was in excellent agreement with an independent determination by flame atomic absorption spectrometry which almost certainly measures total iron. The method provides a convenient means of changing the organic solvent and decreasing the solvent volume.

Sensitive determination of aluminium by detection at 254 nm

8-Quinolinol (5 × 10^{-3} M) in the mobile phase has a strong absorption over a wide range of the u.v. spectrum; this precludes the determination of many metals, despite their high molar absorptivities (ca. 10^4 l mol^{-1} cm^{-1}). However, if the 8-quinolinol concentration is lowered to 5 × 10^{-4} M to minimize the background contribution, the absorbance of species in the eluate can be monitored at 254 nm. The 'external' complex formation method before sample injection was used; the Al(III) solution was mixed with an equal volume of solution containing 10^{-2} M 8-quinolinol, 0.4 M KNO_3 and 0.02 M acetate buffer, pH 6.0. Figure 4 shows the chromatogram obtained for 5.0 ng each of Cu(II), Al(III) and Fe(III). The Al(III) complex gave a sharp peak with good separation from the other complexes. This suggests that the Al/8-quinolinol complex is very stable under these conditions. The detection limit was 0.5 ng Al with 2:3 acetonitrile/water as the eluent and detection at 254 nm. Higher sensitivity for the determination of Al(III) was obtained by this change of chromatographic and detection conditions. However, the copper complex coeluted with the reagent, and the iron complex exhibited a small broad peak, indicating the occurrence of decomposition during the elution. Thus, the conditions are not suitable for either of these elements.

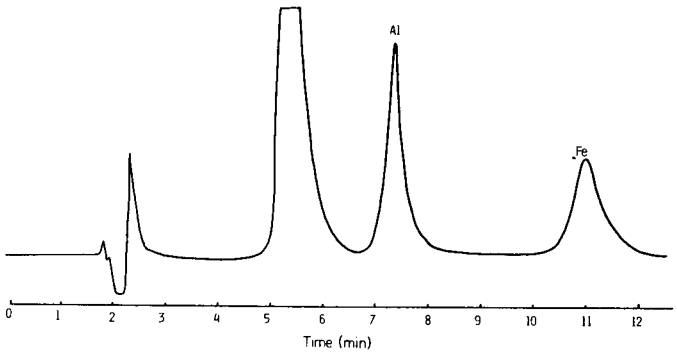

Fig. 4. Sensitive determination of aluminum and iron (5 ng each) based on 'external' complex formation and detection at 254 nm. Conditions: Ultrasphere ODS column; eluent, 2:3 acetonitrile/water with 5 × 10^{-4} M 8-quinolinol, 0.4 M KNO_3 and 0.02 M acetate buffer, pH 6.0; other conditions as for Fig. 1.

Conclusions

8-Quinolinol is a versatile reagent for determining metals by chromatographic separation followed by electrochemical and/or spectrophotometric detection. The results described above demonstrate that a range of methods can be applied to the determination of Cu, Fe, Al and Mn. Clearly, other elements could also be determined by similar procedures based on spectrophotometric and electrochemical detection.

Technical assistance from E. Mocellin and S. Atkinson and discussions with I. Heritage contributed significantly to the work described. Financial support provided by the Deakin University Research Committee for Y. Nagaosa is gratefully acknowledged.

REFERENCES

1 H. Engelhardt, High Performance Liquid Chromatography, Springer Verlag, New York, 1979.
2 M. Brunt and J. F. Lawrence (Eds.), Trace Analysis, Academic Press, New York, 1981.
3 P. C. White, Analyst (London), 109 (1984) 677.
4 P. C. Uden, P. M. Parees and F. H. Walters, Anal. Lett., 8 (1975) 795.
5 E. Gaetani, C. F. Laureri, A. Mangia and G. Parolari, Anal. Chem., 48 (1976) 1725.
6 G. Schwedt, Chromatographia, 11 (1978) 145; 12 (1979) 289; Fresenius Z. Anal. Chem., 295 (1979) 382.
7 O. Liska, J. Lehotary, E. Brandsteterova, G. Guiochon and H. Colin, J. Chromatogr., 17 (1979) 2384.
8 M. Moriyasu and Y. Hashimoto, Chem. Lett., (1980) 593.
9 P. C. Uden and I. E. Bigley, Anal. Chim. Acta, 94 (1977) 29.
10 M. Yamazaki, S. Ichinoki and R. Igarashi, Bunseki Kagaku, 30 (1981) 40.
11 A. M. Bond and G. G. Wallace, Anal. Chem., 53 (1981) 1209; 54 (1982) 1706; 55 (1983) 718; J. Liq. Chromatogr., 6 (1983) 1799.
12 R. M. Smith and L. E. Yankey, Analyst (London), 107 (1982) 744.
13 Y. T. Shih and P. W. Carr, Anal. Chim. Acta, 142 (1982) 55.
14 E. B. Edward-Inatimi, J. Chromatogr., 256 (1983) 253.
15 C. A. Tollinche and T. H. Risby, J. Chromatogr. Sci., 16 (1978) 448.
16 R. C. Gurira and P. W. Carr, J. Chromatogr. Sci., 20 (1982) 461.
17 A. Berthod, M. Kolosky, J.-L. Rocca and O. Vittori, Analusis, 7 (1979) 395.
18 H. Hoshino and T. Yotsuyanagi, Bunseki Kagaku, 29 (1980) 807.
19 C. S. Hambali and P. R. Haddad, Chromatographia, 13 (1980) 633.
20 B. Wenclawiak, Fresenius Z. Anal. Chem., 310 (1982) 144.
21 B. W. Hoffman and G. Schwedt, J. High Resolution Chromatogr. Chromatogr. Commun., 5 (1982) 439.
22 L. H. J. Lajunen, E. Eijarvi and T. Kenakkala, Analyst (London), 109 (1984) 699.
23 B. Wenclawiak and F. Bickman, Bunseki Kagaku, 33 (1984) E67.
24 Y. Nagaosa, Fresenius Z. Anal. Chem., 296 (1979) 259.
25 Y. Nagaosa and K. Kobayashi, Talanta, 31 (1984) 593.
26 L. E. Leon and D. T. Sawyer, Anal. Chem., 53 (1981) 706.
27 H. B. Hanekamp, W. H. Voogt, P. Bos and R. W. Frei, Anal. Chim. Acta, 118 (1980) 81.
28 H. Watanabe, K. Goto, S. Taguchi, J. W. McLaren, S. S. Berman and D. S. Russell, Anal. Chem., 53 (1981) 738, and references cited therein.
29 J. Stary, The Solvent Extraction of Metal Chelates, Pergamon Press, Oxford, 1964.
30 T. Kitagawa and A. Ichimura, Bunseki Kagaku, 24 (1975) 41.
31 T. Fujinaga, M. Murakami and T. Inoue, Nippon Kagaku Zasshi, 92 (1971) 1148.

Analytica Chimica Acta, 178 (1985) 209—215
Elsevier Science Publishers B.V., Amsterdam — Printed in The Netherlands

FLOW INJECTION ANALYSIS FOR TRACES OF ZINC WITH IMMOBILIZED CARBONIC ANHYDRASE

KUNIO KASHIWABARA, TOSHIYUKI HOBO*, EIGO KOBAYASHI and SHIGETAKA SUZUKI

Department of Industrial Chemistry, Faculty of Technology, Tokyo Metropolitan University, 2-1-1 Fukasawa, Setagaya-ku, Tokyo 158 (Japan)

(Received 8th March 1985)

SUMMARY

A small column packed with immobilized bovine carbonic anhydrase is used for determination of traces of zinc in aqueous solution, based on the measurement of recovered esterase activity of the metal-free apoenzyme after taking up zinc from the sample solution. Conditions for the removal of zinc from the immobilized enzyme and for activity measurement are established. A linear calibration graph is obtained between 1×10^{-8} and 4×10^{-7} g of zinc. Then the method is successfully applied to the determination of zinc in tea, sediment and spring water.

Several methods for the determination of trace metals, especially zinc and copper, by using metalloenzymes have been reported [1—9]. In these methods, the metalloenzymes were first deprived of the metals which are essential for their activity. The metal-free apoenzymes were then placed in contact with the sample solution which contained the metal to be determined. By taking up the essential metal from solution, the enzymatic activity measured corresponded to the amount of metal.

Zinc has been the most frequently measured metal. Townshend and Vaughan [1] used filter paper impregnated with apoalkaline phosphatase for a spot test for zinc. The substrate used was *p*-nitrophenylphosphate, and the product, *p*-nitrophenol was yellow. The same enzyme and substrate were used in a spectrophotometric method [2] which could be used for the determination of 6—650 ng of zinc in a 1-ml sample. Later, Lehky and Stein [3] used aminopeptidase in a spectrophotometric method by using L-leucine-*p*-nitroanilide as the substrate. The enzymatic reaction produced *p*-nitroaniline, which had maximum absorbance at 405 nm. As little as 0.1 ng ml^{-1} of zinc could be assayed within an error of 10%.

Kobayashi et al. [5, 6] reported two methods for trace zinc determination by using bovine carbonic anhydrase (BCA) as the metalloenzyme and *p*-nitrophenyl acetate (for esterase activity measurement) or sodium hydrogencarbonate (for hydrolyase activity measurement) as the substrate. The limit of detection was 10 ng ml^{-1} (esterase activity measurement) or 0.9 ng ml^{-1}

0003-2670/85/$03.30

(hydrolyase activity measurement). In these experiments, a batch method was used for the preparation of apoenzyme and measurement of enzymatic activity. Therefore, for each measurement, the apoenzyme has to be replaced. Recently, Risinger et al. [7] developed a flow system in which they used immobilized carboxypeptidase A for the determination of trace zinc ($2-20 \times 10^{-7}$ M). In their system, however, high-performance liquid chromatography was incorporated so as to quantify the reaction products L-phenylalanine and hippuric acid produced by the substrate hippuryl-L-phenylalanine. The chromatographic step makes the method slower (5 samples h^{-1}) than with a more direct method. In the present investigation, based on the work of Kobayashi et al. [5], a new flow system has been developed in which BCA is immobilized on agarose, and esterase activity is measured. The metal ions of the immobilized BCA packed in a small glass column are removed easily by passing a chelating agent solution. In addition, the activity increase after passing sample solution can be measured simply by injecting substrate solution into the buffer stream, which carries it to the column, followed by spectrophotometric detection of the product, *p*-nitrophenol, at 400 nm. The amount of zinc in the sample can be determined by measuring the increase in peak area. The lowest concentration examined was 1.3×10^{-7} g ml^{-1}.

EXPERIMENTAL

Chemicals

Bovine carbonic anhydrase C-7500 (EC 4.2.1.1) was obtained from Sigma Chemical Co. It was immobilized on cyanogen bromide-activated Sepharose 4B (Pharmacia Fine Chemicals) by mixing 10 g of the activated Sepharose and 50 mg of BCA in 1% (w/v) sodium hydrogencarbonate solution for 4 h at room temperature. After reaction, the product was filtered on a glass filter and washed with the 1% sodium hydrogencarbonate solution which contained 0.5 M in sodium chloride, followed by water. It was stored at 4°C until used for packing into the column.

The substrate, *p*-nitrophenyl acetate (GR grade; Tokyo Kasei Co.) was used as a 0.1 M solution in dimethylsulfoxide. Tris buffer (0.03 M, pH 8.0) was used for washing the enzyme column and transporting sample and substrate solutions to the column. In order to remove zinc from the enzyme, aqueous 0.01 M dipicolinic acid (pyridine-2,6-di-carboxylic acid), pH 5.0, was used. Standard aqueous solutions of zinc were prepared from zinc chloride.

Instrumentation

A schematic diagram of the measurement system is shown in Fig. 1. The reaction column, shown in Fig. 2, was prepared by packing a small amount of immobilized enzyme into a Pyrex tube (5 cm × 4 mm i.d.) to a length of 1.5 cm. Both ends of the column were packed with quartz wool to hold the immobilized enzyme. The column was connected to the line through Omnifit connectors type 102 HPO. A simple T-type syringe injection port was used

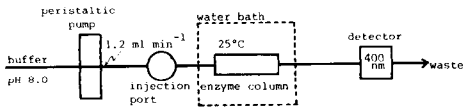

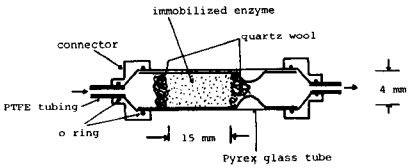

Fig. 1. Schematic diagram of the flow system.

Fig. 2. Enzyme column.

for the introduction of sample and substrate solutions; for sample volumes of $\geqslant 500$ μl a Rheodyne sample injection valve Model 5020 (teflon) was also used. The temperature of the water bath in which the reaction column was placed was controlled by circulating constant-temperature water fed by a Coolnics Circulator Model CTE 220 (Komatsu Electronics, Japan). For the detection of *p*-nitrophenol, a Hirama spectrophotometer type 6 was used. The transmittance output was converted to absorbance by a logarithmic converter (type 3151; Yokogawa Electric Co., Tokyo). The resulting peak was displayed on a chart recorder and the area integrated by a Shimadzu Model ITG-2A digital integrator (Shimadzu, Kyoto). For the construction of the flow system, PTFE tubing (2 mm o.d., 1 mm i.d.) was used.

Procedure

Dipicolinic acid solution is fed through the enzyme column at 1.0 ml min^{-1} until the activity of the enzyme becomes small (5 min). This is replaced by the buffer solution (pH 8.0) pumped at 1.2 ml min^{-1}. A 2-μl portion of substrate solution is injected into the buffer stream, and the response is measured. This measures the extent of removal of zinc from the enzyme.

A zinc sample solution is introduced through the injection port or valve into the buffer stream. After waiting for about 3 min, 2 μl of substrate solution is injected. The difference in peak areas before and after zinc injection corresponds to the amount of enzyme activity restored, and therefore to the amount of zinc in the sample solution. The system is calibrated by injecting 0.05—0.4 μg of zinc.

RESULTS AND DISCUSSION

Typical responses obtained are shown in Fig. 3. Though the peak shapes are similar, i.e., the half-height widths are almost the same, the flow rate of buffer solution and other condition affects the peak shape a little. Therefore, peak areas were measured.

Removal of zinc from the enzyme

The metal ion bound to the enzyme is zinc [10]. Kidani and Hirose [11, 12] reported on the removal of zinc from BCA by various chelating agents.

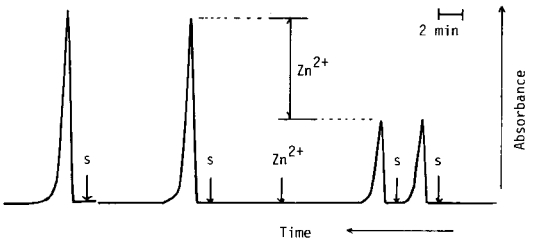

Fig. 3. Typical responses; (s) injection of substrate.

Based on their reports, dipicolinic acid at pH 5.0 was used in the present investigation. EDTA and 1,10-phenanthroline were also examined, but zinc was not removed. Figure 4 shows the time course of zinc ion removal, i.e., the decrease in activity, by the dipicolinic acid solution flowing at 1 ml min^{-1}. As can be seen, 2 min is enough to remove zinc ion from the immobilized enzyme. In subsequent experiments, 5 min was used for the removal of zinc.

Effect of pH, flow rate and substrate concentration

The activity of immobilized BCA is highest at pH 9. However, the higher the pH, the faster the non-enzymatic hydrolysis reaction proceeds. The pH of the buffer solution was chosen to be 8.0. The non-enzymatic reaction takes place slowly at this pH, so that a small response appears even after removal of zinc from the enzyme. The pH of the substrate solution was kept at 4.0 so as to prevent hydrolysis, and the solution was prepared daily. The pH of the sample solution was adjusted to 5 as was that of the chelating agent solution.

The flow rate of the buffer solution should be sufficiently fast that the rate of the enzymatic reaction is not limited by the transport rate of the substrate. The effect of flow rate is shown in Fig. 5. The slower the flow, the higher the response. When the flow rate is too low, however, problems such as peak tailing and a higher blank result. A flow rate of 1.2 ml min^{-1} was chosen for achieving a relatively high response and only slight tailing.

It is essential that the amount of substrate injected should be much larger than that of the enzyme. It was estimated that when the injected volume of substrate solution was 2 μl, 1×10^{-2} M substrate would not be sufficient for maximum sensitivity. When the concentration of substrate was increased above 0.3 M, only an increase of peak width resulted. Accordingly, 0.1 M was chosen for substrate concentration.

Calibration

A linear calibration graph for 1×10^{-8}—4×10^{-7} g was obtained under the recommended conditions. The standard deviation for 0.13 μg of zinc was 4.9% (n = 6). The effect of sample concentration was examined for a fixed amount (130 ng) of zinc by changing the concentration from 0.13 ng ml^{-1}

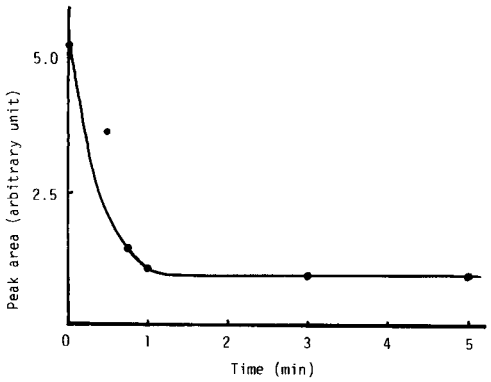

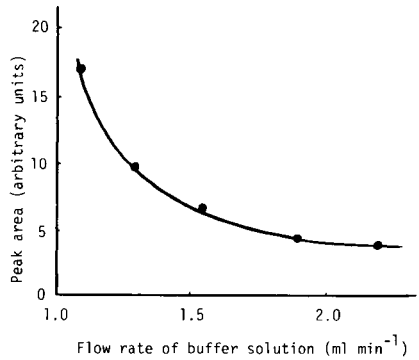

Fig. 4. Time course of the removal of zinc ion under the recommended conditions.

Fig. 5. Effect of flow rate of the buffer solution on response.

(sample volume 1 ml) to 130 ng ml (1 μl). The results (Table 1) show that there is no dependence of response on sample volume. This is an important advantage of the flow injection system, because very low concentration of zinc ions could be concentrated and determined by increasing the sample volume. In this investigation, there was a problem with the sample injection valve for introducing volumes larger than a few ml. Therefore, in this study, 10 ng ml^{-1}—400 μg ml^{-1} was the range of determination.

Effects of other ions

Though the selectivity in the batch method was found earlier to be good [5], the response to zinc ion in the presence of other ions was investigated for the flow procedure. After solutions containing 1 μg Zn^{2+} ml^{-1} and 1, 10 or 100 μg ml^{-1} of other ions had been injected, the changes of response were measured with respect to solutions which contained only 1 μg Zn^{2+} ml^{-1}. The results are presented in Table 2. Similar results were obtained by Kobayashi et al. [5]. Cobalt is another ion which activates apo-BCA. As shown in Table 2, however, its effect is slight at 1 μg ml^{-1}. Mercury(II) is an inhibitor of BCA. When its concentration is ten times more than that of zinc, no recovery of activity on introducing zinc could be observed. Inhibiting metal ions were easily removed from BCA by passing 0.04 M dipicolinic acid through the column for a few minutes, so that its activity was recovered.

Application to real samples

The developed procedure was applied to three samples. One was a hot spring water from Atami (Shizuoka prefecture, Japan), and another two were standard reference materials, Pond sediment and Yabukita tea (green tea, Japan). Before injection, the standard reference materials were digested in 8 M sulfuric acid. The results are presented in Table 3. As can be seen, the

TABLE 1

Effect of sample volume on response from 130 ng of zinc

Zn conc. ($\mu g\ ml^{-1}$)	130	13	1.3	0.13
Sample volume (μl)	1	10	100	1000
Peak area (arb. unit)	123	117	116	114

TABLE 2

Effect of other ions on the response to 1 $\mu g\ ml^{-1}$ zinc ion

Other ion	Concentration of other ion ($\mu g\ ml^{-1}$)[a]		
	100	10	1
—	100	100	100
Cu^{2+}	25	73	88
Ni^{2+}	103	—	—
Cd^{2+}	20	59	106
Fe^{3+}	30	80	100
Co^{2+}	—	327	108
Hg^{2+}	—	0	47
NO_2^-	75	—	—
NO_3^-	96	—	—
CH_3COO^-	100	—	—

[a]Sample volume was 1 ml.

TABLE 3

Application to real samples (1-ml samples injected)

Sample	Zinc content	
	Present method[a]	Reference value
Hot spring water	13 ± 2 ng ml^{-1}	11 ng ml^{-1} [b]
Pond sediment	41 ± 5 $\mu g\ g^{-1}$	34 $\mu g\ g^{-1}$ [c]
Yabukita tea	36 ± 4 $\mu g\ g^{-1}$	37 $\mu g\ g^{-1}$ [d]

[a]Mean of 3 results with standard deviation. [b]By atomic absorption spectrometry. [c]Certified value, National Institute for Environmental Studies (Japan). [d]Certified value, National Chemical Laboratory for Industry (Japan).

results obtained by the proposed method agree reasonably well with the reference values.

Conclusions

The proposed method has been proved to be useful. The advantages of the present method over other reported methods using immobilized apoenzymes are as follows. It is much faster, because removal of metal ions from the

enzyme can be done more easily and quickly than when dialysis is used. The measurement of enzymatic activity needs only a few minutes, and is done in the same apparatus. The immobilized enzyme can be used repeatedly, instead of passing to waste as in the batch method. Finally, zinc may be concentrated on the column, so that the volume of sample could well be very large, and very low concentrations of zinc could be determined [4].

REFERENCES

1 A. Townshend and A. Vaughan, Anal. Chim. Acta, 49 (1970) 366.
2 A. Townshend and A. Vaughan, Talanta, 17 (1970) 289.
3 P. Lehky and E. A. Stein, Anal. Chim. Acta, 70 (1974) 85.
4 J. V. Stone and A. Townshend, Chem. Soc. Chem. Commun., (1972) 502, J. Chem. Soc., Dalton Trans., (1973) 495.
5 K. Kobayashi, K. Fujiwara, H. Haraguchi and K. Fuwa, Bull. Chem. Soc. Jpn., 52 (1979) 1932.
6 K. Kobayashi, K. Fujiwara, H. Haraguchi and K. Fuwa, Bull. Chem. Soc. Jpn., 54 (1981) 2700.
7 L. Risinger, L. Ogren and G. Johansson, Anal. Chim. Acta, 154 (1983) 251.
8 B. Mattiasson, H. Nilsson and B. Olsson, J. Appl. Biochem., 1 (1979) 377.
9 J. J. Jasaitis, V. J. Razumas and J. J. Kulys, Anal. Chim. Acta, 152 (1983) 271.
10 S. Lindskog and B. G. Malmstrom, J. Biol. Chem., 237 (1960) 1129.
11 Y. Kidani and J. Hirose, Biochem. Biophys. Res. Commun., 82 (1978) 506.
12 J. Hirose and Y. Kidani, Biochim. Biophys. Acta, 622 (1980) 71.

Analytica Chimica Acta, 178 (1985) 217—221
Elsevier Science Publishers B.V., Amsterdam — Printed in The Netherlands

DETERMINATION OF PHOSPHATE SPECIES IN NUTRIENT SOLUTIONS AND PHOSPHORUS IN PLANT MATERIAL AS PHOSPHOVANADOMOLYBDIC ACID BY FLOW INJECTION ANALYSIS

ODDVAR RØYSET

Division of Forest Ecology, Norwegian Forest Research Institute, Postbox 61, N-1432 Ås-NLH (Norway)

(Received 4th January 1985)

SUMMARY

A flow-injection spectrophotometric method for the determination of orthophosphate is described. The signal from the yellow phosphovanadomolybdic acid complex is recorded at 400 nm. The detection limit is 0.1 mg P l^{-1} (as orthophosphate), the calibration graph is linear up to 30 mg P l^{-1} and up to 240 samples can be analysed per hour. The method is used in the determination of phosphorus in digested plant material, and is also applicable for separating free orthophosphate from acid-labile aluminium phosphate colloids in nutrient solutions.

The most frequently used spectrophotometric method for determinations of phosphate is the molybdenum blue method, in which the heteropoly acid formed between phosphate and molybdate is reduced. This method has been used in most of the applications for determination of phosphate by flow injection analysis (f.i.a.) [1—6]. Phosphate also forms a yellow heteropoly acid complex with vanadomolybdic acid, which has also been widely used in spectrophotometric determinations of phosphorus [7—9]. The phosphovanadomolybdic acid method is not as sensitive as the reduced phosphomolybdic acid method, but the reaction is very rapid and well suited for adaptation to f.i.a.

The phosphovanadomolybdic acid method has been applied in Auto-Analyzer systems [10, 11]. Basson et al. [12] described a flow-injection procedure which was applied to the determination of phosphorus in rocks and was designed for concentrations from 10 to 1600 mg P l^{-1} (as orthophosphate). The intention of this investigation was to develop a flow-injection method for the determination of phosphate species in nutrient solutions as well as phosphorus in digested plant material. This method is more sensitive than the procedure described by Basson et al. [12]. Only one reagent is necessary, and the manifold is simpler than for the molybdenum blue method [1—6].

0003-2670/85/$03.30

EXPERIMENTAL

Flow-injection equipment

A Bifok FIA-05 unit was used with a Bifok FIA-07 autosampler, Ismatec MP-13 peristaltic pump, Vitatron UPS photometer with a 400-nm filter and a 18-μl flow cell. The manifold is shown in Fig. 1.

Solutions

Vanadomolybdic acid reagent. Ammonium heptamolybdate tetrahydrate (62.5 g) is dissolved in 700 ml of demineralized water. Ammonium vanadate (2.90 g) is dissolved in 200 ml of hot water; after cooling, the solution is slowly mixed with 150 ml of 65% (w/v) nitric acid. The ammonium molybdate solution is mixed into the ammonium vanadate solution with stirring. The solution is stable for at least 4 weeks.

Standard and carrier solutions. For the analysis of plant material, the carrier solution, standards and samples were prepared in 0.10 M hydrochloric acid. For the determination of free orthophosphate in nutrient solutions, the standards and carrier solution were prepared in 0.31 mM hydrochloric acid, corresponding to a pH of 3.5 (which was the pH of the nutrient solution).

RESULTS AND DISCUSSION

Characteristics of the method

The maximum sensitivity of the method is reported to be at 315 nm [7]. The background absorption from the vanadomolybdic acid reagent increases strongly below 400 nm. In the described method, background absorption from the reagents is so high that the lowest practically possible wavelength was at 400 nm. The sensitivity decreased by about 50% at 420 nm compared to 400 nm. A mixing loop of 100 cm was sufficient for full colour development, but the baseline noise decreased with the use of a 200-cm loop.

Composition of the reagent. A nitric acid concentration in the vanadomolybdic reagent lower than 0.8 M led to high background absorption, while a nitric acid concentration above 3.0 M resulted in increased baseline noise and decreased sensitivity. At a nitric acid concentration of 2.2 M in the

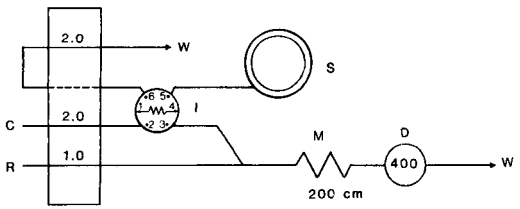

Fig. 1. Manifold for the flow-injection determination of phosphorus by the vanadomolybdic acid method. The numbers refer to pumping flow rates in ml min^{-1}. C, carrier; R, vanadomolybdic acid reagent; S, autosampler; I, injection valve; M, mixing loop; D, detector (photometer); W, waste.

reagent, the sensitivity was highest, the baseline noise was low and the sensitivity was little affected by small differences in acidity in the samples. This corresponds to 0.6 M nitric acid after mixing with the other reagents and agrees well with previous studies [9].

Interferences. According to Kitson and Mellon [14], most of the common cations and anions occurring in digested plant material will not interfere at concentrations lower than 1000 mg l^{-1}. Dissolved silica may form yellow complexes with vanadomolybdic acid, and iron may interfere by formation of yellow chloro complexes [14]. In this investigation, however, neither silica nor iron in concentrations up to 100 mg l^{-1} (highest concentration tested) gave any contribution to the signal from a 10 mg P l^{-1} orthophosphate standard.

Dynamic range and sample throughput. Some typical recorder tracings are shown in Fig. 2. With the use of a 200-μl injection loop and high recorder expansion, the refractive index signals caused by the flow cell becomes high. These false peaks are reproducible and are easily distinguished from real signals; it is therefore possible to obtain a detection limit of 0.1 mg P l^{-1} for orthophosphate. The calibration graph was linear up to 10 mg P l^{-1} and it was possible to analyze up to 100 samples per hour. With the use of a 10-μl injection loop, the linear range was extended up to about 30 mg P l^{-1} and the sample throughput could be increased to 240 h^{-1}. A further increase in the linear range can be obtained by measuring the signal at a longer wavelength.

Applications

Phosphorus in digested plant material. The flow-injection method described was applied in the routine analyses of phosphorus in digested plant material. The typical reproducibility of the method was 0.1 mg P l^{-1} (1—2% relative standard deviation) for samples containing 5—20 mg P l^{-1}. The accuracy of

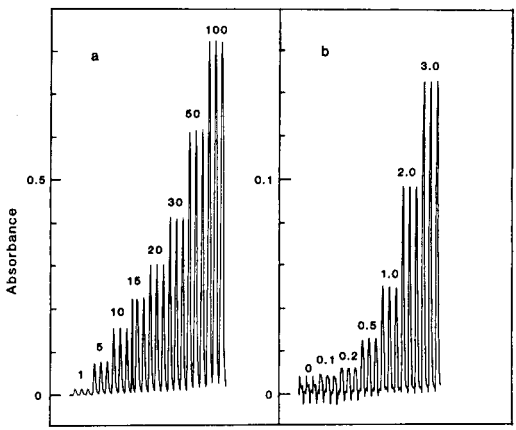

Fig. 2. Recorder signals for the flow-injection determination of phosphate with different injection loops: (a) 10 μl (5 cm); (b) 200 μl (100 cm). The numbers refer to concentrations of standard solutions in mg P l^{-1} (as orthophosphate).

the method was tested by analyzing 100 samples by the method presented here and by the phosphomolybdic acid blue method used previously in this laboratory [13]. Linear regression between the results obtained by the proposed flow-injection method (Y) and the molybdenum blue method (X) gave the regression equation $Y = 1.006\ X + 0.063$ ($r = 0.994$, $S_b = 0.013$, $S_A = 0.18$) for samples containing from 1 to 50 mg P l^{-1}.

Separation of free orthophosphate from colloidal aluminium phosphates. In this Institute, the toxicity of aluminium to small spruce and pine seedlings has been studied; in this connection, nutrient solutions containing increasing amounts of aluminium have been examined. A problem that arose when solutions at pH >3.5 were prepared was that part of the phosphate combined with aluminium, leading to a possible deficiency of phosphorus [15]. The hydrated aluminium phosphates formed to not precipitate, but form colloidal suspensions which are difficult to remove by filtration.

In all spectrophotometric methods for the determination of phosphate with molybdate reagents, the acid concentration after mixing lies between 0.5 and 1.0 M. The colloidal aluminium phosphates decompose very quickly at such acidities, leading to over-estimation of the free phosphate present. This dissolution of the aluminium phosphates can be prevented by using very short reaction times, and f.i.a. is appropriate because the reaction time is only 10 s with the flow manifold in Fig. 1. Figure 3 shows stop-flow signals for the determination of phosphate in two nutrient solutions. The signal from a sample containing only orthophosphate (a) shows that formation of the phosphovanadomolybdic acid complex has reached equilibrium after a reaction time of 10 s. The signal from a sample containing both phosphate and aluminium (e) shows a sharp increase because of dissolution of the phosphate. The two samples were prepared with the same concentration of total phosphate. Figure 3 shows that the signal for the aluminium-containing sample stabilizes in the course of about 2 min at the same height as the top of the signal for the pure orthophosphate sample, indicating that all the aluminium phosphate is completely hydrolyzed by this time. Consequently, all photometric methods operated at such a high acidity with a reaction time exceeding a few seconds will not be capable of discovering these two phosphate species.

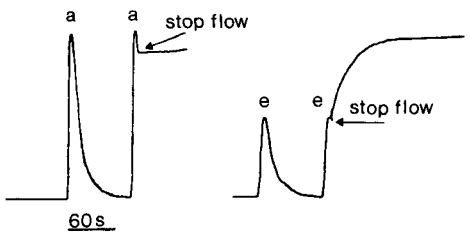

Fig. 3. Normal recorder signals and stop-flow signals for the determination of phosphorus in two nutrient solutions, both containing 4.5 mg P l^{-1} (as orthophosphate) and with a pH of 3.5. Sample (a) does not contain aluminium while sample (e) contains 80 mg Al l^{-1}.

TABLE 1

Determination of phosphate species by the flow-injection method in five nutrient solutions at pH 3.5, with a total phosphate concentration of 4.5 mg l^{-1} and increasing amounts of aluminium

Nutrient solution	Aluminium added (mg l^{-1})	Orthophosphate (mg P l^{-1})[a]	
		Free[b]	Total[c]
a	0	4.5 (±0.1)	4.5 (±0.1)
b	10	3.1 (±0.1)	4.5 (±0.1)
c	20	2.6 (±0.1)	4.5 (±0.1)
d	40	2.1 (±0.1)	4.5 (±0.1)
e	80	1.8 (±0.1)	4.5 (±0.1)

[a]Standard deviation (n = 5) in parentheses. [b]Free orthophosphate was quantified in untreated samples with carrier and standard solutions containing 0.31 mM HCl (pH 3.5). [c]Total orthophosphate was determined in samples preserved with 0.10 M HCl to decompose colloidal aluminium phosphates. The standards and carrier solutions contained 0.10 M HCl.

Table 1 shows the determination of free orthophosphate and total orthophosphate in 5 nutrient solutions. The concentration of free orthophosphate is reduced by over 60% in the nutrient solution with the highest aluminium concentration (e) compared to the sample without aluminium added (a). This possible source of phosphorus deficiency in the nutrient solution would not easily be discovered by conventional manual photometric methods. The results in Table 1 and Fig. 3 demonstrates the benefits of f.i.a. in the determination of labile species, as the reaction time is easily controlled in the flow-injection system.

The author thanks Chem. eng. Gro Sjøtveit for skilful technical assistance.

REFERENCES

1 J. Růžička and J. W. B. Stewart, Anal. Chim. Acta, 79 (1975) 79.
2 J. W. B. Stewart and J. Růžička, Anal. Chim. Acta, 82 (1976) 387.
3 E. H. Hansen, A. K. Ghose and J. Růžička, Analyst (London), 102 (1976) 714.
4 B. F. Reiss, E. A. G. Zagatto, A. O. Jacintho, F. J. Krug and H. Bergamin, Anal. Chim. Acta, 119 (1980) 305.
5 J. Růžička and E. H. Hansen, Flow Injection Analysis, Wiley, New York, 1981, p. 133.
6 Y. Hiray, N. Yoza and S. Ohashi, Chem. Lett., (1980) 499.
7 O. B. Michelsen, Anal. Chem., 29 (1957) 60.
8 H. Baadsgaard and E. B. Sandell, Anal. Chim. Acta, 11 (1954) 183.
9 K. P. Quinlan and M. A. DeSesa, Anal. Chem., 27 (1955) 1626.
10 R. J. Ferreti and W. M. Hoffman, J. Assoc. Off. Agric. Chem., 45 (1962) 993.
11 C. W. Gehrke, J. P. Ussary and J. H. Baumgahrter, J. Assoc. Off. Agric. Chem., 49 (1966) 1213.
12 W. D. Basson, J. F. van Staden and P. M. Cattin, Z. Anal. Chem., 307 (1981) 373.
13 G. Ogner, A. Haugen, M. Opem, G. Sjøtveit and B. Sørlie, The Chemical Analysis Program at The Norwegian Forest Research Institute, N-1432 Ås-NLH, Norway, 1984.
14 R. E. Kitson and M. G. Mellon, Ind. Eng. Chem. Anal. Ed., 16 (1944) 379.
15 F. P. C. Blamey, D. G. Edwards and C. J. Asher, Soil Sci., 136 (1983) 4, 197.

Analytica Chimica Acta, 178 (1985) 223—230
Elsevier Science Publishers B.V., Amsterdam — Printed in The Netherlands

COMPARISON OF FOUR CHROMOGENIC REAGENTS FOR THE FLOW-INJECTION DETERMINATION OF ALUMINIUM IN WATER

ODDVAR RØYSET

Division of Forest Ecology, Norwegian Forest Research Institute, Postbox 61, N-1432 Ås-NLH (Norway)

(Received 14th May 1985)

SUMMARY

Pyrocatechol violet (PCV), aluminon, eriochrome cyanine R (ECR) and eriochrome cyanine R with cetyltrimethylammonium bromide (ECR/CTA) are compared as chromogenic reagents for the flow-injection determination of aluminium in water. The detection limit of the ECR/CTA method is 1 μg Al l^{-1}. The detection limits of the PCV and ECR methods are 5 μg Al l^{-1}. The aluminon method is the least sensitive, with a detection limit of 50 μg Al l^{-1}. Interference from iron, fluoride, phosphate and the acidity of the sample were investigated. The interference from iron is suppressed by hydroxylammonium chloride/1,10-phenanthroline in the PCV and ECR/CTA methods at concentrations less than 5 mg Fe l^{-1}. In the ECR and aluminon methods, iron (< 5 mg l^{-1}) is masked by ascorbic acid. Fluoride at < 0.2 mg l^{-1} can be tolerated in all methods. The aluminon method can tolerate up to about 500 mg l^{-1} phosphate-P, but phosphate interferes at concentrations higher than 5 mg P l^{-1} in the three other methods. All methods are sensitive to changes in acidity of the samples; the acidity should be 0.08—0.12 M HCl.

Numerous chromogenic reagents have been investigated for the spectrophotometric determination of aluminium in water. Among these are pyrocatechol violet (PCV) [1—4], aluminon [5—8] and eriochrome cyanine R (ECR) [9—11]. Some of the characteristic properties of these reagents are shown in Table 1. Aluminon is the least sensitive of these methods. Neither ECR nor PCV can detect concentrations of aluminium lower than 5—10 μg Al l^{-1}. Both the PCV and ECR methods are too insensitive for accurate determinations of aluminium at concentrations lower than about 50 μg Al l^{-1}. Addition of cationic surfactants that form ternary complexes with aluminium and the chromogenic reagent have been shown to increase the sensitivity of some spectrophotometric methods [12]. The molar absorptivity of ECR is approximately doubled by the addition of cetyltrimethylammonium bromide (CTA) (Table 1).

Flow injection analysis is at present one of the most efficient methods of increasing the sample throughput of wet chemical methods. Most spectrophotometric methods can be adapted to this system. The aim of the work presented here was to study the adaptation of four spectrophotometric

0003-2670/85/$03.30

TABLE 1

Characteristic properties of the complexes between aluminium and pyrocatechol violet (PCV), eriochrome cyanine R (ECR), eriochrome cyanine R/cetyltrimethylammonium bromide (ECR/CTA) and aluminon

	λ_{max} (nm)	Optimum pH	ϵ l mol^{-1} cm^{-1}	Ref.
PCV	585	6.1	6.9×10^4	1, 2
ECR	537	6.0	6.5×10^4	9–11
ECR/CTA	590	6.0	1.15×10^5	12
Aluminon	525	4.1	2.0×10^4	5–8

methods to flow injection analysis in order to obtain rugged, rapid and sensitive methods. The main application of the developed methods is to the determination of aluminium in water. The effects of the commonest interfering ions in water were therefore studied.

EXPERIMENTAL

Flow-injection equipment

The apparatus consisted of a Tecator/Bifok FIA-05 flow injection analyser, a Tecator/Bifok FIA-07 autosampler, an Ismatec MP13 peristaltic pump, a Vitatron UPS photometer with 18-μl (10-mm light path) flow cell and a Vitatron UR401 recorder. The flow-injection manifold is shown in Fig. 1. The same manifold was used for all four methods. The length of the injection loop was varied according to the sensitivity required.

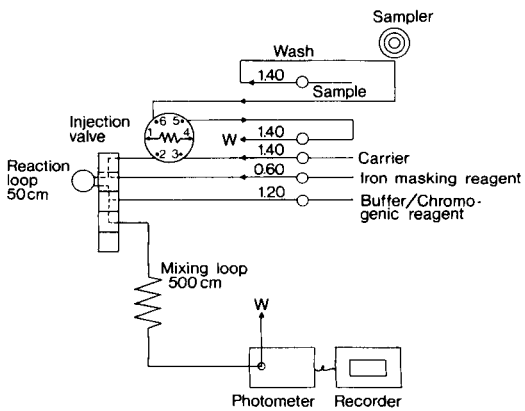

Fig. 1. Schematic flow diagram for the flow-injection manifold used for the four methods. The numbers are pumping rates given in ml min^{-1}. W, waste.

Reagents

The compositions of the reagents are shown in Table 2. To adjust the pH to the optimum level after all reagents had been mixed in the manifold, small amounts of hydrochloric acid were added to the buffer solutions in the PCV, ECR and ECR/CTA methods. In the aluminon method, the acetic acid/acetate buffer of pH 4.2 gave the optimum pH of 4.1 when mixed with the other reagents. The buffer solutions were filtered through paper filters to avoid problems with clogging of the tubings.

In these procedures, the chromogenic reagents were mixed into the buffer solutions to obtain simpler manifolds. The ECR, ECR/CTA and aluminon reagents were stable for at least 4 weeks. The PCV reagent decomposed in the course of a week and was therefore prepared daily. The chromogenic reagents (Sigma Chemical Company) were used as purchased. The qualities of the PCV reagents from various manufacturers differed. The Sigma product has been shown to be of better quality than the PCV from some other manufacturers [13].

All reagents were stored in polyethylene bottles. The carrier solution consisted of 0.10 M hydrochloric acid in demineralized water. Unless otherwise stated, all samples used in this study were prepared in 0.10 M HCl.

TABLE 2

Composition of reagents for the four methods, and wavelength of the filters used in the photometer

Method	Carrier solution	Buffer/chromogenic reagent solution	Iron masking reagent	Wavelength (nm)
PCV	0.10 M HCl	3.0 M HMTA[a] 1.0 mM PCV 0.20 M HCl	0.2 M Hydroxylammonium chloride, 10 mM 1,10-phenanthroline	585
ECR/CTA	0.10 M HCl	3.0 M HMTA 1.0 mM ECR 5 mM CTA[b] 0.25 M HCl	Same as for PCV method	585
ECR	0.10 M HCl	3.0 M HMTA 1.0 mM ECR 0.25 M HCl	0.1 M Ascorbic acid	540
Aluminon	0.10 M HCl	3.0 M Acetic acid 1.0 M Na acetate 1.0 mM aluminon	0.1 M Ascorbic acid	520

[a]Hexamethylenetetramine. [b]Cetyltrimethylammonium bromide (*N*-hexadecyl-*N,N,N*-trimethylammonium bromide).

RESULTS AND DISCUSSION

Adaptation of the methods to flow injection analysis

The pyrocatechol violet method was used earlier in this laboratory for the determination of aluminium in water [4]. Recently, the method has been adapted to a flow-injection system to give a fast method with good reproducibility and sensitivity, which will be described elsewhere. In the adaptation of the other three methods to flow injection analysis, the systems were designed to facilitate comparison with the pyrocatechol violet method. The three other methods therefore do not necessarily represent optimized systems.

Most spectrophotometric methods have relatively narrow pH optima, as the formation of the complex is pH-dependent and the background absorption of the excess of reagent varies with pH. In most cases, the pH therefore must be controlled within 0.1—0.2. Unfortunately there are relatively few buffers with strong buffering capacity around 6.0—6.2, which is the optimum for the PCV, ECR and ECR/CTA methods. Neither phosphate nor di- or tri-carboxylic acids can be used as buffers as they form strong complexes with aluminium. Hexamethylenetetraamine with a pK_a value of 5.1 has been used as a buffer at pH 6.1 in the PCV method [4]. The buffering capacity towards the acidic side is high, but smaller towards the alkaline side. To compensate for the weakness of the buffer in the PCV, ECR and ECR/CTA methods, an almost saturated buffer solution (3 M) was used.

Effect of acidity of samples. The effect of the acidity of the samples on the sensitivity is shown in Fig. 2. The sensitivity varies considerably in all methods when the hydrochloric acid concentration varies from 0.5 M to 0.0001 M. Especially the aluminon method is sensitive to changes in sample pH. It is therefore important that the acidities of the samples, carrier and standards be equal. When the carrier and standards are prepared in 0.10 M HCl, the acidity of the sample must be within 0.08—0.12 M HCl to avoid

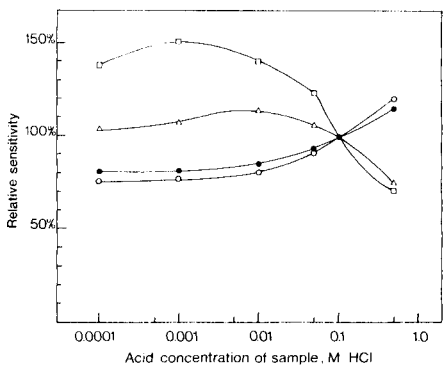

Fig. 2. Effect of acidity of the sample on the determination of aluminium. The sensitivity is calculated relative to a sample containing 0.10 M HCl (= 100%). Reagent: (△) PCV; (○) ECR; (●) ECR/CTA; (□) aluminon.

errors greater than 2—3%. This treatment of the samples is easy to obtain as water samples usually are preserved in 0.10 M HCl.

Interference studies

The most severe interferences in spectrophotometric methods for the determination of aluminium in natural water samples are caused by fluoride, phosphate and iron. Many heavy metal cations also form coloured complexes with these chromogenic reagents, but to give any significant light absorption they must be present in concentrations higher than 0.1 μM, which rarely is the case in natural waters. The interferences from fluoride, phosphate and iron were studied by preparing standard solutions containing 1.0 mg Al l^{-1} plus increasing amounts of the interfering species. The sensitivity was calculated relative to a sample containing 1.0 mg Al l^{-1} without interferent.

Both low-molecular-weight organic acids and high-molecular-weight humic compounds form complexes with aluminium. The stabilities of these organoaluminium complexes are highly variable, and the intensities of these interferences are therefore difficult to predict. Methods for the determination of aluminium in water therefore involve a digestion procedure to remove the organic compounds [4], or a speciation procedure where the organic aluminium complexes are separated from the inorganic species of aluminium [14]. No efforts were made to evaluate these possible interferences.

Iron interference. Iron interferes by forming coloured complexes with most of the chromogenic reagents used for aluminium. This leads to positive errors as the iron complex usually also absorbs at the wavelength used for aluminium. Various masking reagents for iron have been proposed. The best have been shown to be hydroxylammonium chloride/1,10-phenanthroline [1, 2] or ascorbic acid [5, 11].

Figure 3(a) shows that hydroxylammonium chloride/1,10-phenanthroline suppresses the iron interference up to concentrations of about 5 mg Fe l^{-1} in both the PCV and ECR/CTA methods, whereas it does not mask the interference in the ECR method. This is because the iron/1,10-phenanthroline complex (absorption maximum at 510 nm) also absorbs light at the wavelength (540 nm) used for the ECR method. Figure 3(b) shows that ascorbic acid suppresses the iron interference in the aluminon method up to 20 mg Fe l^{-1}, whereas the interference is masked up to about 5 mg Fe l^{-1} in the ECR method. Ascorbic acid does not suppress the iron interference in the PCV and ECR/CTA methods.

Fluoride interference. Fluoride interferes by forming such stable complexes with aluminium that the formation of the complex with the chromogenic reagent is prevented. Figure 4(a) shows that the interference effect produces a <10% reduction in sensitivity for concentrations up to 0.5 mg F l^{-1} in the PCV and ECR methods. The aluminon and ECR/CTA methods are somewhat more sensitive to the fluoride interference, but up to 0.2 mg F l^{-1} can be tolerated.

Phosphate interference. Phosphate interferes in the same manner as

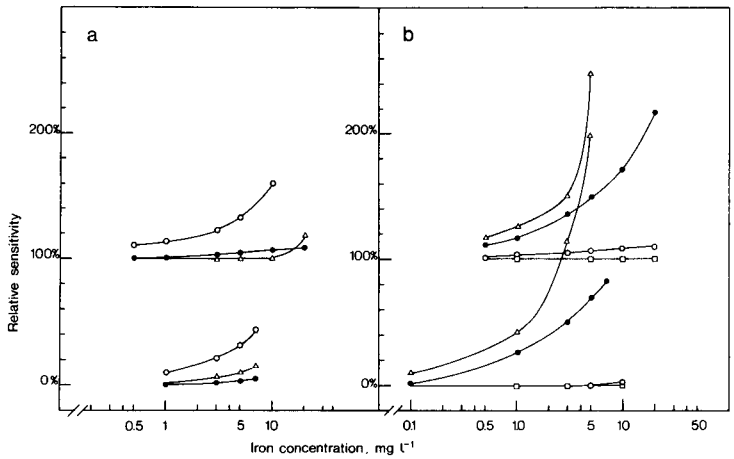

Fig. 3. Interference from iron on the determination of aluminium. Iron is masked by (a) hydroxylammonium chloride (0.2 M)/1,10-phenanthroline (10 mM) or (b) ascorbic acid (0.1 M). The upper curves show the sensitivity of a 1.0 mg Al l^{-1} standard plus increasing amounts of iron (1.0 mg Al l^{-1} = 100%). The lower curves show the signal from iron alone calculated relative to the signal from a sample containing 1.0 mg Al l^{-1}. Reagent: (△) PCV; (○) ECR; (●) ECR/CTA; (□) aluminon.

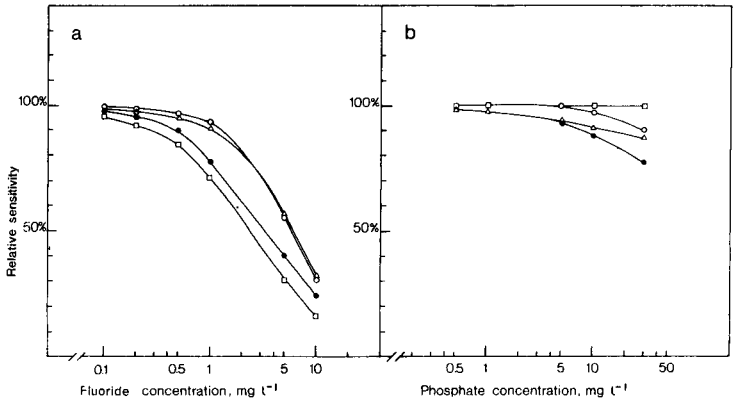

Fig. 4. Interference from fluoride (a) and phosphate (b) on the determination of aluminium. The samples contained 1.0 mg Al l^{-1} plus increasing amounts of fluoride or phosphate. The sensitivity is calculated relative to a sample which contained only 1.0 mg Al l^{-1} (=100%). Reagent: (△) PCV; (○) ECR; (●) ECR/CTA; (□) aluminon. Phosphate concentrations are given for phosphate-P in mg l^{-1}.

fluoride, by forming stable complexes with aluminium. The stability of the aluminium phosphate species is highly pH-dependent. The lowest solubility of the aluminium phosphates is at a pH around 6.0, while it is about 10 000 times more soluble at pH 4.0. Therefore, one might expect that spectrophotometric methods with pH optima around 6.0 would be more affected

than methods with optima at lower pH values. Figure 4(b) shows that the aluminon method which is monitored at pH 4.1—4.2 is unaffected at a concentration of 30 mg l^{-1} phosphate-P. The three other methods showed interference from 1—10 mg l^{-1} phosphate-P. The aluminon method tolerated up to 500 mg l^{-1} phosphate-P without significant interference.

Performance of the methods

Sensitivity. The calibration graphs for the four methods are compared in Fig. 5. The sensitivity of the aluminon method is so low that it cannot be used for the determination of aluminium at concentrations lower than 100 μg Al l^{-1}. The sensitivities of the PCV and ECR methods are nearly identical. With these two methods, it is possible to determine aluminium down to 5—10 μg Al l^{-1}.

The addition of the cationic surfactant CTA to ECR leads to a remarkable increase in sensitivity. The sensitivity of the ECR/CTA method is about three times higher than that of the ECR and PCV methods. The detection limit is about 1 μg Al l^{-1}, and the method is therefore capable of providing very precise determinations of aluminium at low concentrations.

Reproducibility of the methods. The typical reproducibility for the PCV method was 1—2% relative standard deviation for aluminium concentrations in the range of 100—500 μg Al l^{-1}. Both the ECR and ECR/CTA method showed the same reproducibility for the time they were studied. The within-sample precision of the aluminon method was also good, but this method showed up to 5—10% drift in sensitivity within an hour and was therefore inconvenient in use.

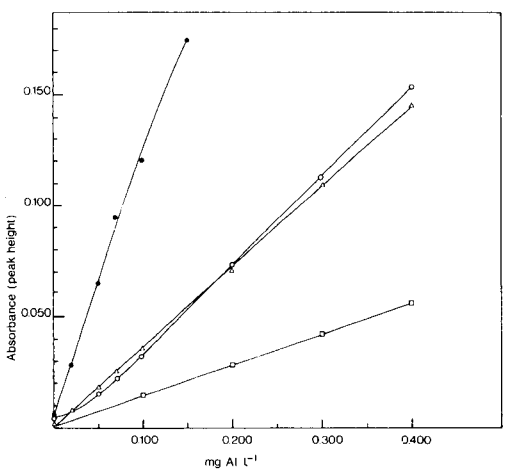

Fig. 5. Calibration graphs for the four methods. The flow injection manifold used was as shown in Fig. 1 with a 100-cm (200-μl) injection loop. The reagents used were as described in Table 2: (△) PCV; (○) ECR; (●) ECR/CTA; (□) aluminon.

Conclusions

The interference study demonstrates that fluoride gives the most intense interference in the four flow-injection spectrophotometric methods presented. In most natural waters, the fluoride concentration is below 0.5 mg l^{-1}. The fluoride interference effect can be neglected in most cases when the PCV and ECR methods are used for determination of aluminium in water. The ECR/CTA and aluminon methods are somewhat more sensitive to interference from fluoride concentrations below 0.5 mg l^{-1}. The iron concentration in natural waters is usually less than 1 mg l^{-1}. When hydroxylammonium chloride/1,10-phenanthroline or ascorbic acid is used as a masking reagent, iron at such concentration levels will not cause serious interference problems. The interference effect from phosphate can also be neglected in most cases, as the phosphate concentration in natural waters is well below 1 mg l^{-1} (as phosphate-P). However, if these methods are used for the determination of aluminium in, for example, digested plant material, the phosphate concentration in the solution may become so high that it causes significant interference. In such cases, the aluminon method might be preferable as it is insensitive to phosphate interference.

The sensitivities of both the ECR and PCV methods are satisfactory for the determination of aluminium in natural waters in most cases. The ECR/CTA method shows very good sensitivity, and this method might be advantageous in determination of aluminium in neutral waters where the concentration is usually below 50 μg l^{-1}. However, the interference effects from the commonest ions in water merit better investigation. For determinations of aluminium in water, the ECR methods seemed to have no special advantages compared to PCV. Pyrocatechol violet is therefore still the chosen chromogenic reagent for routine determinations of aluminium in water in this laboratory.

REFERENCES

1 A. D. Wilson and G. A. Sergeant, Analyst (London), 88 (1962) 109.
2 W. K. Dougan and A. L. Wilson, Analyst (London), 99 (1974) 413.
3 A. Henriksen and I. M. Bergman Paulsen, Vatten, 4 (1975) 339.
4 G. Ogner, A. Haugen, M. Opem, G. Sjotveit and B. Sorlie, The Chemical Analysis program at The Norwegian Forest Research Institute, 1984, Norwegian Forest Res. Inst., 1432 Aas-NLH (1984).
5 T. C. Z. Jayman and S. Sivasubramanian, Analyst (London), 99 (1974) 296.
6 P. M. Bertsch, M. M. Alley and T. L. Ellimore, Soil Sci. Soc. Am. J., 45 (1981) 666.
7 R. A. Khalid, Soil Sci. Soc. Am. J., 41 (1977) 448.
8 P. H. Hsu, Soil Sci., 96 (1963) 230.
9 L. H. Jones and D. A. Thurman, Plant Soil, 9(2) (1957) 131.
10 V. T. Hill, Anal. Chem., 38 (1966) 654.
11 B. F. Reiss, H. Bergamin, E. A. G. Zagatto and F. J. Krug, Anal. Chim. Acta, 107 (1979) 309.
12 Z. Marczenko and M. Jarosz, Analyst (London), 107 (1982) 1432.
13 I. Caspari, Ref bla., Norw. Inst. Water Res., Oslo, 1 (1984) 9.
14 C. T. Driscoll, Ph.D. Thesis, Cornell University (1980); Int. J. Environ. Anal. Chem., 16 (1984) 267.

Analytica Chimica Acta, 178 (1985) 231—237
Elsevier Science Publishers B.V., Amsterdam — Printed in The Netherlands

IN VIVO MEASUREMENTS WITH A POTASSIUM ION-SELECTIVE MICROELECTRODE BASED ON A NEW BIS(CROWN ETHER)

J. TARCALI, G. NAGY, K. TÓTH and E. PUNGOR*

Institute for General and Analytical Chemistry, Technical University of Budapest, Gellért tér 4, 1521-Budapest (Hungary)

G. JUHÁSZ and T. KUKORELLI

Department of Comparative Physiology, Eötvös Loránd University, Budapest (Hungary)

(Received 15th January 1985)

SUMMARY

Potassium ion-selective microelectrodes with a tip diameter of 10 μm are described. The ionophore used is 2,2'-bis[3,4-(15-crown-5)-2-nitrophenylcarbamoxymethyl]tetradecane in a conventional mixture with sodium tetraphenylborate, an ether and PVC. The electrode provides Nernstian response over the range 10^{-5}—10^{-1} M potassium activity. Its selectivity is shown to be similar to that of a valinomycin-based microelectrode. After the electrode has aged for 24 h, the 95% response time at the 10^{-3} M potassium ion level is 2.0 ± 0.5 s. The applicability of the bis(crown ether) electrode for measurements in vivo is proved by monitoring the changes in potassium activity in different areas of the brain of anaesthetized rats after administration of veratrine.

Experimental life sciences are now one of the most exciting fields of application of ion-selective electrodes. The desire to obtain chemical information from living objects with no or only minor invasive effects arising from the chemicals needed in most analytical procedures has produced substantial efforts towards miniaturizing the measuring electrodes. Orme [1] invented the microcapillary type of ion-selective electrode, but many other workers (see, e.g., [2—6]) have contributed to the development of special types of widely applicable microelectrodes, measuring methods and apparatus. Electrodes with measuring tips having submicrometer diameters are now frequently prepared to monitor intracellular ion activities. Easily made electrodes with measuring tips of a few micrometers are regularly used in extracellular measurements.

Among the various potassium-selective electrodes developed so far, the neutral-carrier type based on valinomycin [7] has gained the broadest acceptance in different fields of conventional analysis. The valinomycin-based potassium-selective electrodes outperform the other sorts in the most important aspects of selectivity and sensitivity. Yet, for studies in vivo, microcapillary electrodes based on charged ion-exchanger materials (e.g., Corning type 477317) are often used. This is a compromise with selectivity to gain lower resistance.

0003-2670/85/$03.30

Several groups have studied crown-ether compounds in order to develop ion-selective electrodes. Petranek and Ryba [8], Rechnitz and Eyal [9], and others [10] have described crown ether compounds applicable for potassium ion-selective electrodes. Töke et al. [11] have recently described a bis(crown ether) molecule which is suitable for producing stable potassium-selective electrodes. The new potassium electrode closely approaches the performance of the valinomycin-based ones in most important analytical characteristics. The physical features of the solution used to prepare the membrane proved to be suitable for preparing a micropipette-type potassium electrode based on this ionophore. In the work described below, the selectivities of this potassium-selective electrode and of the valinomycin-based electrode are compared.

The applicability of the electrodes in vivo was proved by following the extra-cellular potassium activity in the cortex of anaesthetized rats. Veratrine was used as a drug to induce substantial changes in the potassium activity in the brain area adjacent to the measuring tip of the potassium-sensing micropipette.

The bis(crown ether) used in these electrodes is 2,2-bis[3,4-(15-crown-5)-2-nitrophenylcarbamoxymethyl] tetradecane (BME 44).

BME-44

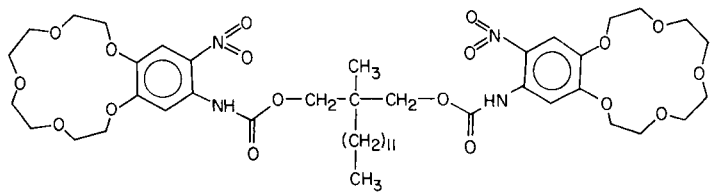

(I)

EXPERIMENTAL

Preparation of the electrodes

To prepare the potassium microelectrodes, micropipettes with tips of 5—10 μm diameter were pulled from ordinary sodium glass capillaries (0.5—0.6 mm i.d.) using a horizontal puller. The glass tubes were previously soaked in a (1 + 1) mixture of concentrated sulphuric acid and 30% hydrogen peroxide for 24 h, washed until neutral with distilled water and dried at 100°C. The tips of the dry pipettes were dipped in silanizing solution for a few seconds so that the liquid rose into the capillary to a length of about 200 μm. The silanization was completed by drying the pipettes in a covered Petri dish at 100°C for 1 h. The ion-exchanger solution was introduced into the silicone-coated pipettes by capillary action and slight suction. The pipettes were back-filled with 0.5 M KCl internal filling solution. Thin chloridized silver wire served as the internal reference electrode. The electrodes were soaked in saline solution when not in use.

The ion-exchanger solution was prepared as follows. First, 80.6 mg of *o*-nitrophenyl octyl ether (Fluka) and 13 mg of powdered poly(vinyl chloride)

(PVC; Ongrovill) were dissolved in 200 μl of tetrahydrofuran (THF). To this solution, 5 mg of BME-44 and 1.36 mg of sodium tetraphenylborate was added. The bright orange solution formed was diluted with THF occasionally if it became too thick as the solvent evaporated.

The silver/silver chloride reference electrodes used were prepared from micropipettes (5—10 μm diameter) with 0.156 M sodium chloride as the filling solution and electrically chloridized silver wire.

A home-made battery-powered apparatus with two symmetric high-impedance inputs was used to measure and follow the cell voltage. The first parts of this equipment (AD-515 IC-based voltage followers) were placed in a shielded small capsule, which could be placed in the immediate vicinity of the electrodes. For in-vivo measurements, the capsule could be attached to the head of the experimental animal.

Surgical procedure

Five Wistar rats (350—400 g) were anaesthetized with nembutal (50 mg kg^{-1}). Animals were fixed in a stereotaxic frame (David Kopf) and the right somatosensory cortex was exposed by removing the bone. The potassium-selective electrode and the Ag/AgCl reference electrode were inserted into the cortex by means of a stereotaxic electrode holder. The distance between the electrodes was less than 100 μm. A gold-plated dental screw was driven into the right frontal bone for grounding. The electrode leads were attached into the input capsule mounted on the electrode holder. Veratrine crystals were placed directly onto the cortical surface in the close vicinity of the electrodes.

RESULTS AND DISCUSSION

Characteristics of the micropipette electrodes

After preparation, the functioning of the micropipette electrodes was checked by calibrating them with standard potassium chloride solution at room temperature. A typical calibration curve is shown on Fig. 1; the linear section of the curve ends at about 10^{-5} M potassium ion; a slope of 56—58 mV/decade was obtained for 10^{-5}—10^{-1} M potassium ion. Electrodes showing calibration slopes less than 50 mV/decade were not considered for further use. In preparing the calibration curves, the activity coefficients used were taken from Dobos [12].

To study the response times of the electrodes, the potassium-selective and reference electrodes were placed in 9.91 ml of a solution containing sodium chloride at the physiological concentration (0.156 M) and 10^{-3} M potassium chloride. A high rate of stirring was maintained with a magnetic stirrer and the cell potential was monitored. After a steady value had been attained, a fast concentration increase was obtained by injection of 90 μl of 1 M KCl. The time between the addition and the attainment of 95% of the total potential change was considered as the response time. It was found to be

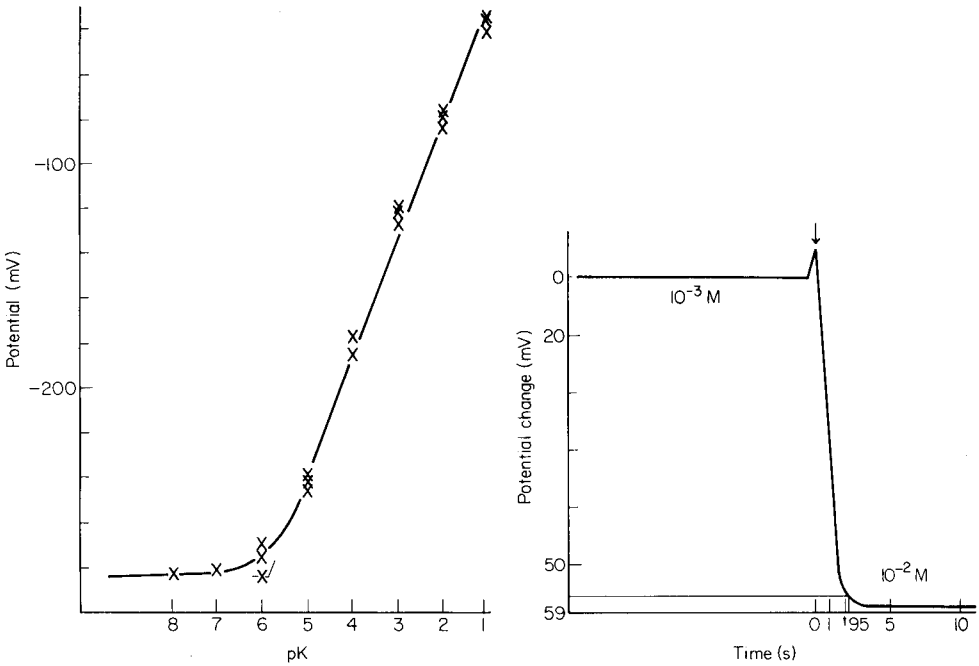

Fig. 1. Response of the BME-44 micropipette electrode with a tip diameter of 10 μm. Potential measured against a double-junction Ag/AgCl reference, with three measurements at each potassium concentration.

Fig. 2. Response time of a 1-day old BME-44 micropipette electrode (10 μm tip diameter) to a change in concentration from 10^{-3} M KCl to 10^{-2} M KCl. The arrow indicates the time of injection. For detail, see text.

ca. 10 s for freshly prepared electrodes. Further experiments showed a dramatic decrease of the response time as the electrode aged. One-day-old electrodes showed an average response time of 2.0 ± 0.5 s (n = 5). A recording of the response to a concentration change obtained with a one-day-old electrode previously used for an in vivo experiment is shown in Fig. 2. The decrease in the response time is most probably caused by structural rearrangements in the ion-selective membrane during solvent evaporation in the early stage of the electrode life.

The selectivity of these electrodes was evaluated by using the mixed solution method. The concentration of the interfering ion was kept constant at 0.1 M and the potassium activity was changed. However, when the sodium selectivity was measured, the physiological concentration (0.156 M) of sodium ion was used. Figure 3 shows the selectivity coefficients obtained for the BME-44 electrode, compared with selectivity data for a valinomycin-based micropipette electrode; the latter were measured [13] by the separate

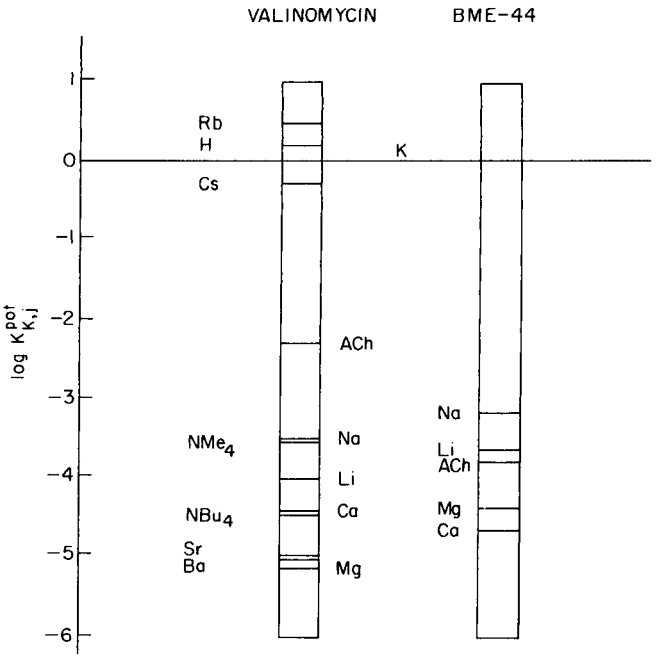

Fig. 3. Comparison of the selectivity coefficients (log $K^{pot}_{K,j}$) for the valinomycin [13] and BME-44 electrodes.

solutions method. Because of the different methods of evaluation, direct comparison of the selectivities of the two types of electrode is questionable, but it can be concluded that the new electrode has adequate selectivity for application to measurements in vivo.

The stability of the microelectrodes appeared to be good. The electrodes could be used or kept in the saline solution containing KCl in 10^{-2} M concentration without noticeable changes of their performance for 3—4 weeks. Electrodes implanted in different brain regions of experimental animals showed a stable function for days and, in most cases, their performance in vitro showed no substantial changes after they had been used for in vivo experiments.

Application to in vivo experiments

In order to prove the applicability of the electrodes in vivo, the potassium electrodes together with the closely attached micro reference electrode were introduced into the cortex of anaesthetized rats as described under Experimental. Introduction of the electrodes produced a relatively high potential, reflecting a high potassium activity. Most probably, this was a consequence of rupture of the tissue around the measuring tip. After some decrease, a steady value was obtained. A small crystal of veratrine was then placed on the cortical surface very close to the electrode. The pharmacological effect of the different veratrum alkaloids has been widely studied [14, 15]. Local

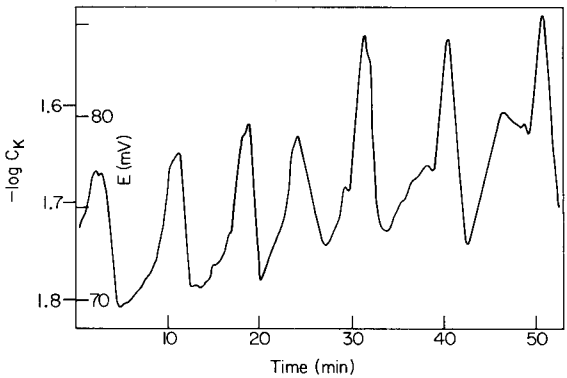

Fig. 4. Recording of cell potential (mV vs. Ag/AgCl) with time after administration of veratrine. The corresponding potassium concentration is also given.

administration of the strongly depolarizing veratrine should induce an increase in the potassium activity in the extracellular space. Indeed, shortly after this administration, there were dramatic changes in the cell potential. A recording of cell potential vs. time for some hours after administration of the drug showed regular oscillations indicating periodic increase of the potassium activity followed by its return to near the original value. Figure 4 shows a typical section of a trace obtained with one of the rats (No. 3); the potassium concentrations given in the figure were evaluated from the cell potentials by using a calibration curve obtained in vitro. Potassium maxima appeared at intervals of 4—8 min. The veratrine-induced depolarization produced changes in extracellular potassium concentration as large as 30 mM in the studied area of the rat cortex.

The repetitive depolarizing action of the veratrum alkaloid cevadine on striated muscle [16, 17] that of veratridine on rat brain [18] has been described earlier. After the veratrine administration, the depth of narcosis decreased and increased respiration frequency was observed. In most cases, an additional dose of nembutal was necessary to maintain the narcosis.

REFERENCES

1 F. W. Orme, in M. Lavallée, O. F. Schanne and N. C. Hebert (Eds.), Glass Microelectrodes, Wiley, New York, 1969, 376.
2 J. L. Walker, Anal. Chem., 43 (1971) 90A.
3 I. Dietzel, U. Heinemann, G. Hofmeier and H. D. Lux, Exp. Brain Res., 40 (1980) 432.
4 R. C. Thomas, Ion-sensitive Intracellular Microelectrodes, Academic Press, London, 1978.
5 F. Vyskocil and N. Kriz, Pfluegers Arch., 337 (1972) 265.
6 C. Nicholson, G. ten Bruggencate, H. Stöckle and R. Steinberg, J. Neurophysiol., 41 (1978) 1027.
7 Z. Stefanac and W. Simon, Chimia, 20 (1966) 436.
8 J. Petranek and O. Ryba, Anal. Lett., 72 (1974) 375.
9 G. A. Rechnitz and E. Eyal, Anal. Chem., 44 (1972) 370.

10 E. Pungor, K. Tóth, in H. Freiser (Ed.), Ion-Selective Electrodes in Analytical Chemistry, Plenum Press, New York and London, 1980, 143 pp.
11 L. Töke, B. Ágai, J. Bitter, E. Pungor, K. Szepesváry, E. Lindner, M. Horváth and J. Havas, Europatent PCT Int. Appl. W 0.8300, 149 ICl. CO7 J5/18/1983; HU. Appl. 81/1999, 1981, 34 pp.
12 P. Dobos, Elektrokémiai táblázatok, Müszaki Könyvkiadó, Budapest, 1979.
13 P. Wuhrmann, H. Ineichen, U. Riesen-Willi and M. Lozzi, Proc. Natl. Acad. Sci. USA, 76 (1979) 806.
14 M. C. W. Minchin, J. Neurosci. Methods, 2 (1980) 111.
15 T. L. Török, Z. Salamon, T. T. Nguyen and K. Magyar, Quart. J. Exp. Physiol., 69 (1984) 1.
16 M. Danko, J. Cseri and E. Varga, Acta Phys. Acad. Sci. Hung., 58 (1981) 103.
17 M. Danko, J. Cseri and E. Varga, Acta Phys. Acad. Sci. Hung., 58 (1981) 275.
18 G. Nagy, A. Oke, B. Moghadam and R. N. Adams, Unpublished work.

Analytica Chimica Acta, 178 (1985) 239—246
Elsevier Science Publishers B.V., Amsterdam — Printed in The Netherlands

MULTICOMPONENT DETERMINATIONS IN FLOW-INJECTION SYSTEMS WITH SQUARE-WAVE VOLTAMMETRIC DETECTION USING THE KALMAN FILTER

CAROLINE A. SCOLARI and STEVEN D. BROWN*[a]

Department of Chemistry-4630, Washington State University, Pullman, WA 99164 (U.S.A.)

(Received 22nd July 1985)

SUMMARY

Electrochemical detection in flow-injection systems has become increasingly popular. Scanning electrochemical methods of detection have received less attention. The use of rapid square-wave voltammetric detection for flow injection is described. Experimental considerations for the use of square-wave voltammetric detection are discussed. Results of the application of this combination are shown for dopamine in 0.28 M sulfuric acid, and for lead(II) and thallium(I) in 0.9 M nitric acid. A linear, recursive estimator known as the Kalman filter is used to resolve overlapping responses. Empirical models consisting of the square-wave voltammetric responses of single species are used. Results are shown for mixtures of lead(II) and thallium(I) in 0.9 M nitric acid.

Flow injection is a technique which involves injection of a sample into a flowing unsegmented carrier stream, followed by controlled dispersion and detection. Electrochemical methods have become increasingly popular for detection because of their sensitivity. Scanning electrochemical methods have received less attention, although these methods have the additional advantages of the positive identification of sample components and the possible identification of interferents. A few applications of scanning voltammetric detection have appeared; Janata and Růžička [1] have successfully shown the application of linear sweep voltammetry, and Wang and DeWald [2] have shown the application of rapid differential pulse voltammetry as a detection method for flow injection. The comparative lack of attention can be attributed to the increased difficulty involved in performing the scanning voltammetric experiment versus the amperometric experiment. In order to get the maximum advantage from rapid-scan voltammetric detection, it is necessary to optimize the electrochemical cell design for maximum sensitivity and lowest possible response time. The more significant difficulty, however, is the necessity that each dispersed zone be sampled at the same point in time and space. This problem is not insurmountable, especially given the availability of microcomputers to sample the data with precise timing. Another difficulty which occurs when scanning voltammetric

[a]Present address: Department of Chemistry, University of Delaware, Newark DE 19716, U.S.A.

0003-2670/85/$03.30

methods are used is overlapping voltammetric responses. Because the sample dispersion, and thus the detector response, is dependent on a number of experimental factors, it is not convenient to use procedures requiring a theoretical model to effect the resolution of these responses. However, the flow-injection sample zone is very reproducible in both space and time, which would make the use of empirical models feasible. The Kalman filter has been demonstrated to allow resolution of overlapped static electrochemical responses using empirical models. The models consist of measured voltammetric responses for single components [3, 4]. This work will demonstrate the use of rapid-scan square-wave voltammetric detection for flow injection, with resolution of closely overlapping responses using the Kalman filter.

Kalman filter

The details of the use of the Kalman filter for multicomponent determinations have been reported elsewhere [3]. The Kalman filter is a recursive linear estimator which, in essence, provides a point-by-point linear mean-square fit of the model component responses to the experimental data.

The filter requires models for the system dynamics and the measurement process. Even though the sample disperses as it traverses the flow-injection system, the dispersion is very reproducible in both space and time. Therefore, the concentration of each component present at each point in the dispersed zone is proportional to the concentration of the original sample injected into the system. So long as the dispersed zone is sampled at the same point in time after injection and the experimental conditions remain constant, the current response will be proportional to the concentration of the component present in the injected sample. Therefore, as in the static case [4], a simple system dynamics model can be used. The model used is

$$Z(k) = \mathbf{S}^{\mathrm{T}} \cdot \mathbf{X}(k) + v(k) \tag{1}$$

which relates the measurement of current, $Z(k)$, at potential k to the component concentrations by a proportionality vector, $\mathbf{S}^{\mathrm{T}}$. The elements of this vector are simply the slopes of the current/concentration relationship obtained for each of the N pure components included in the model. Here, the elements of $\mathbf{X}(k)$ are the N pure component concentrations at potential k, and the elements of $v(k)$ are the measurement noise present at potential k. The output is a statistically optimal estimate of the N component concentrations, provided that certain noise assumptions [3, 5] are met, although substantial deviations from the noise requirements appear to have little effect on the quality of the results [6].

EXPERIMENTAL

Reagents

Two chemical systems were used in this work: dopamine in 0.28 M sulfuric acid, and mixtures of lead and thallium in 0.9 M nitric acid. A stock

solution of 1.014×10^{-2} M dopamine was prepared by dissolving reagent-grade dopamine in 0.28 M sulfuric acid prepared by diluting reagent-grade acid with deionized water. The dopamine stock solution was diluted to desired concentrations with 0.28 M sulfuric acid. A stock solution of 1.877×10^{-2} M lead(II) was prepared by dissolving reagent-grade lead nitrate and then diluting with Super-Q water. A stock solution of 2.24×10^{-2} M thallium(I) was prepared by dissolving reagent-grade thallium(I) sulfate (99.5%) in dilute nitric acid. These solutions were standardized with EDTA by using methods described by Schwarzenbach and Flaschka [7]. Lead(II) and thallium(I) stock solutions were diluted to the desired molarities with 0.9 M nitric acid, prepared by diluting reagent-grade acid with distilled water. A stock solution of 1×10^{-2} M mercury(II) was prepared by dissolving liquid mercury in a minimum amount of dilute nitric acid. The mercury plating solution was 2×10^{-4} M mercury(II) in 0.1 M potassium nitrate, kept at pH 4 with an acetate buffer. The acetate buffer was prepared from reagent-grade sodium acetate and acetic acid.

Apparatus

The carrier and plating solution reservoirs were Omnifit glass reagent bottles with 1-l capacity. Switching between carrier and plating solutions was accomplished with a 3-way Rheodyne type 50 teflon rotary valve. The sample injector was an Altex 202-00 rotary injection valve. A 500-μl sample loop was used for the lead/thallium system on mercury-coated glassy carbon, while a 100-μl sample loop was used for the dopamine runs, and for the lead/thallium system on mercury-coated gold. The trigger to the computer to signal sample injection was a modified event marker (Phase Separations). All connections within the flow-injection system were made with 0.5-mm i.d. teflon tubing. The distance from the injector to the detector was 65 cm. For the dopamine system, the carrier solvent was propelled through the flow-injection system using a Masterflex variable speed pump, which was also used to propel the mercury(II) plating solution. The 0.9 M nitric acid carrier solution for the lead/thallium system was deaerated and propelled through the flow-injection system with argon; the gas pressure was controlled with a Matheson 70A gas microregulator. The Hg(II) plating solution and the Pb(II) and Tl(I) sample solutions were also deaerated with argon before use. The flow rate used in the lead/thallium experiments was 2.0 ml min^{-1}.

Temperature control was achieved with a Haake E-12 water temperature bath with tempering beakers situated at the carrier reservoir, injector, and the stretch of tubing before the detector. All tubing in the system between the carrier reservoir and the detector was placed in 2-mm i.d. tygon tubing for insulation and retardation of oxygen permeation. The entire system was placed inside an insulated aluminum box, which acted as a Faraday cage. The potentiostat used to apply potentials to the cell was an IBM EC-225-3A interfaced to an LSI-11/23 microcomputer, as described previously [8].

Computer programs. The square-wave voltammetric data-collection program has been described previously [4]. The program was modified to allow an external device to trigger the computer to enter a specified wait period, and upon completion of the wait period, to control the square-wave scan. The waiting time is specified by the user, as are the other scan parameters. The resulting voltammograms were Fourier-filtered and background-subtracted prior to application of the Kalman filter. Details of these methods have been reported previously [9]. The Kalman filter was a modified version of the FORTRAN program previously reported [3].

Flow-through cell

The flow-through wall-jet cell configuration used in these experiments is shown in Fig. 1. The wall-jet configuration has the advantages of high sensitivity and minimal electrode fouling. The body of the cell is made of two halves, both constructed of polypropylene, separated by a polyethylene spacer. The bottom half, with dimensions 5 cm × 3 cm × 1.5 cm contains the inlet and outlet channels and the counter electrode, which is a platinum button press-fitted into the polypropylene block. Electrical connection is made to a copper wire with a drop of mercury. The copper wire then extends out of the cell and is fixed in place with epoxy resin. The inlet and outlet channels are threaded to allow connection to standard low-pressure chromatographic fittings. The top block (5 cm × 3 cm × 4 cm) contains the working electrode and the reference electrode. Bioanalytical Systems glassy carbon and gold electrodes were used. The working electrode is pressed into position, and the teflon sleeve is screwed in for a secure fit. The reference electrode chamber is connected to the flow system via a porous teflon frit. Some 3 M sodium chloride solution is introduced into the chamber and a Bioanalytical Systems RE-1 silver/silver chloride reference electrode is pressed into position. The counter electrode is approximately 4 mm from

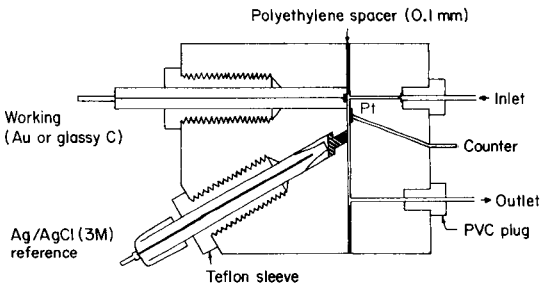

Fig. 1. Electrochemical flow cell.

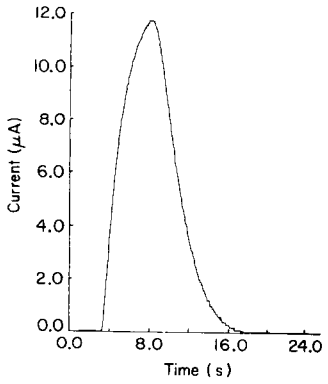

Fig. 2. Amperometric response to dopamine.

the working electrode and 3 mm from the reference electrode, center to center. The polyethylene spacer used in this instance is 0.1 mm thick; multiple pieces of polyethylene can be used to increase the size of the channel. The two halves are held together by six screws with the spacer sandwiched in the middle. The frequency response of the electrochemical cell was investigated by using a square-wave input of amplitude 0.1 V. The −3 dB point for the cell was found to be 4 kHz for both a static solution of 0.28 M sulfuric acid, and for the sulfuric acid solution flowing through the cell at a rate of 3.1 ml min^{-1}.

Procedure

To create the mercury coating on a glassy carbon or gold electrode for the lead/thallium system, the 3-way valve is switched to allow the mercury plating solution to flow through the detector; the mercury is plated onto the working electrode by holding the cell at −1.0 V vs. silver/silver chloride for 5 min, and then at −0.1 V for 2 min. The potential of the cell is then set at −0.2 V vs. the reference and the valve is switched to allow the carrier stream through the detector. The shape of the sample bolus is measured by amperometry at −0.700 V. The square-wave scan timing parameters are chosen from examination of a plot of this current response with time. For the studies on glassy carbon, scans were initiated 10 s after injection; the scans lasted 5 s and the voltage range swept was −0.2 to −0.7 V vs. Ag/AgCl. The square-wave frequency was 100 Hz. For the studies on gold, scans were initiated 15.0 s after injection with the same scan time and voltage range parameters as for the glassy carbon system. The scan range was thus 0.500 V.

For the dopamine system, the shape of the sample bolus is determined by amperometry at +1.2 V, and scan parameters are again chosen from examination of a plot of the current response with time. For the dopamine standard-addition curve, scans were initiated 7 s after injection, and the scans lasted 5 s, with a square-wave frequency of 100 Hz. The voltage range swept was +0.6 to +1.2 V.

For both systems, the square-wave height used was 50.0 mV, and current sampling occurred at 70% of the pulse width. Background scans were initiated using the same procedure, except that the carrier solution, rather than a sample, was contained in the cell during the electrochemical scan.

RESULTS AND DISCUSSION

Dopamine

A typical amperometric response of the electrochemical cell to an injected plug of dopamine is shown in Fig. 2. The small fluctuations in current are attributed to slight pulsations in flow caused by the pump action. The sample zone enters the electrochemical cell after approximately 3 s and reaches a maximum within 8 s. The signal then decays, disappearing completely in 18 s.

Thus, the sample zone is only present in the detector for about 15 s, and is present at analytically useful concentrations for only about 10 s. A set of square-wave scans taken over a series of identical sample zones is shown in Fig. 3. The scans, each 5 s in duration, were initiated at different times after sample injection, as indicated on the figure. As expected, the sensitivity of the square-wave response varies, depending on when the scan is initiated, and thus on the position of the sample zone relative to the detector. Also, the shape of the square-wave response changes as the scans progress in time. The maximum current response shifts in potential cathodically as the scan is initiated later in time after injection. This is also expected, because the current response at each point is a reflection of the concentration of analyte present in the detector at the point in the scan, as well as the response of the analyte at that point in potential. A standard addition curve of dopamine was obtained with square-wave voltammetric detection. The peak responses of the dopamine were found to be linear with concentration, as shown in Table 1.

Lead/thallium mixtures

The linearity of response was also tested with reductive systems. The dependence of Pb(II) and Tl(I) current responses with concentration were investigated using working electrodes of mercury on gold, and mercury on glassy carbon. Lead(II) and Tl(I) responses on both electrodes were linear with concentration as shown in Table 1.

Kalman filter fits to data consisting of overlapped responses of lead and thallium mixtures on mercury-coated gold and mercury-coated glassy carbon electrodes were attempted. Empirical models were used. These models consisted of the square-wave voltammetric response of single species, taken under conditions identical to those used in collecting data on the mixtures. Responses close to the least-squares line and close in time to the mixture

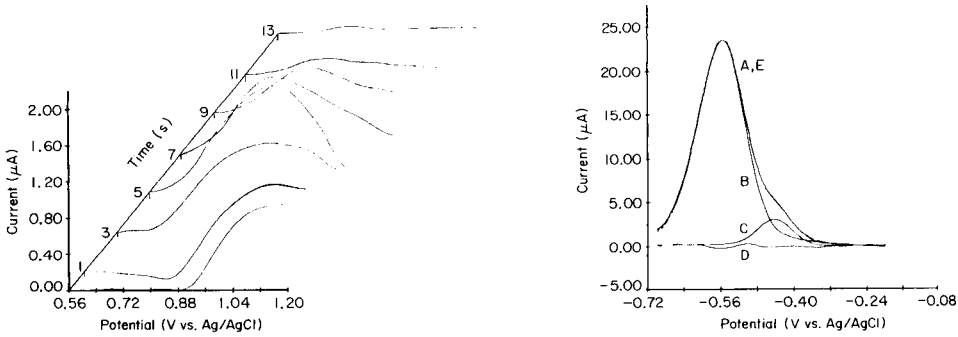

Fig. 3. Square-wave voltammetric scans of dopamine with varying delays.

Fig. 4. Deconvolution of overlapped lead and thallium responses on mercury-coated glassy carbon: (A) experimental data; (B) fitted thallium response; (C) fitted lead response; (D) residuals of the fits; (E) sum of the fitted components.

TABLE 1

Results for square-wave voltammetric standard addition curves

Electrode	Species	Concentration range (10^{-5} M)	Slope[a] (10^{+4} μA M^{-1})	Intercept (10^{-1} μA)	r[b]
Glassy carbon	Dopamine	1.014—10.14	1.47 ± 0.08	0.2 ± 0.5	0.9993
Mercury-coated gold	Lead(II)	0.75—11.3	4.7 ± 0.3	3 ± 2	0.9991
	Thallium(I)	2.32—13.9	8.7 ± 0.5	−3 ± 5	0.9994
Mercury-coated glassy carbon	Lead(II)	0.188—7.51	16.8 ± 1.0	2 ± 3	0.9992
	Thallium(I)	0.224—1.34	49.5 ± 0.8	0.2 ± 5	0.9998

[a]Of peak current response. [b]Correlation coefficient.

TABLE 2

Results for Pb/Tl mixtures

Mix	Pb/Tl ratio	Peak ht. ratio	Concentration (10^{-5} M)				Error (%)		Coefficient of Determination
			Prepared		Estimate				
			Pb	Tl	Pb	Tl	Pb	Tl	
1	3:1	1:1	7.51	2.24	7.30	2.13	−2.8	−4.9	0.9999
2	2:1	1:2	3.75	2.24	3.45	2.28	−8.0	+1.8	0.9999
3	1:2	1:6	1.88	4.48	1.80	4.78	−4.3	+6.7	0.9999
4	1:5	1:13	1.88	8.96	1.97	8.91	+4.8	−0.6	0.9996

injection were selected [4]. This was necessary because drift in the flow rate affected the shape of the electrochemical response with time. The peak current, however, was not affected greatly by these flow fluctuations.

Attempts to fit mixture responses on the mercury-coated glassy carbon electrode were successful. The results of fitting data from this system are shown in Table 2. The model used for mixtures 1 and 4 consisted of the responses of an 8.96×10^{-5} M thallium(I) and 2.25×10^{-5} M lead solution. For mixtures 2 and 3, the responses of a 3.58×10^{-5} M thallium(I) and 3.00×10^{-5} lead(II) solution were used. In all of the mixtures, the initial value for the measurement variance, used in the Kalman filter, was taken as 1×10^{-4} μA^2. The quality of fits is good, as is indicated by the coefficients of determination given in Table 2. A typical fit obtained by use of the filter is shown in Fig. 4, for which the thallium and lead are present at a ratio of 2:1. The difference between the observed (curve A) and the fitted (curve E) voltammograms is very small. The error in concentrations is, in all cases, below 10%. These errors are attributed to long-term flow fluctuations and irreproducibility in the injection process. Attempts at resolving the overlapped Tl(I)/Pb(II) response on mercury-covered gold electrodes failed,

as the models did not adequately describe the individual component responses in the presence of each other.

The combination of square-wave voltammetry and flow injection is a fast and convenient method for detection of electroactive species. The speed and the ability to use empirical models makes the Kalman filter attractive for use in flow-injection systems with square-wave voltammetric detection to resolve closely overlapping responses.

This work was supported by the Division of Chemical Sciences, U.S. Dept. of Energy, through grant DE-FG06-84ER13202.

REFERENCES

1 J. Janata and J. Růžička, Anal. Chim. Acta, 139 (1982) 105.
2 J. Wang and H. D. DeWald, Anal. Chim. Acta, 153 (1983) 325; Talanta, 31 (1984) 387.
3 T. F. Brown and S. D. Brown, Anal. Chem., 53 (1981) 1410.
4 C. A. Scolari and S. D. Brown, Anal. Chim. Acta, 166 (1984) 253.
5 S. C. Rutan and S. D. Brown, Anal. Chim. Acta, 160 (1984) 99.
6 T. F. Brown, PhD Dissertation, University of Washington, 1982.
7 G. Schwarzenbach and H. Flaschka, Complexometric Titrations, Methuen, London, , 1969.
8 D. M. Caster, J. J. Toman and S. D. Brown, Anal. Chem., 55 (1983) 2143.
9 J. J. Toman and S. D. Brown, Anal. Chem., 53 (1981) 1497.

Analytica Chimica Acta, 178 (1985) 247—253
Elsevier Science Publishers B.V., Amsterdam — Printed in The Netherlands

A CARBON ELECTRODE SPUTTERED WITH PALLADIUM AND GOLD FOR THE AMPEROMETRIC DETECTION OF HYDROGEN PEROXIDE

LO GORTON

University of Lund, Department of Analytical Chemistry, P.O. Box 124, S-221 00 Lund (Sweden)

(Received 17th May 1985)

SUMMARY

A modified carbon electrode for the amperometric determination of hydrogen peroxide is described. By deposition of a 15-nm thick layer of a 40:60 mixture of palladium and gold on the surface of the electrode the overvoltages for both the oxidation and the reduction can be decreased by at least 800 mV. When applied as an electrochemical sensor in a flow-injection system, linear calibration graphs were obtained between 10^{-7} and 5×10^{-3} M hydrogen peroxide. The modified electrodes were stable for months.

The importance of hydrogen peroxide in industrial and biotechnological processes as well as in waste water treatment, sterilization and biology is well reflected by the large variety of analytical techniques used for its determination even in classical texts [1—4]. The analytically interesting concentration range varies over at least 9 orders of magnitude. Amperometric detection in flow injection analysis (f.i.a.) is one of the most versatile techniques for the detection of hydrogen peroxide in the μM to M range [5—7]. The electrode reactions, however, suffer from large overvoltages, irreproducible behaviour with time and dependence on electrode prehistory [8—13]. The rates of many electrochemical reactions can be tremendously enhanced by the deposition of very small particles of metals or metal oxides on the surface of the electrode [14—23]. This paper reports on some aspects on the oxidation and reduction of hydrogen peroxide on a carbon electrode, modified by vapour deposition of a thin layer (15 nm) of a mixture of palladium and gold. The electrode was used as an amperometric sensor for hydrogen peroxide in a single-channel flow-injection system.

EXPERIMENTAL

Electrodes were prepared from carbon rods (Ringsdorff-Werke, type 203, diameter 3.1 mm) which were cut and polished on wet, fine emery paper. They were washed thoroughly with deionized water and dried at

0003-2670/85/$03.30

60°C for 2 h. A 150-Å layer of a mixture of palladium and gold (40% Pd/60% Au w/w) was deposited on the surface of the electrode by a vapour sputtering device (Polaron Equipment Ltd, SEM Coating Unit E 5150, sputtering current 20 mA). The covered electrodes were press-fitted into a teflon holder so that only the flat circular end surface (0.0731 cm^2) contacted the solution. An electrode was inserted into a flow-through electrochemical cell [24] and connected to a three-electrode potentiostat with an Ag/AgCl (0.1 M KCl) reference electrode and a platinum wire counter electrode. All potentials except the cyclic voltammograms are referred to this reference electrode (+50 mV vs. SCE). Samples (50 μl) were injected with a pneumatically operated valve (Cheminert, type SVA) into a carrier consisting of a deaerated 0.1 M phosphate buffer. Connections between various parts were made with teflon tubing (0.5 mm i.d.). The dispersion [25] for hydrogen peroxide in the system was found to be 1.08 for flow rates of 0.4—1.2 ml min^{-1}. Triangular sweep voltammetry was made with a modified electrode in quiet solutions using a platinum counter electrode and a SCE with a Luggin capillary as reference. The supporting electrolyte was a 0.25 M phosphate buffer, pH 7.0. Hydrogen peroxide (Merck, p.a., cat. no. 7209) was standardized by titration with potassium permanganate.

RESULTS AND DISCUSSION

Unmodified carbon electrode

The oxidation reaction for samples of 1.05 mM hydrogen peroxide, pH 8.0, was studied by noting the peak currents for successively more positive potentials. A wave starts at +450 mV and reaches the limiting current plateau at about +1200 mV. About 5% higher currents were obtained between +1200 and +450 mV when the potential was stepped in the reverse direction (Fig. 1). High applied voltages will thus activate the electrode so that the oxidation currents become larger.

When the potential is decreased further, a cathodic wave caused by reduction of hydrogen peroxide starts at —30 mV. It is drawn out and is small compared to the anodic currents even at —500 mV (Fig. 1). The overall electrochemical reactions are

$$H_2O_2 \rightarrow O_2 + 2H^+ + 2\,e^- \quad \text{(anodic)} \tag{1}$$

$$H_2O_2 + 2H^+ + 2\,e^- \rightarrow 2H_2O \quad \text{(cathodic)} \tag{2}$$

The formal potentials ($E^{0\prime}$) of Eqns. 1 and 2 are —83 and +1011 mV, respectively, at pH 8.0 [26]. The overvoltages are thus 1.3—1.5 V for both reactions. Besides the reactions mentioned above, the hydrogen peroxide disproportionates to oxygen and water at the electrode surface:

$$H_2O_2 \rightarrow 1/2\,O_2 + H_2O \tag{3}$$

The extent of this side-reaction varies with the type of electrode material and its pretreatment [27, 28].

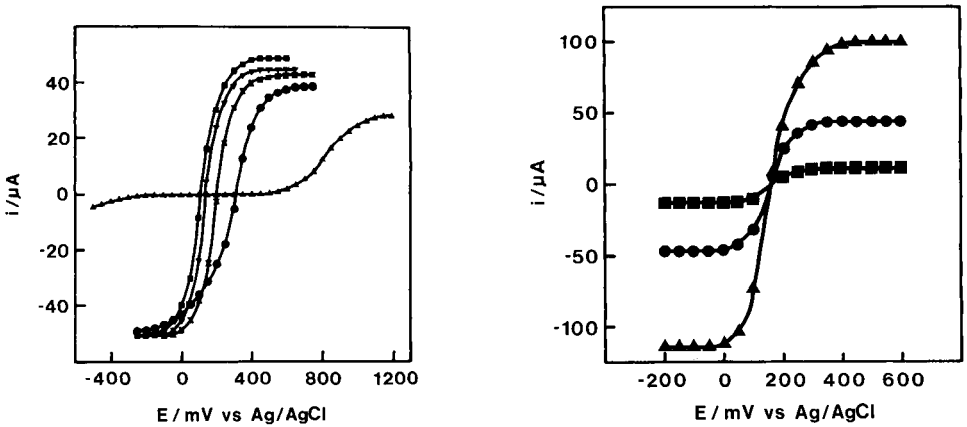

Fig. 1. Current vs. potential for the Pd/Au modified electrode at different pH values: (■) 8.0; (▼) 7.0; (⧗) 6.0; (●) 4.0. (▲) pH 8.0 at a bare electrode. (1.05 mM H_2O_2; 0.1 M phosphate buffer carrier at 0.7 ml min^{-1}.)

Fig. 2. Current vs. potential for the Pd/Au modified electrode at different H_2O_2 concentrations: (▲) 2.0 mM; (●) 0.9 mM; (■) 0.2 mM. (0.1 M Phosphate buffer, pH 7.0, carrier at 0.7 ml min^{-1}.)

Modified carbon electrodes

The oxidation of hydrogen peroxide at a palladium/gold modified electrode at various pH values is also shown in Fig. 1. The measurements were taken in the direction from the most positive potential to the most negative. The currents at such modified electrodes are independent of direction and prehistory except for the first time an electrode is used. The currents will then be somewhat lower if measurements are taken from zero towards positive potentials. The application of a high potential seems therefore to activate the catalytic layer and the activation seems to be constant afterwards.

The overvoltages for oxidation and reduction are decreased drastically by the electrode modification. The anodic and cathodic limiting currents at pH 8.0 are reached at +400 and −150 mV respectively, i.e., the overvoltage for the oxidation is decreased by about 800 mV. The limiting currents (i_d) are also increased compared to an unmodified electrode. The limiting currents for oxidation and reduction are almost equal at pH 8.0 but at pH 4.0 the anodic current becomes 14% less than the cathodic current.

The potentials at which the waves reach the limiting current vary somewhat with the hydrogen peroxide concentration (Fig. 2). The reactions, particularly the anodic reaction, show a more irreversible behaviour the higher the peroxide concentration. The limiting current increase linearly with the concentration (Fig. 3). Strictly linear calibration graphs for the oxidation are obtained from the detection limit (0.3 μM) up to 5 mM where the interference from oxygen bubbles (Eqn. 1) sets the limit. The range of determination can of course be extended upward by dilution in the flow

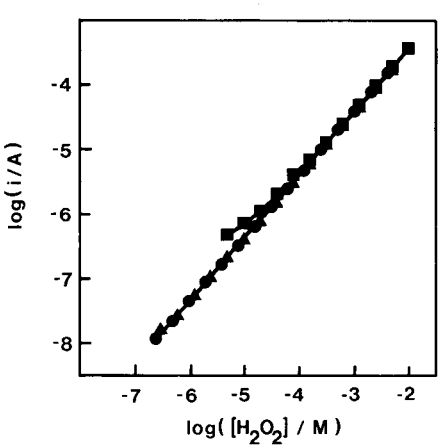

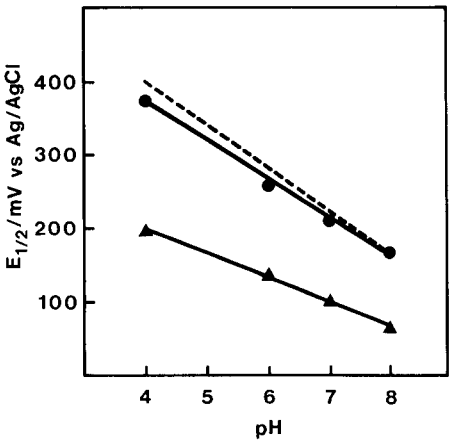

Fig. 3. Current vs. H_2O_2 concentration for the Pd/Au modified electrode. Oxidation: (▲) pH 8.0, +300 mV; (●) pH 7.0, +400 mV; Reduction (■) pH 8.0, —150 mV. (0.1 M Phosphate buffer carrier at 0.7 ml min^{-1}.)

Fig. 4. Half-wave potential vs. pH: (●) anodic wave; (▲) cathodic wave. (0.1 M Phosphate buffer carrier at 0.7 ml min^{-1}, 1.05 mM H_2O_2.) (---) Formal potential ($E^{0\prime}$) of $Pd/Pd(OH)_2$ vs. pH.

system by increasing the dispersion or by decreasing the sample volume. The slopes of the calibration graphs were 34 μA mM^{-1} at pH 7.0 (+400 mV) and 37 μA mM^{-1} at pH 8.0 (+300 mV).

A calibration graph for hydrogen peroxide based on its reduction is also shown in Fig. 3. There is a deviation from linearity below 20 μM probably owing to interference from residual oxygen in the degassed solutions (see below). The calibration graph levels out above 10 mM, although it cannot be seen on the log-log plot. The upper limit on the cathodic side is also set by gas bubble formation. The bubbles are clearly visible.

Oxidation at the modified electrode is reproducible from day to day and from electrode to electrode except for a slight irreproducible electrode variation above 4 mM hydrogen peroxide in the flow-injection system. Interference from gas bubbles will set in at lower concentrations under non-flow conditions. The noise and background currents are low and automatic blanks between samples are provided for by the flow-injection arrangement. A single calibration graph can be used for different electrodes and it is stable with time at constant pH. The sensor seems therefore to be well suited for a number of applications.

Electrochemical behaviour

The oxidation of hydrogen peroxide is considered to occur according to the same scheme as has been reported for the oxidation at platinum electrodes [9]:

$$Pd(OH)_2 + H_2O_2 \rightarrow Pd + 2H_2O + O_2 \quad (4)$$

$$Pd + 2H_2O \rightarrow Pd(OH)_2 + 2e^- + 2H^+ \quad (5)$$

with the overall reaction

$$H_2O_2 \rightarrow 2H^+ + O_2 + 2e^- \quad (6)$$

The hydrogen peroxide reduces the metal oxide film to the metal, which is re-oxidized electrochemically. The standard potential (E^0) of the palladium oxidation (Eqn. 5) is +928 mV vs. NHE and the expected pH dependence of the formal potential ($E^{0\prime}$) can thus be calculated (Fig. 4, broken line). The half-wave potentials ($E_{1/2}$) of the oxidation waves of hydrogen peroxide at different pH values were evaluated from a E vs. log $(i/i_d - i)$ plot and are also given in Fig. 4 (upper solid line). The $E_{1/2}$ values are sufficiently close to the formal potentials of the $Pd/Pd(OH)_2$ couple to give support to the mechanism proposed by Eqn. 4.

The discrepancies between the $E_{1/2}$ and $E^{0\prime}$ values can be explained by the irreversible behaviour of the oxidative reaction. Both $E_{1/2}$ and the potential at which the limiting current (i_d) is reached depend on the peroxide concentration (see Fig. 2). The shapes of the i vs. E waves (Fig. 1) also vary with pH, because the reaction rates are pH-dependent. This is indicated by the variation of the Tafel slope with pH (Table 1). Also, at lower pH values the oxidative limiting current is lower than at higher pH values, making the evaluation of $E_{1/2}$ more uncertain. Probably the disproportionation of hydrogen peroxide (Eqn. 3) competes with the electrochemical oxidation at lower pH values, at which the rate of the electro-oxidation is slower.

Lingane and Lingane [9] showed that solid platinum could be activated by repeated electrochemical cycling so that the reaction with hydrogen peroxide (cf. Eqn. 4) becomes faster. This effect, which has been observed for finely dispersed platinum black, is even more important with the highly active palladium which is produced by sputtering. The gold is assumed not to be directly active in the electro-oxidation but to aid in the fine dispersion of the palladium. It has been shown, however, that the background material may influence the behaviour of the electrode, so in this instance both the carbon support and the sputtered gold may be of importance [29].

The reduction of hydrogen peroxide involves a very complex series of reactions closely related to the reduction of oxygen [10], and several pathways have been proposed [9, 10, 12]. The details of the mechanism are beyond the scope of this paper, but the influence of molecular oxygen is clearly demonstrated in Fig. 5. Cyclic voltammetry at a modified electrode in a deaerated solution (Fig. 5a) produces a background current showing no special features in either direction, except that it is significantly higher than that obtained with an unsputtered carbon electrode of the same material. When the electrode was exposed to air for a moment and repositioned in the deaerated solution (Fig. 5b), the first sweep produced a cathodic peak related to the reduction of adsorbed oxygen [19]. This peak is decreased

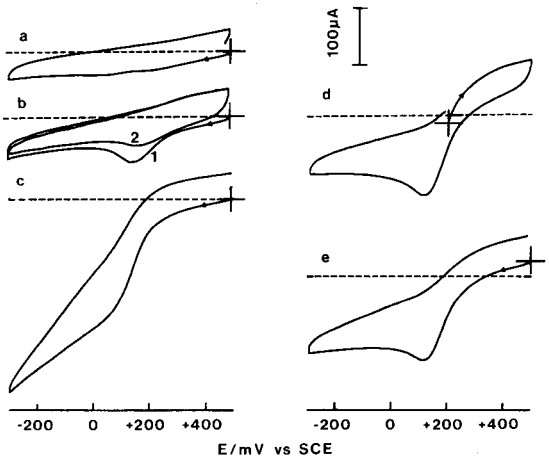

Fig. 5. Cyclic voltammograms of the Pd/Au carbon electrode in: (a) a deaerated buffer; (b) as in (a) with the electrode exposed to air (1 and 2 denote first and second scans); (c) an oxygen saturated solution; (d, e) a deaerated buffer containing 9.8 mM H_2O_2. Conditions: 0.25 M phosphate buffer, pH 7.0; scan rate 50 mV s^{-1}; (+) start potential; (---) line of zero current.

during the next sweep. The reduction of oxygen seems to give some hydrogen peroxide which is oxidized anodically at about 300 mV (cf. the anodic currents in Fig. 5a, b). Formation of hydrogen peroxide from the reduction of oxygen is known to occur at electrodes [10]. When a cyclic voltammogram was taken in an oxygen-saturated solution (Fig. 5c), the oxygen reduction increased drastically but the anodic current at around +300 to 400 mV was the same as in Fig. 5(b). The amount of peroxide formed is not affected by the dissolved oxygen.

Cyclic voltammetry in degassed hydrogen peroxide solutions (Fig. 5d, e) produces cathodic peaks at the same potentials as oxygen, i.e., the reduction waves for hydrogen peroxide and dioxygen are indistinguishable under the present conditions. The disproportionation of hydrogen peroxide (Eqn. 3), catalyzed by the electrode surface, produces oxygen which is known to catalyze the electrochemical reduction of hydrogen peroxide [9]. Similarly to the oxidation, the rate of reduction is faster in more alkaline solutions (see Tafel slopes in Table 1) but the influence of the disproportionation

TABLE 1

Slopes of the Tafel E vs. log $(i/i_d - i)$ plots (1.0 mM H_2O_2; 0.1 M phosphate buffer carrier at 0.7 ml min^{-1})

pH	4.0	6.0	7.0	8.0
Slope (mV)				
Reduction	218	120	110	88
Oxidation	172	149	144	106

in more acidic solution does not decrease the limiting current as the resulting oxygen is reduced at the same potential.

Conclusion

The large decrease in the overvoltages for both the oxidation and the reduction of hydrogen peroxide in combination with a linear response over almost 5 orders of magnitude of concentration and the long-term stability seem to be promising qualities of this electrode. In some fields, especially where hydrogen peroxide-producing oxidases are being used in the analysis of biological fluids, there is a call for a lower applied potential of the amperometric detection device to minimize interfering reactions.

The author thanks Prof. G. Johansson for valuable discussions concerning this work. Miss Birgitta Svensson, Department of Chemical Technology, Lund is gratefully acknowledged for help with the vapour deposition and the Swedish Natural Research Council for financial support.

REFERENCES

1 T. E. Barman, Enzyme Handbook, Vol. 1, Springer Verlag, New York, 1969.
2 J. Fritz and G. Schenk, in Quantitative Analytical Chemistry, Allyn and Bacon, Boston, 1966.
3 I. M. Kolthoff, E. B. Sandell, E. J. Meehan and S. Bruckenstein, in Quantitative Chemical Analysis, 4th edn., Macmillan Co., Toronto, 1969.
4 P. W. Carr and L. D. Bowers, Immobilized Enzymes in Analytical Chemistry, Wiley, New York, 1980.
5 H. Lundbäck, Anal. Chim. Acta, 145 (1983) 189.
6 H. Lundbäck, G. Johansson and O. Holst, Anal. Chim. Acta, 155 (1983) 47.
7 H. Lundbäck and B. Olsson, Anal. Lett., B18 (1985) 871.
8 J. O'M. Bockris and L. F. Oldfield, Trans. Faraday Soc., 51 (1955) 249.
9 J. J. Lingane and P. J. Lingane, J. Electroanal. Chem., 5 (1963) 411.
10 J. Wilshire and D. T. Sawyer, Acc. Chem. Res., 12 (1979) 105.
11 V. G. Prabhu, L. R. Zarapkar and R. G. Dhaneshwar, Electrochim. Acta, 26 (1981) 725.
12 A. J. Appleby and M. Savy, J. Electroanal. Chem., 92 (1978) 15.
13 M. R. Tarasevich and V. S. Bagotskii, Elektrokhimiya, 14 (1978) 1340.
14 J. Zak and T. Kuwana, J. Am. Chem. Soc., 104 (1982) 5514.
15 L. R. Faulkner, Chem. Eng. News, Feb. (1984) 28.
16 V. S. Bagotzky and A. M. Skundin, Electrochim. Acta, 29 (1984) 757.
17 K. Juttner, Electrochim. Acta, 29 (1984) 1597.
18 D. J. Harrison and M. S. Wrighton, J. Phys. Chem., 88 (1984) 3932.
19 O. Outiki, E. Lamy-Pitara and J. Barbier, React. Kinet. Catal. Lett., 23 (1983) 213.
20 L.-C. Jiang and D. Pletcher, J. Electroanal. Chem., 149 (1983) 237.
21 D. Pletcher, J. Appl. Electrochem., 14 (1984) 403.
22 S. Dong and T. Kuwana, J. Electrochem. Soc., 131 (1984) 813.
23 J. Zak and T. Kuwana, J. Electroanal. Chem., 150 (1983) 645.
24 R. Appelqvist, G. Marko-Varga, L. Gorton, A. Torstensson and G. Johansson, Anal. Chim. Acta, 169 (1985) 237.
25 J. Růžička and E. H. Hansen, Flow Injection Analysis, Wiley, New York, 1981.
26 S. Kotrlý and L. Šůcha, Handbook of Chemical Equilibria in Analytical Chemistry, Ellis Horwood, Chichester, 1985.
27 J. E. Harrar, Anal. Chem., 35 (1963) 893.
28 N. D. Koshel' and A. S. Cherednichenko, Elektrokhimiya, 20 (1984) 218.
29 N. V. Korovin, I. G. Shmachkova and A. G. Kicheev, Elektrokhimiya, 15 (1979) 354.

Analytica Chimica Acta, 178 (1985) 255—261
Elsevier Science Publishers B.V., Amsterdam — Printed in The Netherlands

CATALYTIC DETERMINATION OF MOLYBDENUM WITH IMPROVED SENSITIVITY BY MEANS OF THE HYDROGEN PEROXIDE/IODIDE/ ASCORBIC ACID LANDOLT REACTION

J. A. AMBERSON and G. SVEHLA*

Department of Analytical Chemistry, The Queen's University, Belfast (Northern Ireland)

(Received 29th July 1985)

SUMMARY

Modified catalytic procedures are described for the determination of 0—0.1 and 0—1 mg l^{-1} molybdenum in solutions. Reaction times of the hydrogen peroxide/iodide/ ascorbic acid Landolt reaction are evaluated from conductometric or potentiometric traces. Calibration graphs are based on the ratio of the reaction times for the blank and the sample, $t(0)/t(c)$, plotted against the concentration of molybdenum. The shapes of the conductometric and potentiometric traces are explained.

Some years ago, a catalytic method for the determination of 0.1—1 mg l^{-1} molybdenum in solutions was described by Erdey and Svehla [1, 2]; the hydrogen peroxide/iodide/ascorbic acid reaction was monitored visually in buffered solutions. The time elapsed between mixing of the reagents and the appearance of the iodine colour was measured and related, through calibration graphs, to the concentration of molybdenum, which catalyses the reaction of hydrogen peroxide with iodide. The visual end-point detection, however simple, is tedious; it requires constant attention and, should it be missed, a new attempt. Also, reaction times need to be reasonably short (if possible, below 10 min) to make the visual observation less tiresome. It is not suited for automation and cannot be adapted for flow injection analysis.

In the present conversion of this method for the determination of molybdenum traces in industrial samples, electrochemical monitoring techniques were examined. The reaction is optimized for the 0.01—0.1 mg l^{-1} range (the procedure can also be used for higher concentrations). This means that longer reaction times (up to 30 min) are required for the lowest molybdenum concentrations, but this does not cause any difficulties if the monitoring is made automatic by recording the kinetic curve. Further, the overall acidity is changed (to pH 1.5), which means that industrial samples can be prepared with ease by evaporating solutions to dryness and taking them up with hydrochloric acid.

The principle and historic background of the method (with visual monitoring) has been described [1—4], together with the kinetic and mechanistic details of the reactions involved. The present paper is concerned only with

0003-2670/85/$03.30

those aspects which are particular to the conductometric and potentiometric monitoring techniques.

Conductometric monitoring

Among the methods available for monitoring reaction rates, conductometry has been rather neglected in the past. The reason for this is obvious: conductivity is not a specific analytical property. In the reaction systems used in catalytic analysis, conductivities are usually high, specific conductances being in the order of 1—10 mS cm^{-1}, and the changes during the progress of the reaction are low (say 0.01 mS cm^{-1} or less). Even with modern conductometric apparatus, which allows not only direct reading and recording of the conductivity but also compensation of the signal (so that small changes in highly conductive solutions can be monitored), the direct monitoring of reaction rates is impractical. However, when the methods used are connected with an abrupt change in reactant concentrations at a specific point of time (e.g., when a predetermined amount of a reactant has been consumed), the corresponding change in conductivity can be large enough for easy evaluation. Such a method can be based on Landolt-type reactions.

Potentiometric monitoring

Potentiometric monitoring of catalytic reactions has often been used. With Landolt-type reactions, there is an added advantage: the abrupt change in reagent concentrations, and so in the oxidation-reduction potentials, makes the end-point of a reaction clear, as in a potentiometric titration [4, 5]. With bright platinum and saturated calomel electrodes connected to a pH meter, potential vs. time curves can be recorded on a chart recorder and the reaction times evaluated.

EXPERIMENTAL

Reagents

Analytical-grade chemicals and glass-distilled water were used unless otherwise specified.

Potassium iodate standard solution (0.010933 mol l^{-1}) is prepared by dissolving 2.3397 g of potassium iodate in water and diluting to 1 l. Hydrochloric acid solutions (10% and 1% w/v) are needed. The 10% (ca. 2.75 mol l^{-1}) solution is prepared by diluting 235 ml of concentrated hydrochloric acid to 1 l; the 1% solution is then prepared from this by 10-fold dilution. All molybdenum standards and sample solutions must contain 0.1% hydrochloric acid.

Ammonium molybdate stock solution (100 mg l^{-1} molybdenum) is prepared by dissolving 0.1840 g of hexammonium heptamolybdate tetrahydrate in water and diluting to 1 l. From this, 10 and 1 mg l^{-1} solutions are prepared. Standards covering the range to 1 mg l^{-1} are prepared from the 10 mg l^{-1} solution and the 0.01—0.1 mg l^{-1} standards from the 1 mg l^{-1} solution. All

these standards must contain 0.1% hydrochloric acid; this can be achieved by adding 10 ml of the above 1% hydrochloric acid solution before diluting the standards to 100 ml. The ammonium molybdate reagent used contains 3% (w/v) of the heptamolybdate tetrahydrate.

For the hydrogen peroxide stock solution (ca. 0.088 mol l^{-1}) 10 ml of 30% (v/w) hydrogen peroxide solution is diluted to 1 l. For the ascorbic acid stock solution (ca. 0.033 mol l^{-1}) 0.58 g of ascorbic acid is dissolved in 100 ml of water; this solution keeps for 48 h.

Solution A (oxidizing) is made up by diluting 55 ml of 10% hydrochloric acid and V(A) ml of hydrogen peroxide stock solution to 1 l; V(A) is determined by standardization (see below). The solution keeps for 2 weeks.

Solution B (reducing) is prepared by dissolving 6.34 g (0.0382 mol) of potassium iodide, 7.71 g (0.0273 mol) of sodium acetate trihydrate and 0.76 g (0.002 mol) of disodium ethylenediaminetetraacetate in water, to which V(B) ml of ascorbic acid stock solution is added, and diluted to 1 l; the volume V(B) is determined by standardization (see below). The solution keeps for 36 h.

The test solutions contained 0—0.1 (or 0—0.01) mg l^{-1} molybdenum and 0.1% hydrochloric acid. Industrial samples were prepared by dissolution or digestion; the solutions were evaporated to dryness, taken up in 10 ml of 1% hydrochloric acid and diluted to 100 ml.

Standardization of ascorbic acid. To 25.00 ml of 0.010933 mol l^{-1} standard potassium iodate solution, 2 g of solid potassium iodide and 5 ml of 10% hydrochloric acid are added. The iodine produced is titrated with the ascorbic acid stock solution until the last traces of yellow disappear. The volume of ascorbic acid, V(B) (about 25 ml), is noted; the same volume has to be dispensed when 1 l of solution B is prepared.

Standardization of hydrogen peroxide. The hydrogen peroxide stock solution (10 ml) is dispensed from a 50-ml burette into a glass-stoppered titration flask; 10 ml of 10% hydrochloric acid, 2 g of potassium iodide and 5 drops of 3% ammonium molybdate reagent are added. The flask is closed, shaken, and set aside for 5 min. The iodine is then titrated with the ascorbic acid stock solution until the last traces of yellow disappear. The volume, V(1) (25—30 ml) is noted. Volume V(A) is calculated from $V(A) = 19.512\ V(B)/V(1)$. Volume V(A) is dispensed for preparation of 1 l of solution A.

Solutions A and B and all the test and molybdenum standard solutions must be thermostatted to 25 ± 0.1°C before kinetic runs (see below).

Apparatus

Conductometric measurements. It is important to use a device which has facilities for compensation of conductivity, and which can be linked to a chart recorder. In these experiments, a Metrohm E518 conductometer was used in combination with a Metrohm E586 Labograph. A standard Metrohm EA880 TV universal titration vessel (with thermostatted jacket) was used with two Metrohm EA211 platinized platinum sheet electrodes; the electrodes

did not have protecting umbrellas around them, thus allowing free circulation of the liquid. Solutions were stirred magnetically during the kinetic runs; medium speeds ensured that the electrodes were always covered by the liquid. The two electrodes were at a distance of 1.5 cm; their surface area was about 0.56 cm^2. Before the first run on each day, the cell was calibrated with 0.01 mol l^{-1} potassium chloride solution (with a specific conductivity of 1.4087 mS cm^{-1} at 25°C); from then onwards all signals were measured as specific conductivities. The cell constant for this arrangement was 2.6 cm^{-1}. In a typical run, the initial conductivity of 10 ml of solution A mixed with 10 ml of 0.1% hydrochloric acid was 28 mS cm^{-1}; upon addition of 10 ml of solution B, the conductivity decreased by about 0.5 mS cm^{-1}, but, on mixing, the conductivity quickly rose again by almost 0.3 mS cm^{-1}. This was followed by a gradual decrease of about 0.1 S cm^{-1} and the end-point was marked by a sharp increase in the conductivity, bringing its value back near to the initial figure (these changes will be explained later). This meant that a full-scale deflection of 1 mS cm^{-1} could be used throughout, provided of course that most of the original 28 mS cm^{-1} conductivity was compensated initially. This was achieved by moving the control knob until the meter needle came back into the scale; a high scale reading was then adjusted. In practice, it was found that the sharpest end-points were obtained when the 0.3 mS cm^{-1} sensitivity was used; although the recording was then below zero for a short while, resulting in some cutoff (see Fig. 1), the rest of the run was well within scale and the end-points were easy to evaluate. The sensitivity of the chart

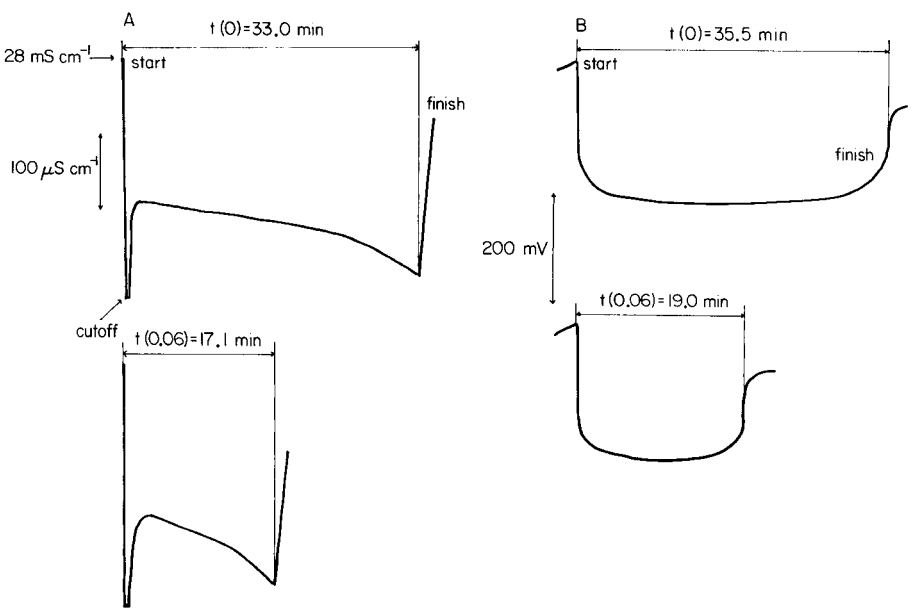

Fig. 1. Recorded traces: (A) conductometric; (B) potentiometric. For details, see text.

recorder had to be chosen appropriately; in the present arrangement, a 1-V full scale sensitivity was satisfactory. A chart speed of 10 mm min^{-1} (for lower concentrations) or 20 mm min^{-1} (for higher ones) was sufficient to obtain sharp end-points.

Potentiometric measurements. Any pH meter that can be linked to a chart recorder is suitable. A Metrohm E632 digital millivoltmeter was used, again in combination with the Metrohm E586 Labograph. The titration vessel was the same as in the conductometric experiments; the electrodes were a bright platinum sheet and a saturated calomel electrode (SCE). All changes of potential were well within 1 V, so that this value for the full-scale deflection of the chart recorder accommodated all the kinetic runs comfortably. The chart speeds were the same as in the conductometric experiments.

Thermostat. As the reaction times depend strongly on temperature, all solutions and the reacting mixture were thermostatted to 25 ± 0.1°C in the same water bath, the temperature of which was kept constant with a BTL Circon heater-circulator unit; this unit also circulated the water through the cell jacket.

Procedures

Solutions A and B are immersed in the thermostat. For each concentration range, five molybdenum standards suffice. Sample solutions can contain up to 1 mg l^{-1} tungsten, 10 mg l^{-1} iron(III) and other metals up to a total of 100 mg l^{-1}. Each sample must contain 0.1% free hydrochloric acid.

The sample (10.00 ml) is placed in the vessel, 10 ml of solution A is added, and recording of the conductivity or the potential is started. Once the response has become nearly constant, 10.00 ml of solution B is added. The response changes immediately, later it becomes nearly constant, and finally an abrupt change occurs on both the conductometric (Fig. 1A) and potentiometric (Fig. 1B) traces. The signal is recorded until the response becomes fairly constant again. The reaction times, $t(c)$, are evaluated in the manner indicated in Fig. 1. In the calibration experiments, the sample solution is replaced by a standard, and the blank reaction time, $t(0)$, is measured with 10.00 ml of 0.1% hydrochloric acid in the cell. The ratios $t(0)/t(c)$ are calculated and plotted as a function of molybdenum concentration (c). The straight line obtained is used as a calibration graph for evaluating the data obtained with the samples.

RESULTS AND DISCUSSION

Typical conductometric (Fig. 1A) and potentiometric (Fig. 1B) traces are shown, together with the way in which the reaction times are evaluated. The shape of the conductometric curve requires some explanation, because if one looks at the chemical reactions taking place during these processes [1—4], one would not expect this type of curve. However, the concentrations of the complexing/buffering agents were here chosen deliberately to cause such

changes in the pH of the solution that the reaction times would be easy to observe. The pH of the pure solution A is 1.0 and that of solution B 5.1; the pH of the final reaction mixture is 1.4 after the reaction has been completed. Thus, when the sample solution and solution A are mixed, the hydrogen ion concentration is high and this produces a high conductivity signal. When solution B is added, this conductivity drops, because of the obvious increase in pH; but at the end, owing to the limited buffer capacity applied, the hydrogen ion concentration and so the conductivity increases again, allowing precise evaluation.

The shape of the potentiometric traces is the consequence of the changes in the oxidation-reduction potentials during the reaction. Initially, the potential is undefined, but the indicator electrode acquires a fairly positive potential. When solution B is added, a change of ca. 260 mV occurs, the potential becoming less positive. As the reaction proceeds, a minimum is observed, followed by a slow movement in the potential towards more positive values. The appearance of iodine in the solution is marked by a sharp increase

TABLE 1

Calibration data

Mo conc. (mg l^{-1})	Conductometry		Potentiometry	
	$t(c)$ (min)	$t(0)/t(c)$	$t(c)$ (min)	$t(0)/t(c)$
For the 0—0.1 mg l^{-1} concentration range				
0	33.0	1.00	35.5	1.00
0.02	25.3	1.30	28.1	1.26
0.04	20.5	1.61	22.8	1.56
0.06	17.1	1.93	19.0	1.87
0.08	14.8	2.23	16.8	2.11
0.10	13.4	2.46	14.7	2.41
Intercept with $t(0)/t(c)$ axis		1.011		0.994
Slope (l mg^{-1})		14.871		14.157
Correlation coefficient		0.9990		0.9995
Lowest determinable concentration [6] (mg l^{-1})		0.007		0.004
For the 0—1 mg l^{-1} concentration range				
0	39.0	1.00	32.8	1.00
0.2	10.3	3.80	8.6	3.81
0.4	5.9	6.60	4.85	6.76
0.6	4.1	9.50	3.4	9.65
0.8	3.15	12.40	2.65	12.38
1.0	2.6	15.00	2.15	15.26
Intercept with $t(0)/t(c)$ axis		1.000		1.008
Slope (l mg^{-1})		14.100		14.271
Correlation coefficient		0.9999		1.0000
Lowest determinable concentration [6] (mg l^{-1})		0.021		0.015

(ca. 100 mV) in the potential. The end-point may be evaluated the same way as that of potentiometric titrations.

Table 1 contains results obtained in the calibration, together with the most important statistical characteristics of the calibration lines, calculated by linear regression analysis. The data clearly indicate that the linearity is excellent in all cases (the correlation coefficient is always greater than 0.999). The results also show the advantage of using the $t(0)/t(c)$ ratio (instead of the reciprocal reaction times) as the analytical parameter for evaluation. While the repeatability of reaction times is excellent (within 5 s at longer reaction times and 2 s at shorter times), their reproducibility obtained with newly prepared solutions is much worse (mainly because of the uncontrollable decomposition of ascorbic acid in the solution). In contrast, the $t(0)/t(c)$ ratios are easily reproducible. There is hardly any variation among the four values of intercept and slope; one could use a single calibration line for the evaluation of all the results, regardless of the method of monitoring or the concentration range.

Interferences were not studied, because it is known [3, 7] that out of 29 important metal cations (and oxoanions) only tungsten ($\geqslant 1$ mg l^{-1}), vanadium ($\geqslant 10$ mg l^{-1}), and cadmium and iron(III) ($\geqslant 100$ mg l^{-1}) interfere. Interference of iron and cadmium can be easily overcome by extraction with benzoin-α-monoxime [7, 8].

REFERENCES

1 L. Erdey and G. Svehla, Acta Chim. Acad. Sci. Hung., 26 (1961) 167.
2 G. Svehla and L. Erdey, Microchem. J., 7 (1963) 206.
3 G. Svehla and L. Erdey, Microchem. J., 7 (1963) 221.
4 G. Svehla, Analyst (London), 94 (1969) 513.
5 H. Weisz and K. Rothmaier, Anal. Chim. Acta, 68 (1974) 93.
6 K. Doerffel, Statistik in der Analytischen Chemie, VEB Deutscher Verlag für Grundstoffindustrie, Leipzig, 1966, p. 177.
7 T. Kennedy and G. Svehla, Z. Anal. Chem., to be published.
8 E. G. Bradfield and J. F. Stickland, Analyst (London), 100 (1975) 1.

Analytica Chimica Acta, 178 (1985) 263—275
Elsevier Science Publishers B.V., Amsterdam — Printed in The Netherlands

THE EFFECTS OF ERRORS IN MEASUREMENTS OF ABSORBANCE AND TIME ON THE CALCULATED VALUE OF A PSEUDO-FIRST-ORDER RATE CONSTANT

EDWARD D. JOHNSON, JON P. WEBER and LOUIS MEITES*

Department of Chemistry, George Mason University, 4400 University Drive, Fairfax, VA 22030 (U.S.A.)

(Received 31st July 1985)

SUMMARY

When data on the variation with time of the absorbance of a reactant or product are used to evaluate the rate constant of a first- or pseudo-first-order reaction, the precision of the result depends on the precisions with which both the time and the absorbance are measured. The natures of the dependences, and the ways in which they are affected by both constant and linearly varying background absorbances, are examined. If the standard error σ_t of a measurement of time is below about 0.005 $t_{1/2}$, the standard error of the rate constant is virtually identical for an experiment in which the concentration of the reactant is followed as for one in which the concentration of the product is followed, but for larger values of σ_t it is better to follow the concentration of the reactant. In any event, errors in the measurements of time are much more likely to be significant than they are usually assumed to be. Other sources of error in such experiments, including constant and time-dependent background absorbances, are examined more briefly, with emphasis on the requirements that should be satisfied in work of the highest quality.

First- and pseudo-first-order rate constants are usually evaluated from data obtained by following the time dependence of the absorbance, or some other quantity proportional to the concentration, of a reactant or product. It is generally assumed that, in consequence of an argument set forth by Zuman and Patel [1], errors in the measurements of time are insignificant by comparison with those in the measurements of absorbance, and that it is therefore "completely unnecessary to scrutinize" the former.

The experimental values of thousands of rate constants are recorded in the literature [2]. Because such experiments are so frequently done, it would clearly be desirable to know whether they yield results that are consistent with the random errors of the experimental measurements, what might be responsible for the discrepancy if there is one, and how small the errors in the measurements of time must be to justify regarding them as negligible. It actually appears that there has been no prior inquiry into whether following the concentration of a reactant is superior or inferior to following that of a product, or whether there is any ground, other than convenience of experimentation, for choosing between these alternatives.

Similar questions arise with respect to all other physicochemical experiments, and they are addressed here in ways similar to those taken in recent studies of the potentiometric titrations of strong [3] and weak [4] acids with strong bases. It is concluded that, in a typical experiment, errors in the measurements of time will not be insignificant unless the standard error is of the order of a ten-thousandth of the half-time. Such precision is rarely sought or achieved. The results of this investigation should make it possible to design experiments that yield results substantially superior to those generally obtained.

THEORY AND PROCEDURE

Six different cases have been examined: three (Cases 1a, 1b, and 1c) in which the concentration of the limiting reactant is followed, and three others (Cases 2a, 2b, and 2c) in which the concentration of a product is followed. In Cases 1a and 2a, which are the simplest, the measured absorbances are entirely attributable to the substance whose concentration is followed; the other cases include the effects of finite background absorbances. In Cases 1b and 2b, the background absorbance is taken to be constant; in Cases 1c and 2c, it is assumed to increase linearly with time. These situations correspond to the equations

$$A = A^0 \exp(-kt) \tag{1a}$$

$$A = A^0 \exp(-kt) + a \tag{1b}$$

$$A = A^0 \exp(-kt) + bt \tag{1c}$$

$$A = A_\infty[1 - \exp(-kt)] \tag{2a}$$

$$A = A_\infty[1 - \exp(-kt)] + a \tag{2b}$$

and

$$A = A_\infty[1 - \exp(-kt)] + bt \tag{2c}$$

where A is the absorbance t s after the start of the reaction, A^0 is the initial and A_∞ the final absorbance related to the substance, the concentration of which is followed, k is the rate constant in s^{-1}, and a and b are parameters, the values of which govern the background absorbance.

Arbitrarily chosen values of the parameters in these equations, which always included $k = 0.1\ s^{-1}$ and A^0 or $A_\infty = 1$, while a and b were assigned values ranging between 1×10^{-4} and 0.03, were used to calculate the coordinates of 30 points on the absorbance/time curve. These were always equally spaced at intervals of 1.5 s, beginning with $t = 1.5$ s and ending with a point at which the reaction was 98.9% complete. It was always assumed that the standard error of the measurements of absorbance was 0.001, but different values ranging from 0.0001 s to 0.15 s were assigned in different calculations to the standard error of the measurements of time.

The corresponding standard error of the rate constant was computed by using the program VARPWR [5], which resembles a program that was described previously [6] but employs weighted non-linear regression to take errors in the independent variable into account. The value A_1 of the absorbance (the dependent variable) at the first point in the set of synthetic data is changed by an arbitrary small amount ΔA (which in this work was always four times the standard error of an absorbance measurement), and the best values of the parameters [$V(1)$, $V(2)$, etc.] are computed by non-linear regression, minimizing the quantity

$$\sum_n [W_n(A_{c,n} - A_{m,n})]^2$$

where $A_{c,n}$ is the calculated and $A_{m,n}$ the "measured" absorbance at the nth point, and W_n is a weighting factor given by

$$W_n = 1/[\sigma_A^2 + \sigma_t^2(dA/dt)^2] \tag{3}$$

in which the necessary expression for the slope dA/dt of the absorbance/time curve is easily obtained by differentiating the equation from which the synthetic data were computed and to which the perturbed data are fitted. The values of $\Delta V(1)/\Delta A_1$, $\Delta V(2)/\Delta A_1$, etc., are stored, A_1 is reset to its original value, the value A_2 of the absorbance at the second point is changed similarly, a new set of values of the parameters is computed, and so on. When this has been done for all the points, the time t_1 at the first point is changed by an amount Δt that is equal to four times the standard error in the measurements of time, and the whole process is repeated to obtain values of $\Delta V(1)/\Delta t_1$, $\Delta V(2)/\Delta t_1$, and so on. The variances of the parameters are finally obtained from equations of the form

$$\sigma_{V(1)}^2 = \sigma_A^2 \sum_{j=1}^{n} [\Delta V(1)/\Delta A_j]^2 + \sigma_t^2 \sum_{j=1}^{n} [\Delta V(1)/\Delta t_j]^2 \tag{4}$$

All the computations were made in single-precision FORTRAN with a Radio Shack TRS-80 Model II microcomputer. Both because only very simple relationships are involved and because stringent criteria were applied in terminating the least-squares fits, replicate calculations indicated that the computed standard errors of the parameters are reliable to about 1%.

RESULTS AND DISCUSSION

Table 1 shows how the relative standard errors of the initial (or final) absorbance and the rate constant depend on the standard error of the measurements of time for data conforming to Eqns. 1(a) and 2(a) and having a standard error of 0.001 absorbance in the measurements of absorbance. The

TABLE 1

The effects of the uncertainty in measuring time on the relative standard errors of the initial or final absorbance and the rate constant in Cases 1a and 2a
(The first column gives the values of σ_t that were used in calculating these results. Since F and $t_{1/2}$ were taken to be equal to 0.001 and to 6.9 s, respectively, the values of σ_t correspond to the values of G/F given in the second column. The remaining columns give the corresponding values of the quantity $\sigma_{V_i^*}$ defined by Eqn. 6.)

σ_t (s)	G/F	Relative standard error (%)			
		Case 1a		Case 2a	
		A^0	k	A_∞	k
0.0001	0.0145	0.0908	0.119	0.0358	0.126
0.001	0.145	0.0914	0.120	0.0358	0.127
0.01	1.45	0.121	0.146	0.0382	0.148
0.02	2.9	0.208	0.288	0.0642	0.288
0.04	5.8	0.450	0.838	0.285	0.890
0.06	8.7	0.699	1.41	0.841	1.86
0.10	14	1.16	2.40	2.33	4.00
0.15	22	1.53	3.12	3.71	5.84

general relationship among these standard errors can be expressed in the form

$$(\sigma_{V_i}/V_i)^2 = (\sigma_A/A^0)^2(\partial V_i/\partial A)^2 + (\sigma_t/t_{1/2})^2(\partial V_i/\partial t)^2 \quad (5)$$

The relation of this equation to Eqn. 4 is apparent. Defining the relative standard errors of measurement of A and t by means of the equations

$$F = \sigma_A/A^0 \text{ and } G = \sigma_t/t_{1/2}$$

makes it possible to rewrite Eqn. 5 as

$$(\sigma_{V_i}/V_i) = F\{[(\partial V_i/\partial A)^2 + (G/F)^2(\partial V_i/\partial t)^2]^{1/2}\} = F\sigma_{V_i^*} \quad (6)$$

where V_i denotes the ith parameter (for example, either A^0 or k in Case 1a) and $\sigma_{V_i^*}$ denotes the quantity within braces, which depends on the value of G/F. From these equations, it is possible to find the relative standard error of k for any combination of standard errors of measurement of absorbance and time, in the following fashion. Consider a relaxation experiment in which the absorbance of a reactant is measured (Case 1a), in which its initial value is 0.02, and in which the standard error of a measurement of absorbance is 0.0001, so that $F = 0.005$. Suppose that the half-time is 1 μs and that the standard error in the measurements of time is 50 ns, so that $G = 0.05$ and $G/F = 10$. By interpolating between the values given in Table 1, it may be found that the relative standard error of k would be approximately 1.6% if $G/F = 10$ and $F = 0.001$. Hence $\sigma_{k^*} = 0.016$ in Eqn. 6 and, because F is five times as large in this hypothetical experiment as it is in Table 1, the relative standard error of k will be approximately 8%.

Several phenomena are prominent in Table 1. First, the precisions of the results deteriorate as the measurements of time become more uncertain, as is of course to be expected, but they do so at different rates in the two cases. If the standard error σ_t of the measurements of time is less than about 0.005 $t_{1/2}$, the precision of the rate constant computed from the data is nearly the same regardless of whether the measured absorbance is due to a reactant (Case 1a) or a product (Case 2a). Hence the structure of the experiment is immaterial if the measurements of time are highly precise. As σ_t increases, however, the standard error of the rate constant increases. It does so more rapidly when the absorbance of a product is measured than it does when the absorbance of a reactant is measured, and can become much larger in the former case than in the latter. Hence it is advantageous to follow the concentration of a reactant if the measurements of time are only moderately precise. Moreover, as will be shown subsequently, the precision of k can be improved, if it is the absorbance of a reactant that is measured, by decreasing the overall duration of the experiment, but this expedient makes matters worse if it is the absorbance of a product that is measured. The results shown in Table 1 therefore understate the advantage of measuring the absorbance of a reactant.

Secondly, provided that the standard error of the measurements of time is extremely small, it has no detectable effect on the standard error of any parameter calculated from the data. In this range, the effects of uncertainties in the measurements of time are certainly insignificant, but the requirement is much more stringent than is generally believed. It corresponds to values of $\sigma_t/t_{1/2}$ no larger than about 0.00015 (= 0.001/6.9) if F = 0.001, as is assumed here. These figures mean that, for a reaction having a half-time of 50 s, the uncertainty in the measurements of time is insignificant only if the standard error of those measurements does not exceed about 7 ms. Precision of that order is rarely sought or achieved.

Thirdly, very few of the rate constants for which values have been recorded in the literature have precisions approaching those recorded in Table 1. One reason for the discrepancy is that the standard errors of measurement embodied in Table 1 are smaller than those achieved in most such experiments. On the fourth line of the Table, for example, the assumed values of F and G are $F = \sigma_A/A^0 = 0.001/1 = 0.001$ and $G = \sigma_t/t_{1/2} = 0.02/6.9 = 0.003$, respectively. A standard error of 0.001 in the measurement of an absorbance is optimistic but not unrealistic for a modern spectrophotometer, but one of 0.01 would be closer to the truth for the older equipment with which many of the values in the current literature were obtained. Moreover, it is the ratio of that standard error to the initial or final absorbance that governs the precision of the value of the rate constant. If, in Case 1a, the initial absorbance were changed from 1 to 0.2 without altering the standard error of measurement, the value of F would be increased from 0.001 to 0.005, and this fivefold increase would cause the relative standard error of the value of k to increase by a factor of approximately 5. If some upper bound is imposed on the concentration of the reaction mixture by the availability or solubility

of the reactant or by any other consideration, it is advisable to adopt special measures (such as the use of a cell having a long optical path) that will increase the initial (or final) absorbance. The ratio of the standard error of a measurement of absorbance to the change of absorbance during the reaction is probably the most important of the factors that affect the precision of the result.

The relatively poor precisions of many of the literature values of k might also reflect large uncertainties in the measurements of time. If the half-time is 50 s, the fourth line of Table 1 corresponds to a standard error of 0.15 s. That is easily within the reach of modern timing and recording devices, and by no means beyond that of older ones. It is not, however, a very large figure, and the notion that uncertainties in the measurement of time are insignificant may well have led some experimenters to look tolerantly on standard errors as large as this.

Another possibility is that other important sources of uncertainty are common in such experiments. Some of these, including background absorbances of various kinds, are considered in subsequent paragraphs.

Before leaving Cases 1a and 2a, however, it is appropriate to examine certain information that these calculations provided with regard to the efficiency of experimentation. Figure 1A shows pointwise-variance-analysis plots [6] for the rate constant in Case 1a. On such a plot the ordinate is the logarithm of the relative influence that a particular point exerts on the value that is assigned to the parameter of interest, and the abscissa is the independent variable in the experiment. Curve (a) duplicates a curve previously published [7] and shows that, if the standard error of the measurements of time is negligibly small, there is a broad region of substantial influence at values of

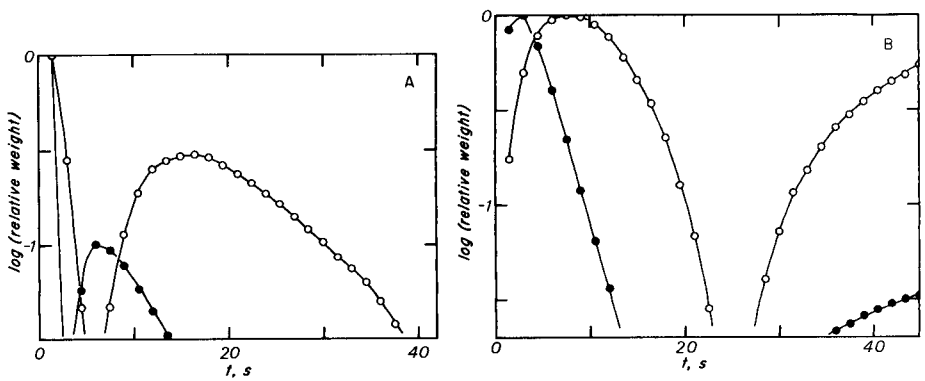

Fig. 1. Pointwise-variance-analysis plots showing how the relative influence of a data point on the computed value of k depends on the time at that point: (A) in Case 1a; (B) in Case 2a. It is assumed that there are 30 data points equally spaced along the time axis from Δt to 30 Δt, that $A^0 = 1$ and $k = 0.1$ s^{-1} in Case 1a (or that $A_\infty = 1$ and $k = 0.1$ s^{-1} in Case 2a) and that the standard errors in the measurements of absorbance and time are 0.001 and 0.001 s (open circles; curve a) or 0.02 s (solid circles; curve b), respectively. These assumptions correspond to $F = 0.001$ and $G = 0.000145$ or 0.0029, respectively.

$t/t_{1/2}$ between about 1.7 and 3.2. This is an important reason why, as is customarily prescribed, the data should cover more than the first half-time or two: the consequences of missing this influential region are illustrated by the last several lines for Case 1a in Table 2. The values given in that Table are based on the assumptions that 30 data points are secured; that they are equally spaced along the time axis from Δt to 30 Δt; that A^0 and k are equal to 1 and 0.1 s^{-1}, respectively; and that the standard errors in the measurements of absorbance and time are equal to 0.001 and 0.02 s, respectively. These assumptions correspond to $F = 0.001$ and $G = 0.02/6.9 = 0.003$. The relative standard error of A^0 decreases monotonically as Δt decreases, because all of the points that appreciably influence the value of A^0 occur at very short times, so that they become proportionately more numerous as the duration of the experiment decreases. As regards the value of k, the situation is more complex. If Δt is moderately large, decreasing it crowds a larger fraction of the points into the two most influential regions, and the precision of k improves. Under the conditions assumed in these calculations the relative standard error of k passes through a minimum if $\Delta t = 0.5$ s. That corresponds to $t = 15$ s, or $t/t_{1/2} = 2.2$, at the last point obtained. Only a very few points are then obtained in the important region $1.7 < t/t_{1/2} < 3.2$. Decreasing Δt still further leads to a decrease of the already small number of those points, and the precision of the result deteriorates rapidly.

When the absorbance of a product, rather than that of a reactant, is followed, very different behavior is observed; this is also outlined in Table 2 (Case 2a). As is shown by the pointwise-variance-analysis plots of Fig. 1B, there are again two regions in which the points exert substantial influence on

TABLE 2

Effects of the range of times covered by the experimental measurements on the standard errors of A_∞ and k computed in Case 1a and in Case 2a.
(The assumptions that lead to these values are described in the text.)

Δt (s)	Fraction of starting material remaining at last point	Relative standard errors (%)			
		Case 1a		Case 2a	
		A^0	k	A_∞	k
1.5	0.989	0.208	0.288	0.0642	0.288
1.3	0.980	0.192	0.272	0.0804	0.305
1.1	0.963	0.175	0.257	0.103	0.331
0.9	0.933	0.157	0.241	0.143	0.380
0.7	0.88	0.138	0.226	0.220	0.473
0.5	0.78	0.120	0.220	0.390	0.682
0.35	0.65	0.104	0.228	0.716	1.07
0.25	0.53	0.0939	0.256	1.31	1.75
0.2	0.45	0.0883	0.286	1.89	2.38
0.15	0.36	0.0829	0.344	2.97	3.53
0.1	0.26	0.0769	0.473	7.25	7.99

the value of k. One occurs shortly after the start of the reaction, and is centered around $t/t_{1/2} = 1$ if $\sigma_t = 0.001$ s ($G/F = 0.145$, curve a); the other occurs as the reaction approaches completion and gives rise to a broad band in which the relative influence of a point increases steadily as the time at that point increases. As Δt becomes larger (curve b), the first region becomes sharper and narrower and moves toward shorter times, while the relative importance of the second is greatly diminished. Because of these phenomena, decreasing the duration of an experiment always decreases the number of points that lie within the second influential region, and decreasing it very largely leads ultimately to a situation in which most of the points lie on the rising part of the first region, so that only a few of them are worth obtaining, and the relative standard error of k again becomes very large.

Tables 3—6 describe the relative precisions that can be obtained in evaluating the parameters in Cases 1b, 1c, 2b, and 2c, respectively. In Cases 1b and 2b (Tables 3 and 5), increasing the value of a has, within the precision of these calculations, no effect whatever on the precisions of the initial (or final) absorbance and the rate constant, and merely improves the precision of a in inverse proportion to its value. In Cases 1c and 2c (Tables 4 and 6) the same thing is true as a first approximation; small deviations can be discerned but do not seem to deserve detailed discussion.

Because the precision that can be attained in evaluating a or b is evidently very poor unless that quantity is moderately large, it is appropriate to inquire into the errors that result from overlooking a background correction and into the ways in which the necessity for such a correction might be detected. Tables 7 and 8 show how the values of a and b affect the values of A^0 (or A_∞) and k that are obtained from ordinary unweighted regression when the data actually conform to Case 1b or 2b (Table 7) or Case 1c or 2c (Table 8), but when failure to recognize the necessity of taking a background correction into account leads to their being erroneously fitted to the equation representing Case 1a or 2a. In Case 1b, for example, a constant background absorbance of 0.03 would cause the measured absorbance to decay from 1.03 to 0.03, and its neglect would lead to a relative error of −3.8% in the rate constant (Table 7, line 5). Nearly the same error is produced in Case 1c if $b = 3 \times 10^{-4}$ (Table 8, line 6), which corresponds to an increase of the background absorbance from 0 to 0.0135 during the time in which the reaction reaches 98.9% completion. The last of these numbers is only 1.3% of the initial absorbance. It would surely be much easier to overlook the background absorbance in the second of these situations, and easier still if the measurements were discontinued before the reaction had reached that degree of completion. The difficulty of identifying a linearly increasing absorbance may be one of the most important factors limiting the precisions of experimental evaluations of rate constants in traditional ways.

Figure 2 shows the deviation pattern obtained when the necessity of taking a linearly increasing background absorbance into account is not perceived, and when data that actually conform to Eqn. 1(c) are accordingly fitted to

TABLE 3

The effects of the uncertainty in measuring time and the value of a on the relative standard errors of the parameters in Case 1b (The first column gives the values of σ_t that were used in calculating these results. Since F and $t_{1/2}$ were taken to be equal to 0.001 and to 6.9 s, respectively, they correspond to the values of G/F given in the second column. The remaining columns give the corresponding values of the quantities of $\sigma_{V_i^*}$ defined by Eqn. 6)

σ_t (s)	G/F	Relative standard error (%)								
		a = 0.001			a = 0.01			a = 0.1		
		A^0	k	a	A^0	k	a	A^0	k	a
0.0001	0.0145	0.0916	0.195	38.4	0.0915	0.195	3.92	0.0915	0.195	0.394
0.001	0.145	0.0919	0.197	38.6	0.0915	0.194	3.90	0.0916	0.195	0.393
0.01	1.45	0.113	0.217	39.7	0.113	0.216	4.05	0.113	0.217	0.408
0.02	2.9	0.166	0.280	44.4	0.166	0.279	4.48	0.166	0.279	0.451
0.04	5.8	0.328	0.508	64.1	0.328	0.509	6.48	0.328	0.506	0.645
0.06	8.7	0.541	0.823	95.5	0.541	0.829	9.64	0.541	0.825	0.955
0.10	14	—	—	—	1.02	1.52	16.4	1.02	1.52	1.64
0.15	22	—	—	—	1.66	2.37	24.3	1.66	2.36	2.38

TABLE 4

The effects of the uncertainty in measuring time and the value of b on the relative standard errors of the parameters in Case 1c (For explanation, see notes on Table 3.)

σ_t (s)	G/F	Relative standard error (%)											
		b = 0.0001			b = 0.001			b = 0.01			b = 0.03		
		A^0	k	b	A^0	k	b	A^0	k	b	A^0	k	b
0.0001	0.0145	0.0982	0.154	9.08	0.0980	0.154	0.915	0.0984	0.155	0.0916	0.0983	0.155	0.0305
0.001	0.145	0.0988	0.155	9.09	0.0982	0.154	0.914	0.0985	0.155	0.0915	0.0978	0.154	0.0304
0.01	1.45	0.130	0.190	9.65	0.129	0.188	0.971	0.122	0.179	0.0946	0.110	0.168	0.0328
0.02	2.9	0.223	0.370	15.1	0.220	0.362	1.49	0.191	0.284	0.113	0.140	0.204	0.0384
0.04	5.8	0.473	1.03	58.1	0.464	0.991	5.45	0.362	0.602	0.183	0.222	0.310	0.0547
0.06	8.7	—	—	—	0.723	1.77	16.6	0.535	0.928	0.261	0.311	0.438	0.0762
0.10	14	—	—	—	1.21	3.87	80.2	0.852	1.50	0.412	0.488	0.736	0.127
0.15	22	—	—	—	—	—	—	1.13	1.97	0.592	0.703	1.18	0.202

TABLE 5

The effects of the uncertainty in measuring time and the value of a on the relative standard errors of the parameters in Case 2b (For explanation, see notes on Table 3.)

σ_t (s)	G/F	Relative standard error (%)								
		a = 0.001			a = 0.01			a = 0.1		
		A_∞	k	a	A_∞	k	a	A_∞	k	a
0.0001	0.0145	0.0939	0.181	99.9	0.0925	0.185	9.92	0.0938	0.187	1.01
0.001	0.145	0.0947	0.185	101	0.0925	0.187	10.0	0.0935	0.187	1.00
0.01	1.45	0.118	0.234	133	0.118	0.235	13.4	0.119	0.236	1.34
0.02	2.9	—	—	—	0.184	0.464	23.1	0.184	0.466	2.31
0.04	5.8	—	—	—	0.309	1.41	50.2	0.306	1.42	5.03
0.06	8.7	—	—	—	0.461	3.00	83.4	0.471	3.01	8.34
0.10	14	—	—	—	—	—	—	2.07	10.7	19.4

TABLE 6

The effects of the uncertainty in measuring time and the value of b on the relative standard errors of the parameters in Case 2c (For explanation, see notes on Table 3.)

σ_t (s)	G/F	Relative standard error (%)											
		b = 0.0001			b = 0.001			b = 0.01			b = 0.03		
		A_∞	k	b	A_∞	k	b	A_∞	k	b	A_∞	k	b
0.0001	0.0145	0.237	0.325	55.1	0.245	0.330	5.64	0.238	0.321	0.554	0.241	0.326	0.183
0.001	0.145	0.221	0.310	51.6	0.241	0.327	5.56	0.235	0.318	0.543	0.238	0.325	0.182
0.01	1.45	0.291	0.406	66.2	0.292	0.404	6.68	0.302	0.422	0.690	0.349	0.486	0.263
0.02	2.9	0.595	0.804	135	0.618	0.827	14.0	0.706	0.924	1.61	0.834	1.08	0.636
0.04	5.8	—	—	—	2.48	2.65	57.6	2.75	2.88	6.49	2.35	2.64	1.82
0.06	8.7	—	—	—	5.55	4.99	131	5.31	4.87	12.7	4.18	4.29	3.26
0.10	14	—	—	—	—	—	—	15.3	9.94	38.4	7.91	7.15	6.12
0.15	22	—	—	—	—	—	—	—	—	—	12.7	10.1	9.67

TABLE 7

The errors caused by an unrecognized constant absorbance
(This table gives the values of the parameters obtained by unweighted regression when synthetic data conforming to Cases 1b and 2b, with A^0 or A_∞ equal to 1 and k equal to 0.1 s^{-1}, are mistakenly fitted to the equations that represent Cases 1a and 2a)

a	Case 1b		Case 2b	
	A^0	k	A_∞	k
0.0001	0.999 999	0.099 962	1.000 08	0.100 017
0.0003	0.999 969	0.099 883	1.000 25	0.100 045
0.001	0.999 886	0.099 610	1.000 83	0.100 149
0.003	0.999 643	0.098 836	1.002 48	0.100 446
0.01	0.998 749	0.096 159	1.008 28	0.101 482
0.03	0.996 144	0.088 877	1.024 97	0.104 448
0.1	0.990 541	0.067 783	1.084 28	0.114 999

TABLE 8

The errors caused by an unrecognized linearly increasing absorbance
(This table gives the values of the parameters obtained by unweighted regression when synthetic data conforming to Cases 1c and 2c, with A^0 or A_∞ equal to 1 and k equal to 0.1 s^{-1}, are mistakenly fitted to the equations that represent Cases 1a and 2a)

b	Case 1c		Case 2c	
	A^0	k	A_∞	k
1×10^{-6}	0.999 96	0.099 990	1.000 04	0.099 954
3×10^{-6}	0.999 88	0.099 968	1.000 13	0.099 985
1×10^{-5}	0.999 60	0.099 893	1.000 41	0.099 952
3×10^{-5}	0.998 80	0.099 679	1.001 26	0.099 852
1×10^{-4}	0.995 99	0.098 928	1.004 19	0.099 509
3×10^{-4}	0.987 80	0.096 768	1.012 59	0.098 539
0.001	0.957 50	0.089 031	1.042 34	0.095 274
0.003	—	—	1.130 25	0.086 947

Eqn. 1(a). A pattern that is nearly the mirror image of Fig. 2 around the abscissa axis is obtained when data that actually conform to Eqn. 2(c) are fitted to Eqn. 2(a). The amplitudes of such plots [8] are difficult to describe meaningfully, and we shall therefore speak instead of the value at the minimum on Fig. 2. If $b = 0.001$, so that the measured value of the absorbance at $t = 45$ s is actually 0.056 (instead of 0.011, as it would be if there were no background absorbance), the difference between the measured and calculated values of the absorbance is —0.0155 at the minimum. If the standard error of a single measurement of the absorbance is 0.001, the minimum will be prominent on the deviation plot, and the necessity of taking a background absorbance into account will be plainly evident. However, as is shown by Table 9, the depth of the minimum decreases as the value of b decreases, and

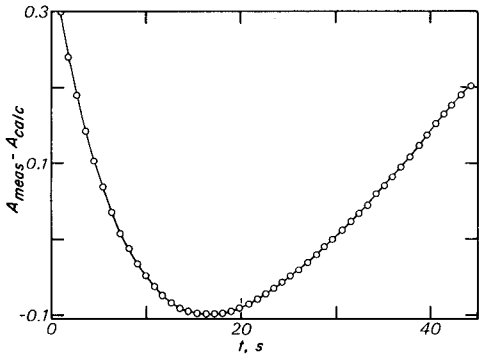

Fig. 2. The deviation pattern obtained when data conforming to Case 1c are erroneously treated as though they conformed to Case 1a. One hundred "data" points equally spaced along the time axis from $t = 0.065\ t_{1/2}$ to $t = 6.5\ t_{1/2}$ were synthesized from Eqn. 1(c) with $A^0 = 1$, $k = 0.1$, and $b = 0.01$. The best fit to Eqn. 1(a) gave $A^0 = 0.659$ and $k = 0.019$, which differ from the values given in Table 8 because the data-acquisition schedules are different.

TABLE 9

Coordinates of the minima on the deviation plots obtained when a system conforming to Eqn. 1(c) is erroneously classified as conforming to Eqn. 1(a)
(To locate the minima as precisely as possible, 90 points at 0.5-s intervals from $t = 0.5$ s to 45 s were synthesized from Eqn. 1(c) with $A^0 = 1$, $k = 0.1$, and the value of b given in the first column. The second and third columns give the values of A^0 and k obtained by fitting these "data" to Eqn. 1(a), and the fourth column gives the deviation at the minimum on the deviation plot (Fig. 2). All these minima occurred at $t = 10.5$ s)

b	Apparent values of		Deviation at the minimum
	A^0	k	
0.001	0.9653	0.0898	0.0155
0.0005	0.9833	0.0950	0.00754
0.0003	0.9900	0.0970	0.00446
0.0002	0.9934	0.0980	0.00296
0.0001	0.9967	0.0990	0.00147
0.00005	0.9984	0.0995	0.000730
0.00003	0.9990	0.0997	0.000439

is nearly but not exactly proportional to that value. If $\sigma_A = 0.001$, it may reasonably be supposed that the shape of the deviation plot will point reliably to the existence of the background absorbance if b exceeds about 1×10^{-4} s^{-1}, but that shape is likely to be obscured by the random errors of measurement if b has a smaller value. With $b = 1 \times 10^{-4}$ s^{-1}, failure to recognize the background absorbance leads to a relative error of 1% in the value of k.

Most of the rate constants tabulated in the literature are generally understood to have relative errors of roughly 3—5%. Very generous assumptions

regarding the values of F and G must be made to account for such figures. Other factors that can limit the precision of the experimental results include: (1) deviations from proportionality between that signal and the corresponding concentration; (2) unsuspected variations of the experimental conditions from one experiment to another or even during a single experiment, or differences between the actual and stated experimental conditions; (3) failure to account for the existence of a finite mixing interval or another source of uncertainty in the initial time; and (4) other sources of error. The first of these can be tested by measuring the signals obtained with stable solutions containing different known concentrations of the reactant or product which is to provide the signal to be followed; correction for any observed deviation from proportionality can then be made, at least in principle and with some loss of accuracy and precision. As regards the second, it is easily shown that a variation of temperature from 25° to 25.15°C will lead to a change of 1% in the rate constant if the energy of activation has the typical value of 50 kJ mol^{-1}. As has long been recognized, failure to control the temperature closely enough may well be the chief source of error in such experiments. Zuman and Patel [1] indicate that control within 0.02—0.05°C suffices in practical experimentation, but even these limits may be too generous if a really precise result is wanted or if the energy of activation may exceed 50 kJ mol^{-1}. It is easy to show that the temperature of a reaction mixture in which the initial concentration of the limiting reactant is 0.01 M may change as much as 0.1°C during a reaction for which the value of ΔH is 40 kJ mol^{-1}: if the reaction is reasonably fast, heat transfer through the walls of the reaction vessel may compensate for only a fraction of this variation, with the result that k may vary by several tenths of a per cent even though a highly precise thermostat is used to control the external temperature. Errors in the initial time may be dismissed as far as first- and pseudo-first-order reactions are concerned, for although they affect the calculated initial value of the signal, they have no effect whatever on the calculated value of the rate constant. All these considerations must be taken into account in designing experiments that will yield results having precisions commensurate with the trouble and time that it costs to perform them.

REFERENCES

1 P. Zuman and R. C. Patel, Techniques in Organic Reaction Mechanisms, Wiley, New York, 1984, p. 7 and p. 13.
2 V. A. Palm (Ed.), Tables of Rate and Equilibrium Constants of Heterolytic Organic Reactions, Vols. I—V, Viniti, Moscow, 1975.
3 H. C. Smit, L. Meites and G. Kateman, Anal. Chim. Acta, 153 (1983) 121.
4 G. Kateman, H. C. Smit and L. Meites, Anal. Chim. Acta, 152 (1983) 61.
5 L. Meites, The General Non-Linear Regression Program CFT4A, The George Mason Institute, Fairfax, VA, 1985, pp. 218—222.
6 L. Meites, Anal. Chim. Acta, 74 (1975) 177.
7 L. Meites, CRC Crit. Rev. Anal. Chem., 8 (1979) 1.
8 L. Meites, Anal. Lett., 15(A5) (1983) 507.

Analytica Chimica Acta, 178 (1985) 277—288
Elsevier Science Publishers B.V., Amsterdam — Printed in The Netherlands

A NEW METHOD FOR THE pH CALCULATION OF SOLUTIONS AND MIXTURES OF ACIDS, BASES AND SALTS

ALBERT E. CLAEYS

Laboratory of Analytical Chemistry, Faculty of Pharmacy, State University of Gent, Harelbekestraat 72, B-9000 Gent (Belgium)

(Received 6th June 1985)

SUMMARY

The improved successive approximation method calculates the exact $[H^+]$ and pH value of solutions and mixtures of acids, bases and salts, and can be applied to titration data. The procedure consists in the calculation of the concentration of all species present in solution, selection of the appropriate rule of electroneutrality and introduction of suitable correction factors in order to obtain a final quadratic equation which is easily solved. Compared with existing methods of pH calculation, which are based on the Newton-Raphson iteration procedure, the proposed method requires a smaller number of iterations and a shorter calculation time. As there are no limitations on the number of compounds, nor on the number or values of acidity and basicity constants, nor on the concentration range, complex problems can be solved and titration curves plotted in a short time.

Problems in the calculation of pH in which a maximum of four constants is involved are discussed in most handbooks and solved in the same way by a chemical and algebraic approach (see, e.g. [1—3]). Introducing the predominant dissociation reaction, taking into account only the principal solute species and assuming that the concentration of the other species is negligible makes it possible to use simplified formulae. Although for some selected examples where the approximations are valid good results are obtained, it can be confirmed easily by a simple checking through the rule of electroneutrality that considerable errors can occur in other cases.

Exact results can only be obtained by methods where a rigorous expression for the $[H^+]$ concentration is used and the equation is solved by a computer program based on the Newton-Raphson procedure. Derived from a Fortran program with a capacity of eight constants [4], the only valuable practical HP program [5] is still restricted to four constants.

There has been a lack of programs for the pH calculation of complex mixtures. This paper introduces a new calculation method, based on an original principle, whereby no limits occur as to the number of constants involved.

In order to avoid all misunderstanding in the description and discussion of the proposed method, it has to be emphasized that a compound (acid,

0003-2670/85/$03.30

base, salt) will be considered as a molecule (Arrhenius concept) and a species as a Brönsted acid or base or both. The term monovalent is used for an acid or base with only one constant, and the term polyvalent for an acid or base with several constants. Furthermore, as in the existing programs for calculation of pH, no account is taken of activity coefficients.

The calculation procedure will be described in detail for an aqueous solution of a polyvalent acid and, by analogy, for a base, a salt and finally for a complex mixture. After the comparison of the method with the Newton-Raphson procedure, a short survey of application possibilities including titration curves is given.

CALCULATION PROCEDURES

All calculations are made on HP-85 personal computer connected to an HP-7225 plotter. The memory requirement is 19.2 kbyte for the first program and 16.4 kbyte for the second (see below). The programs are available from the author on request.

Calculation procedure for a polyvalent acid

An aqueous solution of a polyvalent acid (with x acidity constants K_{a1} to K_{ax}) contains $x + 1$ kinds of species S_i^{-} (numbered S_0 to S_x with subscript i representing the absolute value of the charge on the species). The concentration of each species changes with the pH of the solution; their sum remains constant and is called the analytical concentration C_a.

For a tetravalent acid, the concentration of the different species is given by $[S_0] = D\,[H^+]^4$, $[S_1] = D\,[H^+]^3\,K_{a1}$, $[S_2] = D\,[H^+]^2\,K_{a1}\,K_{a2}$, $[S_3] = D\,[H^+]\,K_{a1}\,K_{a2}\,K_{a3}$ and $[S_4] = D\,K_{a1}\,K_{a2}\,K_{a3}\,K_{a4}$, where $D = C_a/([H^+]^4 + [H^+]^3\,K_{a1} + [H^+]^2\,K_{a1}\,K_{a2} + [H^+]\,K_{a1}\,K_{a2}\,K_{a3} + K_{a1}\,K_{a2}\,K_{a3}\,K_{a4})$.

It is possible to derive $x + 1$ rules of electroneutrality (or R(en), R_r numbered R_0 to R_x) by using the equation

$$[H^+] + \Sigma\{(r-i)\,[S_i]\}_{i=0}^{i=r} = \Sigma\{(i-r)\,[S_i]\}_{i=r}^{i=x} + [OH^-] + r\,C_a \qquad (1a)$$

This equation clearly indicates that the species $S_{i=r}$ is always absent in the R(en) R_r.

For a tetravalent acid, five R(en) equations can thus be obtained

$$R_0\ [H^+] = [S_1] + 2\,[S_2] + 3\,[S_3] + 4\,[S_4] + [OH^-]$$

$$R_1\ [H^+] + [S_0] = [S_2] + 2\,[S_3] + 3\,[S_4] + [OH^-] + C_a$$

$$R_2\ [H^+] + 2\,[S_0] + [S_1] = [S_3] + 2\,[S_4] + [OH^-] + 2\,C_a$$

$$R_3\ [H^+] + 3\,[S_0] + 2\,[S_1] + [S_2] = [S_4] + [OH^-] + 3\,C_a$$

$$R_4\ [H^+] + 4\,[S_0] + 3\,[S_1] + 2\,[S_2] + [S_3] = [OH^-] + 4\,C_a$$

Plotting the % fraction of each species vs. pH, one can distinguish $x + 1$ areas, each of which is characterised by the presence of: (1) a predomi-

nant species S_m; (2) species $S_{i<m}$ with increasing % fraction for increasing values of $[H^+]$ (these $[H^+]$-analogous species are called α species); (3) species $S_{i>m}$ or $[OH^-]$-analogous species with increasing % fraction for increasing values of $[OH^-]$ which are called β species.

Selecting for a given pH, the R(en) with subscript equal to that of the predominant species, one obtains the specific R(en) R_m where the predominant species S_m is absent, given by

$$[H^+] + \Sigma\{(m-i)[S_i]\}_{i=0}^{i=m} = \Sigma\{(i-m)[S_i]\}_{i=m}^{i=x} + [OH^-] + m C_a \qquad (2a)$$

or in a simplified form

$$[H^+] + [\alpha] = [\beta] + [OH^-] + [\delta] \qquad (3a)$$

The term $[\alpha] = \Sigma\{(m-i)[S_i]\}_{i=0}^{i=m}$ or $[\beta] = \Sigma\{(i-m)[S_i]\}_{i=m}^{i=x}$ contains the sum of the concentration of each α species $S_{i<m}$ or β species $S_{i>m}$ multiplied by a coefficient equal to the absolute charge difference versus the predominant species S_m. The term $[\delta]$ contains the analytical concentration of the S species multiplied by a coefficient equal to the subscript of the predominant species.

Because the R(en) equations are used in the calculation procedure, a selection of adequate R(en) has to be made in order to guarantee a minimum of iterations. For a given $\Delta[H^+]$, the relative concentration change of the predominant species is the smallest one, thus use of a R(en) containing that species will result in a high number of iterations and must therefore be avoided. In practice, this means that the specific R(en) R_m has to be selected as this is the only one where S_m is absent.

The procedure starts with the calculation, for an arbitrary value of $[H^+]_0$, of $[OH^-]_0$ and of the species concentrations $[S_0]_0$ to $[S_x]_0$, the selection of the predominant species S_m and of the α species ($S_{i<m}$) and β species ($S_{i>m}$), and the calculation of $[\alpha]_0$, $[\beta]_0$ and $[\delta]_0$. The next step consists in introducing the values $[H^+]_1 = [H^+]_0 p_0$ and $[OH^-]_1 = [OH^-]_0 q_0$. Both values are hypothetical and temporarily unknown because of the correction factors p_0 and q_0; however, their product always remains $p_0 q_0 = 1$, because $[H^+]_0 [OH^-]_0 = K_w = [H^+]_1 [OH^-]_1$. In the same way, the correction factors $s_{0,0}$ to $s_{x,0}$ for the different species concentrations must be introduced; they are rather complex and lead to a polynomial equation of $(x+2)$ degree. For a tetravalent acid, they are given by $s_{i,0} = s_{4,0} p_0^{4-i}$, where $s_{4,0} = ([H^+]_0^4 + [H^+]_0^3 K_{a1} + [H^+]_0^2 K_{a1} K_{a2} + [H^+]_0 K_{a1} K_{a2} K_{a3} + K_{a1} K_{a2} K_{a3} K_{a4})/([H^+]_0^4 p_0^4 + [H^+]_0^3 p_0^3 K_{a1} + [H^+]_0^2 p_0^2 K_{a1} K_{a2} + [H^+]_0 p_0 K_{a1} K_{a2} K_{a3} + K_{a1} K_{a2} K_{a3} K_{a4})$.

Elimination of higher-degree equations can only be achieved by simplifying the correction factors. Taking into account that all the α species $S_{i<m}$ are assembled in the $[\alpha]$ term and that they are all $[H^+]$-analogous species, the assumption is made that the correction factor for the $[\alpha]$ term is equal to p_0. In the same way the correction factor for the $[\beta]$ term containing all the $[OH^-]$-analogous β species $S_{i>m}$ is assumed to be equal to q_0. The specific R(en) then becomes

$$([H^+]_0 + [\alpha]_0)\, p_0 = ([OH^-]_0 + [\beta]_0)\, q_0 + [\delta]_0 \qquad (4a)$$

Multiplication of both sides with p_0 and rearrangement yields the quadratic equation

$$([H^+]_0 + [\alpha]_0)\, p_0^2 - [\delta]_0\, p_0 - ([OH^-]_0 + [\beta]_0) = 0$$

from which the value of p_0 is solved as

$$p_0 = \{[\delta]_0 + \{[\delta]_0^2 + 4([H^+]_0 + [\alpha]_0)([OH^-]_0 + [\beta]_0)\}^{1/2}\}/2([H^+]_0 + [\alpha]_0)$$

The value of the correction factor p_0 is thus obtained by using only the exact true values of $[OH^-]_0$, $[\alpha]_0$, $[\beta]_0$ and $[\delta]_0$ calculated at the start of the procedure.

The next iteration starts with $[H^+]_1 = [H^+]_0\, p_0$ which is used for the calculation of $[OH^-]_1$ and $[S_0]_1$ to $[S_x]_1$, followed by the selection of the specific R(en) (which can be changed when another species becomes predominant) and of the α and β species, the calculation of $[\alpha]_1$, $[\beta]_1$ and $[\delta]_1$, and finally of p_1 in order to obtain $[H^+]_2 = [H^+]_1\, p_1$. This procedure is repeated until $1.0023 > p_n > 0.9977$ (i.e., an error of 0.23% for an accuracy of 0.001 pH), giving the final result $[H^+]_f = [H^+]_n\, p_n$. Checking of this final result can be done in a simple way by introducing the values $[H^+]_f$, $[OH^-]_f$, $[S_0]_f$ to $[S_x]_f$ into the different R(en) equations: for each of them, the left and right sides must be equal within an error of 0.23%.

As an example, the pH is calculated for a 0.01 M solution of pyrophosphoric acid, $H_4P_2O_7$ (for constants, see Table 3). Starting with $pH_0 = 7$, the final result $[H^+]_f = 1.042 \times 10^{-2}$ or $pH_f = 1.982$ is obtained after four iterations and a calculation time of 3.31 s. The selected R(en), value of p and of pH for each iteration are: (1) R_3, 10.5786, 5.9756; (2) R_2, 6631.82, 2.1539; (3) R_1, 1.4831, 1.9828; (4) R_1, 1.00140, 1.9822. Checking of the result shows a 0.048% error between the left and right sides of R(en) R_0. For an erroneous result, pH = 1.981 or 1.983, the error becomes 0.37% or 0.28%, respectively.

Calculation procedure for a polyvalent base

The same principles can be applied for an aqueous solution of a polyvalent base (with y basicity constants K_{b1} to K_{by}) containing $y + 1$ kinds of species $T_{i'}^{i'+}$ (numbered T_0 to T_y with subscript i' corresponding to the absolute value of the species charge) with analytical concentration C_b.

The equation for the $y + 1$ R(en) $R_{r'}$ ($r' = 0$ to y) is given by

$$[H^+] + \Sigma\{(i' - r')\,[T_{i'}]\}_{i'=r'}^{i'=y} + r'C_b = \Sigma\{(r' - i')\,[T_{i'}]\}_{i'=0}^{i'=r'} + [OH^-] \qquad (1b)$$

In a diagram of % fraction versus pH, each of the $y + 1$ areas contains: (1) a predominant species $T_{m'}$; (2) species $T_{i'>m'}$ with increasing % fraction for increasing value of $[H^+]$ and called α' species; and (3) species $T_{i'<m'}$ or β' species because their % fraction increases for increasing value of $[OH^-]$.

The specific R(en) R_m, where the predominant species $T_{m'}$ is absent, is given by

$$[H^+] + \Sigma\{(i' - m')[T_{i'}]\}_{i'=m'}^{i'=y} + m'C_b = \Sigma\{(m' - i')[T_{i'}]\}_{i'=0}^{i'=m'} + [OH^-] \quad (2b)$$

or in a simplified form

$$[H^+] + [\alpha'] + [\delta'] = [\beta'] + [OH^-] \quad (3b)$$

The terms $[\alpha']$ and $[\beta']$ contain the sum of the concentration of each α' species and β' species, respectively, multiplied by a coefficient equal to the absolute charge difference compared to the predominant species. The term $[\delta']$ contains the analytical concentration of the T species multiplied by a coefficient equal to the subscript of the predominant species.

The calculation procedure can be summarised as follows: (1) for a given value of $[H^+]_0$, calculation of $[OH^-]_0$ and $[T_0]_0$ to $[T_y]_0$; (2) selection of the predominant species T_m, and of the α' species ($T_{i'>m'}$) and β species ($T_{i'<m'}$); (3) calculation of $[\alpha']_0$, $[\beta']_0$ and $[\delta']_0$; (4) introduction of the correction factor p_0 for $[H^+]_0$ as well as for $[\alpha']_0$ and of the correction factor q_0 for $[OH^-]_0$ and $[\beta']_0$. The specific R(en) becomes

$$([H^+]_0 + [\alpha']_0)p_0 + [\delta']_0 = ([OH^-]_0 + [\beta']_0)q_0 \quad (4b)$$

Multiplication of both sides with q_0 yields a quadratic equation from which the correction factor is calculated as

$$q_0 = \{[\delta']_0 + \{[\delta']_0^2 + 4([H^+]_0 + [\alpha']_0)([OH^-]_0 + [\beta']_0)\}^{1/2}\}/2([OH^-]_0 + [\beta']_0)$$

The next iteration starts with $[H^+]_1 = [H^+]_0/q_0$ and allows the calculation of q_1. The procedure is continued until $1.0023 > q_n > 0.9977$ to reach the final result $[H^+]_f = [H^+]_n/q_n$. For example, given a 0.05 M solution of codeine with $pH_0 = 7$, four iterations and a calculation time of 1.93 s are needed to obtain $pH_f = 10.324$.

Calculation procedure for a salt

A salt X_aY_b consists of species X (a T species derived from or equal to a parent base with y basicity constants) and of species Y (an S species derived from or equal to a parent acid with x acidity constants). An aqueous solution of molarity M_c behaves as a mixture containing the species S_0 to S_x (analytical concentration $C_a = b\,M_c$) and the species T_0 to T_y (analytical concentration $C_b = a\,M_c$). At each pH it is possible to derive $(x + 1)(y + 1)$ R(en) combinations $R_rR_{r'}$, using as the equation a combination of Eqns. 1(a) and 1(b):

$$[H^+] + \Sigma\{(r - i)[S_i]\}_{i=0}^{i=r} + \Sigma\{(i' - r')[T_{i'}]\}_{i'=r'}^{i'=y} + r'C_b =$$
$$= \Sigma\{(i - r)[S_i]\}_{i=r}^{i=x} + \Sigma\{(r' - i')[T_{i'}]\}_{i'=0}^{i'=r'} + rC_a + [OH^-]$$

The specific R(en) $R_mR_{m'}$, where the predominant species S_m and $T_{m'}$ are absent is a combination of Eqns. 2(a) and 2(b) or, in the simplified form, a combination of Eqns. 3(a) and 3(b):

$$[H^+] + [\alpha] + [\alpha'] + [\delta'] = [OH^-] + [\beta] + [\beta'] + [\delta]$$

Taking $[A] = [\alpha] + [\alpha']$, $[B] = [\beta] + [\beta']$, and $[D] = [\delta] - [\delta']$, one obtains the general equation

$$[H^+] + [A] = [OH^-] + [B] + [D] \quad (5)$$

The calculation procedure is also a combination of the procedures outlined above, resulting in a combination of Eqns. 4(a) and 4(b):

$$([H^+]_0 + [\alpha]_0 + [\alpha']_0)p_0 + [\delta']_0 = ([OH^-]_0 + [\beta]_0 + [\beta']_0)q_0 + [\delta]_0$$

which simplifies, by using Eqn. 5, to

$$([H^+]_0 + [A]_0)p_0 = ([OH^-]_0 + [B]_0)q_0 + [D]_0 \quad (6)$$

Multiplication of both sides with p_0 or q_0 yields two quadratic equations

$$([H^+]_0 + [A]_0)p_0^2 - [D]_0 p_0 - ([OH^-]_0 + [B]_0) = 0$$

or $$([OH^-]_0 + [B]_0)q_0^2 + [D]_0 q_0 - ([H^+]_0 + [A]_0) = 0$$

which can be solved to obtain

for $[D]_0 \geqslant 0$, $p_0 = E_0/2([H^+]_0 + [A]_0)$ and $[H^+]_1 = [H^+]_0 p_0$

for $[D]_0 < 0$, $q_0 = E_0/2([OH^-]_0 + [B]_0)$ and $[H^+]_1 = [H^+]_0/q_0$

using $E_0 = (\text{Abs } [D]_0) + \{[D]_0^2 + 4([H^+]_0 + [A]_0)([OH^-]_0 + [B]_0)\}^{1/2}$

For example, for a 0.02 M solution of strychnine arsenate with $pH_0 = 7$, four iterations and a calculation time of 4.53 s are needed to obtain $pH_f = 4.780$.

Calculation procedure for a mixture

For a mixture of acids, bases and salts containing different series of S and T species the calculation procedures outlined above are applied for each series of species. Taking [A] = sum of all $[\alpha]$ and $[\alpha']$ terms, [B] = sum of all $[\beta]$ and $[\beta']$ terms, [D] = (sum of all $[\delta]$ terms) — (sum of all $[\delta']$ terms), and introducing the correction factors, one obtains the general equation (Eqn. 6) which allows, as indicated above, the calculation of p_0 or q_0. The iteration procedure is continued by using $[H^+]_1 = [H^+]_0 p_0$ or $[H^+]_0/q_0$ and repeated until the final result is obtained.

DISCUSSION

The Newton-Raphson iteration procedure (I), which is the usual method for pH calculation, will be compared with the proposed method (II) with regard to the number of iterations, calculation time, choice of initial value, and maximum number of constants involved.

For solutions of monovalent acids with different pK_a, $pC_a = -\log C_a$ and initial values pH_0, the calculation time and the number of iterations needed

TABLE 1

Number of iterations, n, and calculation time, t (s), for the Newton—Raphson method (I) and the proposed method (II)

pK_a	pC_a	pH_0	n_I	t_I	n_{II}	t_{II}	pH_f
−2	6.0	2.0	17	3.83	2	0.28	5.996
		7.0	—	—	2	0.29	
0	1.0	0.5	6	1.33	3	0.43	1.038
		4.5	—	—	3	0.42	
2	4.0	1.0	17	3.71	3	0.36	4.004
		6.0	—	—	2	0.28	
4	2.0	1.5	12	2.63	3	0.24	3.022
		3.0	3	0.63	2	0.15	
6	3.0	2.5	15	3.39	3	0.24	4.507
		5.0	—	—	3	0.22	
8	5.5	3.0	25	5.69	3	0.23	6.698
		5.5	11	2.50	3	0.24	
10	1.5	2.0	25	5.74	2	0.15	5.749
		5.5	5	1.15	2	0.16	
12	2.5	1.5	35	7.90	2	0.17	6.940
		6.0	9	2.01	2	0.15	
14	1.0	1.0	38	8.54	2	0.15	6.979
		6.5	6	1.36	2	0.16	
1	3.5	−14.0	98	20.75	3	0.38	3.501
		28.0	—	—	2	0.29	
7	3.0	−14.0	112	23.66	3	0.22	5.002
		28.0	—	—	4	0.34	

to obtain the final result are given in the upper part of Table 1. The results clearly indicate the restricted number of iterations needed by method II (34 against 224) as well as the short calculation time (3.11 s against 50.4 s). As can be seen, the number of iterations in method I is considerably influenced by the choice of the starting value and decreases for pH_0 approaching pH_f; in practice, the only way to minimize this number is a preliminary estimate of pH_0 as close as possible to pH_f; however, for $pH_0 > pH_f$, the calculation fails and a new guess has to be made. For method II the number of iterations is practically unaffected by the pH_0 value and no preliminary estimate has to be made because all values (even unrealistic values, as noted in the lower part of Table 1) can be entered as the starting value. In practice, this means that no time-consuming precalculation of pH_0 is needed; for all problems, the starting value can be $pH_0 = 7$.

For a solution containing compounds with a total number of k constants, the equation of method I becomes of the $(k + 2)$ degree; although there are no theoretical limitations, practical problems arise for solving equations of very high degree. The existing programs are limited to the 6th degree and thus allow a pH-calculation of a tetravalent acid, and even the calculation of the titration curve provided that the titrant is the strong base sodium hydroxide.

Because of the additive character of the calculation procedure, method II has no limitations on the number of compounds or on the number of constants. To illustrate the capacity of the method, a program was developed for the pH calculation of a mixture containing a maximum of nine compounds: each of them may be an acid, a base or a salt, each with a maximum of nine constants for the (parent)acid as well as for the (parent)base. When all 162 constants are included the iteration time is about 32 s, which can be considered as quite satisfactory, taking into account that each iteration involves four steps: (1) the concentration of 180 species is calculated; (2) the predominant species for each of the 18 species series is selected; (3) 162 species concentrations are multiplied by an appropriate coefficient to obtain a total of 36 $[\alpha]$, $[\alpha']$, $[\beta]$ and $[\beta']$ terms; and (4) the value of nine $[\delta]$ terms and nine $[\delta']$ terms is calculated.

A practical example is given for a mixture of nine organic salts. Volume and molarity are listed in the upper part of Table 2, and pK values are listed in Table 3. With $pH_0 = 7$ as the starting value, seven iterations with a total calculation time of 58 s are needed to obtain the final result $pH_f = 4.907$, including the concentration and the % fraction (rounded values in lower part of Table 2) of all species present in the mixture. It should be emphasized that this problem needs an equation of the 35th degree when method I is used.

TABLE 2

Mixture of nine organic salts

(1) Cocaine hydrochloride	X_1Y_1	(6) Quinine phosphate	X_3Y_2
(2) Codeine citrate	X_3Y_1	(7) Sparteine sulfate	X_1Y_1
(3) Nicotine salicylate	X_1Y_1	(8) Strychnine arsenate	X_1Y_1
(4) Pilocarpine nitrate	X_1Y_1	(9) Thebaine oxalate	X_2Y_1
(5) Quinidine tartrate	X_2Y_1		

Comp	(1)	(2)	(3)	(4)	(5)	(6)	(7)	(8)	(9)
M[a]	0.10	0.09	0.09	0.09	0.08	0.08	0.10	0.08	0.08
V[b]	6	2	5	9	4	2	10	9	5
Fraction (%) of species at pH 4.907									
S_0	0.00	0.68	1.17	0.00	0.30	0.21	0.00	0.20	0.00
S_1	100.0	40.53	98.83	100.0	22.41	99.30	0.12	98.96	19.07
S_2		56.96			77.29	0.49	99.88	0.84	80.93
S_3		1.83				0.00		0.00	
T_0	0.03	0.09	0.11	1.13	0.02	0.06	0.00	0.08	0.09
T_1	99.97	99.91	98.55	98.84	88.98	85.65	69.99	99.67	99.91
T_2			1.34	0.03	11.00	14.29	30.01	0.25	

[a]Molarity. [b]Volume.

TABLE 3

Values for pK

Acid	pK_{a1}	pK_{a2}	pK_{a3}	pK_{a4}	Base	pK_{b1}	pK_{b2}
HCl	−1.00				NaOH	−1.00	
HNO_3	0.10				Cocaine	5.59	
HBO_2	9.23				Codeine	6.05	
H_2SO_4	0.15	1.99			Nicotine	6.16	10.96
H_2SO_3	1.76	7.21			Pilocarpine	7.15	12.57
H_2CO_3	6.35	10.33			Quinidine	5.40	10.00
H_3PO_4	2.23	7.21	12.32		Quinine	5.96	9.87
H_3AsO_4	2.22	6.98	11.53		Sparteine	2.24	9.46
$H_4P_2O_7$	1.52	2.36	6.60	9.25	Strychnine	6.00	11.70
Acetic acid	4.76				Thebaine	6.05	
Citric acid	3.13	4.76	6.40				
Maleic acid	1.92	6.22					
Oxalic acid	1.25	4.28					
Salicylic acid	2.98						
Succinic acid	4.19	5.48					
Tartaric acid	3.04	4.37					

APPLICATION OF THE METHOD

A titration can be considered as a systematic change of concentration of a mixture containing one or more titrated compounds and the titrant, thus the proposed method can be applied for the calculation and plotting of titration curves. These curves can be obtained quite quickly because of the fast calculation procedure and the restricted numbers of iterations. Among the large number of programs that can be developed for solving specific problems, only two will be mentioned.

The first program is tailored for the titration of a mixture of maximum of three compounds which may be, as well as the titrant, acid or base or salt, each with a maximum of four constants for the (parent) acid and (parent) base. The program offers the following possibilities: (1) calculation of $[H^+]$, pH, concentration and % fraction of species for the original solution and during the separate titration (addition of an arbitrary volume of titrant); and (2) calculation of $[H^+]$, pH and also $\Delta pH/\Delta V$, which reaches a maximum around the equivalence point(s), for part of the titration (between given volume limits of the titrant using prefixed volume increments) and for the full titration (systematic addition of the titrant from 0 ml to a prefixed maximum using volume increments adapted to the pH change in order to obtain a smooth curve). Furthermore, different titration curves can be plotted on the same axes in order to compare the effect of different titrants.

This program can be illustrated by a few examples in which some unusual titrants such as polyvalent acids or salts are involved. In the first series, single compounds are titrated: sodium hydroxide (Fig. 1) and trisodium

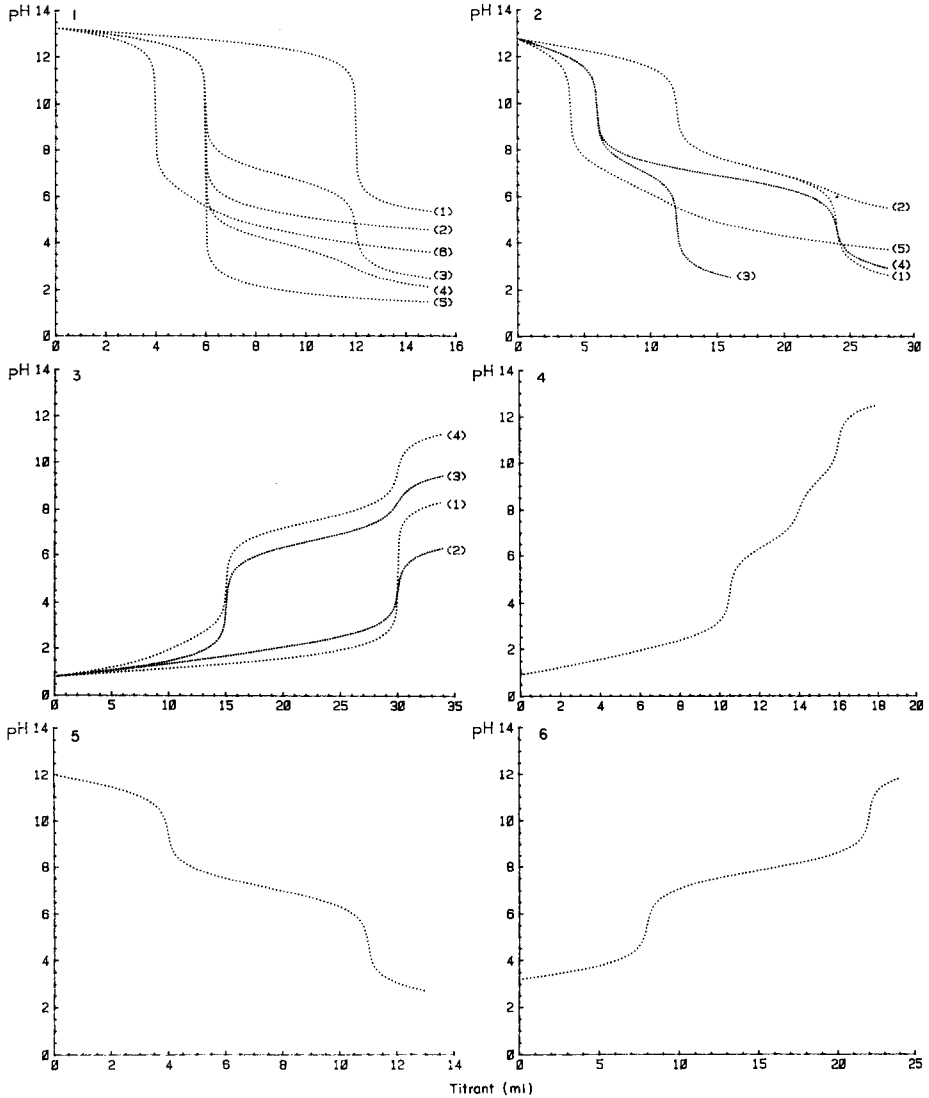

Fig. 1. Titration of 10 ml of 0.18 M sodium hydroxide with a 0.15 M solution of: (1) acetic acid, (2) succinic acid, (3) sulphurous acid, (4) oxalic acid, (5) sulphuric acid, (6) citric acid.

Fig. 2. Titration of 10 ml of 0.24 M trisodium phosphate with a 0.20 M solution of: (1) hydrochloric acid, (2) acetic acid, (3) sulphuric acid, (4) sulphurous acid, (5) citric acid.

Fig. 3. Titration of 20 ml of 0.15 M hydrochloric acid with a 0.10 M solution of: (1) $NaBO_2$, (2) Na_2SO_3, (3) Na_2CO_3, (4) Na_3PO_4.

Fig. 4. A mixture of 3 ml of 0.25 M maleic acid, 5 ml of 0.25 M sulphuric acid and 5 ml of 0.20 M pyrophosphoric acid titrated with 0.50 M sodium hydroxide.

Fig. 5. A mixture of 4 ml of 0.16 M Na_3PO_4 and 4 ml of 0.12 M Na_2HAsO_4 titrated with 0.16 M HCl.

Fig. 6. A mixture of 10 ml of 0.12 M nicotine dihydrochloride and 10 ml of 0.09 M nicotine salicylate titrated with 0.15 M sodium hydroxide.

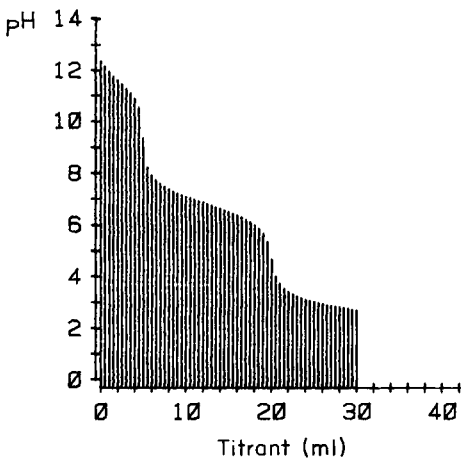

Fig. 7. Titration of 10 ml of 0.20 M trisodium arsenate with 0.20 M phosphoric acid.

phosphate (Fig. 2) with mono- and poly-valent acids, and hydrochloric acid with different salts (Fig. 3). The second series concerns the titration of mixtures of three acids with sodium hydroxide (Fig. 4), two inorganic salts with hydrochloric acid (Fig. 5) and two organic salts with sodium hydroxide (Fig. 6). For all examples, the titration curve clearly indicates that the separate titration of each compound is possible. Calculation time, t, and the number of calculated points, x, differ of course with the complexity of the problem. The minimum values are t = 80 s for x = 39 (Fig. 1, curve 1, with two constants involved), and the maximum values are t = 609 s for x = 81 (Fig. 4, with nine constants involved).

The second program which draws the titration curve on a graphic display is restricted to the titration of 10 ml of one compound with an equimolar solution of a titrant, both having the same specifications as indicated above. This program offers the same possibilities as the first program, except that the full titration curve (to a maximum of 42 ml of titrant) is obtained by addition of fixed volume increments (0.5 or 1 ml). A reproduction of the graphic display is given in Fig. 7 for the titration of 10 ml of 0.20 M trisodium arsenate with 30 ml of 0.20 M phosphoric acid using ΔV = 0.5 ml; seven constants are involved and 61 points are calculated, the calculation time being 405 s.

Conclusion

The proposed method, using an appropriate calculation procedure based on selection of the specific rule of electroneutrality and the introduction of simplified correction factors, allows the pH calculation of complex mixtures of acids, bases and salts and the plotting of titration curves. Compared with the Newton-Raphson procedure, the method is faster, needs a restricted number of iterations and has no limitations on the number of compounds or of constants involved.

REFERENCES

1 I. M. Kolthoff, P. J. Elving and E. B. Sandell, Treatise on Analytical Chemistry, Part 1, Vol. 1, Interscience, New York, 1959, pp. 443—454.
2 I. M. Kolthoff, E. B. Sandell, E. J. Meehan and S. Bruckenstein, Quantitative Chemical Analysis, 4th edn., Macmillan, London, 1969, pp. 80—89.
3 D. A. Skoog and D. M. West, Fundamentals of Analytical Chemistry, 3rd edn., Holt, Rinehart and Winston, New York, 1976, pp. 193—235.
4 G. L. Breneman, J. Chem. Educ., 51 (1974) 812.
5 K. Marhenke, HP-67/HP-97 Users' Library: Solutions, Chemistry, Hewlett-Packard, Corvallis, pp. 11—17.

Analytica Chimica Acta, 178 (1985) 289—298
Elsevier Science Publishers B.V., Amsterdam — Printed in The Netherlands

SEPARATION AND AUTOMATIC SPECTROPHOTOMETRIC DETERMINATION OF LOW CONCENTRATIONS OF CYANIDE IN WATER

M. HANGOS-MAHR and E. PUNGOR*

Technical University of Budapest, Institute for General and Analytical Chemistry, Budapest 1521 (Hungary)

V. KUZNECOV

Mendelev Institute, 125047 Moskow A-47 (U.S.S.R.)

(Received 3rd June 1985)

SUMMARY

Semi-automatic methods are described for the routine determination of cyanide in water. Membrane diffusion and isothermal distillation are examined for the separation/concentration of cyanide; the isothermal distillation procedure is optimized for routine use. An air-segmented flow analyzer is used to quantify cyanide. Two classical spectrophotometric methods are adapted and compared. The method based on reaction with picric acid is applicable at cyanide concentrations exceeding 1 mg l^{-1}. A modified Aldridge method is far better for lower concentrations. Combination of isothermal distillation with the automatic version of the Aldridge method is suitable for the determination of cyanide in waters in the concentration range 0.01—10 mg l^{-1}. Interference by sulphide and sulphite and their removal are described.

The acute toxicity of cyanide-containing compounds is due primarily to hydrogen cyanide. Cyanide groups bound in many inorganic and organic compounds can be converted by dissociation or decomposition to free cyanide which yields hydrogen cyanide below pH 11. In the determination of the cyanide pollution of waters, free and bound cyanides can be measured separately [1] but in practice the determination of the total amount of cyanide is considered sufficient. The maximum allowable cyanide concentrations internationally recommended [2] are 0.01 mg l^{-1} and 0.03 mg l^{-1} in tap water and natural waters, respectively. The aim of the present work was to develop a method for cyanide determination suitable for routine measurements. The preparation of the samples had to be as simple and rapid as possible and the determination had to be completed by a flow-type automatic analyzer.

In all practical determinations of cyanide, the first step is a separation and enrichment in the form of hydrogen cyanide; then the cyanide ions (obtained after absorption in alkaline solution) are quantified by spectrophotometry or by an electroanalytical method. The separation is usually done by distillation

[3]. For flow systems, several methods have been described for transferring cyanides to the gaseous phase; most of them use sweeping with inert gas [4—10]. Some authors do not apply extra gas [11, 12], but purging of the solution with gas at 1 l min^{-1} has been recommended [13]. The hydrogen cyanide in the gaseous phase is absorbed in a solution of sodium hydroxide. This part determines the speed and yield of the whole process [6, 8] therefore absorbers which ensure large contacting surfaces are preferred. A critical survey of the distillation methods used in flowing systems indicates that separation with sufficient yield and reproducibility can only be achieved with complicated glass devices with a controlled-pressure gas inlet.

Separation and concentration are also possible with the Conway microdiffusion method [14]; isothermal distillation is a better name, corresponding to the principle of the method. Several modifications have been developed [15] and the method has been applied to cyanide determinations [15—18], being adopted in a standard method for the analysis of industrial wastes [19]. The isothermal distillation method seems to be very advantageous because of its simplicity and reproducibility. An inconvenience is that it needs a fairly long time (from 30 min to several hours) for efficient distillation.

For separations in flow systems, the dialysis method works well. A Technicon dialysis unit, with use of a special gas-permeable membrane has been used for separating the hydrogen cyanide evolved [20]. The method is of high sensitivity with a detection limit of 1 $\mu g\ l^{-1}$ cyanide but it works at a speed of only 6 samples/hour.

For the determination of cyanide ions, many methods are available [1, 21]. A sensitive spectrophotometric method was described by Epstein [22]; this has been applied to flow-type automatic analyzers [8], but it has the disadvantages that the reagent solutions are unstable and special tubing (Acidflex, Solvaflex) is needed. The method based on a sodium picrate reagent has the advantage that aqueous solutions are used. The mechanism of the reaction between picric acid and cyanide has not been clarified unambiguously; it is supposed that the product is isopurpurate (4,6-dinitro-2-hydroxyamino-3,5-dicyano-phenolate), but the aminophenolate which is formed by reduction from picrate also absorbs at the wavelength for measurement, 520 nm. The picric acid method has been applied manually for many years [23, 24] for cyanide concentrations exceeding 1 mg l^{-1}. The most frequently recommended methods now are variations of the Aldridge method [25], which is suitable for the determination of cyanide in waters. The method is based on the König synthesis; cyanogen bromide reacts with an aromatic amine and with pyridine to give a compound of the Ar—N=CH—CH=CH—CH—CH—Ar type, which can be detected spectrophotometrically. Originally benzidine was used, but it was later replaced by other amines such as barbituric acid [26] and *p*-phenylenediamine [27]. This last variation was adapted for a flow-type automatic analyzer [11], but cyanide concentrations below 0.5 mg l^{-1} could not be determined.

EXPERIMENTAL

Potassium cyanide solutions were prepared in 0.01 M potassium hydroxide. A stock solution (1 g l^{-1}) of cyanide was prepared from potassium cyanide puriss; this solution was standardized by potentiometric titration and standard solutions of 0.01—5 mg l^{-1} cyanide were made by appropriate dilution with the potassium hydroxide solution.

All the other solutions were prepared from reagents of analytical purity and with deionized water.

A Contiflo automatic analyzer (LABOR Instrument Works, Esztergom, Hungary) was used. The determinations can be done with any automatic flow analyzer, e.g., the Technicon II AutoAnalyzer. The instrument was constructed from the following modules: sampler, peristaltic pump, photometer, recorder. The analytical modules were home-made.

A Hewlett-Packard 65 programmable calculator was used as required.

RESULTS AND DISCUSSION

The separation and preconcentration of cyanides

Dialysis method. A gas dialyzer unit was used in the flow manifold shown schematically in Fig. 1. The microporous teflon membranes used were 100 μm thick with an average pore size of 0.2 μm and a porosity of 50—60%. In the 0.01—4 mg l^{-1} cyanide range, the standard deviation was 0.02—0.03 mg l^{-1}; the regression coefficient of the calibration plot was 0.999. Cross-contamination was 2.4% at a sampling rate of 20 h^{-1}.

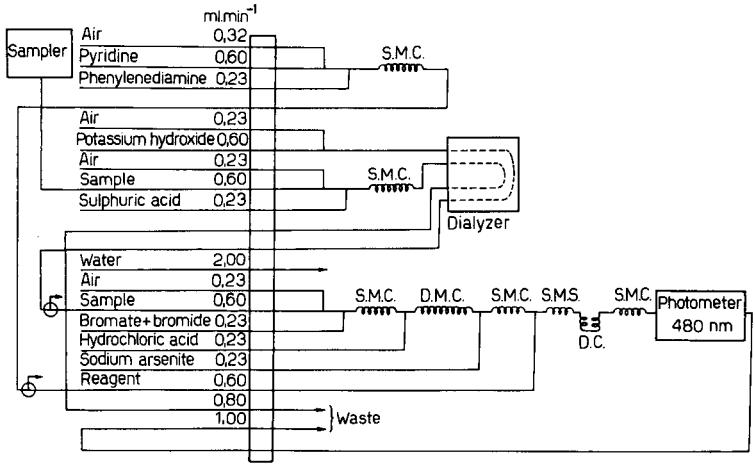

Fig. 1. Manifold for the determination of cyanide by dialysis. SMC's are 50-cm mixing coils; DMC's are 100 cm long; DC is the delay coil (200 cm). Further details given in connection with Fig. 7.

The dialysis technique is very simple and needs no preparation of water samples but it has the disadvantage that it provides no enrichment. Enrichment by a factor of 3—6 can be achieved [20] but only at the price of increased cross-contamination unless the speed of the determination is reduced to a few samples per hour.

Isothermal distillation method. To apply the principles of isothermal distillation, appropriate equipment had to be devised. Several cells of different shape and size were constructed and tested. One simple, but quite efficient cell is shown in Fig. 2. The sensitivity, precision and reproducibility of the whole isothermal distillation process depends on how constant the following factors can be held: the surface-to-volume ratio, the speed of renewal of the surface layer of the liquid, the temperature and the time.

The extent of enrichment depends strongly on the volume of the sample solution. With the cell shown in Fig. 2, the yield diminishes markedly as the volume increased (Fig. 3). Thus it is advantageous to keep the sample volume as small as possible, always provided that enough cyanide can be recovered to suit the range of the procedure for completing the determination. Experience showed that at room temperature (23° C), with magnetic stirring, the standard deviations of the measurements obtained from 20.0-ml samples were less than those from 10.0-ml samples; e.g., 0.0032 mg l^{-1} cyanide for 20-ml samples and 0.0040 for 10-ml samples. The volume of the absorbing solution is governed by the size of the cup and the requirements of the

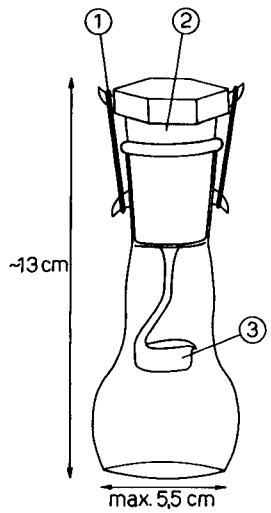

Fig. 2. Cell for isothermal distillation: (1) springs; (2) glass stopper; (3) glass cup containing absorption solution (1.5 ml capacity).

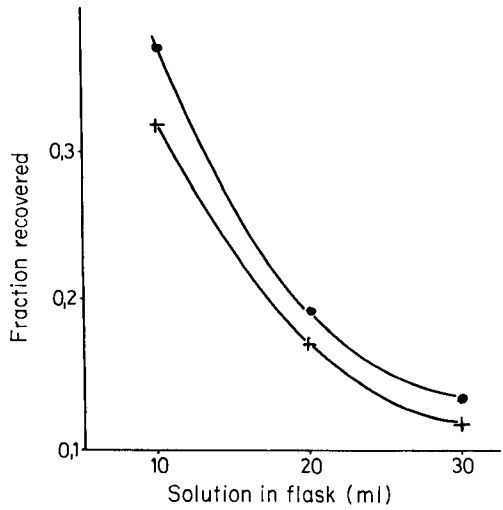

Fig. 3. The fraction of cyanide distilled as a function of the volume of the sample in the cell: (•) 1 μg CN^-; (+) 2 μg CN^-.

automatic measurement; the volume should not exceed 1.00 ml. The relative standard deviation of the volume of absorption solution poured from the cup was found to be 2.3%.

The sample solution, which is originally alkaline or has been made alkaline must, of course, be acidified. The amount and nature of the acid depends on whether the total cyanide or only free cyanide is to be measured, and also on the nature of the cyanide compounds involved. Elevated temperatures and/or auxiliary substances and catalysts can be used in addition to strong mineral acids. For the determination of the free cyanide content and/or of easily dissociated cyanides, the use of a weak acid is sufficient. It is advantageous to use solid acids, because the cell can be closed before the acid has dissolved, so that losses as hydrogen cyanide are avoided. Of the many organic acids tested, citric acid proved to be the best. [When a strong mineral acid is necessary, it is best to use (1 + 1) sulphuric acid added in a thin-walled glass vial or through a small hole in the stopper of the vessel.] The citric acid can be added from a spatula or spoon; 2 g of citric acid measured out ±100 mg was found to be adequate.

In the isothermal distillation, equilibrium distribution of the cyanides between the gas and liquid phase cannot be reached within a reasonable time. Conditions must be chosen so as to transfer as much cyanide as possible to the gas phase quickly and with sufficient reproducibility. The fraction recovered in the absorption solution increases with the temperature, time and contact area between gas and liquid, as indicated in Fig. 4. The standard deviations of measurements are higher when the temperature or the intensity of stirring increases. It is necessary to compromise between the permissible standard deviation, the sensitivity required, and the time available. The effect of time of the isothermal distillation on the concentration factor is shown in Table 1; the standard deviation did not differ significantly at the different times.

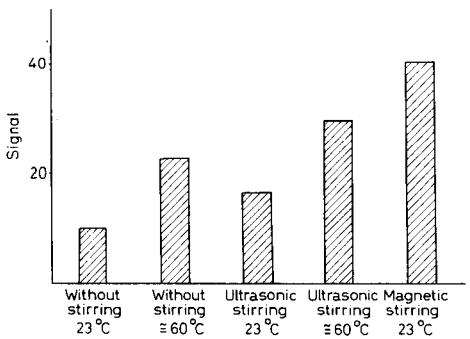

Fig. 4. Effect of temperature and type of stirring on the yield of isothermal distillation from 10 ml of 0.05 μg ml^{-1} cyanide solution. Absorbance measured at 480 nm.

TABLE 1

Data characteristic of the enrichment by isothermal distillation

Cyanide in sample (mg l^{-1})	30-min diffusion time		60-min diffusion time	
	CN^- in absorbing soln. (mg l^{-1})	Average enrichment[a]	CN^- in absorbing soln. (mg l^{-1})	Average enrichment[a]
0.010	—	—	0.055, 0.055, 0.060, 0.065	5.9
0.025	—	—	0.12, 0.17, 0.14	5.7
0.050	0.18, 0.20, 0.18	3.9	0.27, 0.285	5.6
0.100	0.42, 0.39	4.1	0.58, 0.49, 0.53	5.3
0.250	0.98, 0.92	3.8	1.25, 1.30	5.1

[a]Ratio of the cyanide concentration in the absorbing solution to that of the sample solution.

Determination of cyanide in a flow-type automatic analyzer

Picric acid method. The method based on picric acid has not previously been applied in automatic analyzers. The effects of different reagent compositions and concentrations, reaction times and temperatures were examined for manifolds fundamentally similar to that shown in Fig. 5. The sensitivity was found to increase almost linearly with temperature, therefore a 95°C thermostat was fitted in the analytical stream; this was the maximal temperature that could be used for the aqueous solutions without any trouble from bubbles in the flow stream.

Increasing the concentration of sodium carbonate improved the sensitivity (Fig. 6); the blank value from the reagent stream also increased but to a smaller extent. However, too much alkali had an adverse effect on the homogeneity of the liquid stream because of increased density and viscosity. A 0.5 mol l^{-1} concentration of sodium carbonate was found to be best for the proportions of solutions indicated in the flow diagram in Fig. 5. Similarly, increasing the concentration of sodium picrate improved the sensitivity because of solubilities and flow characteristics, 0.08 mol l^{-1} sodium picrate was selected for the manifold in Fig. 5. The cyanide standards and samples were prepared or kept in alkaline solutions of various concentrations, usually 0.1 or 0.01 mol l^{-1} sodium or potassium hydroxide. The sensitivities were essentially the same for these alkalinities.

Statistical data for the method developed are summarized in Table 2. The detection limit (three times the standard deviation of the blank value) was about 0.1 mg l^{-1} cyanide, which is one order of magnitude better than the values given in the literature for the manual methods based on picric acid. However, it is not enough for the purposes of water analysis.

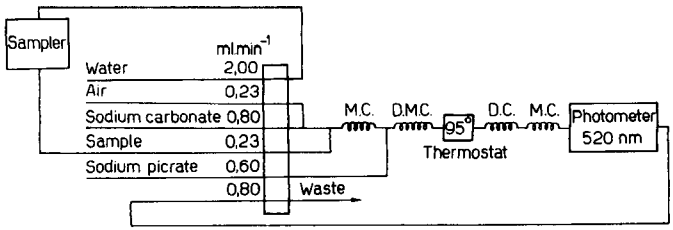

Fig. 5. Manifold for the determination of cyanide with sodium picrate.

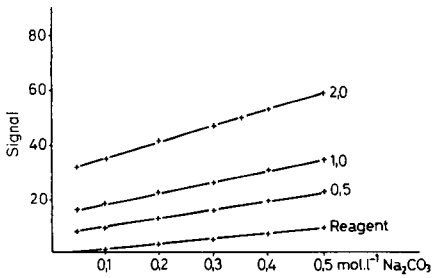

Fig. 6. Sensitivity of the determination with picric acid as a function of the sodium carbonate concentration. The signal was measured at 520 nm. The numbers on the lines are mg l^{-1} cyanide in the sample.

TABLE 2

Statistical data for the automatic cyanide determination with picric acid

Range (mg l^{-1})	0.5—5		0.1—2	
Sampling rate (h^{-1})	40	60	40	60
S.d.[a] (mg l^{-1} CN^-)	0.04	0.03	0.02	0.03
r[b]	0.997	0.998	0.996	1.000
Cross-contamination (mean, %)	0.9	2.6	0.9	2.5

[a]Standard deviation. [b]Regression coefficient.

The only potentially interfering components of the sample solutions that need be considered are those remaining with the hydrogen cyanide after the separation by isothermal distillation (or dialysis). In practice, this means sulphides and sulphites. Table 3 shows the extent of the interferences caused by these ions.

Aldridge method. The Aldridge method has already been adapted for use with the Technicon AutoAnalyzer I [11]. The purpose of this work was to adapt the phenylenediamine modification [27] to the Contiflo analyzer and to work without distillation, but with microdiffusion or dialysis for sample preparation. When the Aldridge method is used, the absorbance is measured

TABLE 3

Selectivity of the picric acid method in the determination of 1 mg l^{-1} cyanide

Concentration ratio (mole/mole) CN^-/X	Apparent cyanide conc. found (mg l^{-1})	
	$X = S^{2-}$	$X = SO_3^{2-}$
1:1	1.01	1.00
1:5	1.15	1.04
1:10	1.25	1.07
1:20	1.57	1.09

at various wavelengths, depending on the aromatic amine selected. Here, an interference filter for 480 nm proved to be the best in terms of sensitivity and linearity of the calibration plot.

The concentrations and proportions of reagents were optimized on the basis of the manifold shown in Fig. 7. The concentrations chosen for the ancillary reagent solutions were 0.08 mol l^{-1} bromate/4% (w/v) potassium bromide and 0.1 mol l^{-1} sodium arsenite. The sensitivity was altered only slightly by changes in the concentrations of phenylenediamine, pyridine and hydrochloric acid. The concentrations selected were 0.6% (w/v) phenylenediamine, 40% (v/v) pyridine and 0.5 mol l^{-1} hydrochloric acid; there was no significant difference in the results when these concentrations were varied within ±30% (relative). The reaction time was also not critical.

Statistical data for the final method are summarized in Table 4. The sensitivity is sufficient for water analysis if some preconcentration can be achieved.

Potentially interfering ions, remaining after separation by isothermal distillation or dialysis, are sulphide and sulphite. Table 5 shows the effects of these ions on sample solutions containing 0.05 mg l^{-1} cyanide. At low concentrations (below 10 mg l^{-1}) no interference was observed, but at higher concentrations there was a significant negative interference. Increasing the

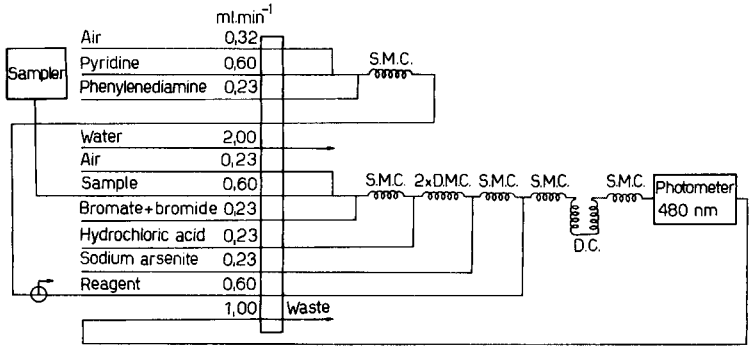

Fig. 7. Manifold for the determination of cyanide by an Aldridge method.

TABLE 4

Statistical data for the automatic cyanide determination based on the Aldridge method

Range (mg l^{-1})	0.01—0.1		0.02—0.2	0.025—0.5		0.1—1.0	
Sampling rate (h^{-1})	40		40	40		40	60
r^a	0.996		0.996	1.00		1.00	—
Cyanide in sample (mg l^{-1})	0.01	0.025	0.1	0.025	0.05	0.5	—
S.d.[a]	0.0009	0.0009	0.0021	0.0015	0.0015	0.1	—
R.s.d. (%)[b]	9.3	3.7	2.1	6.0	3.0	2.6	—
Cross-contamination (mean, %)	1.2		1.0	1.0		0.9	1.5

[a]Regression coefficient. [b]Standard deviation and relative standard deviation.

TABLE 5

Selectivity of the automatic Aldridge method in the determination of 0.05 mg l^{-1} cyanide

Concentration ratio (mole/mole) CN^-/X	Apparent cyanide conc. found (mg l^{-1})			
	$X = S^{2-}$		$X = SO_3^{2-}$	
	No pre-treatment	$Pb(NO_3)_2$ treatment	No pre-treatment	$K_2Cr_2O_7$ treatment
1:100	0.051	—	0.050	—
1:200	0.050	—	0.047	—
1:300	0.049	—	0.030	—
1:400	0.039	0.051	0.013	0.049
1:500	0.030	0.050	0.003	0.051
1:1000	0.004	0.052	0.000	0.048

concentration of the bromine reagent should decrease these interferences, which are thought to occur because the concentration of bromine diminishes. Experience showed, however, that when the bromine concentration was increased by 25%, the sensitivity of the cyanide determination and the stability of the flow deteriorated, so this is not a good solution to the problem. There are chemical methods for eliminating the sulphide and sulphite interferences. Sulphide can be precipitated as lead sulphide, and sulphite is oxidized by dichromate to sulphate. These reactions are easily used with the isothermal distillation process, simply by adding the reagents to the sample solution in the cell and after a short delay (5 min) proceeding with the isothermal distillation. Small volumes of concentrated solutions were used in order not to increase the total volume of the solution (e.g., 0.5 ml of 0.5% (w/v) solutions of lead nitrate or potassium dichromate). As the data in Table 5 show, these treatments were effective.

TABLE 6

Statistical data on the determination of cyanide by isothermal distillation and the automatic determination based on the Aldridge method[a]

Cyanide conc. (mg l^{-1})	0.025	0.033	0.05
No. of measurements	10	15	20
Standard deviation	0.0032	0.0027	0.0046
Relative standard deviation (%)	12.9	8.2	9.1
Standard deviation of the blank	0.0031	0.0024	0.0031

[a]Sample volumes were 20 ml in all cases.

Conclusion

The most useful method for the determination of cyanide in water seems to be to separate hydrogen cyanide by isothermal distillation and then apply an automatic photometric determination based on the Aldridge method. Statistical data of the determination of cyanide by this combination of methods are given in Table 6. The detection limit is 0.01 mg l^{-1} cyanide, which is quite sufficient for the analysis of waters.

REFERENCES

1 W. J. Williams, Handbook of Anion Determination, Butterworths, London, 1979.
2 World Health Organisation (WHO): International standards for drinking water, Geneva, 1958.
3 F. J. Ludzack, W. A. Moore and C. C. Ruchhoft, Anal. Chem., 26 (1954) 1784.
4 B. Pihlar and L. Kosta, Anal. Chim. Acta, 114 (1980) 275.
5 R. F. Roberts and B. Jackson, Analyst (London), 96 (1971) 209.
6 D. B. Easty, W. J. Blaedel and L. Anderson, Anal. Chem., 43 (1971) 1071.
7 A. L. Dennis and D. G. Porter, J. Autom. Chem., 2 (1980) 134.
8 P. D. Goulden, B. K. Afghan and P. Brooksbank, Anal. Chem., 44 (1972) 1485.
9 J. Keay and P. M. A. Menage, Analyst (London), 94 (1969) 895.
10 R. G. Lidzey, P. Sawyer and P. B. Stockwell, Lab. Pract., 20 (1971) 213.
11 P. Casapieri, R. Scott and E. A. Simpson, Anal. Chim. Acta, 49 (1970) 188.
12 J. Crowther and J. Evans, Analyst (London), 105 (1980) 841.
13 R. B. Roy, J. Jansen and M. Sahn, J. Assoc. Off. Anal. Chem., 63 (1980) 931.
14 E. J. Conway, Microdiffusion Analysis and Volumetric Error, Crossley-Lockwood, London, 1947.
15 S. J. Broderius, Anal. Chem., 53 (1981) 1472.
16 J. M. Kruse and L. E. Thibault, Anal. Chem., 45 (1973) 2260.
17 B. Pihlar, L. Kosta and B. Hristovski, Talanta, 26 (1979) 805.
18 S. Baar, Analyst (London), 91 (1966) 269.
19 Am. Nat. Standards Inst., New York, 1978, ANSI PH 4.41.
20 R. A. Durst, Anal. Lett., 10 (1977) 961.
21 S. J. Broderius and L. L. Smith, Anal. Chem., 49 (1977) 424.
22 J. Epstein, Anal. Chem., 19 (1947) 272.
23 G. Gutzeit, Helv. Chim. Acta, 12 (1929) 713.
24 F. B. Fischer and J. S. Brown, Anal. Chem., 24 (1952) 1440.
25 W. N. Aldridge, Analyst (London), 69 (1944) 262; 70 (1945) 474.
26 G. Y. Murty and T. S. Viswanathan, Anal. Chim. Acta, 25 (1961) 293.
27 L. S. Bark and H. G. Higson, Talanta, 11 (1964) 471, 621.

Analytica Chimica Acta, 178 (1985) 299—306
Elsevier Science Publishers B.V., Amsterdam — Printed in The Netherlands

ÉTUDE DE LA COMPLEXATION DES LANTHANIDES TRIVALENTS PAR LES SIX ISOMÈRES DE L'ACIDE DIAMINOCYCLOHEXANE-TÉTRAACÉTIQUE

Partie 3. Relation entre les Constantes d'Acidité et la Structure Moleculaire des Chélatants

J. CHARLIER, E. MERCINY et J. FUGER*

Laboratoire de Chimie Analytique et Radiochimie, Université de Liège, B-4000 Sart Tilman-Liège (Belgium)

(Reçu le 23 Juli 1985)

RÉSUMÉ

Les auteurs ont déterminé, par titrage coulométrique suivi potentiométriquement, dans un milieu de force ionique égale à 1 mol l^{-1} (KCl) et à 25° C, les constantes d'acidité des 6 isomères de l'acide diaminocyclohexane-*N,N,N',N'*-tétraacétique (DCTA). Ils rendent compte des valeurs de ces constantes et étudient l'évolution des deux constantes K_{a3} et K_{a4} en fonction de la distance N—N maximale. Ils associent à cette étude l'acide éthylènediamine-*N,N,N',N'*-tétraacétique (EDTA) et certains de ses homologues dont les acides 1,8-diaminooctane-*N,N,N',N'*-tétraacétique et 1,10-diaminodécane-*N,N,N',N'*-tétraacétiont synthétisés et étudiés dans les mêmes conditions que précédemment. Ils mettent en évidence une relation entre la structure moléculaire et l'affinité pour les protons.

SUMMARY

(Study of the complexation of trivalent lanthanides by the six isomers of diaminocyclohexanetetraacetic acid. Part 3. Relationship between the acidity constants and the molecular structure of the ligands.)

Potentiometric measurements of the acidity constants of the six isomers of diaminocyclohexane-*N,N,N',N'*-tetraacetic acid (DCTA) are reported for an ionic strength of 1 mol l^{-1} (KCl) at 25° C. The values of the two constants K_{a3} and K_{a4} are correlated with the maximum N—N distance for each ligand. Ethylenediamine-*N,N,N',N'*-tetraacetic acid (EDTA) and some homologous ligands, including specially synthesized 1,8-diaminooctane-*N,N,N',N'*-tetraacetic acid and 1,10-diaminodecane-*N,N,N',N'*-tetraacetic acid, are studied under the same conditions. It is proved that there is a relationship between the molecular structure and the affinity for protons.

Dans deux publications précédentes [1, 2], nous avons décrit le protocole expérimental de synthèse de cinq isomères de l'acide diaminocyclohexane-tétraacétique (DCTA) et nous avons déterminé les propriétés acido-basiques des isomères *trans*-1,2- et *trans*-1,4-DCTA [2] (μ = 1, KCl, 25° C) ainsi que leurs propriétés chélatantes vis-à-vis des lanthanides trivalents.

Dans le cadre de ce travail, nous avons été amenés à déterminer les constantes d'acidité des 4 autres isomères dans les mêmes conditions

0003-2670/85/$03.30

expérimentales. Nous avons comparé ces valeurs avec celles de l'EDTA et de ses homologues et, pour compléter cette analyse comparative, nous avons synthétisé l'acide 1,8-diaminooctanetétraacétique et l'acide 1,10-diaminodécanetétraacétique. Les valeurs des constantes d'acidité de ces deux acides ont également été déterminées dans les mêmes conditions de milieu afin d'établir, aussi bien pour les homologues de l'EDTA que pour les isomères du DCTA, une relation entre la structure moléculaire et l'affinité envers les protons.

PARTIE EXPÉRIMENTALE

Caractéristiques des agents complexants étudiés

Les caractéristiques des composés *trans*-1,2-DCTA et *trans*-1,4-DCTA ont été décrites précédemment [1, 2].

Après synthèse, les différents isomères sont purifiés par cristallisation dans l'eau et se présentent alors sous forme de solides blancs cristallins. Dans le cas des composés *cis*-1,2-DCTA et *cis*-1,3-DCTA, cependant, cette purification s'avère impossible, le résultat d'une évaporation poussée, même à basse température, conduisant à des milieux visqueux. On se contente donc de purifier ces composés par passage sur résine cationique.

Détermination du poids moléculaire. Le poids moléculaire (p.m.) théorique des isomères anhydres est de 346,36. Expérimentalement, par titrage à la soude arrêté au premier saut de titrage (neutralisation de deux protons), on obtient respectivement: 356,3 pour le *trans*-1,3-DCTA correspondant à la formule DCTA.1/2 H_2O; 363,4 pour le *cis*-1,4-DCTA correspondant à la formule DCTA.H_2O; 650 environ pour le *cis*-1,2-DCTA; et 670 environ pour le *cis*-1,3-DCTA.

Les deux dernières valeurs sont anormalement élevées. Comme les poids moléculaires ainsi obtenus sont presque le double du poids moléculaire théorique, on peut envisager deux cas: soit, d'une part, le premier saut correspond en fait à un seul proton, ce qui nous donne un p.m. d'environ 325 c'est-à-dire le p.m. théorique moins une molécule d'eau; il y aurait donc eu déshydratation et formation d'un anhydride interne; soit, d'autre part, le premier saut correspond à la neutralisation de deux protons mais de molécules distinctes; il y aurait donc eu association entre deux molécules formant ainsi un anhydride avec perte d'une molécule d'eau.

Le titrage complet des deux composés montre, dans le cas de l'isomère *cis*-1,2, deux sauts situés pour des volumes de titrant identiques et, dans le cas de l'isomère *cis*-1,3, deux sauts situés pour des volumes de titrant dont le rapport est égal à 3:2. Par contre, après hydrolyse dans des conditions très dures (pH > 13, solution portée à reflux pendant plus de 15 h), les courbes de titrage des produits obtenus sont cette fois caractéristiques d'un acide quadribasique ainsi que le montre la Fig. 1 pour le composé *cis*-1,2-DCTA. Par conséquent, le *cis*-1,2-DCTA formerait un anhydride par déshydratation interne (I) tandis que le *cis*-1,3-DCTA formerait un anhydride par association

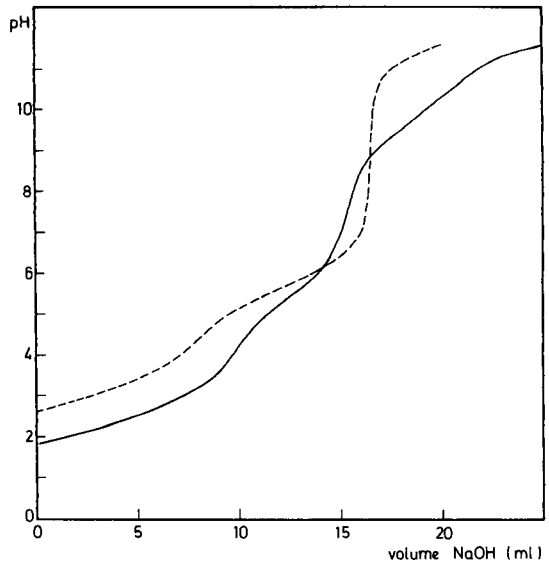

Fig. 1. Titrage par la soude du *cis*-1,2-DCTA avant (– – –) et après (——) hydrolyse.

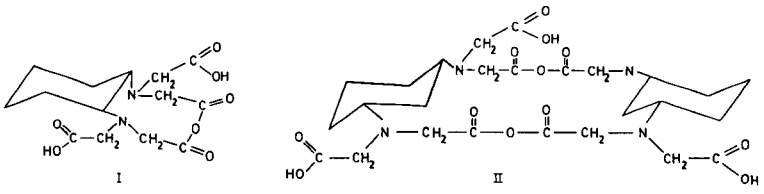

I II

entre deux molécules (II) et les conditions très dures d'hydrolyse montrent à suffisance la stabilité de ces composés. Bien plus, le produit hydrolysé replacé sur échangeur d'ions rend, dans l'éluat, l'anhydride. On peut facilement comprendre cet effet si on se rappelle que les concentrations obtenues localement dans une colonne échangeuse d'ions peuvent atteindre environ 4,5 mol l^{-1}.

En fait, toutes ces considérations peuvent s'interpréter facilement sur base des modèles moléculaires [3]. En effet, dans le cas de l'isomère *cis*-1,2-DCTA, les groupements carboxyliques sont très proches les uns des autres de par leur position adjacente et leur conformation *cis* et les cycles ainsi formés ne sont pas tendus. Pour le *cis*-1,3-DCTA, le plus grand éloignement des fonctions iminodiacétiques est favorable à une association entre deux molécules avec perte d'une molécule d'eau.

Solubilité. Des mesures réalisées à 25° C indiquent que le *trans*-1,3-DCTA est relativement peu soluble (1,8 g l^{-1}) tandis que l'isomère *cis*-1,4 DCTA présente une solubilité plus grande (15 g l^{-1}). Les propriétés particulières évoquées ci-dessus des isomères *cis*-1,2 et *cis*-1,3 interdisent toute mesure de solubilité.

Pour compléter l'étude comparative avec l'EDTA et ses homologues, nous avons également synthétisé les acides 1,8-diaminooctanetétraacétique et 1,10-diaminodécanetétraacétique à partir des diamines correspondantes selon un protocole de synthèse analogue à celui décrit pour les isomères du DCTA [1]. Ces deux composés cristallisent san molécule d'eau et sont assez solubles à température ordinaire: 32 g l^{-1} pour l'acide 1,8-diaminooctanetétraacétique et 19 g l^{-1} pour l'acide 1,10-diaminodécanetétraacétique. A 100° C, ils sont très solubles, soit respectivement plus de 1000 g l^{-1} pour le premier et plus de 700 g l^{-1} pour le second.

*Détermination des p*K

La méthode utilisée pour la détermination des constantes d'acidité et les conditions de titrage sont identiques à celles décrites et réalisées pour le *trans*-1,2-DCTA [1], à savoir: titrage coulométrique suivi potentiométriquement, en milieu KCl 1 mol l^{-1} à 25° C, les solutions étant 10^{-2} mol l^{-1} en complexant (H_4L). Les courbes de titrage sont traitées mathématiquement grâce à un programme sur ordinateur basé sur la méthode des moindres carrés par approximations successives [1].

RESULTATS ET DISCUSSION

Les valeurs des constantes d'acidité obtenues pour les différents agents complexants étudiés sont rassemblées dans le Tableau 1. Dans le Tableau 2, nous réalisons l'étude comparative des pK des isomères du DCTA et des homologues de l'EDTA en fonction de l'éloignement maximal entre les fonctions aminodiacétiques. Par souci d'homogénéité entre les valeurs tirées de la littérature [4] réalisées à 25° C, dans un milieu de force ionique égale à 0,1 (K^+) et nos valeurs obtenues à 25° C, pour un milieu de force ionique égale à 1, nous avons recalculé, pour les composés que nous avons étudiés, les valeurs apparentes de pK_{a4} pour un milieu de force ionique égale à 0,1. En effet, le programme de calcul qui nous permet d'interpréter les courbes de titrage tient compte de la complexation des ions K^+ dans le calcul des constantes d'acidité. Ainsi, il nous fournit une constante réelle $K_{a4} = [H^+][L^{4-}]/[HL^{3-}]$ et une constante de stabilité du complexe $K_{K^+} = [KL^{3-}]/[K^+][L^{4-}]$. Par conséquent, il nous est possible de calculer la constante apparente K'_{a4} en fonction de la force ionique du milieu: $K'_{a4} = K_{a4}(1 + K_{K^+}[K^+])$.

En portant en graphique les valeurs des constantes d'acidité relatives à la fixation du premier proton en fonction de la distance maximale entre les deux azotes (Fig. 2), on observe pour l'EDTA et ses homologues une augmentation de pK_{a4} en fonction de l'accroissement de la distance entre les deux azotes et une stabilisation à partir de 12 Å environ. Il semble donc qu'une distance N—N la plus grande possible soit favorable à la fixation du proton. Ceci semble signifier que le proton présente la même hydratation qu'en solution et qu'il s'insère d'autant mieux entre les deux azotes que ces derniers sont plus éloignés. La diminution de l'attraction électrostatique due

TABLEAU 1

Constantes d'acidité des agents complexants étudiés (KCl 1 M; 25,00 ± 0,01° C)[a]

$pK_{ai} = -\log [H_{4-i}L][H^+]/[H_{4+1-i}L]$; $\log K_{K^+} = \log [KL^{3-}]/[L^{4-}][K^+]$

Complexant	pK_{a0}	pK_{a1}	pK_{a2}	pK_{a3}	pK_{a4}	$\log K_{K^+}$
cis-1,2-DCTA	—	1,54 ± 0,01	2,99 ± 0,01	5,56 ± 0,01	9,67 ± 0,01	0,38 ± 0,01
trans-1,2-DCTA[b]	1,56 ± 0,02	2,42 ± 0,01	3,25 ± 0,01	6,005 ± 0,009	12,73 ± 0,01	0,18 ± 0,03
cis-1,3-DCTA	1,44 ± 0,02	1,86 ± 0,0	2,57 ± 0,01	8,34 ± 0,01	10,68 ± 0,01	−0,08 ± 0,01
cis-1,4-DCTA	1,49 ± 0,02	1,93 ± 0,01	2,44 ± 0,01	8,239 ± 0,009	11,150 ± 0,008	0,18 ± 0,01
trans-1,3-DCTA	1,36 ± 0,05	2,02 ± 0,03	2,48 ± 0,01	7,67 ± 0,01	11,09 ± 0,01	−0,53 ± 0,01
trans-1,4-DCTA[c]	1,66 ± 0,01	1,949 ± 0,005	2,466 ± 0,003	8,419 ± 0,004	11,15 ± 0,01	0,02 ± 0,01
1,8-Diaminooctane-tétraacétique	1,86 ± 0,07	2,03 ± 0,03	2,46 ± 0,02	9,786 ± 0,004	10,761 ± 0,003	−0,19 ± 0,06
1,10-Diaminodécane-tétraacétique	1,83 ± 0,04	2,03 ± 0,02	2,65 ± 0,01	9,79 ± 0,01	10,65 ± 0,01	−0,83 ± 0,03

[a] La façon dont nous calculons les erreurs dont nos constantes sont affectées a été détaillée [1]. Bien que déterminées en milieu KCl 1 M, les valeurs de pK_{a4} sont corrigées de la complexation des ions K^+ pour l'espèce L^{4-}. Il s'agit donc bien du log K_{a4} avec $K_{a4} = [H^+][L^{4-}]/[HL^{3-}]$. [b] Voir 1e partie [1]. [c] Voir 2e partie [2].

TABLEAU 2

Comparaison des valeurs des constantes d'acidité des acides diaminotétraacétiques en fonction de la distance N—N maximale (μ = 0,1 (K^+), 25° C)[a]

Complexant	Dist. N—N max. (Å)		pK_{a1}	pK_{a2}	pK_{a3}	pK_{a4}
EDTA[b]	3,9		2,0	2,68	6,16	10,17
TMDTA[b]	5,2		1,88	2,57	7,96	10,39
TTMDTA[b]	6,5		1,90	2,45	8,98	10,58
$-(CH_2)_5$[b]	7,8		2,30	2,70	9,44	10,60
$-(CH_2)_6$[b]	9,1		2,20	2,70	9,71	10,71
$-(CH_2)_8$	11,7		2,03	2,46	9,79	10,73
$-(CH_2)_{10}$	14,3		2,03	2,65	9,79	10,64
cis-1,2-DCTA	3,1	2,9[c]	1,54	2,99	5,56	9,58
trans-1,2-DCTA	4	3	2,42	3,25	6,005	12,67
trans-1,3-DCTA	5,1	4,4	2,02	2,48	7,67	11,08
cis-1,4-DCTA	5,9	4,8	1,93	2,44	8,24	11,09
cis-1,3-DCTA	5,4	5,2	1,86	2,57	8,34	10,64
trans-1,4-DCTA	6,1	5,8	1,949	2,466	8,42	11,11

[a]La distance entre les deux azotes est simplement estimée à 0,25 Å près, environ, par une mesure sur les modèles moléculaires [3]. Elle ne tient compte en aucun cas d'une éventuelle répulsion électrostatique entre les groupements carboxyliques des deux chaînes opposées, notamment pour les distances les plus faibles. De manière à permettre la comparaison avec les valeurs de la littérature, rapportée pour μ = 0,1 [4], nos valeurs de pK_{a4} mesurées en milieu de force ionique égale à μ = 1, sont recalculées pour μ = 0,1 en tenant compte uniquement de la complexation des ions K^+. [b]Voir [4]. [c]Puisque les études par r.m.n. du *trans*-1,2-DCTA ont montré que le cycle prenait sa conformation chaise et que les groupements iminodiacétiques se plaçaient en position diéquatoriale, nous avons admis qu'il en était de même pour les autres isomères. Ainsi, dans ce tableau, nous donnons, pour chaque isomère, la plus grande distance N—N possible et la distance N—N maximale obtenue compte tenu de la conformation du cycle et des positions axiales ou équatoriales des groupements fonctionnels. C'est cette distance que nous utilisons pour établir les graphiques.

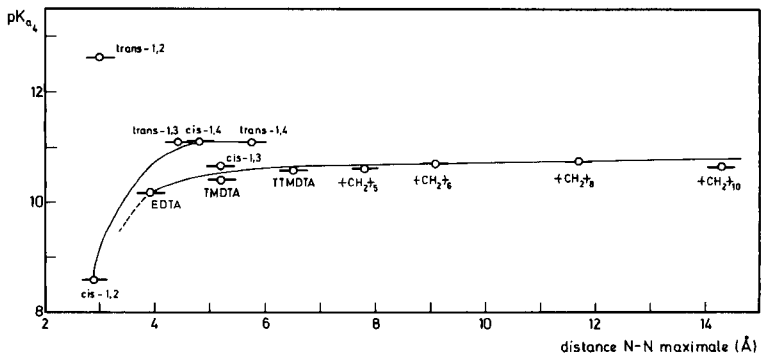

Fig. 2. Evolution de pK_{a4} en fonction de la distance N—N maximale pour les isomères du DCTA et les homologues de l'EDTA.

à l'éloignement des deux groupements fonctionnels est ainsi compensée par un effet entropique favorable dû à des empêchements stériques moins importants.

Dans le cas des isomères du DCTA, les valeurs de pK_{a4} ne s'inscrivent pas tout à fait dans cette ligne générale. Elles sont systématiquement plus élevées que celles des homologues de l'EDTA. Il semblerait que la rigidité de la molécule soit responsable de ce fait. L'isomère *trans*-1,2, en particulier, occupe une position assez singulière avec une valeur de pK_{a4} de 12,73 pour une distance N—N de 4 Å. Une telle valeur de pK_{a4} pour une distance N—N aussi faible ne peut s'interpréter qu'en admettant, dans ce cas particulier, une déshydratation du proton.

L'étude par r.m.n. du *trans*-1,2-DCTA [5] à différents pH montre que les groupements iminodiacétiques occupent les positions diéquatoriales sur le cycle quel que soit le pH. De plus, sur base des déplacements chimiques observés, on peut dire que, lors de la fixation du premier proton, chaque atome d'azote est protoné à 50% et, lors de la fixation du second proton, chaque atome est protoné à 100%. Ces résultats excluent donc l'hypothèse selon laquelle la valeur fort élevée de pK_{a4} proviendrait de la fixation du proton sur un atome d'azote plutôt que sur l'autre. D'autre part, comme les groupements iminodiacétiques sont en position diéquatoriale, la distance N—N maximale à considérer ne serait pas de 4 Å mais de 3 Å environ, de sorte que l'insertion du proton hydraté devrait être plus difficile, autrement dit que ce dernier devrait être au moins partiellement déshydraté pour se fixer aux groupements iminodiacétiques, ce qui expliquerait la valeur de pK_{a4} anormalement élevée observée. Il serait toutefois utile d'étudier ultérieurement par r.m.n. et Raman spectromètrie les différents isomères afin de préciser davantage les conditions de fixation des protons sur les groupements azotés.

L'étude par analyse thermique différentielle des composés de formules $K_3HL.nH_2O$ (avec L = EDTA et *trans*-1,2-DCTA avec respectivement $n = 2$ et $n = 3{,}5$) indique, dans le cas de l'EDTA, le départ de toute les molécules d'eau vers 200° C tandis que dans le cas du *trans*-1,2-DCTA, la perte de toutes les molécules d'eau se produit vers 100° C. Autrement dit, dans le premier cas, l'eau est beaucoup plus fortement retenue. Or, celle-ci ne peut l'être que par le groupement COOH ou les groupements COOK. On peut s'attendre à ce que la déshydratation du groupe acide soit plus difficile et dès lors apparaisse à une température plus élevée que celle des groupes COOK. Dans cette optique, la perte d'eau dans le cas de l'EDTA correspondrait à la déshydratation du groupe COOH; dans le cas du *trans*-1,2-DCTA, par contre, elle correspondrait à la déshydratation des groupes COOK, ce qui implique qu'il n'y aurait donc pas de molécules d'eau retenues sur le groupement acide. Ceci rejoint notre conclusion précédente selon laquelle il devrait y avoir une différence qualitative dans l'hydratation de ces deux entités. Par une étude spectroscopique Raman de ces mêmes composés, nous espérons apporter une preuve supplémentaire et confirmer ainsi notre hypothèse.

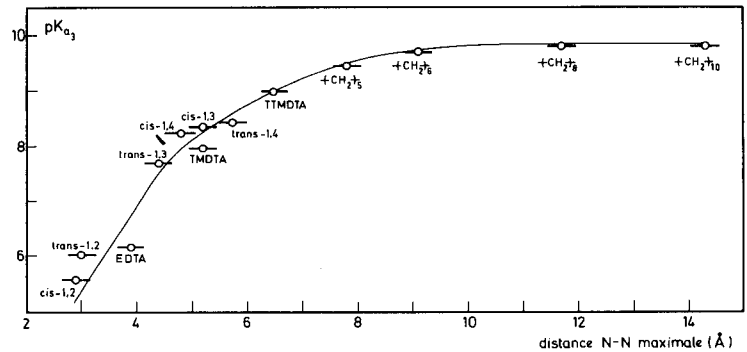

Fig. 3. Evolution de pK_{a3} en fonction de la distance N—N maximale pour les isomères du DCTA et les homologues de l'EDTA.

Le graphique reprenant les valeurs de pK_{a3} (correspondant à la fixation du second proton) des différents acides diaminotétraacétiques en fonction de la distance maximale entre les deux azotes montre, de nouveau, une augmentation continue de pK_{a3} avec la distance (Fig. 3). Il est évident, en effet, que plus la distance N—N sera grande, plus l'insertion du second proton totalement hydraté sera aisée. Dans ce cas-ci, nos valeurs s'inscrivent bien dans l'évolution générale observée pour les homologues de l'EDTA et il est à noter aussi que le *trans*-1,2-DCTA ne se différencie plus des autres composés; il accepte le second proton totalement hydraté. Pour les grandes distances, pK_{a3} tend vers une constante et, tout comme pK_{a4}, ne semble pas diminuer même pour les très grandes distances entre les deux azotes. L'effet entropique l'emporte donc sur la diminution de l'attraction électrostatique due à l'éloignement important des deux groupements fonctionnels. Par conséquent, on peut envisager que, pour des distances suffisamment grandes, les deux pK tendent vers la même valeur; il n'y aurait donc plus différenciation entre les deux azotes.

Enfin, comme nous le montre le Tableau 2, nous constatons que les valeurs de pK_{a1} et pK_{a2} sont très peu affectées par la structure moléculaire des composés. A ce stade, en effet, les protons sont fixés par les groupements carboxyliques (identiques pour tous les composés) et donc ne pénètrent pas dans la cavité chélatante de sorte que la dimension de celle-ci n'influence pas beaucoup la force avec laquelle ces protons sont retenus.

BIBLIOGRAPHIE

1 E. Merciny et J. Fuger, Anal. Chim. Acta, 160 (1984) 87.
2 E. Merciny et J. Fuger, Anal. Chim. Acta, 166 (1984) 199.
3 Framework Molecular Models, Prentice-Hall, Englewood Cliffs, N.J., 1965.
4 A. E. Martell, Critical Stability Constants, Vol. 1: Amino Acids, Plenum Press, New York, 1974.
5 J. L. Sudmeier et C. N. Reilley, Anal. Chim. Acta, 36 (1964) 1707.

Analytica Chimica Acta, 178 (1985) 307—312
Elsevier Science Publishers B.V., Amsterdam — Printed in The Netherlands

Short Communication

USE OF DISPOSABLE CLEAN-UP COLUMNS FOR SELECTIVE REMOVAL OF HUMIC SUBSTANCES PRIOR TO MEASUREMENTS WITH A NITRATE ION-SELECTIVE ELECTRODE

ISTVAN CSIKY*, GYÖRGY MARKO-VARGA and JAN ÅKE JÖNSSON
Department of Analytical Chemistry, University of Lund, P.O. Box 124, S-221 00 Lund (Sweden)

(Received 18th June 1985)

Summary. Measurements of nitrate in natural waters with a nitrate ion-selective electrode are seriously affected by the presence of humic substances. These can be removed quantitatively by a clean-up procedure with cheap disposable adsorption columns packed with chemically-bonded alkylamino silica. The method is applied to natural water samples with high contents of humic substances. The nitrate concentrations found were in good agreement with determinations by ion chromatography.

Determination of nitrate in soils and natural waters is important in studies of eutrophication of waters. Humic substances, the major organic constituents of soil, are inevitably present in such samples and cause severe interferences in most methods for the determination of nitrate. Nitrate is often determined with a nitrate ion-selective electrode, but spectrophotometric and ion-chromatographic methods are also used [1]. Applications of ion-selective electrodes (i.s.e.) for the determination of nitrate in biological and chemical research are numerous, e.g., in the analysis of plants [2—5], soils [2, 5—11] and natural waters [2, 4, 11, 12]. Commonly, the electrodes are used in the batch mode but have also been applied in flow systems [11, 13]. The adsorption of organic matter such as humic substances on the membrane surface of an electrode can create serious errors [14]; potential drifts have been observed in measurements of nitrate in soil extracts and waste waters with both batch and flow techniques [11].

Recently, the use of a clean-up column for selective removal of humic compounds was reported prior to ion-chromatographic determinations of nitrate and sulfate [15]. Several types of chemically-modified packing materials for liquid chromatography were tested and a chemically-bonded primary amine material was found to be best. In the work described here, a sample clean-up step prior to measurements by i.s.e. was investigated. The disposable columns were packed with chemically-bonded amine material.

Experimental

Materials. Solutions of nitrate were prepared from the potassium salt. A 0.5 M acetate buffer (pH 4.5) was prepared from analytical-grade acetic

0003-2670/85/$03.30

acid and sodium acetate. The water was purified by a Milli-Q/RO-4 unit (Millipore, Bedford, MA). Humic acid (Fluka) with a molecular weight of 600—1000 and an ash content of 10—15% was used to prepare reference solutions of humic substances. The solution was stirred for 20 h at 60°C and filtered through a 0.65-μm membrane filter (Millipore). The content of dissolved organic carbon (DOC) was 20 mg l^{-1} [15].

Bond-Elut-NH_2 disposable columns (Analytichem, Harbor City, CA) were used for the adsorption of humic substances. These columns contain ca. 0.5 g of 40-μm silica, surface modified with chemically-bonded alkylamino groups, and packed in a plastic syringe barrel. Solutions were aspirated through the columns by using Vac-Elut equipment (Analytichem). Before use, the columns were rinsed and conditioned by sequentially aspirating 5-ml aliquots of hexane, ethanol, water, 1000 mg l^{-1} potassium sulfate solution, and finally 15 ml of water.

A plastic adapter with low dead-volume enabled the clean-up columns to be connected to a low-pressure flow system comprising a peristaltic pump (Model FIA-08, Bifok, Stockholm, Sweden) and a spectrophotometric detector (Spectromonitor III, LDC, Riviera Beach, FL).

An ion-selective electrode (Philips, Model IS561N03), equipped with a nitrate-selective membrane, was conditioned in a 0.1 M nitrate solution for 24 h as recommended by the manufacturer. The reference electrode was a saturated calomel electrode (Model K401, Radiometer, Copenhagen, Denmark).

Determination of nitrate. The sample (6 ml) was aspirated through a conditioned clean-up column. If the concentration of humic substances was high, two or more clean-up columns might be needed to render the sample completely colourless; this was checked by u.v. spectrophotometry at 225 nm. To 5 ml of the aspirated sample, 0.5 ml of 0.5 M acetate buffer was added as supporting electrolyte. The potential was measured after 3 min of stirring at constant speed and the nitrate concentration was read from a calibration curve. All measurements were made at 22 ± 1°C.

Results

Breakthrough curves of the adsorption of humic substances on the clean-up column. The adsorption capacities of the extraction columns were measured in a continuous flow system by pumping reference humic acid solution (45 mg l^{-1}) through the column at a flow rate of 1.5 ml min^{-1} until breakthrough was sensed by the u.v. detector (225 nm). Two different lots of adsorption columns were compared and the effect of the conditioning procedure was investigated. The measured breakthrough capacities are summarized in Table 1. A considerable variation between batches was observed while the variation within batches was relatively small. After the adsorption columns had been conditioned with a sulfate solution as described above, two-thirds of the adsorption capacity for the humic acid remained. As will be discussed below, the conditioning is necessary for complete recovery of nitrate during the clean-up procedure.

The breakthrough volume was also measured for a ten-fold more dilute

TABLE 1

Adsorption capacity for humic acid (in μg per column) of Bond-Elut-NH_2 disposable columns

Lot	Adsorption capacity (μg/column)	RSD[a] (%)	Lot	Adsorption capacity (μg/column)	RSD[a] (%)
A	67.5	11(9)	B	170	15(5)
A[b]	44.5	10(5)	B[b]	112	16(5)
A[c]	68	12(4)			

[a]Relative standard deviation (%) with number of replicates in parentheses. [b]Conditioned as described in the Experimental section. [c]Concentration of the humic acid solution was only 4.5 mg l^{-1} (see text).

solution of humic acid (4.5 mg l^{-1}). The breakthrough volume was about 10-fold larger than before, so that the adsorption capacity was much the same (Table 1). As the adsorption capacity seems to be independent of the concentration, it can be concluded that the adsorption is irreversible.

Stability of the electrode potential. An electrode with a fresh membrane was immersed in a solution containing 9 mg l^{-1} humic acid and the electrode potential was recorded for 20 h. The experiment was repeated with pure water and with a solution of humic acid, which was cleaned up by passage through a Bond-Elut-NH_2 column. To all solutions (5 ml) was added 0.5 ml of 0.5 M acetate buffer. The results (Fig. 1) show that the membrane is affected by the presence of humic acid, leading to a considerable potential

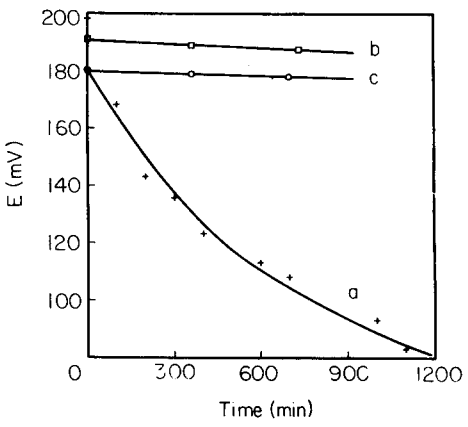

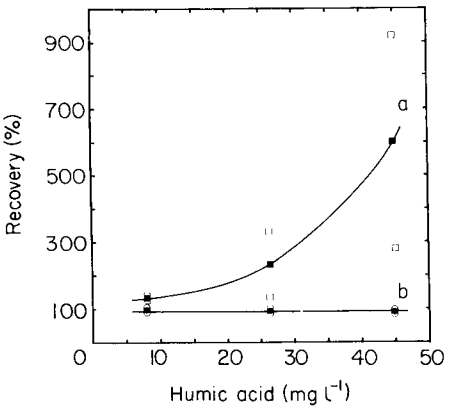

Fig. 1. Potential stability of the nitrate i.s.e. in different media: (a) 9 mg l^{-1} humic acid solution; (b) same as (a) after the clean-up procedure (see text); (c) water.

Fig. 2. Percent recovery of nitrate in solutions containing humic substances before (a) and after (b) the clean-up procedure. Data are presented as means (filled symbols) ± one standard deviation (open symbols).

drift. The use of a clean-up column removes this interference and the drift becomes the same as in pure water.

Selectivity. Selectivity coefficients, evaluated by using a fresh nitrate membrane for potential measurements in solutions of some common interfering ions (Table 2), were in good agreement with those given by the manufacturer. After exposure of the electrode to a solution of humic acid (9 mg l^{-1}) for 20 h, when the membrane should be saturated with humic acid (see Fig. 1), the selectivity coefficients were again evaluated. The selectivity coefficients changed most dramatically for sulfate but significant differences were also noted for chloride and hydrogencarbonate. In practical work, the change in selectivities towards sulphate and chloride are both important. The determination of nitrate in soil is often preceded by an extraction with a concentrated chloride solution [7, 10], and sulphate is often present in relatively high concentration in environmental samples because of deposition from the burning of sulphur-containing fossil fuels.

Analysis of model water samples containing humic substances. Model solutions, containing 0, 9.0, 27 and 45 mg l^{-1} reference humic acid and 30—500 mg l^{-1} nitrate were prepared. The reference humic acid contains some nitrate which was quantified by ion-chromatography [15]. The nitrate concentration of the model solutions was adjusted correspondingly. Nitrate was determined as described under Experimental with and without the clean-up step. Calibration curves were constructed from the solutions without humic acid. The slopes of the calibration curves were close to Nernstian (57.3 mV/decade with the clean-up step, and 57.0 mV/decade without it). Corresponding potential values differed by less than 1 mV.

The percent recovery (concentration found/concentration expected) was calculated in each case; the results are presented in Table 3 and in Fig. 2. When the clean-up procedure was applied, recoveries were around 95% and the reproducibility was independent of the concentration of humic acid (mean of all values 95.0%, RSD 4.2%, n = 36). This contrasts with the direct i.s.e. measurement of nitrate without clean-up, which was highly unreliable; the apparent recoveries were all over 100% and not only increased with the concentration of humic acid but changed with time.

TABLE 2

The influence of membrane contamination by humic acid on selectivity coefficients for various anions

Interfering ion	k_{ij}^{pot}		
	Manufacturer's data	Clean membrane	Contaminated membrane
Cl^-	0.01	0.01	0.02
SO_4^{2-}	1×10^{-4}	$<10^{-3}$	0.01
HCO_3^-	4×10^{-4}	$<10^{-3}$	0.005
NO_2^-	0.05	0.2	0.2

TABLE 3

Percent recoveries of nitrate from solutions containing various concentrations of reference humic acid with and without the clean-up procedure

Nitrate present (mg l^{-1})	Recovery (%)[a] with 9—45 mg l^{-1} humic acid added					
	With clean-up			No clean-up		
	9	27	45	9	27	45
30	99	98	98	143	227	1130
50	96	98	86	132	190	550
70	94	91	94	133	184	556
100	94	92	97	145	407	457
300	96	94	96	—	—	—
500	96	96	96	148	178	324

[a]Mean of two independently treated samples.

Analysis of natural water samples. All the above experiments were done with the same reference humic acid. As there is a wide natural variation in the properties of humic substances, two samples, A and B, of soil lysometer water taken from a forest in south Sweden were also examined as sources of humic materials. These samples had been analyzed by ion-chromatography [15] and found to contain 6.8 and 17 mg l^{-1} nitrate, respectively. The concentration of humic materials was unknown, but the colour was very dark. To sample A, nitrate was added and the percent recovery was found as described above. It was necessary to use three disposable clean-up columns before the effluent was sufficiently colourless (absorbance of >0.01 at 225 nm for 1-cm pathlength). Stable potentials were obtained and the recoveries were satisfactory (Table 4). In sample B, nitrate was determined directly as described under Experimental. The nitrate concentration was found to be 16.4 mg l^{-1} (RSD 2.8%, $n = 4$) in good agreement with the ion-chromatographic determination.

TABLE 4

Percent recoveries of nitrate from a soil lysometer water containing 6.8 mg l^{-1} nitrate

Concentration of nitrate (mg l^{-1})			Recovery (%)
Added	Found	RSD[a]	
60	68.9	4.6	103
80	83.5	3.5	96
100	100.5	1.9	94

[a]Relative standard deviation (%) for 4 replicates.

Discussion

In the previous work [15], when high-quality bonded-phase materials for h.p.l.c. were used, the amine material showed a high adsorption capacity for humic substances (13 mg g^{-1} of adsorbent), but negligible adsorption

of nitrate and sulfate, provided that the ionic strength of the eluent was very low. When the disposable Bond-Elut material was used as described here, the adsorption capacity for humic substances was markedly lower (Table 1) indicating lower surface coverage. The adsorption of humic substances is irreversible [15], preventing regeneration of the columns, but this disadvantage is outweighed by the low cost of the Bond-Elut material. The sorption of nitrate was significant, indicating that the surface charge is higher. The conditioning procedure described above, involving deactivation with sulfate, prevents nitrate adsorption, at the expense of a further 30% reduction in the adsorption capacity of humic substances (Table 1).

The erroneous results obtained with the nitrate i.s.e. placed directly in water samples containing humic substances, were probably due to adsorption of humic substances on the membrane, which contains a quaternary ammonium salt dispersed in plasticized poly(vinyl chloride). A silica surface, chemically modified with quaternary ammonium groups, was found [15] strongly to adsorb humic acid. Humic substances adsorbed on the i.s.e. membrane would probably lead to potential drift and selectivity changes. Some drift could also be caused by fouling of the reference electrode, giving unstable liquid-junction potentials [14, 16].

The disposable columns are well suited for the removal of humic substances prior to i.s.e. measurements in spite of a considerable variation in adsorption capacity and can be used in field applications. Several columns can be connected in series to increase the capacity. Their flow resistance is low, so that they can be connected in a flow system for on-line clean-up.

The authors thank Dr. Lo Gorton and Dr. Arne Torstensson for valuable discussions concerning this work.

REFERENCES

1 K. A. Smith (Ed.), Soil Analysis, Dekker, New York, 1983.
2 P. J. Millham, A. S. Awad, R. E. Paull and J. H. Bull, Analyst (London), 95 (1970) 751.
3 P. J. Millham, Analyst (London), 95 (1970) 758.
4 D. Langmuir and R. L. Jacobson, Environ. Sci. Technol., 4 (1970) 834.
5 A. Raveh, Soil Sci., 116 (1973) 388.
6 H. J. Nielsen and E. H. Hansen, Anal. Chim. Acta, 85 (1976) 1.
7 A. Öien and A. R. Selmer-Olsen, Analyst (London), 94 (1969) 888.
8 M. K. Mahendrappa, Soil Sci., 108 (1969) 132.
9 R. J. K. Myers and E. A. Paul, Can. J. Soil Sci., 48 (1968) 369.
10 A. R. Mack and R. B. Sanderson, Can. J. Soil Sci., 51 (1971) 95.
11 E. H. Hansen, A. K. Ghose and J. Ruzicka, Analyst (London), 102 (1977) 705.
12 A. Hulanicki, R. Lewandowski and M. Maj, Anal. Chim. Acta, 69 (1974) 409.
13 E. H. Hansen, F. J. Krug, A. K. Ghose and J. Ruzicka, Analyst (London), 102 (1977) 714.
14 A. Hulanicki, in E. Pungor (Ed.), Ion-selective electrodes 3, Elsevier, Amsterdam, 1981, p. 103.
15 G. Marko-Varga, I. Csiky and J. Å. Jönsson, Anal. Chem., 56 (1984) 2066.
16 H. Jenny, T. R. Nielsen, N. T. Coleman and D. E. Williams, Science, 112 (1950) 164.

Analytica Chimica Acta, 178 (1985) 313—317
Elsevier Science Publishers B.V., Amsterdam — Printed in The Netherlands

Short Communication

AMPEROMETRIC DETERMINATION OF FORMATE WITH A NICKEL ELECTRODE

H. W. SHIH and C. O. HUBER*

Department of Chemistry, University of Wisconsin-Milwaukee, Milwaukee, WI 53201 (U.S.A.)

(Received 11th June 1985)

Summary. Comparison of the amperometric response of platinum and nickel electrodes for formate showed that the sensitivity of the Pt electrode changed with time while that for Ni did not. The nickel electrode was used in a flow-injection system to monitor formate and other single-carbon species and to study the kinetics of selected reactions that produce formate. The detection limit for formate in a 30 μl sample was 0.02 mM with linear response to 7.0 mM. Rate constants for hydrolysis and hydration of chloroform, carbon monoxide, and dimethylformamide in 0.10 M NaOH solution were found to be $2.30 \pm 0.05 \times 10^{-4}$, $8.5 \pm 0.05 \times 10^{-4}$, and $3.04 \pm 0.003 \times 10^{-4}$ M^{-1} s^{-1}, respectively, at 25°C. Advantages of this technique are direct detection of reaction product, low detection limits, fast measurements, reduced exposure to air, and low sample volumes.

Interest in the oxidation of formate ion arises from several considerations. Its chemical behavior differs from that of typical carboxylic acids, in that its aldehydic group makes it suspectible to oxidation. It is related to important single-carbon species such as methane, methanol, formaldehyde, and carbon monoxide which are of considerable interest in energy-related studies (e.g., fuel cells). It is not easily detected in aqueous systems by spectroscopic methods.

The electro-oxidation of formate ion in alkaline solutions involves a two-electron transfer.

$$HCOO^- + 3OH^- \rightarrow CO_3^{2-} + 2H_2O + 2e^- \quad (1)$$

The reaction rate is slow compared to that for oxidation of formaldehyde and methanol [1]. Several authors have reported on the anodic reaction in acidic solution at platinum and rhodium electrodes; electrode-poisoning effects were caused by adsorption of intermediates or reaction products [2—4]. Previous work in this laboratory has yielded anodic oxidation procedures for many organic molecules in alkaline (e.g., 0.1 M NaOH) solutions [5, 6]. The goal of the work reported here was to characterize the anodic oxidation of formate at platinum and nickel electrodes in alkaline solution and to apply a flow-injection technique to quantitative and kinetic studies. An important advantage of the flow-injection technique when electrochemical detectors are used is the continuous supply of background

0003-2670/85/$03.30

electrolyte; samples only briefly contact the electrodes so that they can be returned quickly to their baseline state. This is particularly important if the electrode surface is part of the electrochemical process.

Fleischmann et al. [7] reviewed the oxidation of organic solutes at nickel oxide electrodes at high pH. The reaction is kinetically controlled. In the rate-determining step, nickel(III) oxide oxidizes the solute in a surface redox reaction. This and other studies have shown that hydration, ion exchange, and crystal morphology as well as redox processes may be involved. The transitions in the surface film of nickel oxide include [8, 9]:

$$\begin{array}{ll} \alpha(\mathrm{II}) \rightleftharpoons \gamma(\mathrm{III}) & \text{hydrated} \\ \uparrow \quad \downarrow & \\ \beta(\mathrm{II}) \rightleftharpoons \beta(\mathrm{III}) & \text{unhydrated} \end{array}$$

In order to maintain the activity of the γ-Ni(III) (NiOOH) for amperometry, nickel(II) is supplied in the form of suspended $Ni(OH)_2$ by addition of nickel sulfate to the sodium hydroxide electrolyte [5]. The amperometric measurements reported here have the advantages that sensitive measurements can be obtained early in the reaction process, and that atmospheric oxygen is excluded from the systems. Three reactions selected for study were the hydrolysis of chloroform, carbon monoxide, and dimethylformamide to give formate. This selection was based on the importance of the reactions and the shortage of literature data on their kinetics. No previous reports on spectroscopic determinations of the respective rate constants were found.

Experimental

Reagents. All chemicals were of reagent grade. Redistilled (glass) water was used to prepare solutions. The background electrolyte was 0.1 M NaOH with 1.0×10^{-4} M nickel sulfate; the nickel precipitates as flocculent nickel hydroxide. Unless otherwise specified, all analytes were prepared in the background electrolyte.

Apparatus. The flow-injection system consisted of a gravity reservoir, 0.8 mm i.d. teflon tubing, a 30-μl injection valve (Rheodyne, Model 50), an 18×0.08-cm mixing tube, and an amperometric detector. The detector cells were three-electrode systems consisting of the working electrode, a stainless-steel counter electrode, and a reference saturated calomel electrode (SCE). The platinum wire electrode (7×0.5 mm) and tubular nickel electrode (1.0 mm $\times$ 0.8 mm) have been described [10]. Both the reference and counter electrodes were in a reservoir 1—2 cm downstream. The potentiostat was based on two operational amplifiers (RCA 3240) with low nanoampere measuring capabilities; it was housed in a small aluminum box and was powered by a Polytron $\pm$ 15 V d.c. supply. A strip-chart potentiometric recorder was used.

When the potential is applied to a nickel electrode, the instantaneous carrier electrolyte current is more than 20 μA, which decays exponentially

as a nickel oxide surface is formed. After 30 min, the steady-state current is about 0.2 μA. When not in use, the electrode is stored in the electrolyte at open circuit. Re-applying the potential yields a steady-state current within 5 min. If the electrode is stored in air and rinsed with water before applying a potential, a period of 15 min or more is needed before a steady-state current is obtained. If needed, a new nickel oxide layer can be obtained by passing 5.0 ml of 0.25 M sulfuric acid or 0.5 M hydrochloric acid through the detector and then re-applying the potential with carrier electrolyte flowing through the electrode.

Procedures. The flow-injection procedure is initiated by adjusting the flow rate (typically 1.5 ml min^{-1}) and offsetting the background current. The signal appears within 10 s of sample injection. Peak heights are measured.

Results and discussion

Formate oxidation at platinum. The response to formate at the platinum electrode is shown in Fig. 1. The sensitivity decreased during several hours of measurement, over the entire useful applied potential range (+0.3 to +0.7 V). Cyclic voltammetry (+0.1 to +0.6 V) showed that both the cathodic and anodic currents decreased more than 50% during several hours. Formate was shown to be stable against air oxidation by bubbling oxygen into the 0.1 M NaOH solution for over 48 h. Adzic and Tripkovic [11] found that a strongly bound intermediate forms during the oxidation of formate at a platinum electrode; the intermediate decreases the effective area of the platinum surface. The loss of electrode activity observed here was probably due to this deactivating species.

Formate oxidation at nickel. Initial studies with a nickel electrode indicated better stability and sensitivity than for platinum. Accordingly, the

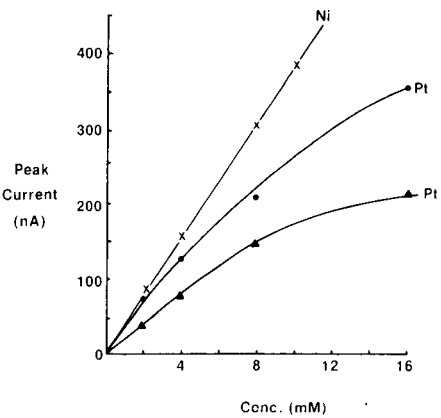

Fig. 1. Peak current vs. concentration for Pt and Ni electrodes: (•) freshly pretreated platinum electrode; (▲) platinum electrode after 5-h use; (×) nickel electrode both freshly prepared and after several hours use.

characteristics of the nickel electrode were examined in detail using the flow-injection technique.

The effect of applied potential for d.c. amperometry was examined using 20-mV increments between 0.490 and 0.560 V. The background current increased with increasing potential. The optimal net signal was obtained at +0.52 V vs. SCE. The signals were unaffected by changes in the hydroxide concentration from 0.10 to 0.40 M. The background current increased about three-fold over this range. When potassium or lithium hydroxide was used in place of sodium hydroxide, no significantly different effects on the signals were observed.

Exhaustive electrolysis was used to determine the number of electrons (n) involved; the flow-injection technique was used to monitor the decreasing formate concentration. The results yielded $n = 1.98 \pm 0.02$ (standard deviation; 5 replicates). Thus it is concluded that a two-electron process occurs to yield carbonate (Reaction 1). The magnitude of the current densities observed were well below those expected for mass-transport rate control. The mechanism of the electrode reaction is probably similar to that proposed by Fleischmann et al. [7]; it probably involves a rate-determining oxidation of the analyte by a higher-oxidation-state nickel oxide species in the surface lattice, probably NiOOH.

The dependence of the signal on temperature was observed over the range 20—30°C by immersing the flow system, including the electrodes in a thermostated water bath. The temperature dependence of the SCE is only 0.10 mV K^{-1} [12] in this range. The observed temperature dependence of the formate signal was positive, approximately 8% K^{-1}. Temperature shifts of more than about 0.5°C between sample and standards should be avoided in routine studies. Effects of flow rate were observed over the range 0.5—5.5 ml min^{-1} by adjusting the height of the electrolyte reservoir. The optimal flow rates were in the range 1.0—2.0 ml min^{-1}. The opposing effects of sample plug dispersion versus rate of mass transport to the electrode surface with increasing flow rate can explain the occurrence of the optimum.

The nickel oxide electrode surface was found to be stable over several hours of use. After the flow rate was reduced, or even stopped for up to 16 h during storage, no change in characteristics was observed when the flow was restored. These results were in sharp contrast to the effects observed at platinum electrodes.

To investigate the quantitative characteristics, formate concentrations from 10^{-5} to 10^{-2} M were examined. The response was linear from 2.0×10^{-5} M to 7.0×10^{-3} M. The standard error of estimate was 0.46 nA and the slope was 40 nA mM^{-1}. At concentrations greater than 7.0×10^{-3} M, the sensitivity decreased, suggesting possible adsorption of formate preceding electron transfer. Peak current measurements for five replicate determinations in the range 0.2 to 4.0 mM yielded relative standard deviations of 1%. The detection limit, defined as the concentration corresponding to a signal three times the peak-to-peak noise (0.2 nA), was 0.02 mM.

Sensitivities for the anodic detection of methanol, formaldehyde, and methylamine were 170, 180, and 830 nA mM^{-1}, respectively.

Kinetic studies. Rates of hydrolysis and hydration of chloroform, carbon monoxide, and dimethylformamide were evaluated as model systems. In each case, the residence time in the sample loop was sufficiently short that any reaction taking place there was judged negligible. For chloroform and carbon monoxide, the only electroactive product was formate:

$$CHCl_3 + 4OH^- \rightarrow HCOO^- + 2H_2O + 3Cl^- \quad (2)$$

$$CO + OH^- \rightarrow HCOO^- \quad (3)$$

For dimethylformamide, both formate and dimethylamine were electroactive:

$$(CH_3)_2\,NCHO + OH^- \rightarrow HCOO^- + (CH_3)_2NH \quad (4)$$

The current was shown to vary linearly with the total concentration of the two species up to 3 mM.

Rate constants were evaluated graphically from plots of $\ln[(C^0_{OH^-} - C_F)/(C^0_R - C_F)]$ in which C^0_{OH} and C^0_R are initial concentrations of hydroxide and reactant and C_F is the time-dependent concentration of formate determined amperometrically. Second-order rate constants for chloroform, carbon monoxide, and dimethylformamide reacting in 0.1 M NaOH at 25°C were $(2.03 \pm 0.05) \times 10^{-4}$, $(8.5 \pm 0.05) \times 10^{-4}$, and $(3.04 \pm 0.003) \times 10^{-4}$ M^{-1} s^{-1}, respectively. Values for chloroform and carbon monoxide can be compared with values of 2.38×10^{-4} and 8.1×10^{-4} M^{-1} s^{-1}, respectively, determined by Hine at 35°C [13, 14]. The rate constant for dimethylformamide was also found to be $(2.85 \pm 0.01) \times 10^{-4}$ M^{-1} s^{-1} at pH 12; below pH 11, the rate was too slow to be measured by the present method.

It should be noted that the nickel electrode is responsive to a variety of organic species and for complex mixtures will need to be coupled with separation methods (e.g., liquid chromatography) to gain the needed selectivity.

REFERENCES

1 W. Vielstich, Fuel Cells, Interscience-Wiley, New York, 1965, p. 76.
2 B. E. Conway and M. Dzieciuch, Can. J. Chem., 41 (1963) 21, 38, 55.
3 R. R. Adzic and M. I. Hofman, J. Electroanal. Chem., 110 (1980) 361.
4 L. Muller and H. Gunther, J. Electroanal. Chem., 103 (1979) 271.
5 B. S. Hui and C. O. Huber, Anal. Chim. Acta, 134 (1982) 211.
6 T. N. Morrison, K. G. Schick and C. O. Huber, Anal. Chim. Acta, 120 (1980) 75.
7 M. Fleischmann, K. Korinek and D. Pletcher, J. Chem. Soc., Perkin Trans. II: (1972) 1396.
8 L. D. Burke and T. A. M. Twomey, J. Electroanal. Chem., 134 (1982) 353.
9 A. J. Arvia, D. Posada and A. J. Bard, The Electrochemistry of Elements, M. Dekker, New York, 1975, Vol. 3, pp. 349—399.
10 C. J. Yuan and C. O. Huber, Anal. Chem., 57 (1985) 180.
11 R. R. Adzic and A. V. Tripkovic, J. Electroanal. Chem., 99 (1979) 43.
12 A. J. Bethone and N. A. S. Loud, Standard Aqueous Electrode Potentials and Temperature Coefficients, C. A. Hampel, Skokie, IL, 1964, p. 15.
13 J. Hine, J. Am. Chem. Soc., 72 (1950) 2438.
14 J. Hine and A. M. Dowell., Jr., J. Am. Chem. Soc., 76 (1954) 2688.

Analytica Chimica Acta, 178 (1985) 319—323
Elsevier Science Publishers B.V., Amsterdam — Printed in The Netherlands

Short Communication

FLOW-INJECTION AMPEROMETRIC DETERMINATION OF CHLORINE AT A GOLD ELECTRODE

ALEXANDRA N. TSAOUSIS and CALVIN O. HUBER*

Department of Chemistry, University of Wisconsin-Milwaukee, Milwaukee, WI 53201 (U.S.A.)

(Received 13th August 1985)

Summary. The applied potential is +0.2 V vs. SCE, flow rate is 1 ml min^{-1} and sample volume is 30 μl. The background electrolyte is 0.05 M phosphate, pH 7.4. Electrode pretreatment is +1.3 V vs. SCE for 40 s, followed by a pre-injection delay of 20 s. Peak current over a receding baseline is used. Linear range extends down to 0.4 μM for chloramine and 0.2 μM for hypochlorite. Sensitivities are 70 and 95 nA μM^{-1} respectively. Time per determination is less than 1.5 min. Monochlorinated glycine is active whereas chlorinated cyanurates show no response. Chlorine and monochloramine in river water were determined.

Chlorination of water is widely used for disinfection, biofouling control, etc., usually at or below 1 mg l^{-1} chlorine concentrations. The major chlorine species with a plus one oxidation state are hypochlorous acid, and hypochlorite ion. If ammonia is present, monochloramine, and unstable dichloramine can form. The various forms differ in toxicity, disinfection efficiency, and longevity under natural conditions. In the presence of natural ammonia in waters, the predominant species are either $HOCl/OCl^-$ or NH_2Cl. For disinfection of swimming pool water, the chlorine is commonly supplied in the form of the sodium salt of dichlorinated cyanuric acid (see below). This chlorine species is used in order to minimize molecular chlorine formation which is catalyzed by ultraviolet radiation. Accordingly, the responses of chlorinated cyanuric acid species were investigated and are described here.

Spectrophotometric molar absorptivities of hypochlorous acid and monochloramine are too low to allow sub mg l^{-1} concentration measurements. Various titrimetric techniques are used to monitor these species [1], however, rapid, direct techniques suitable well below mg l^{-1} levels are often needed.

Amperometric techniques for chlorine species at gold electrodes are often limited by electrode surface maintenance considerations. The flow-injection technique allows for electrode maintenance as well as for rapid, convenient sample handling.

Experimental

The components of the basic flow injection system were a peristaltic pump, an injection valve (Rheodyne, Model 50, four-way), and a flow-

0003-2670/85/$03.30

through thin-layer amperometric detector. Teflon tubing (0.8 i.d.) was used.

The detector was of the thin-layer amperometric design (Bioanalytical Systems). The spacer thickness was 0.010 cm and the circular gold electrode was 3 mm in diameter. To minimize ohmic losses, the auxiliary platinum electrode (6 mm in diameter) was positioned directly across the thin-layer channel. The saturated calomel electrode (SCE) was positioned downstream from the working electrode. The detector was attached to a potentiostat current follower based on two operational amplifiers (RCA 3240) with provisions for switching the applied potential between two values. The output of the potentiostat was read with a potentiometric strip-chart recorder.

The background electrolyte was 0.05 M phosphate buffer, pH 7.4. Unless otherwise specified, all sample analytes were prepared in background electrolyte. Cyanuric acid (Aldrich Chemical Company) was used as obtained. Monochloramine samples were prepared by the addition of the appropriate amount of ammonium nitrate to a buffered solution of hypochlorite to give a final 2:1 nitrogen/chlorine molar ratio. Samples were prepared with water distilled from alkaline permanganate to remove residual chlorine.

Results and discussion

The selected measurement conditions are listed in Table 1. For hypochlorous acid and monochloramine, reduction begins at approximately +0.60 V and +0.55 V vs. SCE, respectively. Currents increased as the applied potential was made more cathodic, but at values more negative than approximately +0.10 V, the signal-to-noise ratio decreased significantly because of increasing background current, including that for oxygen reduction. The maximum signal-to-noise ratio was observed at +0.20 V. The proximity of half-wave potentials for these two species prohibited selectivity via applied potential. The peak currents increased slightly with successive sample injections. In order to avoid this surface activation by analyte reduction, the electrode was pretreated at +1.3 V for 40 s. Increasing either the potential or the time of pretreatment beyond those values showed minimal advantage. Following pretreatment, the 20-s pre-injection delay time allowed the baseline current slope to decay enough for accurate peak-current measurement. In the practical pH range of 6—8, $HOCl/OCl^-$ signals decreased slightly while

TABLE 1

Measurement conditions

Applied potential	+0.20 V vs. SCE	Pre-injection time	20 s
Carrier electrolyte	0.050 M phosphate buffer, pH 7.4	Injector to detector time	3 s
		Sample volume	30 μl
Flow rate	1.0 ml min^{-1}	Maximum sampling rate	50 h^{-1}
Pretreatment	1.3 V, 40 s		

for chloramine, maximum signal was observed at pH 7. A pH of 7.4 was selected for subsequent work. Increased buffer concentrations caused decreased signals, probably because of anion adsorption [2]. Peak currents increased with flow rate, but with decreasing slope from 0.5 to 2 ml min^{-1}. The leveling effect at the higher flow rates may be attributed to the onset of kinetics control. At 1 ml min^{-1}, temperature dependence was about 2% per degree, suggesting predominant diffusion control. The maximum sampling rate was limited by the pretreatment times. Peak width was less than 10 s.

The analytical characteristics are shown in Table 2. The minimum determination limits reach the $\mu g\ l^{-1}$ chlorine range appropriate to environmental applications.

Comparison of sensitivities for hypochlorous acid and monochloramine shows an approximate 25% discrepancy. For applications where the identity of the chlorine species is not known, using the value for hypochlorous acid will result in underestimation of the chlorine concentration by 25% if monochloramine is the active form. It should be noted that considerations of chlorine chemistry indicate that either one or the other of the two species is expected in practical samples. Measurements of hypochlorous acid or monochloramine in filtered (paper) and buffered Wisconsin River water showed sensitivity and linear range in accordance with Table 2, but with an intercept corresponding to a sample chlorine demand of 20 μM. Residual currents associated with chlorine demand species were 0.070 μA. The response for monochloroglycine was examined and found to be linear in the range 2.5×10^{-5}—1.5×10^{-4} M with a sensitivity of 21 nA μM^{-1}. In order to examine the activity of chlorinated cyanurates, determinations were made after additions of hypochlorous acid to a 60 μM solution of cyanuric acid. Chlorine/cyanuric acid stoichiometric mole ratios ranging from 0.5 to 4 were used. Data for the corresponding free chlorine concentrations in the absence of cyanurate were also obtained (Fig. 1). To interpret these data, the chlorination of cyanuric acid must be considered, e.g.,

TABLE 2

Analytical characteristics

Characteristic	Monochloramine	Hypochlorous acid
Linear range (μM)	0.43[a]—143	0.16[a]—290
(mg Cl l^{-1})	0.014[a]—4.8	0.0053[a]—9.7
Sensitivity (nA μM^{-1})	70	95
Standard error of estimate (nA)	10	5
Standard deviation (%)	2[b]	2[b]

[a]These values are also the lower determination limits. [b]For 2 mg Cl l^{-1}; $n = 8$.

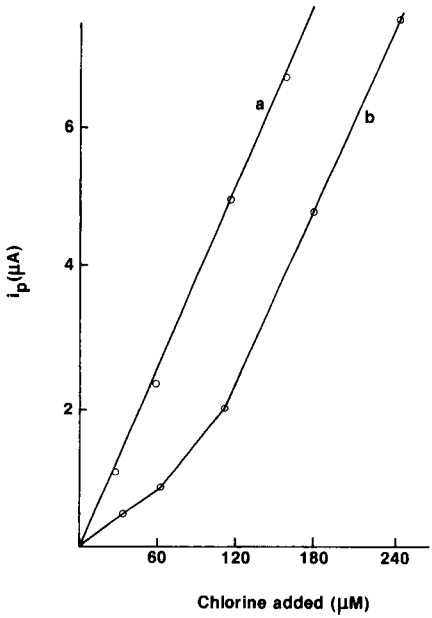

Fig. 1. Peak currents for chlorine solutions: (a) buffer only; (b) buffer plus 60 μM cyanuric acid.

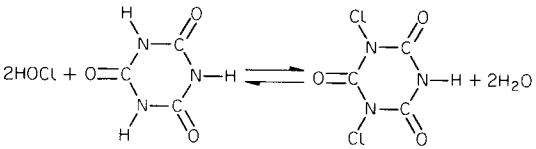

(1)

The various protonation and chlorination equilibria involve ten organic species in addition to HOCl, OCl^-, H^+, and OH^-. These labile equilibria have been carefully evaluated by Brady et al. [3]. At pH 7.5, three predominant species of cyanuric acid (Cy) are related by

$$HClCy^- + OH^- \rightleftharpoons H_2Cy^- + OCl^- \quad (K_1 = 12.6) \tag{2}$$

$$Cl_2Cy^- + OH^- \rightleftharpoons HClCy^- + OCl^- \quad (K_2 = 3 \times 10^{-3}) \tag{3}$$

For a mole ratio of 0.5 (see Fig. 1), $[H_2Cy^-] \approx [HClCy^-]$ and $[OH^-] = 10^{-6.5}$, then the concentration of free chlorine can be computed as 8 μM which corresponds to a signal of 0.27 μA, in reasonable agreement with the experimental value of 0.32 μA observed.

At a mole ratio of 1.5, $[HClCy^-] \approx [Cl_2Cy^-]$ and using K_2, the concentration of total free chlorine can be computed as 30 μM corresponding to a signal of 1.2 μA, in acceptable agreement with the extrapolated signal of 1.3 μA observed. The hydrolysis constant for the trichlorinated form of cyanuric acid indicates that the formation of this species is insignificant. At mole ratios greater than 2, a linear response parallel to that for

free chlorine suggests that the electrode response can be attributed to hypochlorous acid/hypochlorite and that the chlorinated forms of cyanuric acid are not active at the electrode under these conditions.

REFERENCES

1 Standard Methods for the Examination of Water and Wastewater, 14th edn., Am. Public Health Assoc., Washington, D.C., 1975, p. 318.
2 R. Gorbet, W. S. Metcalf and F. G. Soper, J. Chem. Soc. London, (1953) 1927.
3 A. P. Brady, K. M. Sancier and G. Sirine, J. Am. Chem. Soc., 85 (1963) 3101.

Analytica Chimica Acta, 178 (1985) 325—330
Elsevier Science Publishers B.V., Amsterdam — Printed in The Netherlands

Short Communication

COMBINED EXTRACTION/MULTIWAVELENGTH SPECTROPHOTOMETRIC METHOD FOR QUANTIFICATION OF GOLD IN GEOLOGICAL SAMPLES

S. O. FARWELL* and C. T. KAGEL
Department of Chemistry, University of Idaho, Moscow, ID 83843 (U.S.A.)
(Received 5th June 1985)

Summary. The capabilities of a combined liquid-liquid extraction/spectrophotometric method for the trace determination of gold in geological samples are presented. After extraction with ethyl acetate, gold in the extracts is quantified as tetrachloroaurate with the multicomponent data-processing programs inherent in a diode-array u.v.-visible spectrophotometer. This method has an overall detection limit of 0.4 μg Au g^{-1} sample and a combined extraction/measurement imprecision of less than ±12%.

Although considerable research has been done on the problem of determining trace amounts of gold in geological samples by spectrophotometric methods, relatively little of it is of known practical value. Many reports use synthetic solutions to test for interference and pay no attention to the methods of dissolution which must be used to obtain liquid samples. Aqua regia is the commonest medium for dissolution, and even traces of nitric acid will interfere in most classical procedures [1].

The more successful applications of molecular absorption to the determination of gold in geological samples have utilized the extractive and absorptive properties of the tetrabromoaurate ion [1—3]. Procedures utilizing the absorptive properties of tetrachloroaurate [4] are not widely used, especially for complex samples [5]. Whereas the corresponding bromo complex is more stable and has a higher absorbance, other metal/bromide complexes are likewise more stable and more intense chromophores than the respective chloride complexes. The lower stability of most metal/chloride complexes at low hydrochloric acid concentrations gives the chloroaurate complex an advantage of increased extraction selectivity over the bromoaurate. Thus, tetrachloroaurate seems to be the ideal form because it is selectively extractable, absorptive, and formed directly during aqua regia dissolution.

This study involved the characterization of typical aqua regia digests of geological materials by ultraviolet(u.v.)-visible and atomic absorption spectrometry (a.a.s.). In addition several solvent extraction techniques were evaluated for their recovery of gold, reduction of interference, u.v.-visible transparency, quantification of major interferents and limits of determination

0003-2670/85/$03.30

in their presence, and comparison of results for gold using u.v.-visible and a.a.s. detection on the same sample digests. Overall measurement accuracy and precision for the combined extraction/spectrophotometric method developed in this work were compared to more conventional techniques using well characterized geological reference materials.

Experimental

Materials. The concentrated acids used for sample digestions were J. T. Baker reagent grade. J. T. Baker Spectrograde solvents were used for extraction without further purification. The standard solutions of metals (1000 μg ml^{-1}) were obtained from Anderson Laboratories while the geological reference samples were supplied by either the Canada Center for Mineral and Energy Technology (CANMET) or the U.S. Geological Survey (USGS).

Instrumentation. A Hewlett-Packard Model 8450A rapid-scan diode-array spectrophotometer equipped with a HP-9895 disk drive and HP-7470A plotter was used to record all u.v.-visible spectra and compute multicomponent analyses. Matched rectangular 1-cm quartz cells were used for all u.v.-visible measurements in solution. The solvent of interest was used in the reference beam whenever spectra were taken in nonaqueous media. Comparative determinations of gold by a.a.s. were done with an Instrumentation Laboratories Model 353 atomic absorption spectrometer.

Methods. The sample digestions were done in the following manner. Each sample (29.17 g) of pre-roasted (1 h at 600°C) and ground (200-mesh) material was weighed into a 500 ml Florence flask, 50 ml of concentrated hydrochloric acid was added, and the covered solution was boiled for 0.5 h. Then, 15 ml of concentrated nitric acid was added and the digestion was continued for 1 h. Next, 20 ml of 6 M HCl was added and the digestion was continued for another hour. The digest solutions were cooled and filtered through Whatman 4 filter paper into 100-ml volumetric flasks.

Extractions were done in 125-ml separatory funnels by successive 10-ml portions of solvent (either diethyl ether, ethyl acetate, or methyl isobutyl ketone) added to 20-ml aliquots of the digestate solutions. The organic phase was drawn into a calibrated conical centrifuge tube for volume measurement after backwashing with approximately 10 ml of 1 M HCl. This backwashing procedure was used to remove co-extracted covalent chlorides of Fe, Ge, As, Mo, Ga, and Te [6].

Results and discussion

Spectra of typical aqua regia digests showed intense absorption throughout the 200—800 nm region. Dilution failed to clarify peak structure, demonstrating the need for selective extraction procedures. Ethyl acetate was finally selected as an appropriate extraction solvent because of its high selectivity for such gold complexes, its low volatility, and its optical transparency in the region of interest. Investigation of typical ethyl acetate

extracts of standards, potential interferents, and typical digests showed that the major absorbing interferents were $FeCl_4^-$ and nitric acid. The spectra of these components were more distinct from $AuCl_4^-$ spectra in ethyl acetate than in aqueous solution, thus experiments directed toward returning the analyte to the aqueous phase were not continued.

Limits of multicomponent quantification. For the successful use of the multicomponent algorithm resident in the HP-8450A software, certain boundary conditions must be met. First, because only one standard per chromophore is used for multicomponent calibration, it was necessary to demonstrate that Beer's law applies in the spectral region and concentration range of interest. This requirement for $AuCl_4^-$ in ethyl acetate was examined by plotting the actual gold concentration in five standard solutions (ranging from 0.2 to 23 mg Au l^{-1}) versus the gold concentrations computed for these standards by the multicomponent algorithm. The resulting linear graph had a regression equation of $Y = (1.03 \pm 0.02)X + (0.07 \pm 0.70)$ and $r = 0.9996$, which corroborates that the absorption obeys Beer's law. Secondly, the more identical spectra of different components are, the more difficult it is to deconvolute a mixed spectrum of those components. The experimental range of quantifiable mixtures is presented in Table 1. Thirdly, the total absorbance in the mixture must not exceed the linear range of the instrument, conservatively estimated as an absorbance of 2. Because the HP-8450A multicomponent algorithm attempts to fit a measured "unknown" spectrum by taking multiples of stored standard spectra, increases in measurement noise seriously degrade the ability to "match" spectra reliably. For this reason, the maximum absorbance of 2 is especially important.

Validation by recovery studies. Preliminary recovery experiments showed that 90—100% of gold in 3 M HCl was recovered by the ethyl acetate extraction, with the principal losses caused by backwashing. Recoveries from sample digests were studied to evaluate not only the physical recovery of gold added in solution to the digests, but also to test for accurate quantification of gold by u.v.-visible spectrophotometry in the resultant extract. The experimental recoveries of gold obtained from the additions of 21 mg l^{-1}

TABLE 1

Interference limits for multicomponent quantification

Mixture	Concentration (mg l^{-1})			Error (%)
	Au	HNO_3	Fe	
1	12	200	2	+2.3
2	4.6	200	2	+13
3	2.3	200	2	+14
4	1.2	200	2	+10
5	0.2	200	5	+67
6	2.3	100	5	−26
7	2.3	20	5	−25

to a blank and 30 mg l^{-1} each to CMS-1 and USGS-GXR-2 sample digests were 95%, 93%, and 85%, respectively. As shown in Fig. 1, the corresponding spectral environments for the extracted blank digests were relatively clean. Gold-free digests were split, one aliquot spiked with 3 mg l^{-1} gold, and both aliquots extracted. Spectra for extracts of the spiked digest, the unspiked digest, and their difference are shown in Fig. 2. The difference is clearly attributable to absorption by $AuCl_4^-$, although there is some variation in the amount of iron co-extracted in the two digests.

Table 2 shows that apparent recovery was better than 94% for a reference sample (CANMET MA-1) containing approximately 18 $\mu g\ g^{-1}$ gold.

Validation by comparison with other methods. Standard reference materials analyzed by more conventional techniques such as fire assay and a.a.s. were used to validate the u.v.-visible procedure. Parallel a.a.s. quantification of gold in extracts from standard reference materials was used to establish whether errors were due to incomplete extraction or measurement inaccuracy. As illustrated in Table 2, good agreement was found

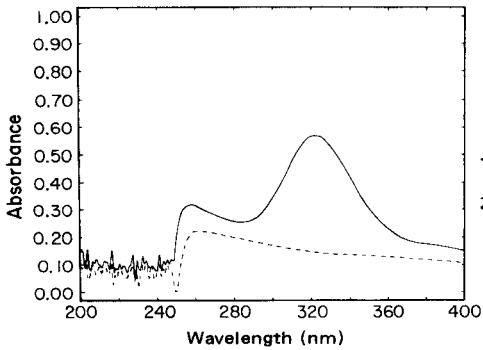

Fig. 1. Absorption spectrum of extracted blank digest with (—) and without (---) 21 mg l^{-1} gold added as tetrachloroaurate.

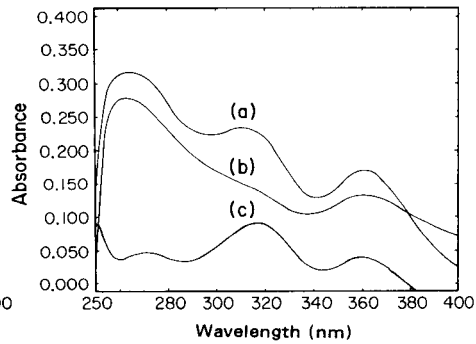

Fig. 2. Absorption spectra of extracts of spiked and unspiked digests. Spectra: (a) a digest to which 3 mg l^{-1} Au has been added; (b) the unspiked digest; (c) the difference between spectra (a) and (b).

TABLE 2

Comparison of results for proposed and conventional methods

Sample	Gold concentration ($\mu g\ g^{-1}$)		
	Fire assay	A.a.s.	U.v.-visible
MA-1	17.8	18	17
USGS-GXR-2	<0.3	<0.4	<0.4
USGS-GXR-4	0.7	<0.4	<0.4
ID-C	—	2.3	0.7
CFC	—	42	38

between the two conventional techniques and the proposed u.v.-visible procedure. The *t*-test value for 5 determinations on sample MA-1 was 1.8, showing no significant difference with the certified value at the 95% confidence level (the critical *t* is 2.8).

The u.v.-visible results in Table 2 for sample USGS-GXR-2 show that false positive identification of gold is not an apparent problem, while the results obtained for sample USGS GXR-4 demonstrate the working limit of quantification. The final two samples in Table 2 are mining industry materials, ID-C being an incompletely leached residue from cyanidation and CFC being a float concentrate. These two representative samples contain quite low and high amounts of gold, respectively, and the u.v.-visible results on these samples demonstrate the ruggedness of this technique. Spectra of extracts from such real ore samples verified the need for interference compensation via multiwavelength data processing.

The imprecision for the u.v.-visible method is ±2%, which is lower than the 5—10% imprecision related to the digestion and/or extraction procedures. Thus, the u.v.-visible measurement of gold in ethyl acetate extracts is comparable in speed, sensitivity, precision, and cost to the a.a.s. measurement of gold in MIBK extracts. For both techniques, the limitations of digestion and extraction are the factors governing accuracy of individual analyses.

Conclusions

Whereas the performance characteristics of this u.v.-visible multicomponent quantification method for gold are comparable to those of a.a.s., each method has distinct advantages. The major advantages of this u.v.-visible method compared to flame a.a.s. are a more rugged optical system and the lack of required flame gases. The primary advantages of a.a.s. are its inherently greater selectivity, a corresponding simplicity in required sample preparation, and established procedures for other sequential trace element determinations. However, the many existing photometric methods for metals of geochemical interest [7, 8] could potentially be adapted to utilize the capabilities of rapid-scan, diode-array, molecular absorption spectrophotometry for similar sequential multi-element determinations. For example, James [9] has shown that this idea is feasible with chloro complexes of various metals.

This project was supported by funding from the University of Idaho Research Council. Steve Sibley of Hewlett-Packard is acknowledged for the loan of the HP-8450A spectrophotometer system.

REFERENCES

1 F. E. Beamish and J. C. Van Loon, Analysis of Noble Metals, Overview and Selected Methods, Academic Press, New York, 1977.
2 W. A. E. McBryde and J. H. Yoe, Anal. Chem., 20 (1948) 1094.

3 W. B. Holbrook and J. E. Rein, Anal. Chem., 36 (1964) 2451.
4 L. Goodkin, M. D. Seymour and J. S. Fritz, Talanta, 22 (1975) 245.
5 E. B. Sandell and H. Onishi, Photometric Determination of Traces of Metals, General Aspects, 4th edn., Wiley-Interscience, New York, 1978.
6 G. H. Morrison and H. Freiser, Solvent Extraction in Analytical Chemistry, Wiley, New York, 1957.
7 A. A. Levinson, Introduction to Exploration Geochemistry, 2nd edn., Applied Publishing, Willmette, IL, 1980.
8 Y. A. Zolotov and I. A. Blyum, Pure Appl. Chem., 44 (1975) 671.
9 G. E. James, Am. Lab., 14 (1982) 79.

Analytica Chimica Acta, 178 (1985) 331—335
Elsevier Science Publishers B.V., Amsterdam — Printed in The Netherlands

Short Communication

AN IMPROVED METHOD FOR THE SPECTROPHOTOMETRIC DETERMINATION OF FLUORIDE BY ADDITION OF SODIUM DODECYL SULPHATE TO THE FLUORIDE/LANTHANUM (III)/ ALIZARIN FLUORINE BLUE SYSTEM

M. E. LÉON-GONZÁLEZ, M. J. SANTOS-DELGADO and L. M. POLO-DIEZ*
Department of Analytical Chemistry, Complutense University, 28040 Madrid (Spain)
(Received 22nd April 1985)

Summary. The conventional spectrophotometric method for the determination of fluoride, based on the fluoride/lanthanum(III)/alizarin fluorine blue ternary complex, is improved by addition of sodium dodecyl sulphate. In 15% (v/v) acetone medium, the absorbance of the binary reagent complex is decreased and the reaction time is only 3 min under sonication. Beer's Law is obeyed at 574 nm for fluoride concentrations in the ranges 0.075—0.30 and 0.20—1.2 mg l^{-1}; the apparent molar absorptivities are $(1.6 \pm 0.1) \times 10^4$ and $(1.5 \pm 0.1) \times 10^4$ mol^{-1} cm^{-1}, respectively. Relative standard deviations are 5.3 and 2.5% at the 0.20 and 0.60 mg l^{-1} fluoride levels, respectively. This method is applied to the determination of fluoride in bottled mineral waters.

The direct methods most often used for the spectrophotometric determination of fluoride are based on the formation of ternary complexes of the La(III) or Ce(III) chelates of alizarin complexan [(3,4-dihydroxy-2-anthraquinonyl)-methyliminodiacetic acid; alizarin fluorine blue; AFB] [1—3]. The sensitivity and precision of these methods in aqueous organic media are limited by overlapping of the absorption bands of the La(III)/AFB complex and the ternary complex. In this communication, the anionic surfactant sodium dodecyl sulphate (SDS) is shown to have beneficial effects on the spectrophotometric determination of fluoride with the La(III)/AFB complex. The sensitivity and precision of the method are improved.

Experimental

Apparatus. A Pye-Unicam SP8-200 spectrophotometer was used with 1-cm lidded cuvettes. A Radiometer M-82 pH meter was used with a GK-2320-E combined glass/calomel electrode. The Selecta ultrasonic bath supplied 50 kHz.

Reagents. The stock standard fluoride solution (100 mg l^{-1}), prepared from analytical-grade sodium fluoride (dried at 110°C) and water, was diluted as required for the working solutions. A 1.5×10^{-3} M AFB solution was prepared by dissolving 0.0578 g of AFB (BDH Chemicals) in 25 ml of water containing 0.2 ml of ammonia liquor, adding 0.2 ml of anhydrous acetic acid and diluting to 100 ml with water. A 3.0×10^{-3} M lanthanum(III)

0003-2670/85/$03.30

solution was prepared by dissolving 0.0489 g of lanthanum trioxide in 2.5 ml of hot (1 + 1) hydrochloric acid and diluting to 100 ml with water. A sodium dodecyl sulphate (SDS) solution (50 mg ml^{-1}) was prepared in water. All chemicals used for interference studies were of analytical-reagent grade. Distilled water was used for all solutions and dilutions.

Determination of 0.075—0.30 mg l^{-1} fluoride. To a 25-ml beaker add, in the following order, 0.4 ml of 0.5 M acetic acid/acetate buffer (pH 4.2), 0.3 ml of the La(III) solution, 1.5 ml of acetone, 0.6 ml of the AFB solution, and an aliquot of fluoride solution, to give a final concentration in the 0.075—0.30 mg l^{-1} range, and 3.4 ml of the SDS solution; adjust the pH to 4.8 (pH-meter) with hydrochloric acid or sodium hydroxide. Transfer this solution to a 10-ml volumetric flask, dilute with water to the mark and place in the ultrasonic bath for 3 min. Measure the absorbance at 574 nm against a reagent blank solution prepared in the same way.

Determination of 0.20—1.2 mg l^{-1} fluoride. Apply the above procedure, but use 0.5 ml of the La(III) solution and 1 ml of the AFB solution.

Results and Discussion

Spectral characteristics. As Fig. 1 shows, SDS causes a slight hypochromic effect in the absorption band of the fluoride/La(III)/AFB ternary complex, but the shape remains practically unchanged. In contrast, the main absorption band for the La(III)/AFB solution with SDS present undergoes a dramatic change; the band at 430 nm corresponds to AFB itself and only a shoulder remains at 530 nm. The combination of these effects means that,

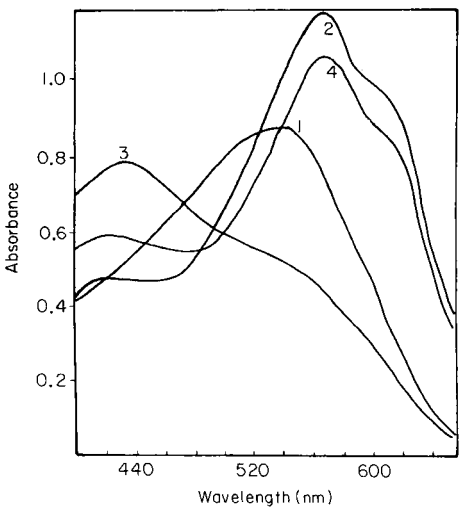

Fig. 1. Absorption spectra: (1) La(III)—AFB; (2) F^-—La(III)—AFB; (3) La(III)—AFB in presence of SDS; (4) F^-—La(III)—AFB in presence of SDS. Conditions: 1.2 mg l^{-1} fluoride, 20% (v/v) acetone, 1.5 × 10^{-4} M La(III)—AFB, pH 4.6, 17.0 mg ml^{-1} SDS (where applicable); all measured against a water reference.

when absorbances are measured at 574 nm against a reagent blank solution, sensitivity is enhanced compared to the method in the absence of SDS, and reproducibility is improved because both the binary and ternary complexes show less variation of absorbance with wavelength in the presence of surfactant around 574 nm.

Choice of experimental conditions. Changes in the surfactant concentration over the range 5—18 mg ml^{-1}, which was always higher than the critical micelle concentration [4], increased the absorbance by only about 10%. There was a slight decrease in absorbance at surfactant concentrations higher than 18.0 mg ml^{-1}, which is probably associated with a change in the micelle structure [4] causing steric hindrance of fluoride coordination. The SDS concentration chosen was 17.0 mg l^{-1}. The influence of the La(III)/AFB concentration was studied at this SDS concentration for 0.6 mg l^{-1} fluoride. The absorbance increased as the La(III)/AFB concentration was increased from 0.8 to 1.4 × 10^{-4} M, but then decreased as the binary complex concentration was raised to 2.2 × 10^{-4} M; the latter effect is due to the excessive correction then needed for the blank absorbance. Maximum sensitivity, at this fluoride concentration was obtained for a fluoride/La(III)-AFB mole ratio of 1:5. In the conventional La(III)/AFB method, 20—25% (v/v) acetone is generally added to intensify the absorbance of the complex. In the presence of 17.0 mg ml^{-1} SDS, only 15% (v/v) acetone was needed to yield the maximum effect; and in fact > 17% acetone reduced the surfactant effect, possibly because of the formation of reverse micelles [4]. In the presence of SDS, maximum absorbance was obtained at pH 4.8, which is similar to the optimum pH suggested originally [1, 2].

Stability of the system. In the presence of 17.0 mg ml^{-1} SDS and 15% acetone, the fluoride complex was formed very rapidly and the absorbance remained practically constant for at least 15 min after ultrasonication. The mechanism of formation of the ternary complex has never been fully elucidated; the effect of SDS may be to alter the nature of the solvation around both the binary and ternary complexes. The absorbance reaches a maximum value for ultrasonication times above 3 min; this time is necessary to obtain homogeneous micellar solutions.

With regard to the sequence of reagent addition, it was shown that, once acetone has been added, it is essential to form the La/AFB complex before the fluoride solution is added. The order of addition of SDS is not important.

Calibration, sensitivity and reproducibility. Under the working conditions specified under Experimental, the ternary complex obeyed Beer's Law at 574 nm for fluoride concentrations up to 0.30 and 1.2 mg l^{-1}. Ringbom plots showed that the concentration intervals for minimum error were 0.050—0.30 and 0.20—1.2 mg l^{-1}, respectively. The molar absorptivities were (1.6 ± 0.1) × 10^{-4} and (1.5 ± 0.1) × 10^{4} l mol^{-1} cm^{-1}, respectively, which are higher than the values commonly given for the ternary fluoride complex in the absence of SDS [2, 3]. The relative standard deviations (n = 10) for 0.60 and 0.20 mg l^{-1} fluoride were 2.5 and 5.3%, respectively.

The precision is good because of the improved nature of the spectra in the presence of SLS (see above). The lower limit of determination is 0.075 mg l^{-1}.

Interferences. The admissible upper limits for several species are shown in Table 1. The most important interferences are from phosphate, nitrate, Al, Fe(III), Ni and Zn ions. Apart from nitrate, these interferences are common to La/AFB procedures. The interference of nitrate is probably due to interaction with SDS; in fact, a white gelatinous precipitate is formed when high concentrations of SDS and nitrate are mixed.

Determination of fluoride in bottled mineral waters. In order to establish the validity of the proposed method, it was applied to the determination of fluoride in six bottled mineral waters, and the results were compared with those obtained by using a method of Hanocq and Molle [3] in which dimethylsulphoxode is added instead of acetone, without the surfactant. The results, summarized in Table 2, show that the average values obtained by both

TABLE 1

Upper tolerable limits for interferences, causing errors of ⩽3%, in the determination of 0.6 mg l^{-1} fluoride

Tolerable S/F^- ratio	Species (S)
2500	I^-, HCO_3^-, CO_3^{2-}, Cl^-
1500	Br^-, Ca(II), K(I)
500	NO_2^-
300	SO_4^{2-}
250	SiO_3^{2-}
150	Mg(II)
10	NO_3^-
5	PO_4^{3-}, Fe(III)
1	Al(III), Ni(II), Zn(II)

TABLE 2

Determination of fluoride in mineral waters by different La/AFB methods

Sample No.	Type	Proposed method			Hanocq/Molle method		
		V (ml)[a]	F^- (mg l^{-1})[b]		V (ml)[a]	F^- (mg l^{-1})[b]	
1	Vichy Catalan	1.0	0.76	(2.06)	1.0	0.79	(6.3)
2	Mondariz	2.0	0.12	(8.0)	2.0[c]	0.65	(9.9)
3	Viladrau	1.0	0.79	(0.60)	1.0	0.78	(7.7)
4	Fontenova	1.0	0.93	(0.62)	1.0	0.93	(1.6)
5	Fontacelta	1.0	1.01	(0.95)	1.0	0.99	(2.1)
6	Cabreiroa	2.0	0.55	(1.5)	2.0	0.54	(5.4)

[a]Volume of sample taken. [b]Mean of four determinations with relative standard deviation (%) in parentheses. [c]Concentrated 8-fold.

methods agree quite well, except in the case of sample 2, which was concentrated for the comparison method; fluoride may have been lost in the concentration. The proposed method is obviously more precise than the comparative method. Statistical comparison of the average values by a method allowing for the difference in standard deviations [5] showed that there are no significant differences between the averages at the 95% probability level.

REFERENCES

1 M. A. Leonard and T. S. West, J. Chem. Soc., (1960) 4477.
2 R. Belcher and T. S. West, Talanta, 8 (1961) 853.
3 M. Hanocq and L. Molle, Anal. Chim. Acta, 40 (1968) 13; 42 (1968) 349.
4 D. Attwood and A. T. Florence, Surfactant Systems, Chapman and Hall, London, 1983.
5 J. A. Hammerly, J. M. Marracino and R. O. Piagentini, Curso de Química Analítica. El Ateneo, Buenos Aires, 1984.

Analytica Chimica Acta, 178 (1985) 337—339
Elsevier Science Publishers B.V., Amsterdam — Printed in The Netherlands

Short Communication

A SENSITIVE SPECTROFLUORIMETRIC DETERMINATION OF HUMAN SERUM ALBUMIN WITH CHROME AZUROL S

YUTAKA SAITO*, YUKIKO INDEN-OKAZAKI, SHOKO WADA-YANO, ATSUKO KANETSUNA, KEI-ICHI MIYAZAKI, MASAKI MIFUNE and YOSHIMASA TANAKA

Faculty of Pharmaceutical Sciences, Okayama University, 1-1-1, Tsushima-Naka, Okayama 700 (Japan)

HIDEKI OKUDA

Shionogi & Co. Ltd., 192 Imafuku, Amagasaki 660 (Japan)

(Received 18th July 1985)

Summary. A simple and sensitive method for assay of human serum albumin (5—80 μg) is based on binding of chrome azurol S by the albumin and determination of the bound dye spectrofluorimetrically. The method is sufficiently sensitive for application to spinal fluid (20—100 μl).

The bromcresol green (BCG) method [1—3], used routinely in clinical assay for human serum albumin (HSA), is not sensitive enough for samples low in HSA, such as spinal fluid. This communication shows that the complex of chrome azurol S (CAS) with HSA fluoresces at 616 nm, which enables a more sensitive fluorimetric method for HSA to be developed; it can be applied to the determination of down to one-thirtieth of the concentration of HSA determined by the BCG method.

Experimental

Reagents and materials. Reagent-grade CAS (Merck) was purified by two precipitations with hydrochloric acid [4]. The HSA (fraction V, Sigma Chemical Co.) and polyethylene glycol-*p*-nonylphenyl ether (PGNP-10; Tokyo Kasei Co.) were used as received. Control normal and abnormal sera (sera I and II) and spinal fluid were purchased from Hyland Diagnostics. The clinical kit for the BCG method used as control was the Albumin B-Test (Wako Junyaku Co.).

The reagent solution was a 2:2:1 (v/v) mixture of CAS (5.0×10^{-6} M), PGNP-10 (2.5×10^{-3} M) and pH 3.0 citrate buffer (0.1 M).

Apparatus. Fluorescence spectra and relative fluorescence intensities were measured on a Shimadzu RF-500 fluorescence spectrometer equipped with a R928 photomultiplier tube (Hamamatsu Photonics). Quartz cells (10 mm) were used for the measurements.

0003-2670/85/$03.30

Procedure. The reagent solution (5.0 ml) was added to a sample solution (20 or 100 μl) containing 5—80 μg of HSA, and the mixture was incubated at around 27.5 for 30 min. The fluorescence intensity was measured against the reagent blank at 616 nm (excitation at 493 nm, slits 20—40 nm).

Results and discussion

The conditions described above gave satisfactory results. Addition of PGNP-10 is necessary for dissolution and stabilization of the CAS/HSA complex. Lactate, glycine and tartrate buffers (pH 3.0) gave almost the same intensity, but acetate buffer (pH 3.0) gave only half the intensity.

The calibration graph was linear in the range 5—80 μg of HSA (r = 0.9998, 6 points). The range of linearity depended on the concentration of CAS. The relative standard deviation was 1.3% for the determination of 40 μg of HSA (n = 10). The sensitivity was ca. 30 times better than that of the BCG method.

The change in intensity for 50 μg of HSA caused by the presence of 500 μg of calcium ion or phosphate was less than 3%. A serious decrease in intensity was caused by aluminium(III) and iron(III) which form chelates with CAS; this effect was negligible when the amount of these ions was ⩽5 μg. The extent of interference of bilirubin and γ-globulin was the same as in the control BCG method.

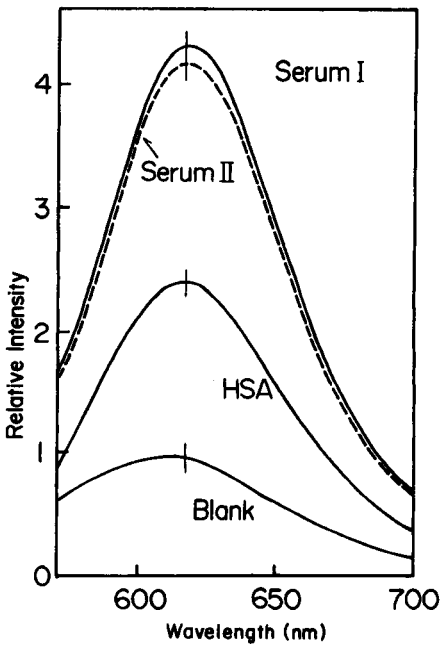

Fig. 1. Emission spectra for serum I and serum II (both from 20 μl of 5% solutions), HSA (20 μg/100 μl) and a blank solution.

TABLE 1

Comparison of the chrome azurol S method with the control bromcresol green method

Sample	HSA found (g dl^{-1})	
	BCG	CAS[a]
Serum I (normal)	4.72[b]	4.73[c] (1.39)
Serum II (abnormal)	4.61[b]	4.56[c] (0.59)
Spinal fluid	0.059[d]	0.055[e] (0.77)

[a]Average of 10 results with standard deviations in parentheses. [b—e]Sample amounts: [b]20 μl of serum; [c]20 μl of 5% serum; [d]1.0 ml of fluid; [e]100 μl of fluid.

The emission spectra obtained for sera I and II are shown in Fig. 1, together with the reagent blank and the spectrum for standard HSA. The spectra coincided, indicating that other components in sera hardly affected the spectrum. Similar results were obtained for 20 and 100 μl of spinal fluid. As shown in Table 1, the HSA values obtained by the new procedure were in agreement with those obtained by the BCG control method, which required 20 μl of undiluted sera I and II and 1.0 ml of spinal fluid. The present method can therefore be regarded as convenient and sensitive enough for assay of HSA in 20—100 μl of spinal fluid.

REFERENCES

1 F. L. Rodkey, Clin. Chem., 11 (1965) 478.
2 O. Hernández, L. Murray and B. T. Doumas, Clin. Chem., 13 (1967) 701.
3 B. T. Doumas, W. A. Watson and H. G. Biggs, Clin. Chim. Acta, 31 (1971) 87.
4 F. J. Langmyhr and K. S. Klausen, Anal. Chim. Acta, 29 (1963) 149.

Analytica Chimica Acta, 178 (1985) 341—345
Elsevier Science Publishers B.V., Amsterdam — Printed in The Netherlands

Short Communication

THE GAS CHROMATOGRAPHIC SEPARATION OF ANAESTHETIC AGENTS AND AEROSOL PROPELLANTS IN OPERATING ROOM AIR USING SERIALLY PACKED COLUMNS

JOHN M. THOMPSON* and WILLIAM I. STEPHEN

Department of Chemistry, University of Birmingham, P.O. Box 363, Birmingham B15 2TT (Great Britain)

BAJADURAI SITHAMPARANADARAJAH[a]

Dutom Meditech, Warwick St., Birmingham (Great Britain)

(Received 5th July 1985)

Summary. The use of gas chromatographic columns serially packed with molecular sieve 5A and Porapak-Q (both with particle sizes in the range 50—80 mesh) is described for the analysis of operating theatre air for nitrous oxide, halothane, trichloroethylene, enflurane, Freon-11 and Freon-12. Various combinations of lengths of the two packings were evaluated; the most suitable was 2.75 m of Porapak-Q and 0.29 m of molecular sieve 5A with a column temperature of 250°C. With the electron capture detector used, the optimum temperature to give high sensitivity for nitrous oxide was 350°C.

There is increasing concern about the possible harmful effects of trace concentrations of gaseous and volatile anaesthetics agents in the air in operating theatres on personnel working in such an environment. It is now widely accepted that it is desirable to minimize the contamination of operating theatre air by such gases and vapours [1]. Any study of the extent of such contamination and its control needs an accurate, precise, rapid and economical method of analysis. The importance of the latter has been discussed [2], along with the problems of sampling, measurement and calibration. The need for care in the choice of statistical methods of analysis of data obtained was stressed.

Various methods have been used for the determination of anaesthetic gases and vapours; gas chromatographic methods have been particularly popular. The advantages of gas chromatography are that (i) sensitivity and selectivity are easily varied to suit a particular application, (ii) only a very small volume of sample is required, and (iii) repeated measurements may be made at frequent intervals. Thus, because microlitre-sized samples can be taken from the monitored air, the rate at which the air is sampled need not be very high. Portable infra-red gas analysers, having sample cells as large as

[a]Present address: Institute of Naval Medicine, Alverstoke, Gosport, Hampshire, Great Britain.

0003-2670/85/$03.30

5 l, require air to be sampled at rates as high as 30 l min^{-1}. Consequently, considerable disturbance of the air at the sampled position occurs, unlike the situation when samples are taken for gas chromatography.

Maintenance of inhalational anaesthesia usually involves the administration of oxygen or of oxygen/nitrous oxide mixtures supplemented with one of the volatile anaesthetic agents. Therefore, operating theatre air is likely to contain much more than the usual ambient concentrations of nitrous oxide and also the vapour of at least one volatile organic anaesthetic agent. In addition, other pharmaceutical agents may be administered in aerosols where the usual propellants used are the chlorofluorocarbon propellants, Freon-11 and Freon-12 (trichlorofluoromethane and difluorodichloromethane). Hence, it would be advantageous if the gas chromatographic method chosen enabled the simultaneous determination of nitrous oxide, volatile anaesthetic agents and aerosol propellants to be achieved with a single column and detector and without the need for temperature programming. No such method has previously been reported. In general, two columns and two detectors have been used for the simultaneous determination [3].

The use of mixed stationary phases, in order to achieve certain difficult separations, is well established in gas chromatography [4]. Computer programs have been utilized to select the best mixed bed column for separation of a known mixture of compounds by isothermal gas chromatography [5]. To increase the resolving power, two or more stationary phases can be used in various ways: (a) two or more separately packed columns can be coupled together in series; (b) two or more stationary phases are mixed to form a single mixed-bed column; (c) two or more stationary phases are packed serially in a single column; or (d) homogeneous mixed liquid (stationary) phase columns are prepared by mixing two or more liquid phases and coating on a single solid support in a single column.

Keller and Stewart [6] in their thermodynamic treatment concluded that coupled columns are equivalent to mixed bed columns. But Keller and Pilgrim [7] later concluded that pressure gradients in the system had a considerable influence on the behaviour of coupled columns. Such problems can be eliminated by the use of stationary phases with similar ranges of particle sizes. With coupled columns, the dead volume between the stationary phases may lead to peak broadening and thus, a loss of resolving power. Serially packed columns have no such problems of dead volume, nor do they have the problem of achieving a homogeneous mixture of stationary phases that arises with mixed bed columns. In serially packed columns, very different lengths of the various stationary phases can be used. In a mixed bed it would be difficult to achieve reproducible homogeneous packing with stationary phase ratios far removed from 1:1. Serially packed columns were, therefore, chosen for analysis of the mixtures of nitrous oxide, anaesthetic agent vapours and aerosol propellants in air.

Experimental

Pyrex glass tubing (4-mm bore) was used to make columns with five different packed lengths. The stationary phases investigated were molecular sieve (zeolite) 5A (MS-5A) and Porapak-Q, both with a particle size range of 50—80 mesh after removal of fines. The packed columns were coupled to a Hewlett-Packard series 5700 gas chromatograph with graphite ferrules. A variable-frequency pulsed electron capture detector was used at 350°C (unless otherwise indicated). The carrier gas was a mixture of argon (95%) and methane (5%) (B.O.C. Special Gases) at a flow rate of 60 ml min^{-1}. Samples were injected via a Taylor-Servomex slide valve (10-μl volume), either manually or automatically [8]. All chromatography was done isothermally.

Results and Discussion

Table 1 lists the retention times obtained with various combinations of Porapak-Q and MS-5A serially packed in columns of different lengths. Molecular sieve 5A could not be used alone because of the lack of resolution of the Freons, halothane and trichloroethylene (Trilene). With Porapak-Q, the retention time for trichloroethylene was too long for automatic sampling from several sites within a room, because the interval between samples from the same site would be excessive. The aim was to achieve an analysis within a cycle time of 5—6 min.

The use of aerosol propellants and of trichloroethylene in operating theatres is not very great. Attention was mainly directed towards achieving a satisfactory determination of nitrous oxide and halothane, the major anaesthetic agents. The results of most interest in this respect are underlined in Table 1. The effect of changing column temperature on the behaviour of nitrous oxide was examined for the 2.75/0.29-m Porapak-Q/MS-5A column; the results are shown in Table 2.

TABLE 1

The retention data for various air contaminants on different serially packed columns

Length of packings (m)		Column temp. (°C)	Retention time (s)				
			N_2O	Freon-12	Freon-11	Halothane	Trilene
P—Q[a]	MS-5A						
0	0.92	230	81	22	22	29	29
0.31	1.22	200	200	10	10	74	120
0.31	1.22	250	140	8	8	62	74
1.22	0.31	200	54	52	128	212	316
1.53	0	200	29	61	136	228	389
1.83	0.61	250	91	101	160	200	313
2.75	0.29	250	72	98	181	237	360
3.05	0.31	250	82	110	194	265	ND[b]

[a]Porapak-Q. [b]Not determined.

TABLE 2

Data for nitrous oxide on a serially packed column at different column temperatures[a]

Column temp. (°C)	Peak area (cm^2)	HETP (mm)	Attenuation	Relative peak height
250	2.49	2.2	4	1
240	2.52	2.8	8	0.47
230	2.50	3.2	16	0.22
210	2.55	4.7	16	0.19

[a]3.04 m column packed with 2.75 m of Porapak-Q and 0.29 m of molecular sieve 5A; 1798 $\mu g\ l^{-1}$ nitrous oxide; other conditions as in the Experimental section.

The sensitivity of the electron capture detector depends on the temperature [9]. Table 3 shows the influence of detector temperature on the measurement of halothane and nitrous oxide. Increasing the detector temperature from 250°C to 350°C caused an approximately four-fold increase in the sensitivity to nitrous oxide. Wentworth et al. [10] explained this as an easier attachment of low-energy electrons to nitrous oxide molecules when their molecular structure is distorted by thermal agitation (increased intensity of the "wagging" vibrational mode). The sensitivity of halothane decreased by about 20% when the detector temperature was increased from 200 to 350°C. The threshold temperature required for homolytic cleavage of the carbon-bromine bond of halothane was stated [11] to be about 400°C, and when halothane is prepared by thermal bromination, the temperature used is 425—475°C. Therefore, it seems unlikely that halothane breakdown occurs in the electron capture detector at 350°C.

A typical chromatogram obtained with the 3.04-m serially packed column (2.75/0.29-m Porapak-Q/MS-5A) at 250°C is shown in Fig. 1. The nitrous oxide peak broadened at 230°C. The retention time of another volatile anaesthetic agent of growing importance, enflurane, was measured on this column at 250°C and was found to be 265 s. With continuous use of this serially packed column for sampling contaminated air, a column lifetime

TABLE 3

The effect of electron-capture detector temperature on the peak heights for halothane and nitrous oxide[a]

Temperature (°C)	200	250	300	350
Relative pk. height				
Halothane	1.25	1.14	1.06	0.49
N_2O	ND[b]	0.21	0.49	1.00

[a]Other conditions as in Table 2. [b]Not determined.

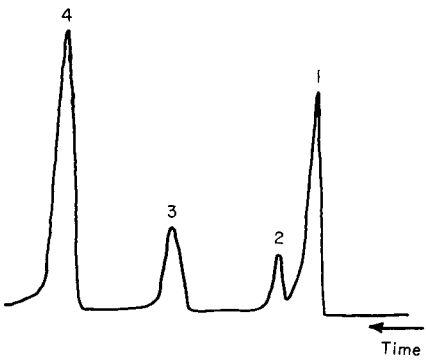

Fig. 1. Chromatogram showing the separation of (1) nitrous oxide, (2) Freon-12, (3) Freon-11, and (4) halothane in operating theatre air.

of less than six months was found; this could be extended if the temperature were reduced during periods of non-use.

The system has recently been used for comparative measurements of natural ventilation in rooms in which halothane, nitrous oxide and Freon-11 and 12 served as tracer gases [12].

REFERENCES

1 National Institute of Occupational Safety and Health (NIOSH), Health Education Report Number 80-56-743 (1980).
2 J. S. Robinson, J. M. Thompson, R. S. Barratt, R. Belcher and W. I. Stephen, Br. J. Anaesth., 48 (1976) 167.
3 L. A. Salamonsen, W. J. Cole and R. F. Salamonsen, Br. J. Anaesth., 50 (1978) 221.
4 M. J. Molera, J. A. Garciá-Dominguez and J. Fernández-Biarge, J. Chromatogr. Sci., 7 (1969) 305.
5 M. D. Cabezudo, E. F. Gorostiza, M. Herraiz, J. Fernández-Biarge, J. A. Garciá-Dominguez and M. J. Molera, J. Chromatogr. Sci., 16 (1978) 61.
6 R. A. Keller and G. H. Stewart, Anal. Chem., 36 (1964) 1186.
7 R. A. Keller and G. W. Pilgrim, J. Chromatogr. Sci., 11 (1973) 206.
8 J. M. Thompson, R. S. Barratt, P. Hutton, J. S. Robinson, R. Belcher and W. I. Stephen, Br. J. Anaesth., 51 (1979) 845.
9 W. E. Wentworth and R. Freeman, J. Chromatogr., 79 (1973) 322.
10 W. E. Wentworth, E. Chen and R. Freeman, J. Chem. Phys., 55 (1971) 2075.
11 M. B. Chenweth (Ed.), Handbook of Experimental Pharmacology, Springer-Verlag, Berlin, 172.
12 F. Abu-Jarad, R. Sithamparanadarajah, J. M. Thompson and J. M. Fremlin, Phys. Med. Biol., 27 (1982) 1393.

Analytica Chimica Acta, 178 (1985) 347—353
Elsevier Science Publishers B.V., Amsterdam — Printed in The Netherlands

Kurze Mitteilung

ELUTIONSEIGENSCHAFTEN DES ETHYLENDIAMINS ZUR IONEN-CHROMATOGRAPHIE VON METALLIONEN

DA-REN YAN

Zentral-südliche Hochschule für Bergbau und Hüttenwesen, Changsha (China)

G. SCHWEDT*

Institut für Lebensmittelchemie der Universität, Pfaffenwaldring 55, D-7000 Stuttgart 80 (Bundes Republik Deutschland)

(Eingegangen den 16 Juli 1985)

Zusammenfassung. Aus Untersuchungen über die Wirkungen von Ethylendiamin und Citronen- bzw. Oxalsäure im Eluenten auf die Trennungen von Schwermetallen und von Erdalkalien an der Säule niedriger bzw. höherer Austauschkapazität wurde festgestellt, daß der Einfluß von Ethylendiamin auf die Retentionen der Erdalkalien und des Mangans größer ist als derjenige der organischen Säuren, während andererseits der Einfluß der organischen Säuren auf die Retentionen der Schwermetalle größer ist als derjenige von Ethylendiamin. Diese Gesetzmäßigkeit läßt sich für die Trennungen der Schwermetalle und Erdalkalien nutzen.

Summary. (*Elution characteristics of ethylenediamine in ion-chromatography of metal ions*). Studies are reported on the action of ethylenediamine with citric or oxalic acid in the eluent on separations of heavy metals, magnesium and alkaline earth elements on columns of Nucleosil SA-10 and Dionex CS-2. The effect of ethylenediamine on the retention times of the alkaline earth elements and manganese is greater than that of the two organic acids, whereas these organic acids have a greater effect on the retention times of heavy metals. This regularity is useful in separations of the heavy metals and alkaline earth elements.

Ethylendiamin wurde zusammen mit Weinsäure als Eluent niedriger Leitfähigkeit zur ionen-chromatographischen (IC-) Trennung von Metallionen mit Leitfähigkeits-Detektion eingesetzt [1, 2]. Bereits von Fritz und Mitarbeitern [1, 2] wurde festgestellt, daß Ethylendiamin im Eluenten bei pH-Werten unter 5 als protoniertes Kation vorliegt. Mit der Weiterentwicklung der IC von Metallionen erwies sich Ethylendiamin auch in Kombination mit Oxalsäure [3], Citronensäure [3, 4], Sulfosalicylsäure [5] und α-Hydroxyisobuttersäure [6] für IC-Analysen von Metallionen mit postchromatographischer Derivatisierung als geeignet. Die Abhängigkeiten der Retentionen verschiedener Metallionen vom Ethylendiamin wurden jedoch bisher nicht systematisch untersucht. Es wurden deshalb die im folgenden beschriebenen experimentellen und theoretischen Untersuchungen darüber durchgeführt.

0003-2670/85/$03.30

Experimentelles

Zur Ionen-Chromatographie wurde eine HPLC-Pumpe (Knauer-64), ein Probeventil (Rheodyne 7010) mit 20 µl-Probeschleife sowie als Trennsäulen die Fertigsäulen Nucleosil SA-10, 250 × 4,0 mm (Kationenaustauscher höherer Kapazität, Macherey-Nagel) bzw. Dionex CS-2, 250 × 4,0 mm (Kationenaustauscher niedrigerer Kapazität) verwendet. Zur Detektion wurde in Kombination mit der Trennsäule Dionex CS-2 ein Leitfähigkeits-Detektor (Knauer) mit Spectra-Physics SP-4100 computing integrator eingesetzt.

Der Reaktionsdetektor für die post-chromatographische Derivatisierung [3] bestand aus einem Cecil Spectrophotometer CE-373 mit 70 µl-Durchflußzelle (1 cm Schichttiefe, Hellma), einer peristaltischen Schlauchpumpe (Gilson Minipuls-2, Einstellung auf 500 Skt) und folgenden Reaktorteilen (s. auch in [3, 7]): Luftsegmentierungsschlauch Farbcode rot (I.D. 1,14 mm), Farbreagenzschlauch gelb (I.D. 1,02 mm), Gesamtförderschlauch blau (I.D. 1,65 mm), Glasmischspirale mit 14 Windungen (I.D. 2,4 mm), Debubbler C5 (alle Einzelteile sowie Verbindungsstücke und Teflonnippel von Kleinfeld, Hannover: Hajoka-Einzelteile).

Weiterhin werden folgende Reagentien und Lösungen benötigt: Ethylendiamin (zur Synth., Merck); Weinsäure, Oxalsäure, Citronensäure (alle p.a., Merck); 4-(Pyridylazo)resorcinol (PAR; Baker Analyzed Reagent); EDTA (Titriplex III, Titrisol, Merck); Zink-Lösung (Titrisol, Merck); Triton X-100 (für Scintillationsmessungen, Merck); Ammoniak (25%ig, p.a., Merck); Salzsäure (37%ig, Suprapur, Merck).

Von den Metallen Zn, Mn, Mg, Ca, Cu, Ni, Pb, Fe(II), Sr und Ba wurden Stammlösungen mit je 1 mg ml^{-1} an Element aus den Chloriden bzw. Nitraten (p.a.) in bidest. Wasser bzw. unter Zusatz von verdünnter Säure hergestellt. (Weitere experimentelle Einzelheiten s. auch [3, 7].)

Ergebnisse und Diskussion

Die Untersuchungen über die Wirkung von Ethylendiamin im Eluenten wurden mit verschiedenen Konzentrationen an Ethylendiamin in Kombination mit Citronensäure bzw. Oxalsäure an Säulenmaterialien sowohl höherer als auch niedriger Austauschkapazität für Trennungen von Schwermetallen und von Erdalkalien durchgeführt. Abbildung 1 zeigt, daß bei der Trennung von Ni, Zn, Pb, Mn, Ca, Mg, Sr an der Säule Dionex CS-2 (niedrige Kapazität) mittels Ethylendiamin/Citronensäure sowohl bei pH 4 als auch bei pH 5 der Einfluß von Ethylendiamin auf die Retentionszeiten der Erdalkalien, des Magnesium und des Mangans deutlich größer ist als auf diejenigen der Schwermetalle (siehe auch [4]).

Weiterhin wurde Ethylendiamin in Kombination mit Oxalsäure an der Säule Nucleosil SA-10 (höhere Kapazität) für die Trennung von Cu, Ni, Zn, Fe(II), Mn, Mg und Ca eingesetzt. Die Konzentration an Ethylendiamin wurde von 2 auf 3 mmol l^{-1} heraufgesetzt, die an Oxalsäure von 1,5 auf 0,2 mmol l^{-1} verringert. Die Ergebnisse sind in Tab. 1 sowie in Abb. 2 dargestellt. Die Differenz der Retentionszeiten von Mn bis Ca nimmt nur mit der Zunahme

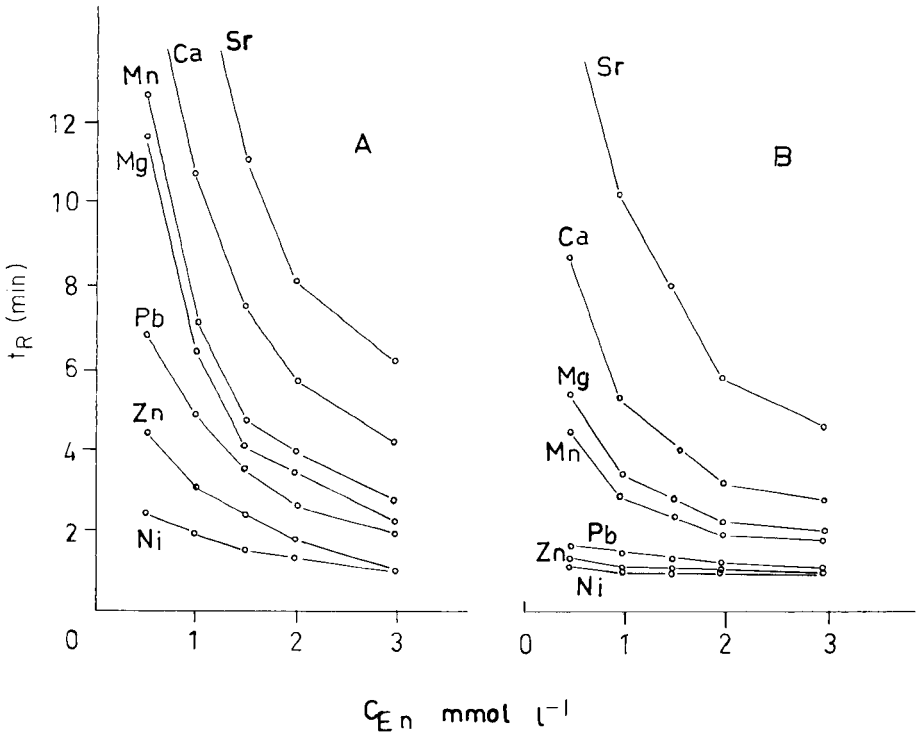

Abb. 1. Einfluß von Ethylendiamin auf die Retentionszeiten der Erdalkalien und Schwermetalle: (A) pH 4,0; (B) pH 5,0. (Säule: Dionex CS-2 250 × 4 mm. Eluenten: x mmol l^{-1} Ethylendiamin (En)/2 mmol l^{-1} Citrat. Flußrate: 1,5 ml min^{-1}. Leitfähigkeits-Detektor.

der Ethylendiamin-Konzentration ab, und nicht mit Verringerung der Oxalsäure-Konzentration zu. Demgegenüber nimmt die Differenz der Retentionszeiten von Cu bis Fe(II) nur mit der Abnahme der Oxalsäure-Konzentration zu und nicht mit Zunahme der Ethylendiamin-Konzentration ab. Das bedeutet, daß der Einfluß von Ethylendiamin auf die Retention der Erdalkalien

TABELLE 1

Abhängigkeiten der retentionszeiten der schwermetalle und erdalkalien von der konzentration an ethylendiamin und oxalsäure

Eluent			Bruttoretentionszeit t_R (min)						
Ethylendiamin (mmol l^{-1})	Oxalat	pH	Cu	Ni	Zn	Fe(II)	Mn	Mg	Ca
2,0	1,5	4,0	2,1	2,9	3,5	6,0	10,0	16,0	21,2
			$\Delta t_{R\,(Cu/Fe)} = 3,9$				$\Delta t_{R\,(Mn/Ca)} = 11,2$		
3,0	0,2	4,0	2,5	5,1	6,8	11,6	14,6	16,4	18,4
			$\Delta t_{R\,(Cu/Fe)} = 9,1$				$\Delta t_{R\,(Mn/Ca)} = 3,8$		

und des Mangans größer ist als derjenige von Oxalsäure, während der Einfluß von Oxalsäure auf die Retention der Schwermetalle größer ist als derjenige von Ethylendiamin.

Der Grund für die unterschiedliche Wirkung von Ethylendiamin bzw. die Oxalsäure und andere organische Säuren auf die Gruppen der Erdalkalien und des Mangans bzw. der Schwermetalle läßt sich mittels der Komplexbildungskonstanten näher erläutern. Ethylendiamin, Oxalat, Citrat und Tartrat protonieren je nach dem entsprechenden pK_a- und pH-Wert. Ethylendiamin protoniert in der Lösung folgenderweise:

$$En \underset{pK_{a2}}{\overset{+H^+}{\rightleftharpoons}} EnH^+ \underset{pK_{a1}}{\overset{+H^+}{\rightleftharpoons}} EnH_2^{2+}$$

Der Protonierungskoeffizient eines Liganden (L) ist:

$$\alpha_{L(H)} = ([L] + [HL] + ... + [H_xL])/L$$
$$= 1 + ([H]/K_{a1}) + ([H^2]/K_{a1}K_{a2}) + ... + ([H]^x/K_{a1}K_{a2}...K_{ax})$$
$$= 1 + 10^{(pK_{a1} - pH)} + 10^{(pK_{a1} + pK_{a2} - 2pH)}$$
$$+ 10^{(pK_{a1} + pK_{a2} + ... + pK_{ax} - xpH)} \quad (1)$$

Die nach der Formel 1 berechneten $\alpha_{L(H)}$-Werte für Ethylendiamin, Citrat, Oxalat und Tartrat im pH-Bereich 3—6 sind in Tab. 2 zusammengestellt.

Daraus ist zu entnehmen, daß Ethylendiamin im pH-Bereich 3—6 gegenüber anderen Liganden stark protoniert ist. Diese Liganden können mit Metallionen zu entweder ML_n oder MH_xL_n Komplexen reagieren. Die effektiven Komplexbildungskonstanten β' lassen sich folgenderweise berechnen:

$$\beta' = [ML_n]/[M]([L] + [HL] + ...)^n = \beta/(\alpha_{L(H)})^n$$

$$\log \beta' = \log \beta - n \log \alpha_{L(H)} \quad (2)$$

Diese Formel läßt sich auch für den Komplex MH_xL_n anwenden, da es gilt:

$$\beta' = [MH_xL_n]/[M][H]^x([L] + [HL] + ...)^n = \beta/(\alpha_{L(H)})^n$$

Tabelle 3 zeigt die log β'-Werte der Metall-Komplexe ML_n bzw. MH_xL_n von

TABELLE 2

pH-Abhängigkeit des protonierungskoeffizienten ($\alpha_{L(H)}$) für verschiedene liganden des ionen-chromatographischen elutionsmittels

Ligand	pK_{a1}	pK_{a2}	pK_{a3}	log $\alpha_{L(H)}$			
				pH 3	pH 4	pH 5	pH 6
Ethylendiamin	10,3	7,3	—	11,4	9,4	7,4	5,4
Citronensäure	6,1	4,4	3,0	4,8	2,7	1,2	0,4
Oxalsäure	4,0	1,1	—	1,1	0,3	0	0
Weinsäure	4,1	2,9	—	1,3	0,3	0,1	0

TABELLE 3

Effektive komplexbildungskonstanten β' von Zn, Mn, Mg und Ca mit den liganden aus Tabelle 2[a]

Metall	Ligand	log β	log β'			
			pH 3	pH 4	pH 5	pH 6
Zn	Citrat	ZnL 11,4—ZnHL 20,8—ZnH_2L 25,0	15,4	19,6	22,6	24,2
	Oxalat	ZnL 3,88—ZnL_2 6,4—ZnHL 5,5—ZnH_2L_2 10,72	8,5	10,1	10,7	10,7
	Tartrat	ZnL 2,68—ZnHL 5,5	3,4	4,9	5,3	5,3
	Ethylendiamin	ZnL 5,71—ZnL_2 10,37—ZnL_3 12,9	<0	<0	<0	<0
Mn	Citrat	MnL 19,7—MnH_2L_2 24,2—	14,6	18,8	21,8	23,4
	Oxalat	MnL 2,7—MnL_2 4,1	1,9	3,5	4,1	4,1
	Ethylendiamin	MnL 2,73—MnL_2 4,79—MnL_3 5,67	<0	<0	<0	<0
Mg	Citrat	MgHL 19,29—MgH_2L 23,7—	14,1	18,3	21,3	22,9
	Oxalat	MgL 2,4	0,2	1,8	2,4	2,4
	Tartrat	MgL 1,39—MgHL 5,0	2,4	4,4	4,8	5,0
	Ethylendiamin	MgL 0,37	<0	<0	<0	<0
Ca	Citrat	CaHL 20,68—CaH_2L 25,1—CaH_4L 27,6	18,0	22,2	25,2	26,8
	Oxalat	CaL 3,0	0,8	2,4	3,0	3,0
	Tartrat	CaL 1,8—CaHL 5,2	2,6	4,6	5,0	5,2
	Ethylendiamin	—	—	—	—	—

[a] log β-Werte aus [8]; log β' nach der Formel 2 berechnet.

Ethylendiamin, Citrat, Oxalat und Tartrat, an Beispielen von Zn, Mn, Mg und Ca.

Alle Metall-Komplexe von Ethylendiamin wiesen im pH-Bereich 3—6 negative Werte auf. Das bedeutet, daß unter diesen Bedingungen Ethylendiamin nicht mehr als Ligand sondern als Kation eine Substitutionswirkung hat. Demgegenüber sind Oxalat, Citrat und Tartrat noch als Ligand wirksam: z.B. ergeben sich bei pH 4 die log β'-Werte der Oxalat-Komplexe von Zn 10,1; von Mn 3,5; von Mg 1,8; von Ca 2,4. Die Wirkung der Oxalsäure auf Zink ist also wesentlich stärker als auf Ca, Mg und Mn. Dies ist der Grund dafür, weshalb die Retentionen der Erdalkalien und des Mangans hauptsächlich von Ethylendiamin und die der Schwermetalle vor allem von Oxalat o.ä. beeinflußt werden.

Die Austauschreaktion lautet:

$$\text{Res. } M^{2+} + EnH_2^{2+} \rightleftharpoons \text{Res. } EnH_2^{2+} + M^{2+};\ M^{2+} + L^{2-} \rightleftharpoons ML$$

Anhand dieser unterschiedlichen Abhängigkeiten der Retentionen der Schwermetalle bzw. der Erdalkalien und des Mangans von Ethylendiamin und Oxalsäure o.ä. lassen sich für vorgegebene Trennungen die Konzentrationen an Ethylendiamin und Oxalsäure optimieren: z.B. ergibt der Eluent (2 mmol l^{-1} En/1,5 mmol l^{-1} Oxalat pH 4) in Abb. 2(a) eine optimale Trennung von

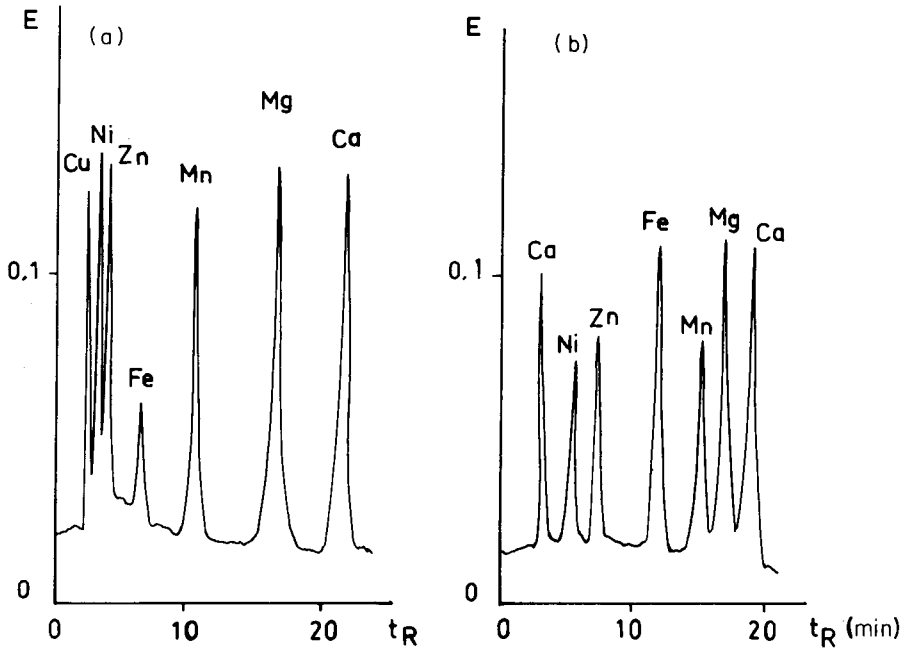

Abb. 2. Einflüsse von Ethylendiamin und Oxalsäure auf die Retentionen der Ca, Mg, Mn, Fe(II), Zn, Ni und Cu. (Säule: Nucleosil SA-10, 250 × 4 mm. Flußrate: 2 ml min^{-1}. Detektion: post-chromatographische Derivatisierung mit PAR/Zn/EDTA.) Eluent: (a) 1,5 mmol l^{-1} Oxalat/2 mmol l^{-1} Ethylendiamin/pH 4,0; (b) 0,2 mmol l^{-1} Oxalat/3 mmol l^{-1} Ethylendiamin/pH 4,0.

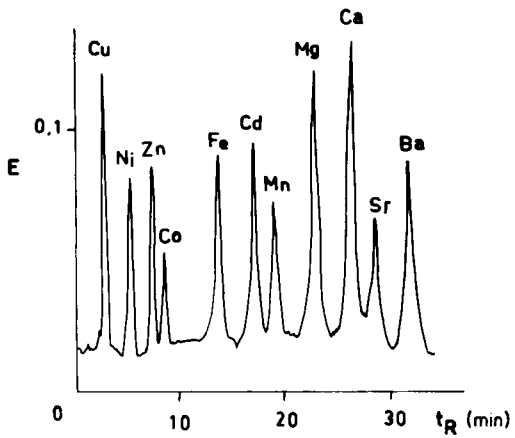

Abb. 3. Multi-Element-Trennung mittels 0,5 mmol l^{-1} Oxalat/2 mmol l^{-1} Ethylendiamin/pH 3,5 Eluenten; sonst wie Abb. 2. (Probe: 20 µl.) Metalle-Konzentrationen (mg l^{-1}): Cu 4; Ni 3; Zn 3; Co 5; Fe(II) 10; Cd 10; Mn 4; Mg 4; Ca 8; Sr 10; Ba 30.

Mn, Mg, Ca und anderen Erdalkalien während der Eluent (0,2 mmol l^{-1} Oxalat/3 mmol l^{-1} En pH 4) in Abb. 2(b) für die Trennung von Schwermetallen besser geeignet ist. Wenn also der Eluent nach den Bedingungen in Abb. 3 eingesetzt wird (0,5 mmol l^{-1} Oxalat/2 mmol l^{-1} En pH 3,5), so ist eine Multielement-Trennung von Cu, Ni, Zn, Co, Fe(II), Cd, Mn, Mg, Ca, Sr und Ba möglich.

LITERATUR

1 J. S. Fritz, D. T. Gjerde und R. M. Becker, Anal. Chem., 52 (1980) 1519.
2 G. J. Sevenich und J. S. Fritz, Anal. Chem., 55 (1983) 12.
3 D. Yan und G. Schwedt, Fresenius Z. Anal. Chem., 320 (1985) 325.
4 D. Yan und G. Schwedt, Fresenius Z. Anal. Chem., 320 (1985) 121.
5 D. Yan und G. Schwedt, Fresenius Z. Anal. Chem., 320 (1985) 252.
6 J. S. Fritz, D. T. Gjerde und C. Pohlandt, in Ion Chromatography, A. Hüthig, Heidelberg, 1982.
7 G. Schwedt, in Chemische Reaktionsdetektoren für die schnelle Flüssigkeits-Chromatographie. A. Hüthig: Heidelberg, 1980, S. 27—54.
8 I. M. Kolthoff und P. J. Elving (Eds.), Treatise on Analytical Chemistry. Part 1, 2nd edn., Vol. 2, pp. 562, Wiley-Interscience, New York, 1979.

Analytica Chimica Acta, 178 (1985) 355—359
Elsevier Science Publishers B.V., Amsterdam — Printed in The Netherlands

Short Communication

REJECTION OF A DEVIANT POINT FROM A STRAIGHT-LINE REGRESSION

LOWELL M. SCHWARTZ
Department of Chemistry, University of Massachusetts, Boston, MA 02125 (U.S.A.)
(Received 7th August 1985)

Summary. A statistical procedure is described to help decide whether or not to reject a data point which deviates markedly from a straight-line regression. A Beer's law plot is used to illustrate the procedure.

It is common to encounter a plot of experimental data in the form of a straight line where a point appears to deviate from the line substantially more than the other points. It is necessary to decide if this large deviation is due to the vagaries of statistical scatter or to a perturbation in experimental conditions which introduce a systematic error, i.e., an outlier. Whereas a real outlier can rationally be discarded from the straight-line evaluation, a point should not be discarded simply because it appears to deviate more than other points. It is useful to have a reliable statistical test to decide on such outliers. An extensive body of literature in mathematical statistics exists on outlier problems [1]. The purpose here is to select appropriate techniques from that literature to apply to regression problems of interest to analytical chemists.

This communication is concerned only with those problems for which ordinary least-squares regression is appropriate for finding the straight-line parameters. This means that the plotted points (x, y) are such that the x values are either experimental settings or have statistical uncertainties (standard deviations) much less than those of the y values. A further limitation will be that the statistical scatter of each y datum can reasonably be characterized by a normal (Gaussian) distribution function. However, it is not assumed that the variance of the y data is uniform provided that the variance changes along the line in a regular rather than an unpredictable way. Most chemical regression problems conform to this set of conditions.

Theory

Behnken and Draper [2] showed how to estimate the variance of residuals along a regression line and Lund [3] presented a table which uses the residual variances to test if a deviant point is an outlier. The derivation by Behnken and Draper [2] treats the general case of a regression on several

0003-2670/85/$03.30

independent variables whereas here only a single independent variable is considered. Behnken and Draper [2] limited their treatment to situations in which the variances of the dependent-variable measurements are uniform, but this limitation is relaxed here.

In the situation considered, an independent variable x and a dependent variable y are linearly related but the y vs. x data points deviate from an exact straight line because of normally distributed errors of measurement in the y direction. If the standard deviations of the response measurements are known to vary, their variation must be known. For example, if the relative standard deviation of the response is constant, the standard deviation is proportional to the response level. The proportionality constant in such a case may not be known. Nevertheless, it is essential to provide a variance function from which the variance of a y datum can be calculated. This variance function is in the general form $\text{var}(y) = V\phi(y,x)$, where $\phi(y,x)$ is a completely specified function of the variables y and/or x, and V is a constant multiplier; the value of V may or may not be known.

Here, the method of ordinary weighted least-squares is applied to a set of n data points y_i vs. x_i to calculate a straight line in the form $\hat{y} = b(x - \bar{x}) + \bar{y}$, where $b = S_{xy}/S_{xx}$ is the least-squares slope, $\bar{x} = S_w^{-1} \Sigma_i w_i x_i$ is the weighted mean of the x data, and $\bar{y}$ is the weighted mean of the y data; $w_i^{-1} = \text{var}(y_i)$ defines the weighting factors, $S_w = \Sigma_i w_i$, $S_{xy} = \Sigma_i w_i y_i (x_i - \bar{x})$ and $S_{xx} = \Sigma_i w_i (x_i - \bar{x})^2$.

The extent of the deviation of individual data points from the least-squares line is the problem considered here. The residual e_j of point j is

$$e_j = y_j - \hat{y}_j = y_j - b(x_j - \bar{x}) - \bar{y} \tag{1}$$

Substituting for the slope b yields

$$e_j = y_j - (x_j - \bar{x}) S_{xx}^{-1} \Sigma_i w_i y_i (x_i - \bar{x}) - \bar{y}$$

The summation Σ_i refers to all data points including the particular point j. If that point is removed from the second term, then

$$e_j = [1 - w_j (x_j - \bar{x})^2 S_{xx}^{-1}] y_j - (x_j - \bar{x}) S_{xx}^{-1} \Sigma_{i \neq j} w_i y_i (x_i - \bar{x}) - \bar{y}$$

Thus e_j is a linear combination of all the y_i and the variance of e_j is

$$\text{var}(e_j) = [1 - w_j f_j]^2 \text{var}(y_j) + f_j \Sigma_{i \neq j} w_i^2 f_i \text{var}(y_i) + S_w^{-1}$$

where $f_j \equiv (x_j - \bar{x})^2 S_{xx}^{-1}$ is defined to help reduce the clutter of the symbols. This expression is simplified by first expanding the squared bracketed quantity and recognizing that $w_i \text{var}(y_i) \equiv 1$, so that

$$\text{var}(e_j) = \text{var}(y_j) - 2f_j + w_j f_j^2 + f_j \Sigma_{i \neq j} w_i f_i + S_w^{-1}$$

The third term on the right is, indeed, the single term omitted from the summation in the fourth term. Thus combining the third and fourth terms yields

$$\text{var}(e_j) = \text{var}(y_j) - 2f_j + f_j \Sigma_i w_i f_i + S_w^{-1}$$

The definitions of S_{xx} and f_i lead to $\Sigma_i w_i f_i = S_{xx}^{-1} \Sigma_i w_i (x_i - \bar{x})^2 = 1$ so that $\mathrm{var}(e_j)$ simplifies to

$$\mathrm{var}(e_j) = \mathrm{var}(y_j) - (x_j - \bar{x})^2 S_{xx}^{-1} + S_w^{-1} \tag{2}$$

The corresponding result for cases where the y_i variances are uniform is Eqn. 10 in the paper by Behnken and Draper [2].

Method

The procedure for using the published table (see Table 32 [1] and table in [3]) for testing a suspicious point is to calculate the least-squares line from all n data points, calculate the residual at each point from Eqn. 1, calculate the variance of each residual from Eqn. 2, and finally calculate the standardized residual E_j defined by

$$E_j \equiv |e_j / [\mathrm{var}(e_j)]^{1/2}| \tag{3}$$

The procedure continues by making the null hypothesis that none of the data is an outlier and testing this hypothesis by comparing the largest E_j to the appropriate entry in the table of critical values E_{crit} as shown in Table 1. If E_j exceeds the tabulated 5% E_{crit} value, the probability is $<5\%$ that the null hypothesis is correct. The null hypothesis is thus rejected at the 5% confidence level and one can be "reasonably" confident in concluding that the data point with the largest E_j is an outlier. Alternatively, one can use a more stringent test of the null hypothesis by comparing the largest E_j with the tabulated 1% E_{crit} value. If E_j exceeds this 1% E_{crit} value, the probability is $<1\%$ that the null hypothesis is correct. One can then be "very" confident that the point is an outlier.

Example

Table 2 shows a set of $n = 8$ artificial data from a Beer's law spectrophotometric experiment. The dependent variable measurements, y_i, are fixed-wavelength absorbances of solutions containing known concentrations x_i. The noise component of the absorbance measurements increases with absorbance level in such a way that the relative standard deviation (RSD) is approximately constant. In terms of the general function for $\mathrm{var}(y)$, the function $\phi(y)$ is y^2 and the multiplier V is the square of the RSD. In this case, a value for the unknown V is calculated from the scatter of the data points from the regression line by the procedure described by Brownlee [4]. The unknown V is provisionally set to unity so that the weighting factors w are taken as the reciprocal of $\phi(y)$ or y^{-2}. Because these weighting factors should not reflect the random fluctuations in the y_i data, w_i is set equal to $\hat{y}_i^{-2}$, which are the values of y^{-2} predicted at x_i by the regression. An iterative procedure starts by taking $w_i = y_i^{-2}$, solving for the regression line, refining w_i using $\hat{y}_i^{-2}$, and recalculating the regression. This iteration generally converges to an invariant regression line within two or three cycles. Column 3 of Table 2 shows the predicted ordinates after convergence,

TABLE 1

Critical standardized residuals for testing an outlier from a two-parameter straight-line regression on 6—100 data points [3]

No. of points	E_{crit} (5%)[a]	E_{crit} (1%)[b]	No. of points	E_{crit} (5%)[a]	E_{crit} (1%)[b]	No. of points	E_{crit} (5%)[a]	E_{crit} (1%)[b]
6	1.93	1.98	16	2.66	2.92	45	3.12	3.47
7	2.08	2.17	18	2.72	3.00	50	3.16	3.51
8	2.20	2.32	20	2.77	3.06	60	3.23	3.59
9	2.29	2.44	25	2.88	3.19	70	3.29	3.65
10	2.37	2.55	30	2.96	3.29	80	3.33	3.70
12	2.49	2.70	35	3.02	3.36	90	3.37	3.74
14	2.58	2.82	40	3.08	3.42	100	3.41	3.78

[a]At 5% probability. [b]At 1% probability.

TABLE 2

Illustrative example

Conc. (mM) x_i	Absorbance y_i	Predicted $\hat{y}_i$	Weight w_i	Residual e_j	Residual variance var (e_j)	Standardized residual E_j
0.8	0.316	0.3168	9.97	—0.0008	0.24×10^{-4}	0.15
1.2	0.485	0.4798	4.34	0.0052	0.55×10^{-4}	0.70
1.6	0.642	0.6429	2.42	—0.0009	0.91×10^{-4}	0.09
2.0	0.797	0.8059	1.54	—0.0089	1.32×10^{-4}	0.78
2.4	0.961	0.9690	1.07	—0.0080	1.78×10^{-4}	0.60
2.8	1.124	1.1321	0.78	—0.0081	2.28×10^{-4}	0.53
3.2	1.331	1.2951	0.60	0.0359	2.84×10^{-4}	2.13
3.6	1.446	1.4582	0.47	—0.0122	3.44×10^{-4}	0.65

column 4 shows the corresponding weighting factors, and column 5 shows the residuals e_j from Eqn. 1. The unknown variance multiplier V is calculated as $\Sigma_i e_i^2/df$, where the number of degrees of freedom $df = n - 2$ for this two-parameter regression. For the data in Table 2, $V = 2.01 \times 10^{-4}$ is calculated. Other intermediate results are $\bar{x} = 1.344, S_{xx} = 11.15$, and $S_w = 21.18$. Column 6 shows var(e_j) values obtained from Eqn. 2 in which the first term on the right-hand side is the variance of y_j as given by $V\hat{y}_j^2$. Column 7 shows the standardized residuals E_j from Eqn. 3.

The residual in column 5 of Table 2 at the 3.2 mM point is obviously much larger in magnitude than any other residual. Before this point can be omitted from the regression, the null hypothesis must be made that none of the eight data points is an outlier, and this hypothesis must be tested at a "reasonable" confidence level by comparing the largest standardized residual 2.13, observed at the 3.2 mM point, with the 5% entry $E_{crit} = 2.20$ in Table 1.

Because the largest standardized residual is less than this E_{crit}, the null hypothesis is accepted and the point is retained. Based on the eight-point regression line, the slope is 0.4076 with standard error estimate 0 0042 and the intercept is −0.0094 with standard error estimate 0.0065.

The above procedure for examining deviant points was done on a microcomputer with a program written in BASIC. This program (on 5.25-in. floppy diskette in CP/M or MS-DOS formats) is available from the author at nominal cost.

REFERENCES

1 V. Barnett and T. Lewis, Outliers in Statistical Data, Wiley, New York, 1978.
2 D. W. Behnken and N. R. Draper, Technometrics, 14 (1972) 101.
3 R. E. Lund, Technometrics, 17 (1975) 473.
4 K. A. Brownlee, Statistical Theory and Methodology in Science and Engineering, 1st Edn., Wiley, New York, 1960, Sect. 11.12 and 11.13.

Analytica Chimica Acta, 178 (1985) 361
Elsevier Science Publishers B.V., Amsterdam — Printed in The Netherlands

Errata

Niels Pind, Application of a Fundamental Parameter Technique for Solving Peak-Overlap Problems in Quantitative Energy-Dispersive X-Ray Fluorescence Spectrometry.

Anal. Chim. Acta, 172 (1985) 381—386.

Equation 2b (p. 382) should be written:

$$a_{r,s} = [GK_s(1 + H_s) \sin \psi_1] / I_r[\mu_r^0 + \mu_r^{r'} \sin \psi_1 / \sin \psi_2]$$

T. Hori, M. Moriguchi, M. Sasaki, S. Kitagawa and M. Munakata, Preconcentration of some Phosphorus-containing Anions by Adsorption on Hydrated Iron(III) Oxide.

Anal. Chim. Acta, 173 (1985) 229—303.

The penultimate sentence on p. 300 should read:

After pH measurement at equilibrium, the precipitate was separated by filtration on a Nuclepore membrane filter (0.4-μm pore size) and then the phosphorus compounds adsorbed were determined spectrophotometrically by a phosphomolybdate-extraction method [1].

The second sentence of paragraph 3 on p. 301 should read:

Although these buffers are so-called "Good's Buffers" [5] and are expected to be mostly inert to iron(III) ions, a slight decrease in the percent adsorption was observed at concentrations higher than 0.2 M.

0003-2670/85/$03.30

ANALYTICA CHIMICA ACTA, VOL. 178 (1985)

AUTHOR INDEX

ACA announcements

ANNOUNCEMENTS OF MEETINGS

1986 JOINT SYMPOSIUM ON DRY SULFUR DIOXIDE AND SIMULTANEOUS SO_2/NO_x CONTROL TECHNOLOGIES, KANSAS CITY, MO, U.S.A., JUNE 2–6, 1986

The U.S. Environmental Protection Air and Energy Engineering Research Laboratory, Research Triangle Park, NC, and the Electric Power Research Institute, Palo Alto, CA, are co-sponsoring the "1986 Joint Symposium on Dry SO_2 and Simultaneous SO_2/NO_x Control Technologies". The symposium will be held June 2–6, 1986, at the Hyatt Regency, Kansas City, MO, U.S.A. The five-day programme is intended to provide for the exchange of knowledge on research, development and applications of this technology, and to stimulate new ideas on emissions control processes based on the injection of dry calcium or sodium sorbents. This technology may offer a simple alternative to wet scrubbers and spray dryers in meeting SO_2 regulations for coal-fired power plants. In some instances, this technology may also provide for the simultaneous control of SO_2 and NO_x. Papers are being solicited on the following topics: process research; sorbent selection, preparation, and performance; mixing and dispersion of sorbent with combustion gases; applications engineering; economics; post-furnace SO_2 removal; slagging combustors; system impacts; and commercial-scale field experience.

For general symposium information, please contact: Jack H. Greene, Symposium Coordinator, MD-60, U.S. EPA, AEERL, Research Triangle Park, NC 27711, U.S.A. Tel.: (919) 541 2903, or J. Pekar, tel.: (919) 541 3995.

1st SYMPOSIUM ON PATTERN RECOGNITION METHODS IN ANALYTICAL SPECTROSCOPY, SALT LAKE CITY, UT, U.S.A., JUNE 16–18, 1986

The goal of the meeting is to provide a direct interface between the fields of analytical spectroscopy and chemometrics.

The following topics fall within the scope of the programme: Spectral Enhancement and Deconvolution, Data Reduction and Compression, Library Storage and Retrieval, Cluster and Classification Analysis, Factor and Discriminant Analysis, Multicomponent ("mixture") Analysis, Automated Spectral Interpretation, Multisource Data Base Integration, Modeling and Prediction. Keynote lectures will be presented by: Thomas Clerc, Peter R. Griffiths, Stephen R. Heller, Peter C. Jurs, Hal. J.H. MacFie, Edmund R. Malinowski, Harald Martens, Abraham Savitzky, Charles L. Wilkins, Willem Windig, Carla Wong, and Hugh B. Woodruff.

The three-day schedule is patterned after the well-known Gordon Research Conference format with morning and evening lecture sessions and afternoons available for social interactions or recreational activities. Each morning or evening session features only two keynote speakers with ample time for discussions. The official conference language is English.

All contributed papers will be presented in poster form. Posters will remain displayed during the entire conference.

Exhibition space will be available for companies interested in demonstrating relevant software or hardware products.

The symposium will be held at the Snowbird Resort at the foot of Hidden Peak Mountain (11 000 ft.) in beautiful Little Cottonwood Canyon, only 31 miles from Salt Lake City International Airport. Transportation to and from the airport will be arranged. A broad choice of individual afternoon activities include hiking, sightseeing, cable tram rides, swimming, exercising, tennis and volleyball.

Further information may be obtained from: Merlinda Van, Conference Secretariat, Biomaterials Profiling Center, University of Utah, Salt Lake City, UT, U.S.A. Tel.: (801) 581-8431, telex: GRAPHNET 3789459 UNIV UTAH SLC.

22nd INTERNATIONAL SYMPOSIUM ON ADVANCES IN CHROMATOGRAPHY, HOUSTON, TX, U.S.A., SEPTEMBER 15–18, 1986

The 22nd International Symposium on Advances in Chromatography will be held on September 15–18, 1986, at the Hotel Inter-Continental in Houston, TX, U.S.A. The meeting will cover all fields of chromatography. Authors desiring to present papers must submit 200-word abstracts by March 15, 1986; complete manuscripts of accepted papers will be due on September 15, 1986 at the meeting in Houston. There will also be a commercial exhibition of the latest instrumentation and books. The Gulf Coast Analytical Conference will be held at the same location later in the week.

All correspondence pertaining to the symposium and exhibition space should be directed to: Professor A. Zlatkis, Chemistry Department, University of Houston, Houston, TX 77004, U.S.A. Tel. (713)-749-2623.

FACSS '86, FEDERATION OF ANALYTICAL CHEMISTRY AND SPECTROSCOPY SOCIETIES, ST. LOUIS, MO, U.S.A., SEPTEMBER 29–OCTOBER 3, 1986

FACSS '86 will be held in historic St. Louis, MO, U.S.A. The technical programme and exhibition of scientific instrumentation, services, and publications will be held at the Cervantes Convention Center in downtown St. Louis (20 minutes from Lambert Airport). Workshops, meetings, and the employment bureau will be held at the adjacent Sheraton Hotel.

Further information may be obtained from: General Chairman: Dr. Marshall Fishman, U.S. Department of Agriculture, 600 E. Mermaid Lane, Wyndmoor, PA 19118, U.S.A. Tel.: (215) 233 6450. Programme Chairman: Dr. Alex Scheeline, University of Illinois, 1209 W. California Avenue, Urbana, IL 61801, U.S.A. Tel.: (217) 333 2999.

THE SILVER JUBILEE EASTERN ANALYTICAL SYMPOSIUM, NEW YORK, NY, U.S.A., OCTOBER 6–10, 1986

A limited number of oral and poster presentations on new developments in analytical chemistry will be accepted for the Silver Jubilee Eastern Analytical Symposium. These contributed presentations will be grouped into several sessions to complement the invited technical sessions at this, the celebration of the twenty-fifth annual EAS. Prospective authors should submit a 50–100 word abstract on the proposed presentation before the deadline (*February 15, 1986*), indicating preference for oral or poster format, to Concetta M. Paralusz, EAS Program Chairman, Permacel/Avery International, P.O. Box 671, New Brunswick, NJ 08903, U.S.A., tel.: (201) 524-5633. Care should be exercised in considering the title and authors of the proposed presentation; if the presentation is accepted, both title and authors will be considered final and not subject to change. Authors of accepted presentations will receive forms for submission of a 200–300-word abstract which will appear in the final programme. The Silver Jubilee EAS will be held at the New York Hilton Hotel.

For further information about the symposium, contact: Dr. S. David Klein, EAS Publicity, 642 Cranbury Cross Road, North Brunswick, NJ 08902, U.S.A. Tel.: (201)846-1582.

4th INTERNATIONAL CONFERENCE ON QUANTITATIVE SURFACE ANALYSIS, TECHNIQUES AND APPLICATIONS, TEDDINGTON, U.K., NOVEMBER 18–20, 1986

The above-mentioned conference will be held at the National Physical Laboratory in Teddington, Middlesex, U.K.

The conference will consider the quantitative use of Auger electron spectroscopy (AES), X-ray photoelectron spectroscopy (XPS), secondary ion mass spectrometry (SIMS) and related surface analytical techniques, together with ion sputtering and depth profiling.

The Versailles Project on Advanced Materials and Standards (VAMAS) is a scheme to stimulate the introduction of advanced materials into high technology products and engineering structures with the overall aim of encouraging trade therein. This will be achieved through international agreement on

codes of practice and performance standards and through multilateral research aimed at furnishing the enabling scientific and metrological base necessary for agreement on standards.

Abstracts of papers on the theme of the conference are invited. Some contributed papers will be presented orally and others in poster sessions. Papers, subject to refereeing, will be published in special issues of the journal *Surface and Interface Analysis* following the conference. Abstracts must be submitted by 1 September 1986.

For further details contact: Conference Secretary, Dr. G.C. Smith, Division of Materials Applications, National Physical Laboratory, Teddington, Middlesex, TW11 0LW, U.K., Tel: (01) 977 3222, telex: 262344.

INTERNATIONAL SYMPOSIUM ON ELECTROANALYSIS IN BIOMEDICAL, ENVIRONMENTAL AND INDUSTRIAL SCIENCES, CARDIFF, U.K., APRIL 6–9, 1987

The above symposium organised by the Electroanalytical Group and Education and Training Group of the Analytical Division of the Royal Society of Chemistry (London) will be held at the University of Wales Institute of Science and Technology (UWIST), Cardiff, Wales, U.K. from Monday 6 April to Thursday 9 April 1987. It will be the sixth in the series of biennial conferences of the Electroanalytical Group.

The programme will be on aspects of electroanalysis relating to biomedical, environmental and industrial sciences. Emphasis will be laid on methodology and applications of the various electroanalytical methods, especially reagarding the use of amperometric and potentiometric membrane and membrane-clad electrodes, gas sensors, polarography, etc. Development, operation and mechanisms will be included where these relate to electroanalysis in the theme areas, including biosensors. Principles and methods of teaching electroanalysis to practitioners in the theme areas will also be included.

The symposium language will be English. An exhibition is being planned.

For further details, please contact: Short Courses Section, UWIST, P.O. Box 68, Cardiff CF1 3XA, Wales, U.K. Tel.: (0222) 42588, ext. 2213.

9TH AUSTRALIAN SYMPOSIUM ON ANALYTICAL CHEMISTRY, SYDNEY, AUSTRALIA, APRIL 28–MAY 1, 1987

The Analytical Chemistry Division of the Royal Australian Chemical Institute will host the 9th national conference at the Centrepoint Conference Centre in Sydney, Australia. This exciting city venue will enable presentation of plenary lectures, contributed papers, specialist workshops, posters and a large scientific instrument exhibition under ideal conditions.

The symposium will highlight new developments in analytical research over a wide range of topics, provide one-day specialist meetings in carbohydrate chemistry and computers in laboratory automation, and encourage exchange of information among participants. Speakers from within and outside Australia will be invited to renew areas of current world interest and present research findings.

A full social programme will take advantage of the city location, and the outstanding tourist attractions available in the Sydney area.

For further information contact the Secretary 9AC, Mr. John Eames, P.O. Box 137, North Ryde, N.S.W. 2113, Australia. Tel.: (02) 887-8688.

2nd INTERNATIONAL SYMPOSIUM ON QUANTITATIVE LUMINESCENCE SPECTROMETRY IN BIOMEDICAL SCIENCES, MAY 11–14, 1987, GHENT, BELGIUM

An international symposium on quantitative luminescence spectrometry in biomedical sciences, sponsored by the Faculty of Pharmaceutical Sciences of the State University of Ghent, the National Foundation of Scientific Research (N.F.W.O. - F.N.R.S.), and the Ministry of Education, will be held in Ghent, Belgium, from Monday, 11th May to Thursday, 14th May 1987, at the Farmaceutisch Instituut. The scope of the symposium will be similar to that of the first meeting held in Ghent, 1984, and will cover current research on all aspects of luminescence analysis.

The scientific programme will consist of plenary and invited lectures, submitted research papers and posters.

Five plenary lectures will be presented by outstanding specialists in the field of quantitative luminescence spectrometry: U.A.Th. Brinkman (Free University of Amsterdam), luminescence detection in high-performance liquid chromatography; J.C. Hummelen (State University of Groningen), thermochemiluminescence techniques; L.J. Kricka (Queen Elizabeth Medical Centre, Birmingham), chemiluminescence immunoassays; S.G. Schulman (University of Florida), fluorescence techniques; O.S. Wolfbeis (Karl-Franzens University, Graz), fiber optic sensors.

Contributed papers (20 min lectures or poster communications) will cover the following topics: drug and bioanalysis via fluorescence and phosphorescence; fluorescence and chemiluminescence immunoassays; detection techniques in chromatography; solid surface luminescence methods; thermochemiluminescence techniques; chemical derivatization methods; use of fluorescence labels; luminescence applications and drug metabolism, clinical chemistry, biochemistry, pharmacokinetics, toxicology, ecology, protein tagging.

The conference language will be English. There will be an exhibition of commercial instruments for luminescence analysis.

As with the earlier symposium, the Proceedings will be published in a special issue of *Analytica Chimica Acta.* Information for authors will be provided in later announcements.

Authors who wish to present papers (oral or poster) should submit abstracts before December 31, 1986.

The symposium registration fee will be about 100 U.S.$ or 5500 BF. This fee includes a copy of the final programme, an abstracts volume; a copy of the Proceedings; part of the social events and refreshments during the breaks. Wagons-Lits Tours, Cantersteen 41, B-1000 Brussels has been appointed the Official Travel Agent.

All correspondence should be sent to: Dr. W. Baeyens, Symposium Chairman, Laboratory of Pharmaceutical Chemistry and Drug Analysis, State University of Ghent, Harelbekestraat 72, B-9000 Ghent, Belgium.

SCIENTIFIC SOFTWARE

SOFTWARE AVAILABLE FROM AUTHORS

A new section of this journal has started, which will give authors of computer programs the opportunity to announce software that they are willing to share with their colleagues. The aims of the section have been outlined in an Editorial (*Anal. Chim. Acta,* 173 (1985) 1). The programs offered will be listed in this section of the journal, as information becomes available.

Further details and forms for entry are available from Professor J.T. Clerc, Universität Bern, Pharmazeutisches Institut, Baltzerstrasse 5, CH-3102 Bern, Switzerland.

CALENDAR OF FORTHCOMING MEETINGS

March 10–14, 1986 Atlantic City, NJ, U.S.A.	**37th Pittsburgh Conference and Exposition on Analytical Chemistry and Applied Spectroscopy** Contact: Mrs. Alma Johnson, Program Secretary, 12 Federal Drive, Suite 322, Pittsburgh, PA 15235, U.S.A.
April 15–17, 1986 Aberdeen, U.K.	**Microbial Problems in the Offshore Oil Industry** Contact: Caroline Little, Conference Officer, The Institute of Petroleum, 61 New Cavendish Street, London W1M 8AR, U.K. Tel.: (01) 636 1004, telex: 264380.
April 21–23, 1986 Neuherberg, F.R.G.	**4th International Workshop on Trace Element Analytical Chemistry in Medicine and Biology** Contact: Dr. P. Schramel, Gesellschaft für Strahlen- und Umweltforschung mbH, Institut für Angewandte Physik, Physikalisch- Technische Abteilung, Ingolstädter Landstrasse 1, D-8042 Neuherberg, F.R.G. (Further details published in Vol. 175.)

April 22–24, 1986 Noordwijkerhout, The Netherlands	**Anatech '86 – An International Symposium on Applications of Analytical Chemical Techniques to Industrial Process Control** Contact: Prof. W.E. van der Linden, Laboratory for Chemical Analysis, Department of Chemical Technology, Twente University of Technology, P.O. Box 217, 7500 AE Enschede, The Netherlands. (Further details published in Vol. 169.)
April 22–26, 1986 Kuala Lumpur	**Asian Health and Lab-Tec Asia Exhibits** Contact: Tony Cascardi, AP-TEX International, 350 5th Ave., Room 4920, New York, NY 10118, U.S.A.
April 24–25, 1986 Neuherberg, F.R.G.	**2nd International Symposium on Biological Reference Materials** Contact: Dr. M. Stoeppler, Institut für Angewandte Physikalische Chemie, Kernforschungsanlage GmbH, Postfach 1913, D-5170 Jülich, F.R.G. (Further details published in Vol. 175.)
May 18–23, 1986 San Francisco, CA, U.S.A.	**HPLC '86. New Frontiers in HPLC. 10th International Symposium on Column Liquid Chromatography** Contact: Ms. Shirley Schlessinger, 400 E. Randolph Drive, Chicago, IL 60601, U.S.A. (Further details published in Vol. 169.)
May 26–29, 1986 Lerici, Italy	**III CAC – Meeting of the Chemometrics Society** Contact: Prof. M. Forina, Istituto di Analisi e Tecnologie Farmaceutiche ed Alimentari, Via Brigata Salerno (ponte), I-16147 Genova, Italy. Tel.: (010) 3993656. (Further details published in Vol. 172.)
May 27–30, 1986 Brussels, Belgium	**2nd International Symposium on Drug Analysis** Contact: Mrs. C. van Kerchove, c/o Société Belge des Sciences Pharmaceutiques, Rue Stévinstraat 137, B-1040 Brussels, Belgium. Tel: (02) 230 26 85, ext. 33. (Further details published in Vol. 175.)
June 2–6, 1986 Raleigh, NC, U.S.A.	**1986 Joint Symposium on Dry Sulfur Dioxide and Simultaneous SO_2/NO_x Control Technologies** Contact: Jack H. Greene, Symposium Coordinator, MD-60, U.S. EPA, AEERL, Research Triangle Park, NC 27711, U.S.A. Tel.: (919) 541 2903, or J. Pekar, tel.: (919) 541 3995.
June 3–6, 1986 Munich, F.R.G.	**Analytica 86, 10th International Trade Exhibition and 10th International Conference 'Biochemical Analytics'** Contact: Dr. Rosemarie Vogel, Nymphenburgerstrasse 70, D-8000 München 2, F.R.G.
June 10–12, 1986 Dublin, Ireland	**Electroanalysis na h'Eireann** Contact: Dr. Malcolm R. Smith, School of Chemical Sciences, National Institute for Higher Education, Glasnevin, Dublin 9, Ireland.
June 16–18, 1986 Salt Lake, City, UT, U.S.A.	**1st Symposium on Pattern Recognition Methods in Analytical Spectroscopy** Contact: Melinda Van, Conference Secretariat, Biomaterials Profiling Center, University of Utah, Salt Lake City, UT, U.S.A. Tel.: (801) 581-8431, telex: GRAPHNET 3789459 UNIV UTAH SLC.
June 23–27, 1986 Copenhagen, Denmark	**Modern Trends in Activation Analysis, 7th International Conference** Contact: Dr. K. Heydorn, General Chairman MTAA-7, Risø National Laboratory, Post Box 49, DK-4000 Roskilde, Denmark. (Further details published in Vol. 169.)

July 7–10, 1986 Bordeaux, France	**2nd International Meeting on Chemical Sensors** Contact: Dr. Claude Lucat, 2nd International Meeting on Chemical Sensors, Université de Bordeaux I, 351, cours de la Libération, 33405 Talence, Cedex, France.
July 14–17, 1986 Ottawa, Canada	**10th International CODATA Conference** Contact: Mrs. Lois Baignée, Executive Secretary CODATA '86, Conference Services, National Research Council of Canada, Montreal Road, Ottawa, K1A OR6 Canada. (Further details published in Vol. 172.)
July 20–26, 1986 Bristol, U.K.	**SAC 86 – International Conference and Exhibition on Analytical Chemistry** Contact: Miss P.E. Hutchinson, Royal Society of Chemistry, Analytical Division, Burlington House, London W1V 0BN, U.K. Tel.: (01) 734-9971, (Further details published in Vol. 169.)
Aug. 10–17, 1986 Ottawa, Canada	**6th International Congress of Pesticide Chemistry** Contact: T.H.G. Micheal, Chemical Institute of Canada, 151 Slater Street, Suite 906, Ottawa, Ontario, Canada K1P 5H3. Tel.: (613) 233-5623. Telex: 053-4306 AIC.
Aug. 25–29, 1986 Antwerp, Belgium	**10th International Symposium on Microchemical Techniques** Contact: Dr. R. Dewolfs, University of Antwerp, Department of Chemistry, Universiteitsplein 1, B-2610 Wilrijk, Belgium. Tel.: 03/828.25.28 (ext. 204). Telex: 33646. (Further details published in Vol. 169.)
Aug. 26–29, 1986 Dunedin, New Zealand	**10th Conference of the Australian and New Zealand Society for Mass Spectrometry** Contact: Dr. J. Cutfield, Department of Biochemistry, University of Otago, Box 56, Dunedin, New Zealand. (Further details published in Vol. 175.)
Sept., 1986 Graz, Austria	**4th Conference on Computer Based Analytical Chemistry** Contact: Dr. Wolfhard Wegscheider, Institut für Analytische Chemie, Mikro- und Radiochemie, Technische Universität, Technikerstrasse 4, A-8010 Graz, Austria. Tel: (0316) 7061-8300/8301. (Further details published in Vol. 172.)
Sept. 8–10, 1986 Freiburg, F.R.G.	**4th International Symposium on Bioluminescence and Chemiluminescence** Contact: Dr. J. Schölmerich, Medizinschi Universitätsklinik, D-7800 Freiburg, F.R.G.
Sept. 9–12, 1986 London, U.K.	**5th Meeting of the International Electrophoresis Society, "Electrophoresis '86"** Contact: Dr. M.J. Dunn, Muscle Research Unit, Royal Postgraduate Medical School, DuCane Road, London W12 0HS, U.K., Tel.: 01-743-2030 ext. 338.
Sept. 9–12, 1986 Preveca, Greece	**2nd International Symposium on Kinetics in Analytical Chemistry** Contact: Prof. N. Evmirides, Laboratory of Analytical Chemistry, Chemistry Department, University of Ioannina, Ioannina, Greece.
Sept. 15–18, 1986 Houston, TX, U.S.A.	**22nd International Symposium on Advances in Chromatography** Contact: Professor A. Zlatkis, Chemistry Department, University of Houston, Houston 77004 TX, U.S.A. Tel.: (713) 749 2633.

Sept. 29–Oct. 3, 1986 St. Louis, MA, U.S.A.	**FACSS '86, Federation of Analytical Chemistry and Spectroscopy Societies 1986 Meeting** Contact: Dr. Marshall Fishman, U.S. Department of Agriculture, 600 E. Mermaid Lane, Wyndmoor, PA 19118, U.S.A. Tel.: (215) 233-6450.
Oct. 6–10, 1986 New York, NY, U.S.A.	**The Silver Jubilee Eastern Analytical Symposium** Contact: Dr. S. David Klein, EAS Publicity, 642 Cranbury Cross Road, North Brunswick, NJ 08902, U.S.A. Tel.: (201) 846-1582.
Nov. 18–20, 1986 Teddington, U.K.	**4th International Conference on Quantitative Surface Analysis, Techniques and Applications and VAMAS Workshop** Contact: Conference Secretary, Dr. G.C. Smith, Division of Materials Applications, National Physical Laboratory, Teddington, Middlesex, TW11 OLW, U.K. Tel.: (01) 977 3222, telex: 262344.
April 6–9, 1987 Cardiff, U.K.	**International Symposium on Electroanalysis in Biomedical, Environmental and Industrial Sciences** Contact: Short Courses Section, UWIST, P.O. Box 68, Cardiff CF1 3XA, Wales, U.K. Tel.: (0222) 42588, ext. 2213.
April 28–May 1, 1987 Sydney, Australia	**9th Australian Symposium on Analytical Chemistry** Contact: The Secretary 9AC, Mr. John Eames, P.O. Box 137, North Ryde, N.S.W. 2113, Australia. Tel.: (02) 887-8688.
May 11–14, 1987 Ghent, Belgium	**2nd International Symposium on Quantitative Luminescence Spectrometry in Biomedical Sciences** Contact: Dr. W. Baeyens, State University of Ghent, Laboratory of Pharmaceutical Chemistry and Drug Quality Control, Harelbekestraat 72, B-9000 Ghent, Belgium.
June 21–26, 1987 Toronto, Canada	**XXV Colloquium Spectroscopium Internationale** Contact: Mr. L. Forget, Executive Secretary XXV CSI, National Research Council of Canada, Ottawa, K1A 0R6 Canada. Tel.: (613) 993-9009, telex: 053-3145. (Further details published in Vol. 172.)
Aug. 24–28, 1987 Vienna, Austria	**6th International Conference on Fourier Transform Spectroscopy** Contact: Interconvention, P.O. Box 80, A-1107 Vienna, Austria. Tel.: (222) 57 63 05, 57 62 88, telex: 11 12 10.

CHEOPS

Chemometrical Optimization by Simplex

Authors: P.F.A. van der Wiel, B.G.M. Vandeginste and G. Kateman

A Program offering an *intelligent sequential* optimization plan for a wide range of applications, e.g.

- optimize the yield of a synthesis
- maximize the output of a production plant
- optimize the separation factors for two compounds in a chromatographic separation
- optimize the composition of a polymer
- optimize the determination of an enzyme in blood plasma etc.

- Incorporates the modified and supermodified sequential simplex optimization methods
- Optimization can be tailored by the user to meet his requirements
- Optimizations involving variation of up to ten parameters can be carried out
- Organizes optimization procedures efficiently to save both time and money
- Available for the Apple II series and IBM-PC
- Includes tutorial
- Full source code listings
- Clear fully descriptive manual
- US $ 360.00

AVAILABLE FROM:

Elsevier Scientific Software (JIC)
52 Vanderbilt Avenue
New York, NY 10017 USA
Phone: (212) 916 1250
Telex: 420643

or

Elsevier Scientific Software
P.O. Box 330
1000 AH Amsterdam
THE NETHERLANDS
Phone: (020) 5862 828
Telex: 18582

Write to us for further information on our other programs

No shipping charge if paid in advance

ELSEVIER SCIENTIFIC SOFTWARE

Apple is a registered trademark of Apple Computer Inc.
IBM-PC is a registered trademark of IBM

Now Available

LIQUID CHROMATOGRAPHY DETECTORS

Second, completely revised edition

by **R.P.W. SCOTT**, *Perkin-Elmer Corporation, Instrument Group, Main Avenue, Norwalk, CT, U.S.A.*

Journal of Chromatography Library - Volume 33

The renaissance of liquid chromatography, provoked by the spectacular development of gas-liquid chromatography, took place in the late 1960's and early 1970's. The first edition of this book published in 1977 describes the detectors that were available at that time and which provided a performance matching that of the contemporary equipment with which they were associated. It is interesting to note that the most popular detectors then, the UV detector, the refractometer detector, the fluorescence detector and the electrical conductivity detector are still the most commonly used detectors today, nearly a decade later. Detector design, however, has changed very significantly over the intervening years. Modern high-efficiency columns provide very narrow peaks and very fast separations, and thus the physical design of the detectors had to change to meet these new challenges. In 1977, there was little real understanding of the important role played by the detector in the overall function of the chromatographic system and although some of the factors were pointed out in the first edition of this book, in retrospect they appeared to be little understood.

This second edition gives an entirely new presentation of the subject of liquid chromatography detectors. It contains sections dealing with the fundamental aspects of the interaction between columns and detectors and the interaction between ancillary equipment and the detector. It brings the reader up-to-date with new designs and novel detecting systems that have been developed since 1977 and extends significantly the subject of the association of the liquid chromatography detector with spectroscopic techniques. In particular the book now explores the association of liquid chromatography with nuclear magnetic resonance spectroscopy, infrared spectroscopy and atomic absorption spectroscopy. This book not only gives a comprehensive treatment of the subject of liquid chromatography detectors and provides a rational procedure for defining their performance and so permit valid comparisons, but also discusses detector performance in relation to the whole of the chromatographic system.

Like the first edition, this book is expected to be well received.

REVIEW

"This book . . . is a well-balanced, practical review of modern LC detectors. This first comprehensive book devoted to LC detectors . . . valuable to workers in academic and industrial laboratories who desire a clear understanding of the principles of detection in order to choose a detector suitable for their research needs." (Journal of the American Chemical Society)

"It is recommended to any liquid chromatographer who desires to have a thorough knowledge of detection principles, who would like to get the most information from his available detectors, or who is interested in pursuing development of a new detector." (Analytical Chemistry)

March 1986 xvi + 272 pages
Price: US $ 64.75 / 175.00 Dutch guilders
ISBN 0-444-42610-8

To Elsevier

Please supply ..... copy(ies) of
Liquid Chromatography Detectors 2nd edition
by R.P.W. Scott
Price: US $ 64.75 or 175.00 Dutch Guilders

☐ I enclose my cheque
☐ Please charge my ..... card
No ..... Valid until .....

Name .....
Full address .....
.....
..... Postal code .....

Signature

ELSEVIER

Elsevier Science Publishers
P.O. Box 211
1000 AE Amsterdam
The Netherlands

Elsevier Science Publishing Co., Inc.
P.O. Box 1663
Grand Central Station
New York, NY 10163, USA

7352

A new comprehensive text

Contemporary Practice of Chromatography

by **COLIN F. POOLE** *and* **SHEILA A. SCHUETTE**, *Department of Chemistry, Wayne State University, Detroit, MI, USA*

Here is a book written for scientists in a wide variety of disciplines who use chromatography as an analytical tool.
It satisfies the need for:

- a graduate-level student textbook in chromatography / separation science
- a text for professional institutes offering short courses in chromatography
- a text for chromatographers who graduated some time ago and who wish to keep up to date with the field
- a comprehensive review of modern separation techniques.

All areas of gas, liquid, and thin-layer chromatography are covered; **no other book available offers the same scope.**

Emphasis is on the practice of chromatographic methods, including "how to" sections and numerous examples of calculation methods. Extensively illustrated, it contains a great many tables of all useful constants, materials and formulas frequently used by chromatographers. Valuable features are the chapters on sample preparation for chromatographic analysis, and on instrumental methods for sample identification, plus the comprehensive up-to-date literature review.

The authors have considerable experience teaching graduate-level courses and the material presented here has been tried and tested, having formed the basis for short courses taught to groups of industrial chemists. A must for chemists, clinical chemists, biologists, pharmacists, environmental scientists, instrument manufacturers and many others.

1984 x + 708 pages
US $ 59.00 (USA & Canada)
Dutch guilders 159.00 (Elsewhere)
ISBN 0-444-42410-5

ELSEVIER

P.O. Box 211
1000 AE Amsterdam
The Netherlands

P.O. Box 1663
Grand Central Station
New York, NY 10103, USA

Completely Revised

Instrumental Liquid Chromatography

A Practical Manual on High-Performance Liquid Chromatography Methods

Second, completely revised edition

by **N.A. PARRIS,** E.I. du Pont de Nemours & Company, Biomedical Products Department, Research and Development Division, Experimental Station Laboratory Wilmington, DE, USA

Journal of Chromatography Library 27

This extensively revised and up-to-date book is an essential tool for the HPLC user in the laboratory. It first appeared in 1976, was twice reprinted and was described in Laboratory Practice as "one of the more useful and successful texts on HPLC . . . a most readable book packed with valuable information and advice . . . strongly recommended."

Practically orientated, it is an easy-to-follow guide containing the minimum essential theoretical background. The majority of the material is based on practical experience and highlights details which may have important operational value for laboratory workers. It helps the HPLC user to select the most appropriate instrumentation, injectors, columns etc.

Applications of liquid chromatography are described with reference to the potential of the technique for qualitative, quantitative and trace analysis as well as for the preparative application. Numerous applications from the literature are tabulated and cross-referenced to sections concerned with the optimization procedures of the particular methods. The format of the original edition proved so successful that it has remained unchanged, but some 45% of the material is either new or completely revised in order to bring the column technology and applications data up-to-date.

"The style . . . is clear. The subject is placed in perspective by comparisons with other separation techniques and should provide a good reference book for all involved in practical LC," (Laboratory Practice).

"Overall the book is well written, and because of its practical emphasis, it is highly recommended for both the aspiring and experienced chromatographer," (J. Am Chem. Soc.).

1984 xiv + 432 pages. Price: US $ 83.25 / Dfl 225.00 (including postage).
ISBN 0-444-42061-4

ELSEVIER SCIENCE PUBLISHERS

P.O. Box 211, 1000 AE Amsterdam, The Netherlands
P.O. Box 1663, Grand Central Station, New York, NY 10163, USA

ontinued from outside back cover)

ort Communications

CONTENTS

Abstracted, Indexed in: Anal. Abstr.; Biol. Abstr.; Chem. Abstr.; Curr. Contents Phys. Chem. Earth Sci.; Life Sci.; Index Med.; Mass Spectrom. Bull.; Sci. Citation Index; Excerpta Med.)

(continued on inside back cover)